Aspects of the chemistry of transition metal complexes

McInnes, Jacqueline M.

Award date:
1995

Awarding institution:
University of Bath

ASPECTS OF THE CHEMISTRY OF TRANSITION METAL COMPLEXES CARRYING η^2(4e)-ALKYNE AND η^4-CYCLOBUTADIENE LIGANDS.

submitted by Jacqueline M. McInnes
for the degree of PhD
of the University of Bath
1995

COPYRIGHT

ProQuest LLC
789 East Eisenhower Parkway
P.O. Box 1346
Ann Arbor, MI 48106-1346

MEMORANDUM

The work described in this thesis was carried out by the author between October 1992 and October 1995 within the School of Chemistry at the University of Bath, under the supervision of Professor Michael Green. Unless otherwise indicated, the work is original and has not been submitted for any other degree.

Some of the results contained within this thesis have been published in the following papers :

- Formation of *cisoid*-η^4-(5e)-Butadienylrhenium Complexes by Coupling of Alkene and Alkyne Ligands.
  S.J. Dossett, M. Green, M.F. Mahon and J.M. McInnes.
  J. Chem. Soc. Chem. Commun., 767, **1995**.
- Reactions of Co-ordinated Ligands. Part 59. Deprotonation of η^2(4e)-Bonded Alkynes as a Pathway to σ,η^2(3e)-Prop-2-ynyl, η^5-*S*-Pentadienyl and η^4-*trans*-1,3-Diene Substituted Molybdenum Complexes.
  C. Carfagna, R.J. Deeth, M. Green, M.F. Mahon, J.M. McInnes, S. Pellegrini and C.B. Woolhouse.
  J. Chem. Soc., Dalton Trans., in press.

ACKNOWLEDGEMENTS

Firstly, I would like to thank Professor Michael Green for his encouragement and guidance throughout the course of this research.

Also, I am grateful to several people without whom some of this work would not have been possible, namely Dr. Mary Mahon for all nine single crystal X-ray structure determinations and for her perseverance when crystals just would not behave, Dr. Rob Deeth for the theoretical studies, Dr. Adrian Fisher for the electrochemical study, Dr. Richard Kinsman for teaching me various NMR techniques and Alan Carver for CHN analysis.

SERC are, also, acknowledged for the funding of this studentship.

Thanks are also due to all the people who have worked with me in Lab 2.31 for their general tolerance of me and, in particular to Dr Sylvain Pellegrini, Steve Dossett and Nick Carr for all their practical help and advice at various stages of this PhD.

Thank you also to my parents, Sybella and Thomas Bambrough, for their support throughout all my student life in both Glasgow and Bath.

Finally, I would like to thank some very special friends for their support, encouragement and understanding over the last few years, Isabell Stewart, Alan Dow, David Evans (soon to be Doctor Dave) and Dr. John McGinley. Life during my PhD would not have been as interesting or bearable without them.

SUMMARY

This thesis is concerned with the reactivity and structure of transition metal complexes of molybdenum and rhenium, which contain either an η^2(4e)-alkyne ligand or an η^4-cyclobutadiene ligand.

In Chapter 2, deprotonation of the X-ray crystallographically identified η^2-alkene/η^2(4e)-alkyne substituted complex $[Mo\{\eta^2(4e)\text{-}MeC_2Ph\}(dpps)(\eta\text{-}C_5H_5)][BF_4]$ **1** (dpps = *o*-diphenylphosphinostyrene), resulted in the unexpected formation of the η^5-*S*-pentadienyl complex $[Mo\{\eta^2,\eta^3(5e)\text{-}S\text{-}CH_2CHC(Ph)CH{=}CH\text{-}o\text{-}C_6H_4PPh_2\}(\eta\text{-}C_5H_5)]$ **2**, which was structurally characterised by single crystal X-ray crystallography. Subsequent reactions of **2** resulted in the formation of *cis* and *trans* substituted η^4-1,3-diene complexes, the *trans* diene complex **3** being stabilised by a Mo(μ-H)C interaction. Also included in Chapter 2 is an investigation of the synthesis and reactivity of the cationic η^4(5e)-butadienyl complexes $[Re{=}C(Ph)\text{-}\eta^3\text{-}\{C(R)CHC(H)C_6H_4PPh_2\text{-}o\}(\eta\text{-}C_5H_5)][BF_4]$ (R = Me **13** and R = Ph **14**); the methyl substituted system was structurally characterised by a single crystal X-ray diffraction study.

In Chapter 3, an investigation was carried out on ancillary ligand substitution of the cyclobutadiene complex $[ReBr_2(\eta\text{-}C_4Ph_4)(\eta\text{-}C_5H_5)]$. Of particular interest was the reaction of $[ReBr_2(\eta\text{-}C_4Ph_4)(\eta\text{-}C_5H_5)]$ with two equivalents of lithium aluminium hydride to afford the dihydride complex $[ReH_2(\eta\text{-}C_4Ph_4)(\eta\text{-}C_5H_5)]$ **20**, which was structurally identified by NMR spectroscopy and single crystal X-ray diffraction studies. This complex (**20**) subsequently underwent a ring opening reaction of the C_4 ring in the presence of trifluoroacetic acid to afford the 1,3-diene complex $[ReH\{\eta^2,\eta^2\text{-}PhC(H){=}C(Ph)C(Ph){=}C(Ph)H\}(CF_3C(O)O)(\eta\text{-}C_5H_5)]$ **22**, the structure and orientation of which was identified crystallographically.

In Chapter 4, the nature of the M-(σ,η^2-C_3H_3) bonding in complexes $[Mo\{\sigma,\eta^2(3e)\text{-}CH_2C_2R\}\{\eta^2(4e)\text{-}MeC_2Me\}(\eta\text{-}C_5H_5)]$, $[Mo\{\sigma,\eta^2(3e)\text{-}CH_2C_2H\}(CO)_2(\eta^6\text{-}C_6Me_6)][BF_4]$ and $[Zr(Me)\{\sigma,\eta^2(3e)\text{-}CH_2C_2Ph\}(\eta\text{-}C_5H_5)_2]$ have been examined using a comparative standard Extended Hückel Molecular Orbital (EHMO) study. Finally, the reactivity of $[Mo\{\sigma,\eta^2(3e)\text{-}CH_2C_2R\}\{\eta^2(4e)\text{-}MeC_2R\}(\eta\text{-}C_5H_5)]$ (R = Me or Ph) towards trifluoroacetic acid and excess hexafluorobut-2-yne gas was investigated.

CONTENTS

ABBREVIATIONS

R	:	alkyl or aryl group
Me	:	methyl
Ph	:	phenyl
Cp	:	cyclopentadienyl
L	:	ligand
M	:	metal
X	:	halide
s	:	secondary
t	:	tertiary
MO	:	molecular orbital
HOMO	:	highest occupied molecular orbital
LUMO	:	lowest unoccupied molecular orbital
Δ	:	heat
NMR	:	nuclear magnetic resonance
EPR	:	electron paramagnetic resonance
IR	:	infra-red
ν(CO)	:	wavelength of carbonyl stretch in cm^{-1}
mol	:	mole
mmol	:	milli-mole
thf	:	tetrahydrofuran

Relating to NMR.

δ	:	chemical shift relative to TMS
J	:	scalar coupling constant in hertz
Hz	:	hertz
TMS	:	tetramethylsilane
s	:	singlet
d	:	doublet
dd	:	doublet of doublets

t	:	triplet
q	:	quartet
m	:	multiplet
br	:	broad
COSY	:	correlated spectrosopy

Relating to Mass Spectral Data.

M^+	:	parent molecular ion

Relating to X-ray Diffraction Data.

a, b, c	:	unit cell edge lengths in Å
α, β, γ	:	angles between pairs of sides in °
Z	:	number of molecules per unit cell
U	:	volume of unit cell in $Å^3$
D_c	:	density in gcm^{-3}
F(000)	:	total number of electrons per unit cell
μ(Mo-K_α)	:	linear absorbance coefficient for molybdenum K_α radiation.

LIST OF NEW COMPLEXES

COMPLEX	No.
$[Mo(\eta^2\text{-}MeC_2Ph)(dpps)(\eta\text{-}C_5H_5)][BF_4]$	1
$[Mo\{\eta^2,\eta^3(5e)\text{-}S\text{-}CH_2CHC(Ph)CH{=}CH\text{-}o\text{-}C_6H_4PPh_2\}(\eta\text{-}C_5H_5)]$	2
$Mo\{\eta^2,\eta^2(\mu_{Mo\text{-}C}\text{-}H)\text{-}CH_3CHC(Ph)CH{=}CH\text{-}o\text{-}C_6H_4PPh_2\}(\eta\text{-}C_5H_5)][BF_4]$	3
$[Mo\{OC(O)CF_3\}\{\eta^2,\eta^2,CH_3CH{=}C(Ph)CH{=}CH\text{-}o\text{-}C_6H_4PPh_2\}(\eta\text{-}C_5H_5)]$	4
$[Mo(NCMe)\{\eta^2,\eta^2,CH_3CH{=}C(Ph)CH{=}CH\text{-}o\text{-}C_6H_4PPh_2\}(\eta\text{-}C_5H_5)][BF_4\}$	5
$[MoI\{\eta^2,\eta^2\text{-}CH_3CH{=}C(Ph)CH{=}CH\text{-}o\text{-}C_6H_4PPh_2\}(\eta\text{-}C_5H_5)]$	6
$[MoBr\{\eta^2,\eta^2\text{-}CH_3CH{=}C(Ph)CH{=}CH\text{-}o\text{-}C_6H_4PPh_2\}(\eta\text{-}C_5H_5)]$	7
$[MoCl\{\eta^2,\eta^2\text{-}CH_3CH{=}C(Ph)CH{=}CH\text{-}o\text{-}C_6H_4PPh_2\}(\eta\text{-}C_5H_5)]$	8
$[Mo(CO)\{\eta^2,\eta^2\text{-}CH_3CH{=}C(Ph)CH{=}CH\text{-}o\text{-}C_6H_4PPh_2\}(\eta\text{-}C_5H_5)][PF_6]$	9
$[MoI\{\eta^2,\eta^2\text{-}CH_3CH{=}C(Ph)CH{=}CH\text{-}o\text{-}C_6H_4PPh_2\}(\eta\text{-}C_5H_5)][BF_4]$	10
$[Mo(\eta^2\text{-}MeC_2Ph)(dpps)(\eta^5\text{-}C_9H_7)][BF_4]$	11
$[Mo\{\eta^2,\eta^3(5e)\text{-}S\text{-}CH_2CHC(Ph)CH{=}CH\text{-}o\text{-}C_6H_4PPh_2\}(\eta^5\text{-}C_9H_7)]$	12
$[Re{=}C(Ph)\text{-}\eta^3\text{-}\{C(Me)CHCHC_6H_4PPh_2\text{-}o\}(\eta\text{-}C_5H_5)][BF_4]$	13
$[Re{=}C(Ph)\text{-}\eta^3\text{-}\{C(Ph)CHCHC_6H_4PPh_2\text{-}o\}(\eta\text{-}C_5H_5)][BF_4]$	14
$[Re\{\eta^4\text{-}CH(Ph){=}C(Ph)CH{=}CH(C_6H_4PPh_2\text{-}o)\}(\eta\text{-}C_5H_5)]$	15
$[Re(OH_2)\{\eta^4\text{-}CH(Ph){=}C(Ph)CH{=}CH(C_6H_4PPh_2\text{-}o)\}(\eta\text{-}C_5H_5)]$	16
$[ReBr(PPh_3)(\eta^4\text{-}C_4Ph_4)(\eta\text{-}C_5H_5)][BF_4]$	17
$[ReH(Br)(\eta^4\text{-}C_4Ph_4)(\eta^5\text{-}C_5H_5)]$	18
$[ReH(PPh_3)(\eta^4\text{-}C_4Ph_4)(\eta^5\text{-}C_5H_5)][BF_4]$	19
$[ReH_2(\eta^4\text{-}C_4Ph_4)(\eta\text{-}C_5H_5)]$	20
$[ReH\{\eta^2,\eta^2\text{-}PhC(H){=}C(Ph)C(Ph){=}C(Ph)H\}(\eta\text{-}C_5H_5)][BF_4]$	21
$[ReH\{OC(O)CF_3\}\{\eta^2,\eta^2\text{-}PhC(H){=}C(Ph)C(Ph){=}C(Ph)H\}(\eta\text{-}C_5H_5)]$	22
$[ReD\{OC(O)CF_3\}\{\eta^2,\eta^2\text{-}PhC(H){=}C(Ph)C(Ph){=}C(Ph)H\}(\eta\text{-}C_5H_5)]$	23
$[Mo\{OC(O)CF_3\}(\eta^2\text{-}MeC_2Ph)_2(\eta\text{-}C_5H_5)]$	24
$[Mo\{OC(O)CF_3\}(\eta^2\text{-}MeC_2Me)_2(\eta\text{-}C_5H_5)]$	25
$[Mo(\eta\text{-}C_5H_5)(\eta^3,\eta^4$ bicyclo[4,3,0]nonyl)]	26

1. INTRODUCTION

1.1 Four-electron Alkyne Transition Metal Complexes.

Early organometallic literature indiscriminately associated alkene and alkynes as "interchangeable" ligands and although it is true that there are numerous examples of analogous alkene and alkyne complexes for the later transition metals there are also important characteristic differences between the two types of ligands. Firstly, alkynes are stronger π-acids and secondly, alkynes have two orthogonal π-systems and, hence, can donate more than two electrons to a metal centre.(Figure 1.1).

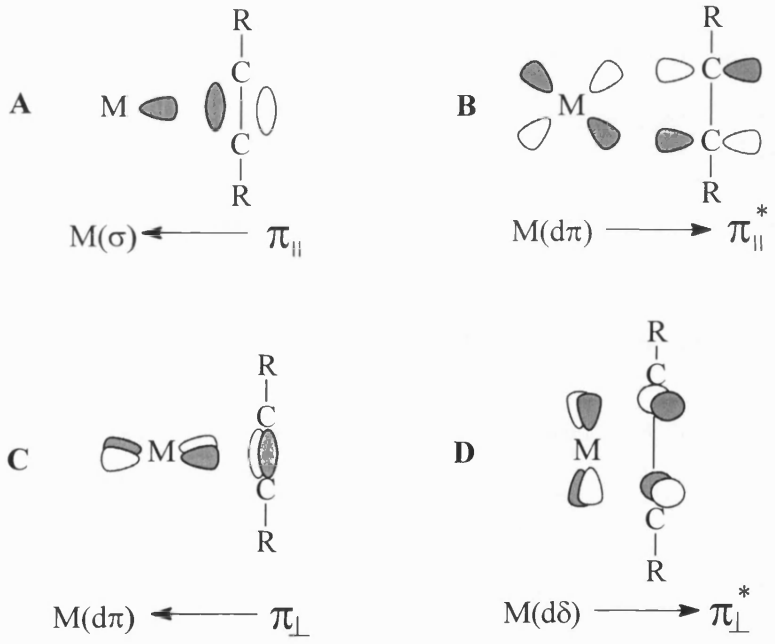

FIGURE 1.1

Calculations have shown that the σ interaction (**A**, Figure 1.1), exhibits the largest overlap and the dπ-$\pi_{\parallel}$* (**B**) and dπ-$\pi_{\perp}$ (**C**) are similar but smaller than **A**. The dδ-$\pi_{\perp}$* interaction (**D**) has been shown to be negligible.

The availability of filled or vacant orbitals and the energy levels of the σ and dπ interactions determine how many electrons an alkyne formally donates to a transition metal centre. The bonding of a two -electron alkyne is analogous to the metal-alkene bonding description by the Dewar-Chatt-Duncanson model.[1]

Alkynes are considered four-electron donors when there is donation from the filled $\pi_\perp$ orbital of the alkyne to an empty dπ orbital of the transition metal (**C**, Figure 1.1). Since the dδ-$\pi_\perp$* interaction (**D**) is negligible there is no back donation to the $\pi_\perp$* orbital of the alkyne and hence, four-electron alkynes are always net electron donors.

The importance of the role played by both filled π orbitals ($\pi_\parallel$ and $\pi_\perp$) in binding to a single metal centre was recognised, initially, by Tate and Augl.[2] They reported the synthesis of [W(CO)(hex-3-yne)$_3$] **1.1** (Figure 1.2) in 1963 and correctly assigned the geometry as pseudotetrahedral, which was confirmed in 1972 by single crystal X-ray crystallography.[3] The spectroscopic data for **1.1** indicated that the three alkynes were equivalent, but that the two ends of the alkyne ligand were situated in different environments. Thus, it was suggested that the alkyne was "doubly π-bonded" to the tungsten with two of the three alkyne ligands donating four electrons because if each alkyne only donated two electrons the complex would have an effective electron count of only fourteen, which is highly unlikely for a centrally placed transition metal in a low oxidation state. It was suggested that the three alkynes were rapidly alternating in their bonding mode i.e. 4e → 2e and 2e → 4e and so, overall, each alkyne was effectively donating $3^1/_3$ electrons.

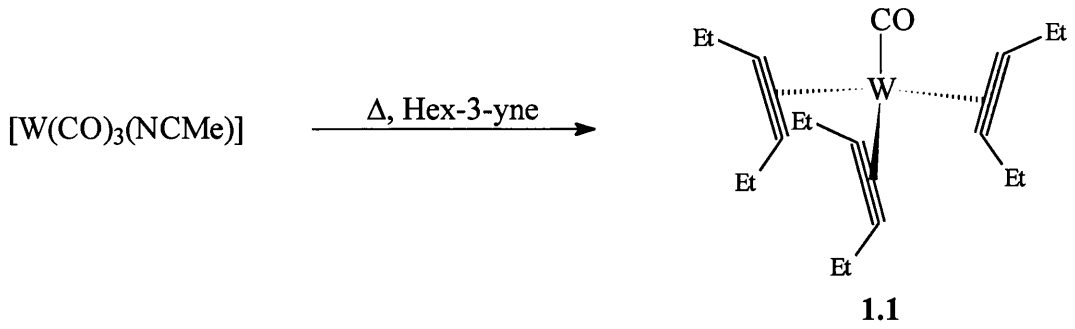

1.1

FIGURE 1.2

The insight and accuracy of this early work in characterising the anomalous $[M(CO)(RC_2R)_3]$ complexes set the stage for further developments of four-electron alkynes. Since that time a plethora of literature has been published regarding four-electron alkynes and was the subject of a review by Templeton in the late 1980's.[4]

This thesis is concerned with the reactivity of molybdenum and rhenium complexes which contain four-electron alkynes, and so, the synthesis, spectroscopic, structural and bonding features of these alkynes will be briefly reviewed.

1.2. Synthesis of Mono- and Bis-Alkyne Complexes.

There are now numerous examples of mono- and bis-alkyne complexes, which are prepared by various synthetic routes with the cyclopentadienyl derivatives of molybdenum and tungsten, i.e. $[M(RC{\equiv}CR)_x(\eta\text{-}C_5H_5)]$, being the most extensively studied class.

The main synthetic routes to mono-alkyne derivatives can be divided broadly into three groups. The first category of reactions involves the addition of free alkyne to a metal complex, e.g. $[MoX(CO)_3(\eta\text{-}C_5H_5)] + RC{\equiv}CR \rightarrow [MoX(CO)(RC{\equiv}CR)(\eta\text{-}C_5H_5)]$.[5] The second class of reactions are those in which one alkyne of a bis-alkyne precursor is replaced. For example, an extensive series of cationic $[MoL(CO)(RC{\equiv}CR)(\eta\text{-}C_5H_5)][BF_4]$ complexes have been prepared from $[Mo(CO)(RC{\equiv}CR)_2(\eta\text{-}C_5H_5)][BF_4]$ reagents by the substitution of one of the co-ordinated alkyne ligands, e.g. the reaction of **1.2** with lithium bromide occurs smoothly at room temperature to afford the neutral, mono-alkyne product $[MoBr(CO)(RC{\equiv}CR)(\eta\text{-}C_5H_5)]$ **1.3** (Figure 1.3).[6]

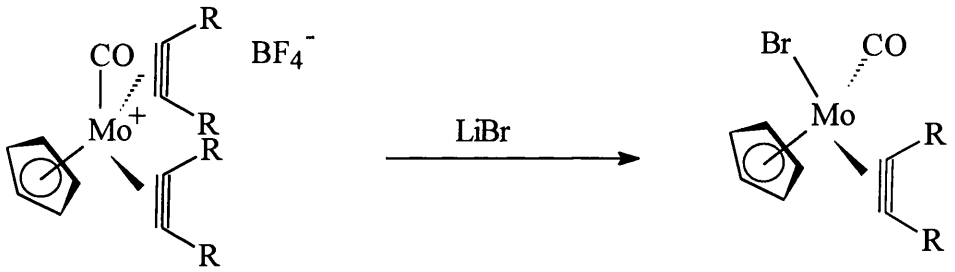

1.2 **1.3**

FIGURE 1.3

Finally, mono-alkyne metal complexes can be synthesised *via* simple ancillary ligand substitution of a mono-alkyne metal complex. For example, displacement of the timethyl phosphite ligand from $[Mo\{P(OMe)_3\}_2(MeC{\equiv}CMe)$

$(\eta\text{-}C_5H_5)]^+$ with anionic sulphur nucleophiles produces neutral mono-alkyne molybdenum derivatives, $[Mo\{P(OMe)_3\}(MeC{\equiv}CMe)(\eta\text{-}C_5H_5)(SR)]$.[7]

Bis-alkyne complexes have been exploited to synthesise mono-alkyne monomers as well as for alkyne coupling reactions and ligand based transformations. In particular, bis-alkyne derivatives of molybdenum and tungsten were prominent in the development of alkyne chemistry in the 1980's. An important category of this chemistry is the cationic, cyclopentadienyl derivatives of bis-alkynes, which can be accessed by the oxidative cleavage of $[Mo(CO)_3(\eta\text{-}C_5H_5)]_2$ **1.4** dimer in the presence of alkyne (Figure 1.4). This is a versatile route and a wide range of $[Mo(CO)(RC{\equiv}CR)_2(\eta\text{-}C_5H_5)][BF_4]$ **1.6** (Figure 1.4) complexes has been synthesised by this route.[4]

This is not the sole route to cationic bis-alkyne complexes but it is a high yield, clean reaction. One alternative is the electrophilic $[Mo(CO)_3(\eta\text{-}C_5H_5)][BF_4]$ reagent prepared by hydride abstraction from $[Mo(CO)_3(H)(\eta\text{-}C_5H_5)]$ with trityl tetrafluoroborate. This readily adds alkyne to form mono-alkyne and bis-alkyne products depending upon the reaction conditions and the alkyne substituents.[8]

However, oxidative cleavage of the indenyl dimer $[Mo(CO)_3(\eta^5\text{-}C_9H_7)]_2$ **1.5** does not yield cationic bis-alkyne complexes in the same facile manner as **1.4**. Instead the indenyl complexes are better synthesised by reducing $[Mo(CO)_3(\eta^5\text{-}C_9H_7)]_2$ with sodium amalgam in the presence of methyl iodide to afford $[Mo(CO)_3(Me)(\eta^5\text{-}C_9H_7)]$ **1.7** (Figure 1.4). Protonation of **1.7** in the presence of acetonitrile affords the cationic bis-(acetonitrile) complex $[Mo(CO)_2(NCMe)_2(\eta^5\text{-}C_9H_7)][BF_4]$ **1.8**, which subsequently reacts with alkynes to form $[Mo(CO)(RC{\equiv}CR)_2(\eta^5\text{-}C_9H_7)][BF_4]$ **1.9** products. Alternatively, protonation of **1.7** at low temperature followed by the addition of an alkyne results in the loss of methane and the formation of **1.9**.

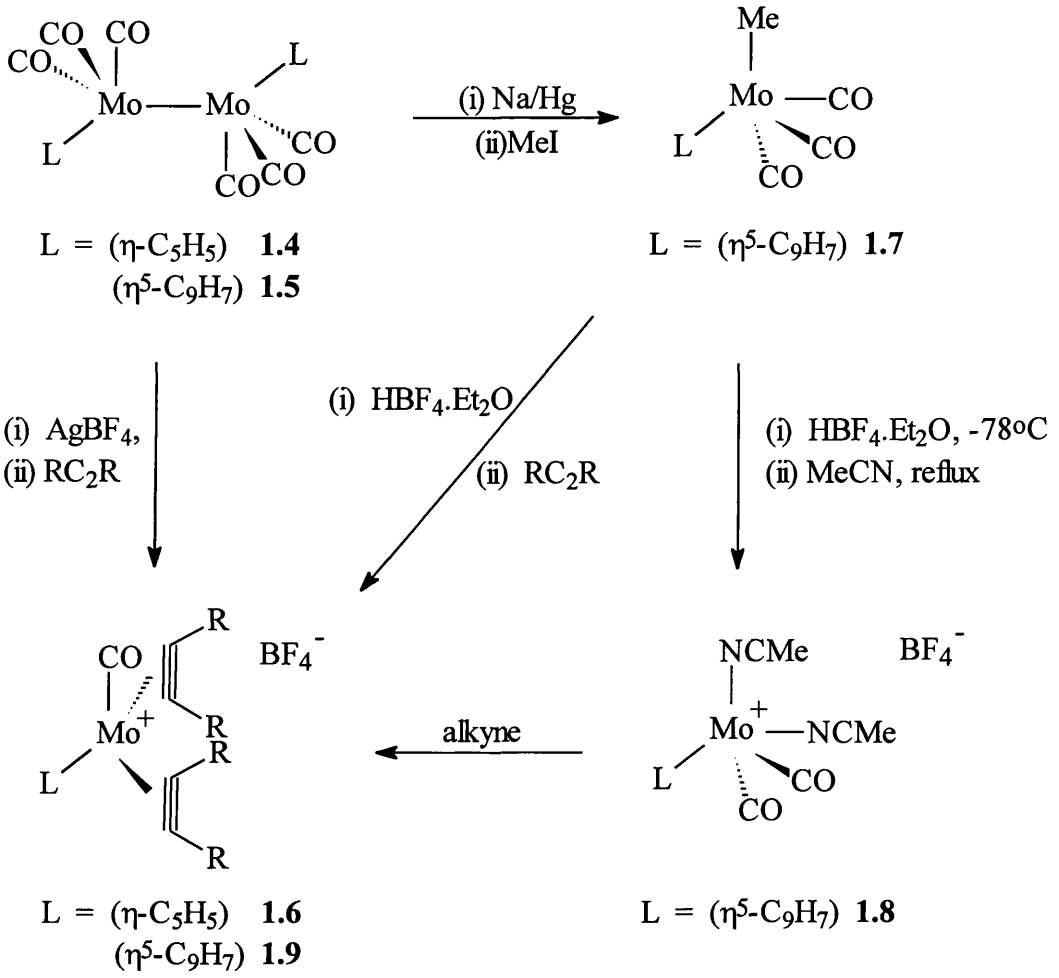
CO CO
CO
Mo — Mo
L
L
CO
CO CO
(i) Na/Hg
(ii)MeI
Me
Mo —CO
L
CO
CO
L = (η-C5H5) 1.4
(η5-C9H7) 1.5
L = (η5-C9H7) 1.7
(i) AgBF4,
(ii) RC2R
(i) HBF4.Et2O
(ii) RC2R
(i) HBF4.Et2O, -78oC
(ii) MeCN, reflux
CO
R
BF4-
Mo+
R
L
R
R
alkyne
NCMe
BF4-
Mo+ —NCMe
L
CO
CO
L = (η-C5H5) 1.6
(η5-C9H7) 1.9
L = (η5-C9H7) 1.8

FIGURE 1.4

1.3 Structure and Physical Properties of Alkyne Complexes.

The number of electrons an alkyne donates in metal complexes is reflected in various properties, such as metal-ligand bond lengths, selected bond angles, ^{1}H and ^{13}C NMR data.[9]

The use of ^{1}H NMR spectroscopy to probe the bonding of alkynes is limited to terminal alkynes. However, $^{13}C\{^{1}H\}$ NMR spectroscopy has proved to be a more useful tool and an empirical correlation between δ values in ^{13}C NMR spectra and the electron donation of bound alkynes were first noted by Templeton and is useful for recognising donation from $\pi_{\perp}$ as well as $\pi_{\parallel}$. A plot of alkyne ^{13}C chemical shifts, which spans over 100 ppm, *versus* the number of the electrons (N) donated per alkyne to fulfil the effective atomic number guideline (Figure 1.5), revealed that two-, three- and four-electron donor co-ordinated alkynes fall into distinct regions i.e. δ 100-130, δ 140-190 and δ 175-230, respectively.

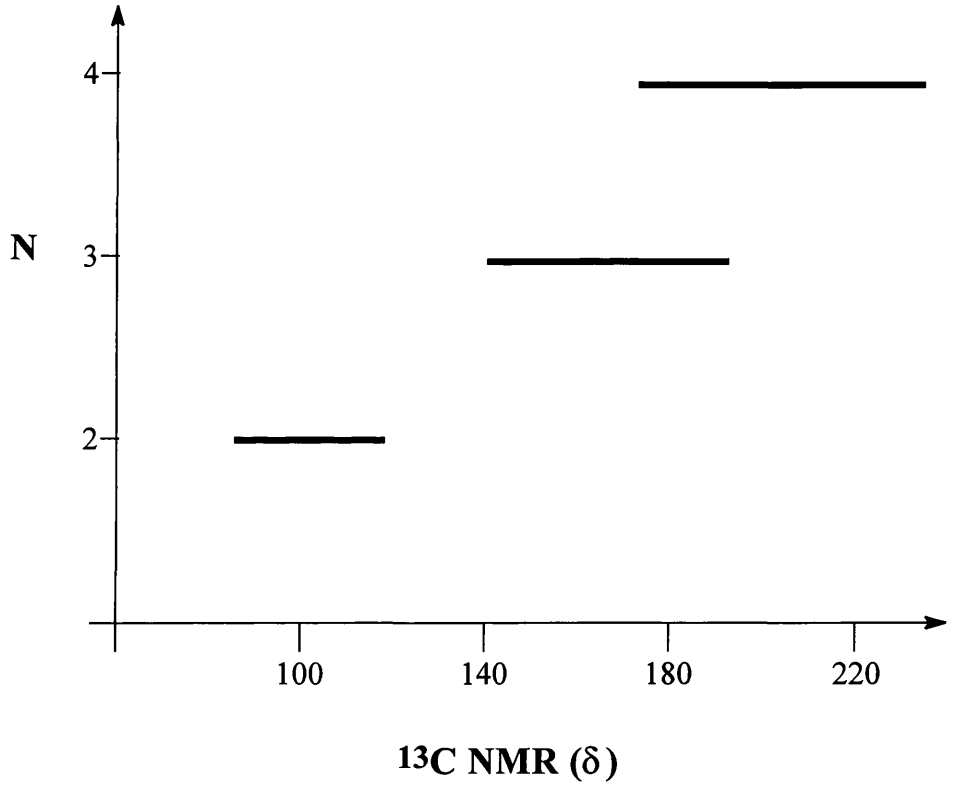

FIGURE 1.5 : Plot of ^{13}C Shifts (δ) *versus* Number of Electrons Donated (N).

Alkynes in transition metal complexes can undergo rotation if the barrier to rotation is low. The barrier to rotation of a variety of alkyne complexes has been probed using variable temperature NMR spectroscopy and typical values for *bis*-alkyne complexes are listed in Table 1.1. In general, cationic bis-alkyne complexes exhibit relatively high rotational barriers (67-88 $kJmol^{-1}$). The rationalisation of trends is difficult since not only do $\pi_{\parallel}^*$ acceptance and $\pi_{\perp}$ donation influence the size of the barrier but steric factors play an important role as well.

TABLE 1.1 : Rotation Barriers ($kJmol^{-1}$) of Selected Complexes.

COMPLEX	$\Delta G_{Tc}^{\ddagger}$
$[MoCl(\eta^2\text{-}MeC{\equiv}CMe)_2(\eta\text{-}C_5H_5)]$[10]	38.9
$[MoBr(\eta^2\text{-}MeC{\equiv}CMe)_2(\eta\text{-}C_5H_5)]$[10]	60.2
$[Mo(CO)(\eta^2\text{-}MeC{\equiv}CMe)_2(\eta\text{-}C_5H_5)][BF_4]$[11]	81.2
$[Mo(PEt_3)(\eta^2\text{-}MeC{\equiv}CMe)_2(\eta\text{-}C_5H_5)][BF_4]$[12]	62.8

The structural parameters, as determined by crystallography, of four-electron alkynes are also noteworthy. The metal-carbon bond distances of four-electron alkynes are relatively consistent across the wide range of complexes (2.00-2.10 Å) and are generally shorter than those observed for two-electron alkyne complexes. Both the two- and four-electron alkynes exhibit relatively short C≡C distances (≤ 1.30 Å) and so this cannot distinguish between the two types. Another germane structural parameter is the deviation of the alkynes from linearity, with angles which range from 130 to 150° (Table 1.2).

TABLE 1.2 : Structural Parameters of Selected Four-electron Alkynes.

COMPLEX	**M-C (Å)**	**C≡C (Å)**	**∠ C≡C-R (°)**
$[Mo(MeC{\equiv}CMe)_2\{S_2CN(Et)_2\}_2]$[13]	2.02, 2.06, 2.04, 2.09	1.24, 1.25	146
$[WCl(CF_3C{\equiv}CCF_3)_2(\eta\text{-}C_5H_5)]$[14]	2.05, 2.06, 2.07, 2.07	1.23, 1.28	139
$[Mo(CO)(MeC{\equiv}CMe)_2(\eta\text{-}C_5H_5)][BF_4]$[11]	2.06, 2.08, 2.12, 2.14	1.27, 1.28	146
$[Mo(NCMe)(MeC{\equiv}CMe)_2(\eta\text{-}C_5H_5)][BF_4]$[11]	2.06, 2.07, 2.06, 2.07	1.27, 1.28	145

2. REACTIVITY OF MIXED η^2(2e)-ALKENE and η^2(4e)-ALKYNE COMPLEXES.

2.1 Introduction

The reactivity of co-ordinated η^2(4e)-alkynes has been extensively studied. Of particular note are the deprotonation reactions, which can lead to reactive η^2(3e)-allenyl[15,16] or η^3(3e)-prop-2-ynyl species.[17] For instance, it has been established that treatment of the cationic complex $[Mo(\eta^2\text{-}PhC_2CH_2Ph)\{P(OMe)_3\}_2(\eta\text{-}C_5H_5)][BF_4]$ **2.1** with $KH/Bu^tOH/Et_2O$ resulted in the loss of H_2 and formation of the isomeric η^2(3e)-allenyl complexes $[Mo\{=C(Ph)C=C(H)Ph\}\{P(OMe)_3\}_2(\eta\text{-}C_5H_5)]$ **2.2a** and **2.2b** (Figure 2.1).[16] The low field carbon resonance of δ 253.5, attributable to the alkylidene α-carbon, was typical of an η^2-allenyl. In a related study reported by Templeton and co-workers[18] it was shown that deprotonation of $[W(CO)(dtc)(\eta^2\text{-}MeOC_2CH_2Ph)(dppe)][X]$ $[dtc=R_2NCS_2;\ dppe=(Ph_2PCH_2)_2;\ X=CF_3SO_3,\ BF_4]$ affords the analogous species $[W(CO)(dtc)\{=C(OMe)C=C(H)Ph\}(dppe)]$.

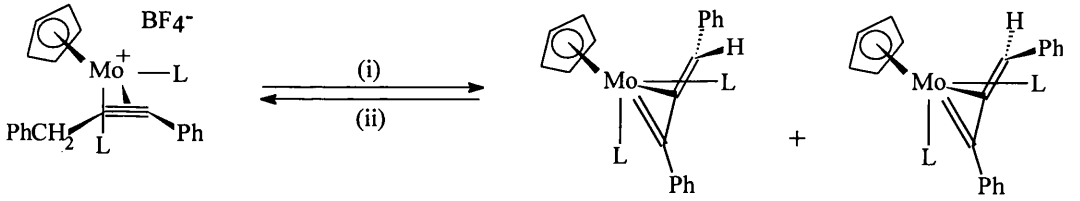

2.1 **2.2a** **2.2b**

FIGURE 2.1 : L = $P(OMe)_3$; i) KH, Et_2O, ^tBuOH, $-H_2$; ii) $HBF_4.Et_2O$.

In contrast, deprotonation of the neutral, *bis*-alkyne complex $[MoBr(RC_2Me)_2(\eta\text{-}C_5H_5)]$ (R = methyl **2.3**, phenyl **2.4**) with lithium bis(trimethyl) silyl amide resulted in the transformation of one of the co-ordinated alkyne ligands into a three-electron σ,η^2-prop2-ynyl[17] (complexes **2.5** and **2.6**, respectively, Figure

2.2). Unlike the allenyl complexes the $^{13}C\{^1H\}$ NMR spectrum of **2.5** and **2.6** did not display a low field signal attributable to an alkylidene α-carbon. These neutral four-electron η^2-alkyne/ three-electron prop-2-ynyl complexes were obviously of interest from the standpoint of reactivity towards donor ligands as both the alkyne (4e → 2e) and prop-2-ynyl (3e → 1e) ligand have the ability to switch bonding modes. Unusual chemical reactivity with carbon monoxide has already been demonstrated for these compounds[17a] and will be discussed in more detail in Section 4.1.

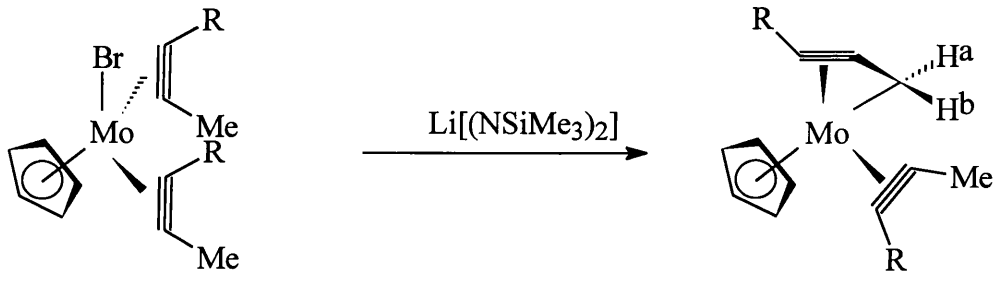

R = Me **2.3**
Ph **2.4**

R = Me **2.5**
Ph **2.6**

FIGURE 2.2

Although complexes containing co-ordinated alkynes have been the subject of many investigations,[4] complexes containing both a co-ordinated η^2-alkene and an η^2-alkyne are a relatively unexplored class of compound and there are only a few reported examples, one of the first being the crystallographically identified complex $[Mo(\eta^2\text{-}MeC_2Me)(dpps)(\eta\text{-}C_5H_5)][BF_4]$[19] (dpps = *ortho*-diphenylphosphinostyrene) **2.7**. In addition to this there is also a group of tungsten complexes with the general formula $[W(\eta^2\text{-}PhC_2H)(\eta^2\text{-alkene})(S_2CNEt_2)]$ (alkene = maleic anhydride or tetracyanoethylene), which derive stability from the presence of the electronegative substituents on the alkene ligand.[20] More recently, the synthesis of $[Mo(CO)(\eta^2\text{-}C_2H_4)(\eta^2\text{-}MeC{\equiv}CMe)(\eta\text{-}C_5H_5)][BF_4]$ **2.9**, *via* halide abstraction from $[MoBr(CO)(\eta^2\text{-}MeC{\equiv}CMe)(\eta\text{-}C_5H_5)][BF_4]$ **2.8** in the presence of a stream of ethylene, has been reported (Figure 2.3).[21]

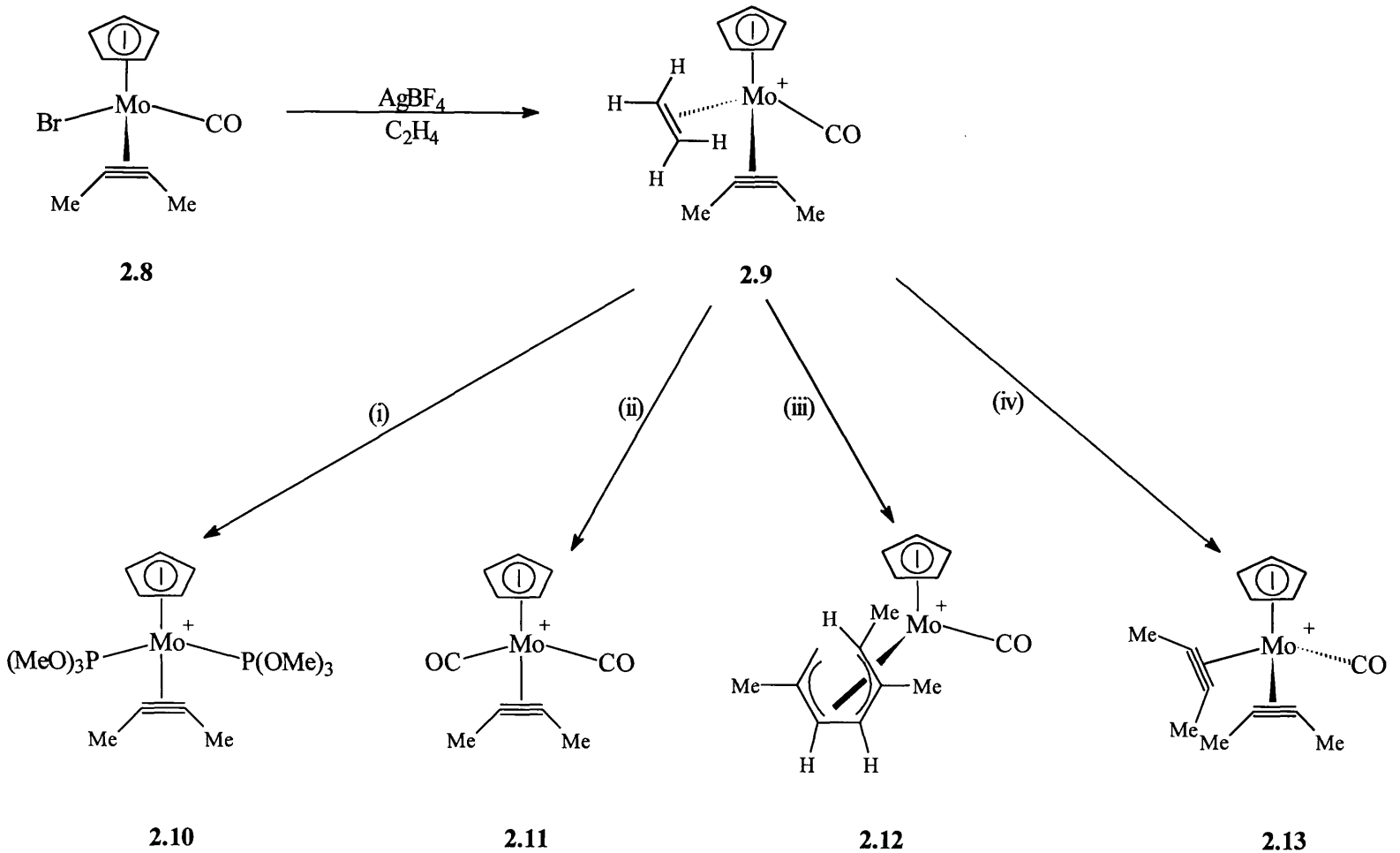

FIGURE 2.3 : (i) $P(OMe)_3$; (ii) CO ; (iii) isoprene ; (iv) but-2-yne.

The reactive nature of this complex mainly arose from the lability of the η^2-alkene ligand and it was discovered that the alkene could be easily displaced by phosphites, carbon monoxide, 1,3-dienes and alkynes to afford the complexes **2.10**, **2.11**, **2.12** and **2.13**, respectively (Figure 2.3). However, unlike **2.9** the alkene in the dpps complex **2.7** was not as labile because it was anchored to the metal centre *via* the phosphine atom and as a consequence the alkene was not displaced when **2.7** was exposed to acetonitrile but instead a coupling of the alkene and alkyne moiety occurred to afford the 1,3-diene complex **2.14** (Figure 2.4).[19] The exact nature of this coupling reaction will be discussed in more detail in section 2.7.

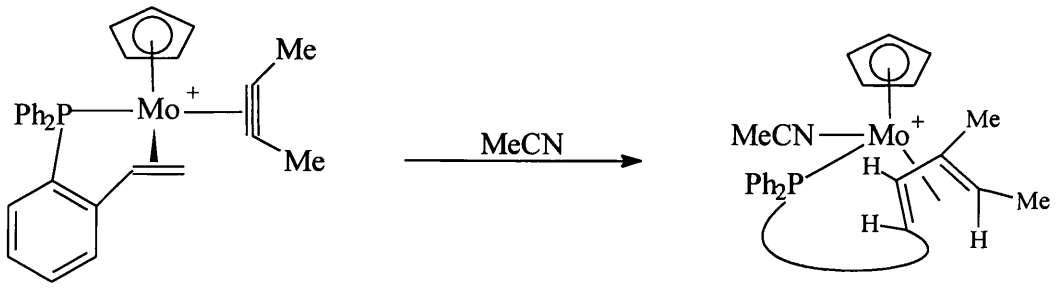

2.7 **2.14**

FIGURE 2.4

Therefore, having shown that in previous studies deprotonation of the cation $[Mo(\eta^2\text{-}PhC_2CH_2Ph)\{P(OMe)_3\}_2(\eta\text{-}C_5H_5)][BF_4]$ **2.1** afforded isomeric η^2(3e)-allenyl complexes, whereas dehydrohalogenation of the bis(alkyne) complexes $[MoBr(\eta^2\text{-}MeC_2R)_2(\eta\text{-}C_5H_5)]$ (**2.3** and **2.4**) resulted in the formation of σ,η^2(3e)-prop-2-ynyl/η^2(4e)-alkyne substituted complexes **2.5** and **2.6** (Figure 2.2), it was obviously interesting and important to extend our studies and examine the deprotonation of an η^2-alkene/η^2(4e)-alkyne substituted molybdenum complex such as $[Mo(\eta^2\text{-}MeC_2Me)(dpps)(\eta\text{-}C_5H_5)][BF_4]$ **2.7**, and discover which of these two different types of product was formed. However, although a reaction did occur on the addition of lithium bis(trimethyl)silyl amide to a thf solution of **2.7**, attempts to isolate a stable product proved unsuccessful. Thus, attention was turned to the phenyl substituted alkyne analogue of **2.7**.

2.2 Synthesis and Reactivity of $[Mo(\eta^2\text{-}MeC_2Ph)(dpps)(\eta\text{-}C_5H_5)][BF_4]$ 1.

The phenyl substituted complex, $[Mo(\eta^2\text{-}MeC_2Ph)(dpps)(\eta\text{-}C_5H_5)][BF_4]$ **1** was formed in high yield (98%) by the reaction of $[Mo(CO)(\eta^2\text{-}MeC_2Ph)_2(\eta\text{-}C_5H_5)][BF_4]$ **2.15** with dpps in refluxing dichloromethane (Figure 2.5). The ^1H and $^{13}C\{^1H\}$ NMR spectra are similar to the analogous complex $[Mo(\eta^2\text{-}MeC_2Me)(dpps)\ (\eta\text{-}C_5H_5)][BF_4]$ **2.7**. The $^{31}P\{^1H\}$ NMR spectrum confirmed the presence of only one isomer. Furthermore, variable temperature NMR studies showed that the methyl singlet at δ1.75 in the ^1H NMR spectrum remains unchanged with temperature, thus indicating that the co-ordinated alkyne of **1** was not undergoing "propeller rotation" about the metal alkyne axis.[19] This contrasts with the MeC≡CMe ligand of **2.7** and is probably a consequence of steric interactions between the phenyl substituent of the alkyne and the bulky dpps ligand.

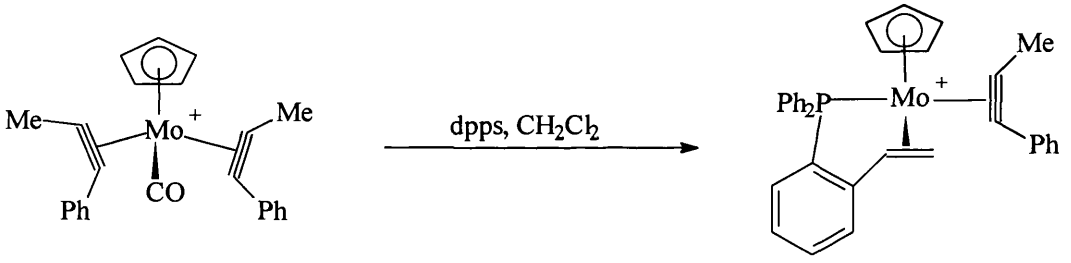

2.15 **1**

FIGURE 2.5.

A crystallographic study established (Figure 2.6, selected bond lengths and angles listed in Table 2.1) that the cation adopts a similar structure to that found in the but-2-yne complex with the C-C vectors of the co-ordinated alkene (dpps) and η^2-MeC_2Ph ligand lying essentially parallel to the Mo-P axis. As anticipated from the NMR data, the molybdenum atom is bonded to an η-C_5H_5 ring and an η^2-alkyne ligand, with the phenyl substituent of the alkyne *trans* to the phosphorus atom in order to minimise steric interactions. In addition, the o-diphenylphosphinostyrene

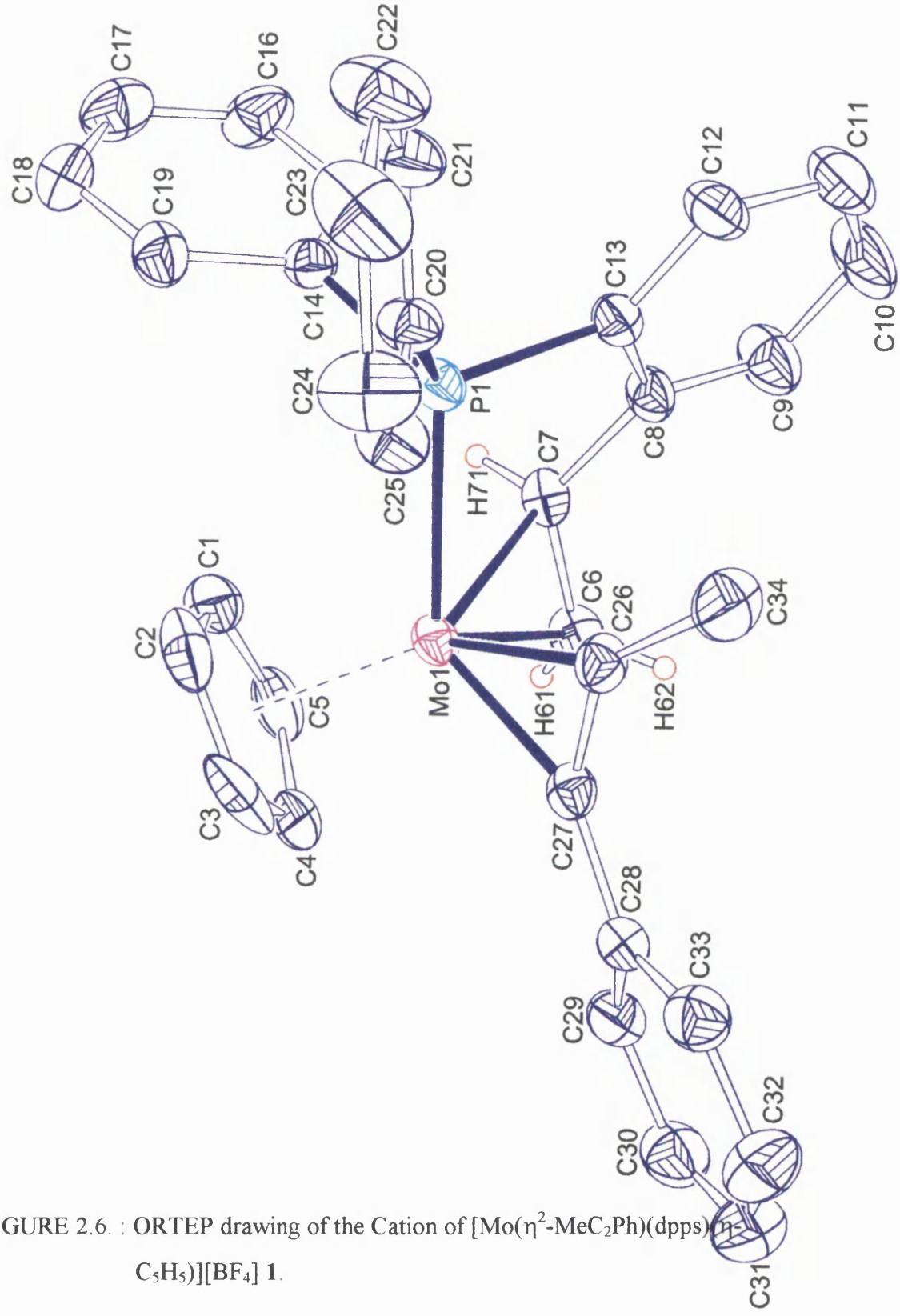

FIGURE 2.6. : ORTEP drawing of the Cation of $[Mo(\eta^2\text{-}MeC_2Ph)(dpps)(\eta\text{-}C_5H_5)][BF_4]$ **1**.

is acting as a bidentate ligand, bonding to the metal through the phosphorus atom and the η^2-alkene substituent. The alkyne shows bending back of its phenyl and methyl substituents in a *cisoid* manner, with the angles C28-C27-C26 139.7(6)° and C34-C26-C27 134.7(6)° being consistent with a four-electron donor alkyne ligand, as are the observed contact carbon resonances of the alkyne (δ 220.5 and δ 229.6) (see section 1.3).[4]

TABLE 2.1 : Selected Bond Lengths (Å) and Angles (°) for [Mo(η^2-MeC_2Ph)(dpps)(η-C_5H_5)][BF_4] **1**.

Atoms	Bond Length	Atoms	Bond Length
P(1)-Mo(1)	2.455(4)	C(7)-Mo(1)	2.278(9)
C(6)-Mo(1)	2.269(9)	C(27)-Mo(1)	2.005(8)
C(26)-Mo(1)	2.026(8)	C(7)-C(8)	1.506(10)
C(7)-C(6)	1.401(10)	C(28)-C(27)	1.447(9)
C(27)-C(26)	1.311(9)	C(34)-C(26)	1.503(10)

Atoms	Angle	Atoms	Angle
C(6)-C(7)-Mo(1)	71.7(5)	C(8)-C(7)-Mo(1)	113.5(5)
C(8)-C(7)-C(6)	124.0(7)	C(9)-C(8)-C(7)	122.9(7)
C(27)-C(26)-Mo(1)	70.2(5)	C(34)-C(26)-Mo(1)	154.6(5)
C(34)-C(26)-C(27)	134.7(6)	C(26)-C(27)-Mo(1)	71.9(5)
C(28)-C(27)-Mo(1)	148.4(5)	C(28)-C(27)-C(26)	139.7(6)

Treatment (-78° → +25°C) of a suspension of **1** in thf with a molar equivalent of Li[$N(SiMe_3)_2$] led, on stirring, to the rapid dissolution of the solid and a colour change from red to yellow. Unlike the product from the analogous reaction with cation **2.7** this product proved easier to handle. Thus, column chromatography of the reaction mixture and elution with a 4:1 hexane: dichloromethane mixture afforded yellow crystals of **2** in excellent yield (80%) (Figure 2.7). Elemental analysis and a mass spectrum of **2** showed that a molecule of HBF_4 had indeed been eliminated. Examination of the ^{1}H NMR spectrum of the neutral product revealed that the resonance due to the methyl group (δ1.75) in **1**, was no longer present, thus indicating that a proton had been abstracted from the

methyl substituent of the η^2(4e)-bonded alkyne. The absence of CH_3 groups was confirmed by a 135° DEPT NMR experiment, which revealed that the complex contained only one quaternary carbon, one CH_2 group (δ37.0) and three CH groups (δ55.7, 77.5 and 77.9). However, resonances characteristic of either a σ,η^2(3e)-prop-2-ynyl[17a] or a η^2(3e)-allenyl ligand[16] were absent from the spectra suggesting that an unexpected reaction had occurred. This was confirmed by a single crystal X-ray diffraction study (Figure 2.8, selected bond lengths and angles are listed in Table 2.2) , which showed that the product of the deprotonation reaction was, surprisingly, a d^4 molybdenum η^5-pentadienyl complex.

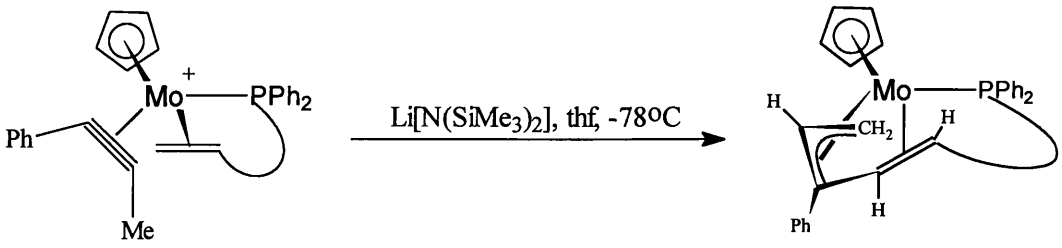

1 **2**

FIGURE 2.7

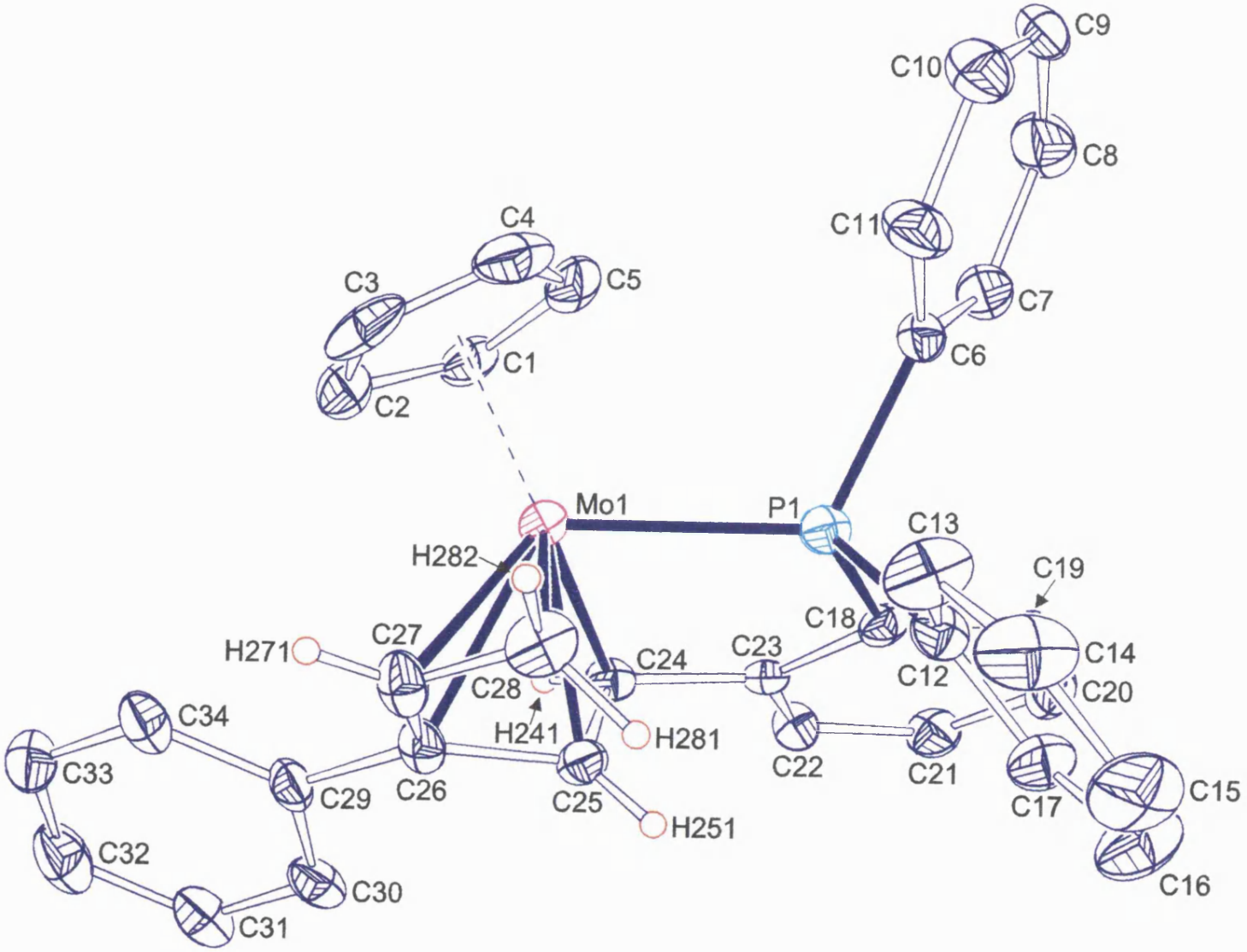

FIGURE 2.8 : ORTEP drawing of **2**

TABLE 2.2 : Selected bond lengths (Å) and Angles (°) for **2**

Atoms	Bond Lengths (Å)	Atoms	Bond Lengths (Å)
Mo1 -P1	2.433(3)	Mo1 -C24	2.235(8)
Mo1 -C25	2.139(8)	Mo1 -C26	2.182(8)
Mo1 -C27	2.231(9)	Mo1 -C28	2.292(8)
C23 -C24	1.502(11)	C24 -C25	1.439(11)
C25 -C26	1.484(11)	C26 -C27	1.403(12)
C26 -C29	1.509(10)	C27 -C28	1.416(13)

Atoms	Angle (°)	Atoms	Torsion Angle
C29-C26-C27	123.3(7)	H251-C25-C26-C29	118.36
C26-C25-C24	113.0(7)	H251-C25-C24-H241	-131.38
C29-C26-C25	122.1(7)	C27-C26-C25-24	121.78
C25-C24-C23	116.4(8)	C29-C26-C27-C28	179.19
C27-C26-C25	114.6(8)	H281-C28-C27-H271	-137.18
C28-C27-C26	119.8(8)	H282-C28-C27-H271	3.67

The pentadienyl ligand adopts the relatively rare η^5-S(sickle) conformation and is wrapped around the molybdenum centre resulting in a dihedral angle of 122° for C27-C26-C25-C24, indicating a twist of the C24-C25 vector out of the C25-C26-C27-C28 plane by 58°. This results in the effective bonding of all five carbon atoms of the pentadienyl ligand and this is reflected in the Mo-C distances which are in the range 2.139(8) - 2.292(8) Å. The C-C bond distances C26-C27 1.403(12) and C27-C28 1.416(13) show slight asymmetry in the bonding of the allylic fragment. However, the most significant feature is the bond length C25-C26 of 1.484(11) Å, which is consistent with there being little interaction between the two π-systems. There is no evidence that this η^5-S conformation rearranges in solution to the more common η^5-U conformation.

There is no precedent for such a carbon-carbon forming reaction and this represents a new synthetic approach to these C_5 ligands, in which interest has grown in recent years.[22] In comparison with their allyl analogues, the chemistry of metal pentadienyl complexes should, in principle, be more interesting because of

the various geometries possible for a pentadienyl ligand bound to a metal centre (Figure 2.9).

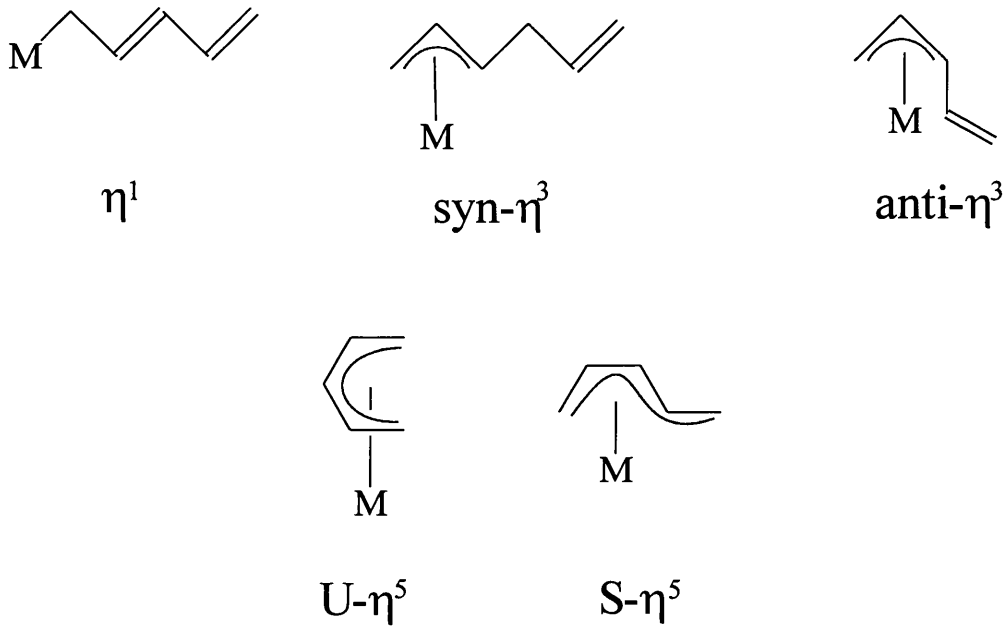

FIGURE 2.9 : Geometries of Pentadienyl Ligand.

The U-η^5 and η^3 bonding modes are the most common and there are numerous examples of both.[23] However, the S-η^5 conformer is rarer and there are only a few examples in the literature which have been structurally characterised by single crystal X-ray diffraction.[24,25,26,27,28] The S-η^5 pentadienyl was first identified in cationic iron tricarbonyl complexes[29] but, in general, these complexes readily rearranged to the more characteristic U conformation, or there were no structural data. More recently, there have been reports of η^5-S-pentadienyl ligands, prepared by a variety of methods (Figure 2.10), which do not rearrange. The first opportunity to examine the geometric characteristics of an η^5-S-pentadienyl emerged in 1985 when Ernst reported that the reaction of $[MCl_4(PEt_3)_2]$, where M = Zr, Nb and Mo **2.16**, reacted with excess 2,4-dimethylpentadienyl anion in thf to form the complexes $[M(PEt_3)(2,4\text{-}C_7H_{11})_2]$.[24] Each complex was thoroughly characterised and it was found that in the Zr and Nb analogues the pentadienyl

ligands adopted a *syn*-eclipsed conformation. In contrast, however, in the molybdenum analogue **2.17** one of the pentadienyl ligands had adopted an unusual S conformation (Figure 2.10).

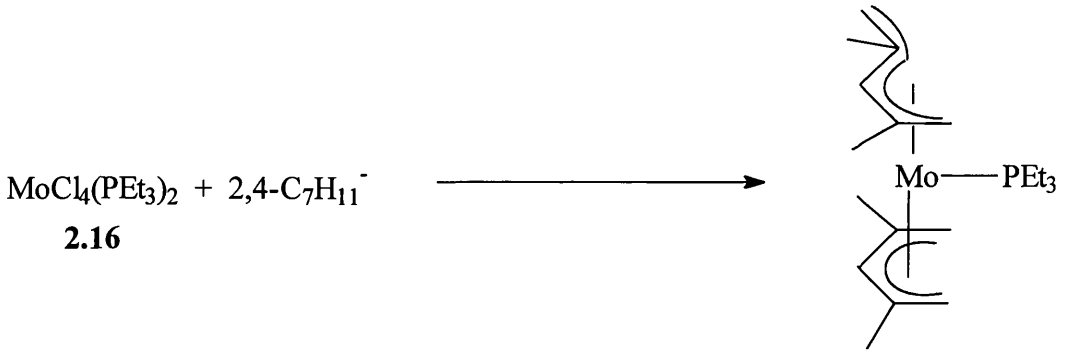

2.17

FIGURE 2.10

Prior to this report, the only other crystallographically determined structure of a similar ligand was of a highly modified pentadienyl, which was prevented from adopting the U configuration by its partial fusion into a lactone ring **2.18** (Figure 2.11).[28]

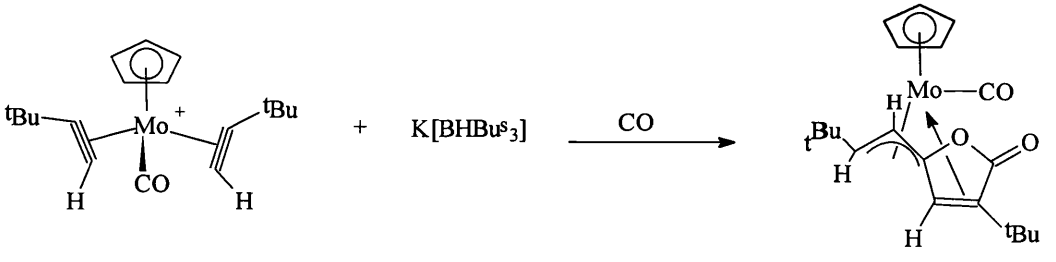

2.18

FIGURE 2.11

Soon after the initial report of **2.17** it was reported that the reaction of 2-ethenyl-2'-ethynyl-1,1'-biphenyl **2.19** with bromotetracarbonyl(ethylidyne) tungsten **2.20** produced an isolatable tungsten pentadienyl **2.21**, which had a sickle

shape and was fully characterised using single crystal X-ray diffraction (Figure 2.12).[25]

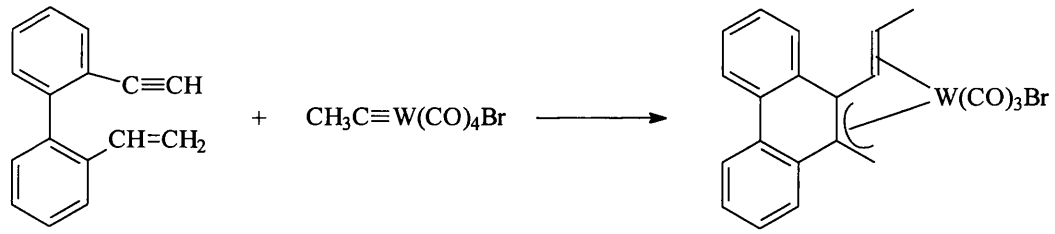

2.19 **2.20** **2.21**

FIGURE 2.12

More recently, Ernst has also reported that in the eighteen-electron half-open chromocene adduct **2.22** (Figure 2.13) the open pentadienyl adopted the unusual η^5-*S* configuration, which was again confirmed by crystallography.[26]

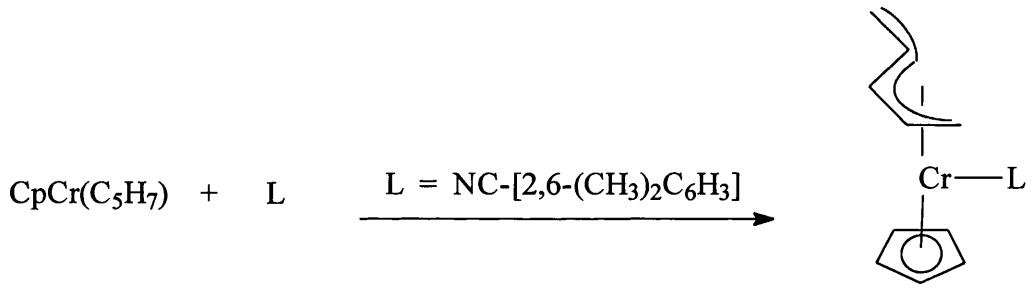

2.22

FIGURE 2.13

Thus far all the examples of S-pentadienyl ligands have been of Group 6 metals, but in 1992 Orpen[27] reported a zirconium complex **2.23** (Figure 2.14) which contained an open C_5R_5 chain which adopted an unusually distorted configuration. The C_5 chain had adopted an S-shape similar to that mentioned previously for complexes **2.17**, **2.18**, **2.21** and **2.22**. However the chain was bound

to the metal centre *via* a σ-bond and two weak unconjugated η^2 interactions with two double bonds.

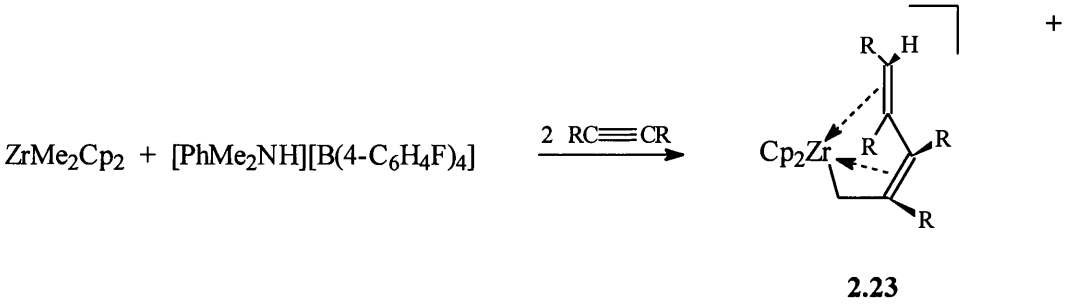

2.23

FIGURE 2.14

TABLE 2.3 : Selected Bond Lengths (Å) and Angles (°) of Complexes **2.17, 2.21, 2, 2.22** and **2.23**.

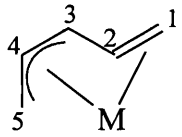

	2.21 (W)	**2.17** (Mo)	**2**	**2.22** (Cr)	**2.23** (Zr)
C1-C2	1.377(7)	1.366(11)	1.439(11)	1.389(7)	1.356(9)
C2-C3	1.475(7)	1.481(11)	1.484(11)	1.437(7)	1.492(9)
C3-C4	1.438(8)	1.327(11)	1.403(12)	1.412(7)	1.387(9)
C4-C5	1.394(9)	1.380(11)	1.416(13)	1.390(7)	1.443(9)
M-C1	2.530(8)	2.285(19)	2.235(8)	2.228(5)	2.759(7)
M-C2	2.275(7)	2.164(14)	2.139(8)	2.080(5)	2.602(7)
M-C3	2.317(7)	2.208(16)	2.182(8)	2.084(5)	2.712(6)
M-C4	2.369(6)	2.390(15)	2.231(9)	2.159(5)	2.705(6)
M-C5	2.330(6)	2.349(16)	2.292(8)	2.246(5)	2.315(7)
Torsion angle C1-C2-C3-C4 (°)	130	128	122.3	123.4(6)	-
Twist out of plane of vector C1-C2	50	52	58	56.6	-

There are only limited structural data available on η^5-S pentadienyl complexes but a comparison of the structural parameters of complexes **2.17, 2.21, 2, 2.22** and **2.23** (Table 2.3) revealed that the bonding in the majority of η^5-S-pentadienyl ligands can best be described in terms of a combination of vinyl and allyl units bonded to the transition metal and electronically isolated from one another by substantial rotation about the single bond linking them together. The comparison also showed that, in general, the sickle "handle" (C1-C2) vector is twisted by *ca.* 50°out of the C2-C3-C4-C5 plane, *via* a rotation about C2-C3. In complexes **2.17**, **2.21** and **2** the bond lengths of the allyl carbons, C3-C4 and C4-C5, are similar and shorter than the single bond (C2-C3). This differs from complex **2.22** with the short-long-short alternation of bond lengths, which is more indicative of a resonance structure **A** (Figure 2.15) with a contribution from hybrid **B**. However, it may also be possible that the simultaneous participation of the two vinyl- allyl hybrids (**C** and **D**) could also lead to the observed pattern of bond lengths. The zirconium complex **2.23**, however, cannot be described as an allyl-vinyl and is best represented as a σ-bond with two unconjugated η^2 carbon-carbon double bond interactions (Figure 2.14). Thus, by comparison, complex **2** is best described as an η^5-S-pentadienyl containing electronically separate vinyl and allyl units

A **B** **C** **D**

FIGURE 2.15

The coupling of an η^2(4e) alkyne and η^2-alkene represents a new synthetic pathway to these unusual C_5 ligands and in considering how the η^5-S-pentadienyl

complex **2** is formed, it is reasonable to assume that the first step involves the loss of a proton from the co-ordinated alkyne methyl group resulting in the formation of the η^2(3e)-allenyl substituted complex **A** (Figure 2.16). Because **A** contains a metal to carbon double bond and a co-ordinated alkene with a relative *cis*-configuration it might, at first sight, be assumed that these ligands would react to form a metallocyclobutane as in the metathesis reaction.[30] Such a step is, however, unlikely because the alkene ligand is not free to rotate and cannot therefore be orientated parallel to the metal carbene bond for the formation of a metallocyclobutane. Parallel orientation of the alkene is normally a geometrical pre-requisite for this type of coupling, although recently, evidence was put forward for the perpendicular approach of an alkene to an iridium carbene bond. However, this type of reaction was facilitated by the electron withdrawing substituents on the alkene.[31] Therefore, it is proposed that **A** (Figure 2.16) must first rearrange into the σ,η^2(3e)-prop-2-ynyl/η^2-alkene substituted species **B** before transforming into **C** *via* an insertion reaction. In order to convert **C** (Figure 2.16) into the isolated product **2** it is necessary for the co-ordinated allene to dissociate from the metal centre so that following C-C bond rotation the *cis*-coplanar geometry needed for a β-hydrogen elimination reaction **D** → **E** (Figure 2.16) can be attained. Insertion of the η^2-co-ordinated allene into the Mo-H bond, i.e. **E** → **F** (Figure 2.16), followed by rotation about the C-C bond **F** → **G** then provides access to **2** with the observed stereochemistry.

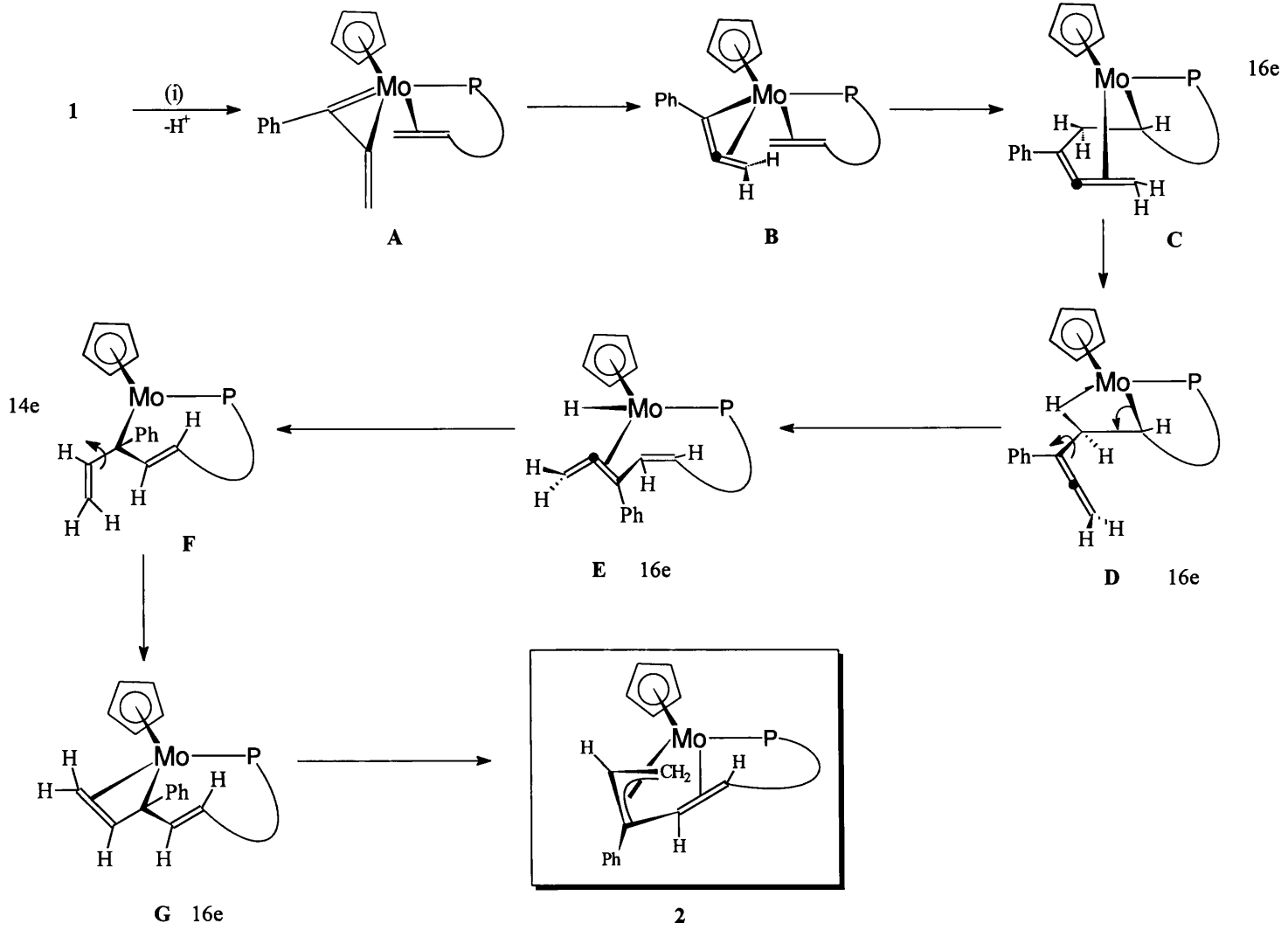

FIGURE 2.16 : (i) $Li[N(SiMe_3)_2]$, thf, -78°C → 25°C.

2.3 Reactivity of [Mo{η^2,η^3-(5e)-S-$CH_2CHC(Ph)CH{=}CH$-*o*-$C_6H_4PPh_2$}(η-C_5H_5)] 2.

Having elucidated the precise molecular structure of the electron-rich pentadienyl complex **2** the reactivity of this complex towards proton sources was examined. An Extended Hückel Molecular Orbital (EHMO) calculation based on the bond parameters derived from the X-ray crystallographic study of complex **2** established the electron density distribution listed in Table 2.4. This indicated that charge controlled protonation should be directed to the terminal carbon, C1, (C28 crystallographic numbering) of the pentadienyl chain, which should result in the formation of a co-ordinatively unsaturated cationic *trans*-η^4-1,3-diene complex. In order to stabilise such a product it was expected that an additional two-electron donor ligand, such as carbon monoxide, would be required.

TABLE 2.4. : Relative Charge Distribution of the Pentadienyl Chain of Complex **2**.

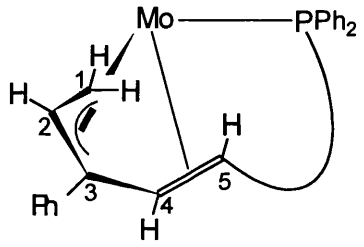

Mo	C1	C2	C3	C4	C5
0.197	-0.266	0.013	-0.096	-0.134	-0.168

Treatment (-78°C → +25°C) of a dichloromethane solution of **2** with a molar equivalent of $HBF_4.Et_2O$ in the presence of a stream of carbon monoxide led to a rapid change in colour from yellow to orange. Addition of diethylether afforded orange crystals of the cationic complex **3** (Figure 2.17). Surprisingly, the IR spectrum of **3** showed no evidence for the presence of a co-ordinated carbon monoxide ligand and it was also discovered that **3** could be formed in equally excellent yield (77%) without the presence of carbon monoxide. Examination of the ambient temperature ^1H NMR spectrum of **3** showed a high field broad singlet

resonance at δ -2.0 attributable to three hydrogens, suggesting the presence of an agostic methyl group, which in solution at room temperature was undergoing "in-place rotation". This was supported by the observation that at low temperature (-80°C) the high field signal at δ -2.0 was replaced by three resonances at δ 2.33, -1.13 and -7.56, each integrating for one hydrogen. Also, when it was ascertained that **2** could be reformed in excellent yield by reacting **3** with one equivalent of the base $Li[N(SiMe_3)_2]$ it became apparent that the product of the protonation reaction **2** → **3** derived stability from an agostic Mo (μ-H)C interaction.[32]

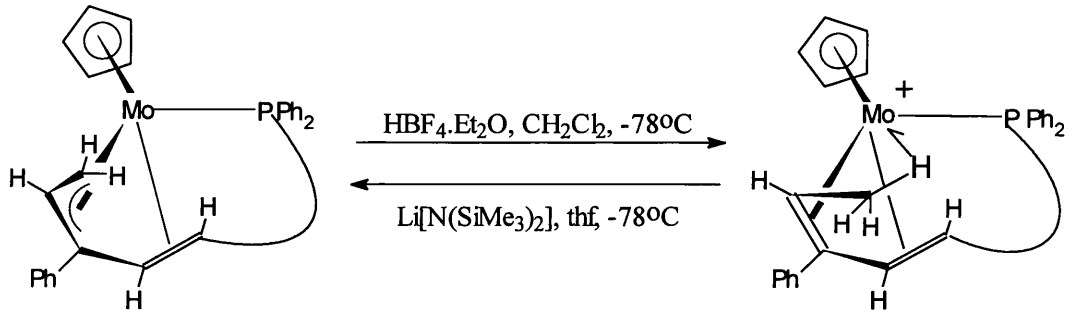

2 **3**

FIGURE 2.17

The reactivity of the pentadienyl complex **2** is similar to that exhibited by other open pentadienyl ligands,[33,34,35] where protonation usually occurs by the open edge of the ligand and then several fluxional processes occur equilibrating the terminal hydrogens of the ligand. Originally, the protonated compounds ground states were formulated as metal-hydrides[33,36] (**A**, Figure 2.18) but, recently, a second ground state in which the complex contains an agostic interaction,[34,35,37] has been accepted (**B**, Figure 2.18). In this second ground state a C-H bond serves as a non-classical donor ligand through the sharing of its σ electrons with the metal and, hence, the formation of a two-electron, three-centre M--H--C. Complexes which contain agostic CH bonds are of interest as they may act as important model systems for C-H activation.[38]

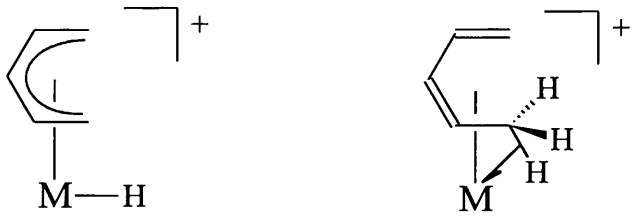

A **B**

FIGURE 2.18

The complexes $[Mn\{(Me_2PCH_2)_3CMe\}(\eta^5\text{-}C_5H_7)]$[33] **2.24** (Figure 2.19) and $[Re(PMe_2Ph)_3(\eta^5\text{-}2,4\text{-dimethylpentadienyl})]$[33] **2.26** (Figure 2.20) both react with acid to generate protonated products **2.25** and **2.27**, respectively, but with different ground states. In the manganese product **2.25** the hydrogen resides in an agostic position, whilst the protonated rhenium complex **2.27** contains a normal (terminal) metal hydride with the H^- ligand lying beneath the "back bone" of the dimethylpentadienyl ligand.

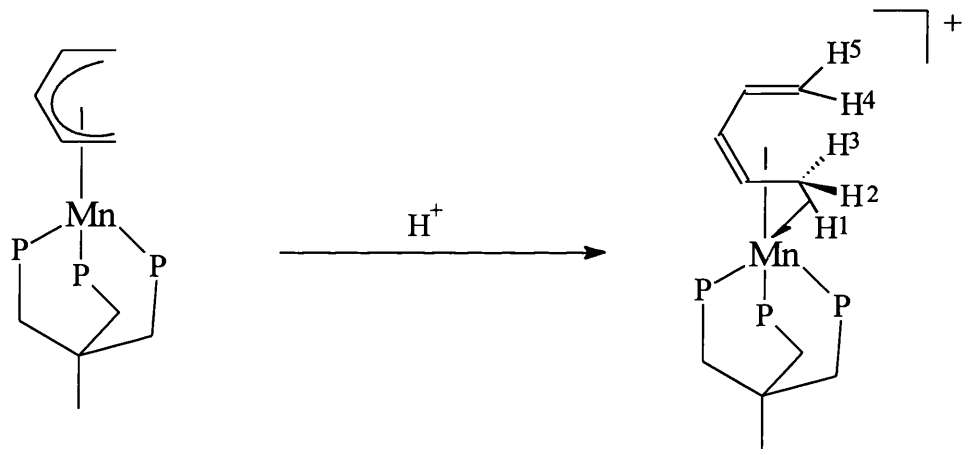

2.24 **2.25**

FIGURE 2.19

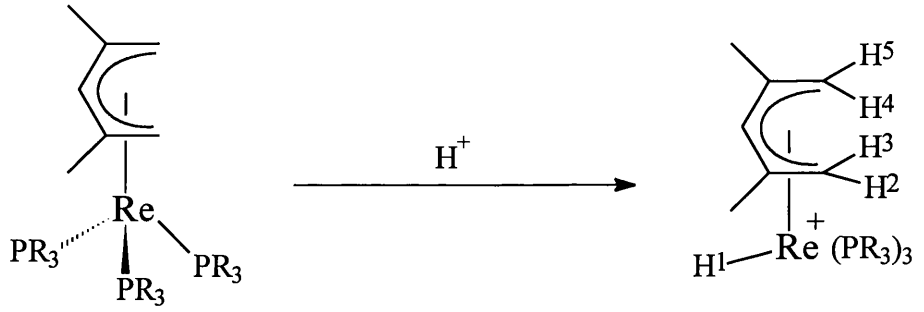

2.26 **2.27**

FIGURE 2.20

Both complexes are fluxional in solution such that H^1-H^5 appear as one signal at room temperature but variable temperature NMR studies show that these fluxional processes can be frozen out at *ca.* -80°C. A common mechanism for H exchange can be postulated for these, and similar complexes, involving a hydride (**C**), an agostic (**B**) and an unsaturated $16e^-$ (**A**) species in equilibrium (Figure 2.21).[35] In species **A** the CH_3 is free to rotate resulting in the equivalence of all five hydrogens.

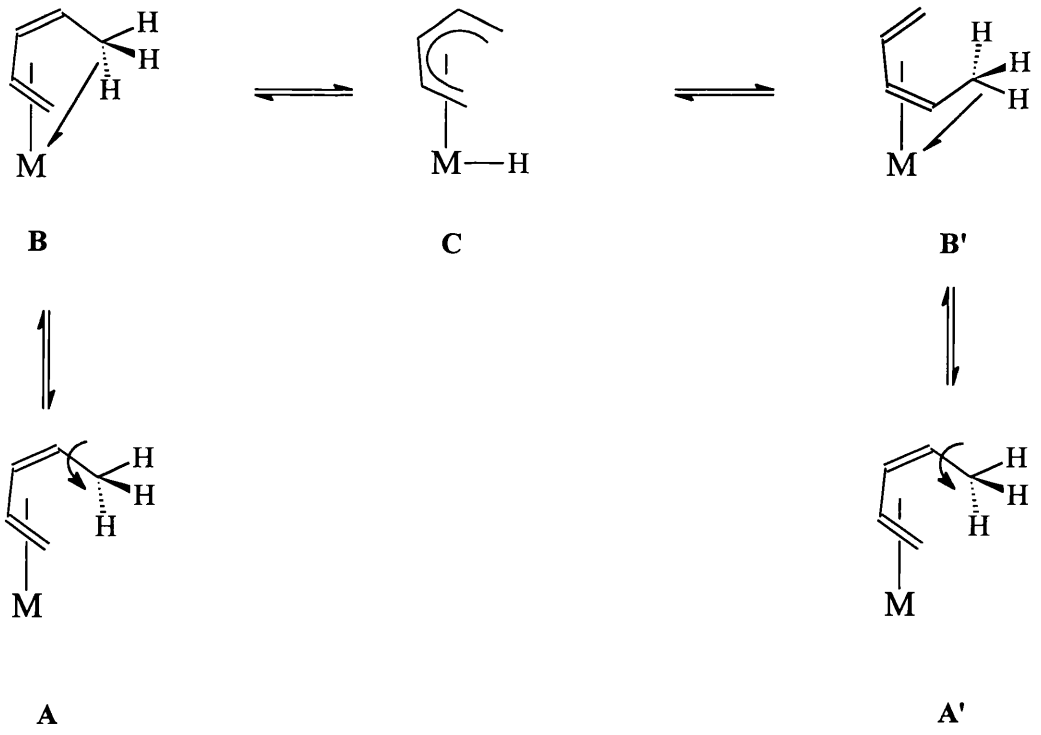

B **C** **B'**

A **A'**

FIGURE 2.21

A single crystal X-ray diffraction study on the cationic complex **3** established the solid state structure (Figure 2.22, selected bond lengths and angles are listed in Table 2.5). and the presence of an agostic methyl group was confirmed by the bond parameters : Mo-H281 1.915(48)Å, Mo-C28 2.437(6)Å, C28-Mo-H281 24.3(13)°. A structural feature of special interest involved the carbon atoms C24, C25, C26 and C27, which adopt a twisted, nonplanar arrangement with a dihedral angle of 123° very similar to that observed (122°) in the parent complex **2**. The central carbon atom C25 and C26 are slightly closer to the molybdenum centre [Mo-C25 2.151(7), Mo-C26 2.232(7)Å] than the terminal carbons C24 and C27 [Mo-C24 2.290(7), Mo-C27 2.246(5)Å].

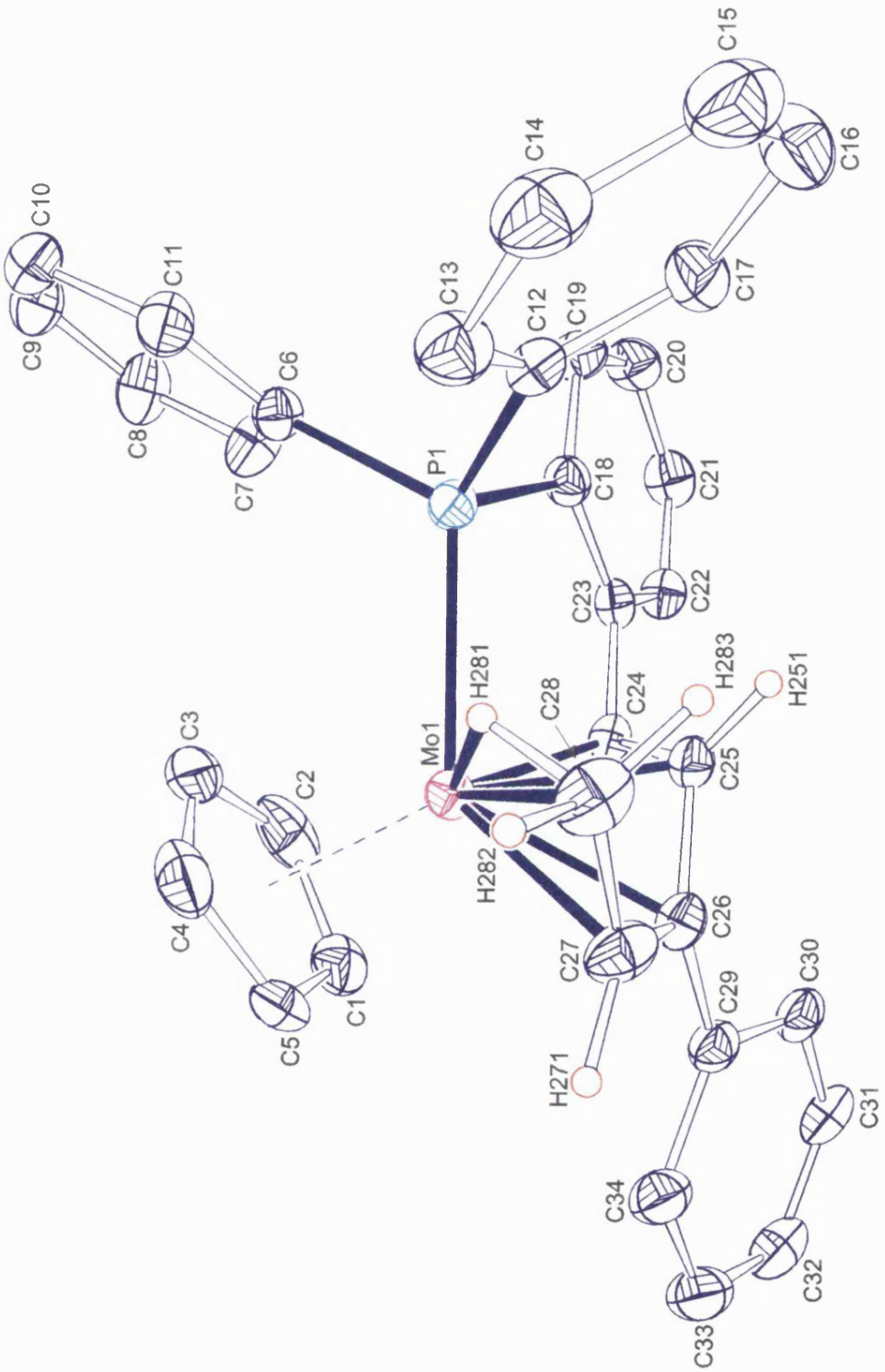

FIGURE 2.22 : ORTEP Drawing of the cation of **3**.

TABLE 2.5 : Selected Bond Lengths (Å) and Torsion Angles (°) of **3**.

Atoms	Bond Length	Atoms	Bond Length
Mo-P1	2.505(4)	Mo-C24	2.290(7)
Mo-H281	1.915(48)	Mo-C24	2.290(7)
Mo-C28	2.437(6)	C28-C27	1.496(11)
Mo-C27	2.246(5)	C27-C26	1.403(9)
Mo-C26	2.232(7)	C26-C25	1.442(8)
Mo-C25	2.151(7)	C25-C24	1.448(7)

Atoms	Angle	Atoms	Angle
C28-C27-C26-C25	-9.36	C24-C25-C26-C27	-123.04
H241-C24-C25-H251	142.25	H282-C28-C27-H271	-105.94

Therefore, it is proposed that complex **3** has an agostic ground state structure in which the pentadienyl ligand is unsymmetrical and in a twisted *transoidal* conformation. The three terminal hydrogens are equivalent in solution at room temperature due to the fluxional process[35,34] involving breaking of the agostic interaction (**A→C**), followed by rotation of the methyl group (**B**) and finally, reformation of the agostic M-H-C bond (**B→A**) (Figure 2.23). Variable temperature ^{1}H NMR studies showed that this process was arrested at -80°C resulting in the hydrogens being non-equivalent at δ 2.33, δ -1.13 and δ -7.56.

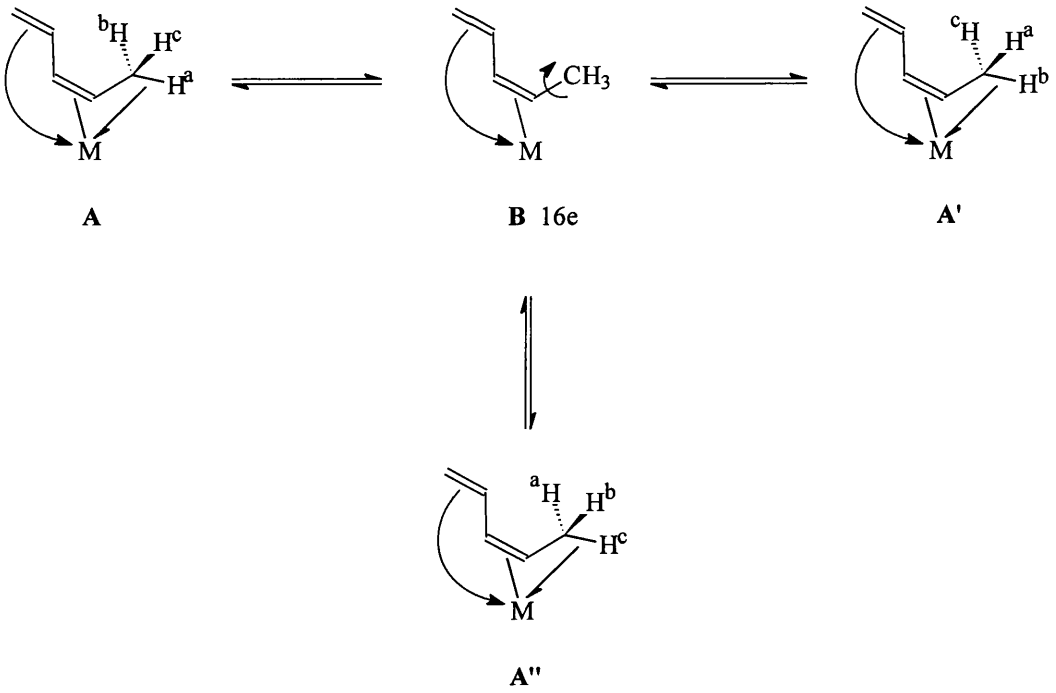

FIGURE 2.23

Although, there have been numerous monomeric, transition metal complexes containing conjugated dienes,[39] in the vast majority the diene is attached to the metal centre in an η^4-*cis* manner.[40] The first examples of η^4-*trans* diene co-ordination to a single metal centre, which were structurally characterised by single crystal, X-ray crystallography, occurred with the early transition metals zirconium[41] **2.28** and niobium[42] **2.29** (Figure 2.24) in which the L_nM-diene moiety may be viewed as being predominantly metallacyclic in character.

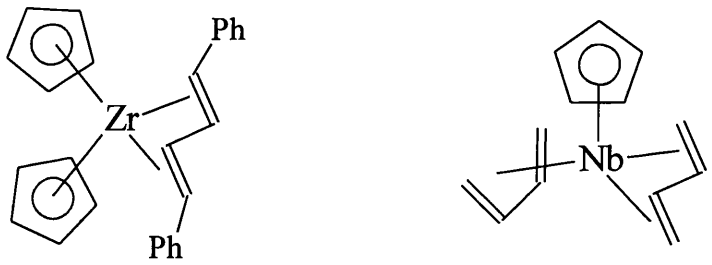

2.28 **2.29**

FIGURE 2.24

More recently, there have been other structurally characterised examples of *trans*-dienes with group 6 metals[28,43] and ruthenium.[44] Legdzins[45] reported in 1991 that the reduction of $[MoI_2(NO)(\eta\text{-}C_5Me_5)]_2$ with sodium amalgam in the presence of an isomeric mixture of (*E*)-1,3-pentadiene afforded the complex of $[Mo(NO)(\eta^4\text{-}$*trans*-1,3-pentadiene$)(\eta\text{-}C_5Me_5)]$ **2.30** (Figure 2.25). The most significant feature of the solid state structure was the fact that the buta-1,3-diene was *transoidal* with the methyl substituent pointing away from the cyclopentadienyl ring.

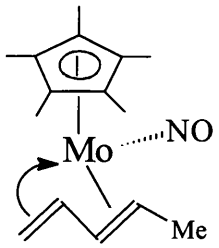

2.30

FIGURE 2.25

Also, in 1991, Ernst[46] reported that the reduction of $[Ru(acac)_3]$ (acac = acetyl acetonate) with zinc in the presence of 1,3-dienes led to the formation of $[Ru(\eta^4\text{-}$*trans*-diene$)(acac)_2]$ complexes (diene = 2,3-dimethyl-1,3-butadiene, 2,4-hexadiene and 2,4-dimethyl-1,3-pentadiene), the 2,4-dimethyl-1,3-pentadiene **2.31** (Figure 2.26) analogue being structurally characterised by X-ray crystallography.

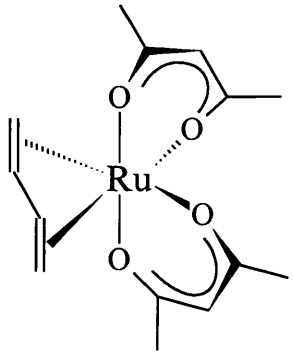

2.31

FIGURE 2.26

This geometric preference of most transition metal fragments for the *cis* conformer is in contrast to the free C_4H_6 molecule, which can exist in the two possible planar conformations illustrated in Figure 2.27, but the *trans* conformer is markedly favoured.[47]

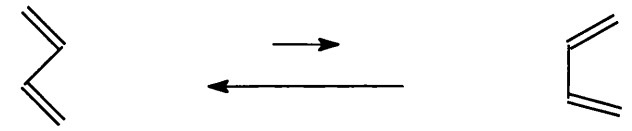

trans ***cis***

FIGURE 2.27

Interestingly, a comparison of the structural parameters (Table 2.6) of [Mo(NO)(η^4-*trans*-(E)-1,3-pentadiene)(η-C_5Me_5)] **2.30**, [Mo(NO)(η^4-*trans*-2,3-dimethylbutadiene)(η-C_5H_5)][48] **2.32** and [Zr(η^4-*trans*-PhCH=CH.CH=CHPh)(η-$C_5H_5)_2$][41] **2.28** and complex **3** reveal that the diene in complex **3** is in the rare twisted *trans* configuration with the carbon-carbon bond lengths C1-C2, C2-C3 and C3-C4 (crystallographic numbering C26-C27, C25-C26 and C24-C25, respectively) being approximately equivalent This is consistent with the current bonding rationale suggested by Legdzins for [Mo(NO)(η^4-*trans*-2,3-dimethylbutadiene)(η-C_5H_5)] **2.32** and [Mo(NO)(η^4-*trans*-(E)-1,3-pentadiene)(η-C_5Me_5)] **2.30** complexes but is in marked contrast to the η^4-*trans*-1,3-complex

[Zr(η^4-*trans*-PhCH=CH.CH=CHPh)(η-C_5H_5)$_2$] **2.28**, which exhibits short-long-short carbon-carbon bond lengths characteristic of a diene. It is reasonable to suggest, therefore, that **3** is a cationic η^4-*trans*-1,3-diene complex (Figure 2.17). In all the reported cases of *trans* diene co-ordination, there is a marked deviation from planarity, with a torsion angle for C1-C2-C3-C4 of *ca.* 120°. Furthermore, as in the [Mo(NO)(*trans*-diene)(η-C_5R_5)] complexes, **3** shows no evidence of isomerisation of the bound diene to the *cis* form.

TABLE 2.6 : Comparison of Structural Parameters of **2.28**, **2.30**, **2.32** and Complex **3**.

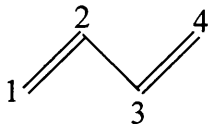

Complex (M)	φ **C1-C2-C3-C4** (°)	**C1-C2** (Å)	**C2-C3** (Å)	**C3-C4** (Å)
3 (Mo)	123	1.403(9)	1.442(8)	1.448(7)
2.30 (Mo)	123.9	1.407(4)	1.387(4)	1.408(4)
2.32 (Mo)	124.8	1.401(4)	1.408(4)	1.418(4)
2.28 (Zr)	126.1	1.40	1.48	1.40

In contrast, when a proton source containing a strongly co-ordinating anion, e.g. trifluoroacetic acid, is used the agostic interaction observed in complex **3** is displaced and the *trans* diene rearranges to the more common *cis* diene. Addition of excess trifluoroacetic acid at -78°C, to a yellow solution of **2** results in a dark green solution. The neutral, green product can be chromatographed and eluted with a 2:1 hexane/ dichloromethane mixture to afford the green, *cis* diene complex [Mo{OC(O)CF_3}{η^2,η^2-CH_3CH=C(Ph)CH=CH-o-$C_6H_4PPh_2$}(η-C_5H_5)] **4** (Figure 2.28) in excellent yield (80%). There is no high field signal due to an agostic methyl but instead a doublet at δ 1.46 is observed, which, in a H-H COSY NMR experiment, is clearly coupled to H^a [δ 3.99, J(H^aMe) 6.9Hz]. Low temperature NMR studies showed the molecule was not undergoing any rotational processes but

did serve to resolve the splitting of the resonances due to H^a and H^c. At room temperature these resonances were broad but at -50°C, H^a and H^c were a quartet of doublet and a doublet of doublets, respectively. Further 2D correlation NMR studies showed that the resonances at δ 60.1, 64.3 and 113.1 in the $^{13}C\{^1H\}$ NMR spectrum, were attributable to carbons C_1, C_4 and C_3, respectively. The presence of a trifluoroacetate group was evident from the $^{13}C\{^1H\}$ {δ 163.1 quartet, CCF_3, $^2J(CF)$ 24 Hz and δ 115.3 quartet, CF_3, $^1J(CF)$ 294 Hz]}, ^{19}F (δ -74.5) NMR spectra and mass spectrum [680 (M^+), 565 (M^+-CF_3CO_2)].

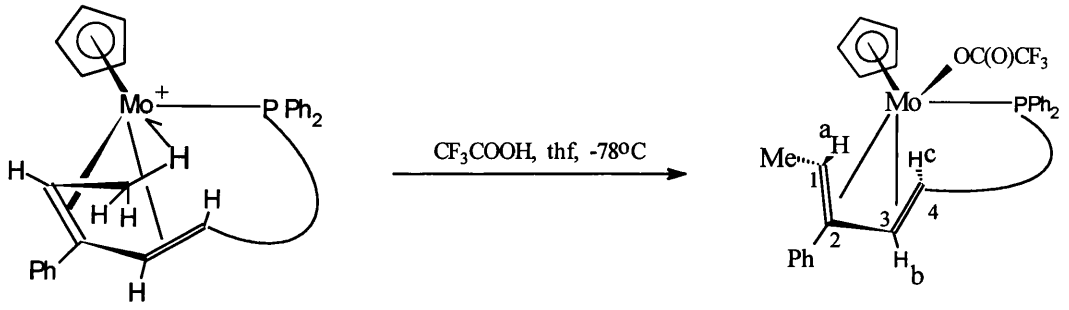

3 4

FIGURE 2.28

2.4 Reactivity of $Mo\{\eta^2,\eta^2(\mu_{Mo,C}\text{-}H)\text{-}CH_3CHC(Ph)CH{=}CH\text{-}o\text{-}C_6H_4PPh_2\}(\eta\text{-}C_5H_5)][BF_4]$ 3.

As previously ascertained the agostic methyl interaction in complex **3** could not be displaced by carbon monoxide but could be in the presence of the co-ordinating anion trifluoroactetate. Against this background the reactivity of $[Mo\{\eta^2,\eta^2(\mu_{Mo,C}\text{-}H)\text{-}CH_3CHC(Ph)CH{=}CH\text{-}o\text{-}C_6H_4PPh_2\}(\eta\text{-}C_5H_5)][BF_4]$ **3** with acetonitrile and lithium halides was examined.

Addition of acetonitrile to a dark orange solution of **3** at room temperature results in the formation of the dark purple complex $[Mo(NCMe)\{\eta^2,\eta^2\text{-}CH_3CH{=}C(Ph)\ CH{=}CH\text{-}o\text{-}C_6H_4PPh_2\}(\eta\text{-}C_5H_5)][BF_4]$ **5** (Yield 80%) after stirring at room temperature for twelve hours (Figure 2.29). In a similar manner to **4** the ^1H NMR spectrum was better resolved at low temperature (-60°C) with a doublet of doublets [δ 3.27 H^c, $J(H^cH^b)$ 5.9 Hz, $J(H^cP)$ 10.2 Hz], doublet of quartet [δ 3.54, H^a, $J(H^aMe)$ 7.0 Hz, $J(H^aH^b)$ 1.9 Hz], and a doublet of doublet of doublets [δ 5.78 H^b, $J(H^bH^c)$ 6.0 Hz, $J(H^bP)$ 8.0 Hz, $J(H^bH^a)$ 2.2 Hz]. The high field, agostic methyl signal was no longer present but was replaced by a doublet at δ 1.47 [$J(MeH^a)$ 7.0Hz]. The presence of a co-ordinated acetonitrile was confirmed by resonances in the ^1H NMR spectrum [δ 1.56, s, 3H, *Me*CN], the $^{13}C\{^1H\}$ NMR spectrum [δ 3.5, broad singlet, *Me*CN, and δ 99.9, singlet, *C*N] and mass spectrum [(M^+) 607, (M^+-MeCN) 567, (BF_4^-) 87].

In a similar fashion, addition of lithium iodide also results in the displacement of the agostic methyl and co-ordination of a one-electron σ donor. Addition of lithium iodide at room temperature to a solution of **3** results in an immediate colour change of orange to dark green, which after column chromatography, afforded the green complex $[MoI\{\eta^2,\eta^2\text{-}CH_3CH{=}C(Ph)CH{=}CH\text{-}o\text{-}C_6H_4PPh_2\}(\eta\text{-}C_5H_5)]$ **6** (Figure 2.29) in good yield (70%). The ^1H NMR spectrum was similar to that observed for **4** and **5** with a doublet at δ 1.42 [methyl group, $J(MeH^a)$ 7.3 Hz], a doublet of doublet of doublet at δ 6.37 [H^b, $J(H^bH^c)$ 7.8

Hz, $J(H^bP)$ 5.4 Hz, $J(H^bH^a)$ 2.0 Hz] and two broad signals at δ 2.99 [H^c] and δ 4.12 [H^a], with the mass spectrum confirming the presence of the iodide [(M^+) 694, (M^+-I) 565]. The diene carbons resonated at δ 54.8, 63.2, 89.5 and 109.4 and, after C-H NMR correlation studies, the signals were assigned to C_1, C_4, C_2 and C_3, respectively (Figure 2.29). This reaction worked equally well with lithium bromide and lithium chloride to afford the green complexes [MoBr{η^2,η^2-CH_3CH=C(Ph)CH=CH-o-$C_6H_4PPh_2$}(η-C_5H_5)] **7** and [MoCl{η^2,η^2-CH_3CH=C(Ph)CH=CH-o-$C_6H_4PPh_2$}(η-C_5H_5)] **8**, respectively (Figure 2.29) in good yield.

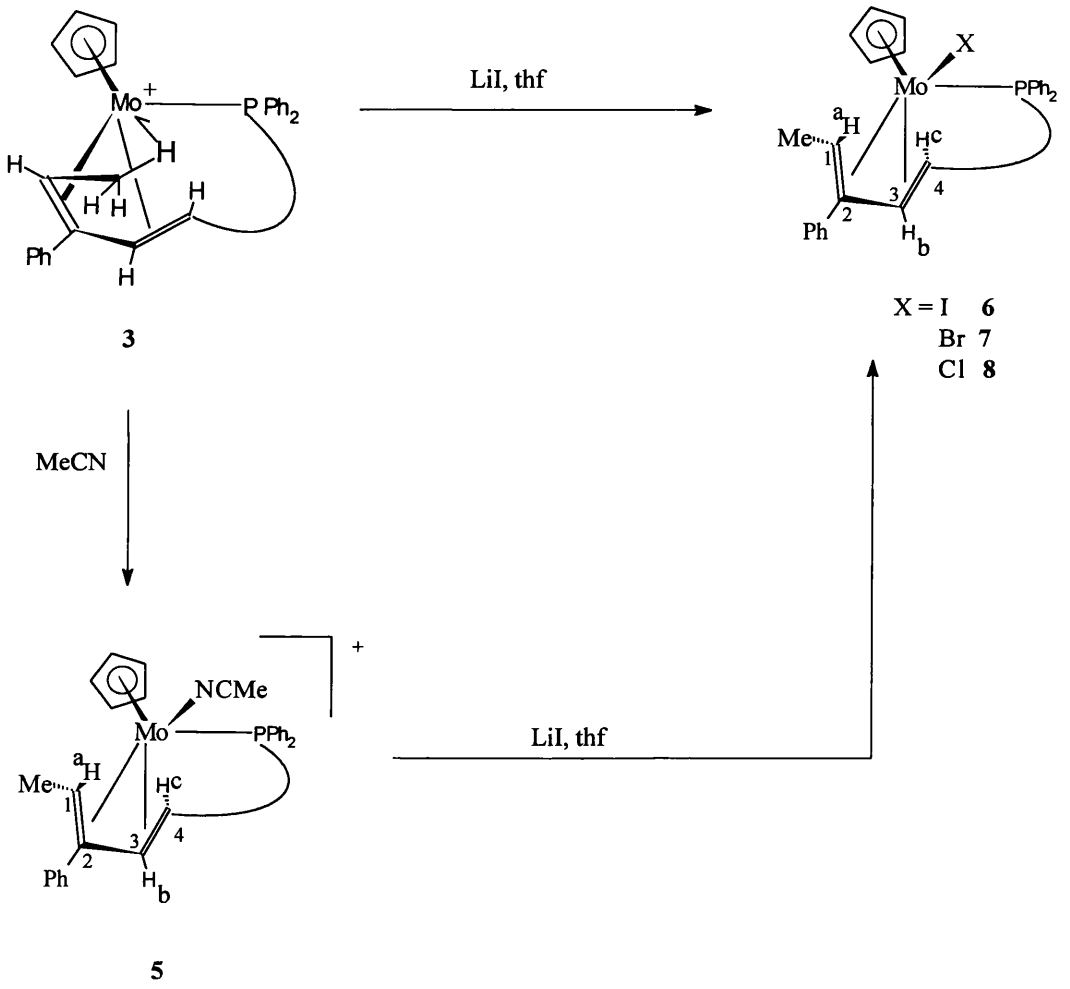

FIGURE 2.29

Alternatively complex **6** could be formed in equally good yield from complex $[Mo(NCMe)\{\eta^2,\eta^2\text{-}CH_3CH{=}C(Ph)CH{=}CH\text{-}o\text{-}C_6H_4PPh_2\}(\eta\text{-}C_5H_5)]$ **5** (Figure 2.29) by the addition of one equivalent of lithium iodide at room temperature, followed by column chromatography work-up. The product, **6**, was confirmed by ^1H and $^{31}P\{^1H\}$ NMR spectroscopy.

Although it was clearly evident that the agostic interaction had been displaced in these reactions, the conformation of the diene could not be conclusively determined from the NMR data alone and, therefore, a single crystal X-ray diffraction study was undertaken with $[MoI\{\eta^2,\eta^2\text{-}CH_3CH{=}C(Ph)CH{=}CH\text{-}o\text{-}C_6H_4PPh_2\}(\eta\text{-}C_5H_5)]$ **6** (Figure 2.30, selected bond lengths and angles are listed in Table 2.7). This confirmed the orientation of the diene moiety as *cis*, with a torsion angle for C27-C26-C25-C24 (crystallographic numbering) of *ca.* 0°. Interestingly, the C26-C25 (1.393 Å) bond distance is significantly shorter than the C27-C26 (1.439 Å) and C25-C24 (1.448 Å) bond distances, which is opposite to the expected short-long-short alternation usually observed in free *cis*-butadiene.

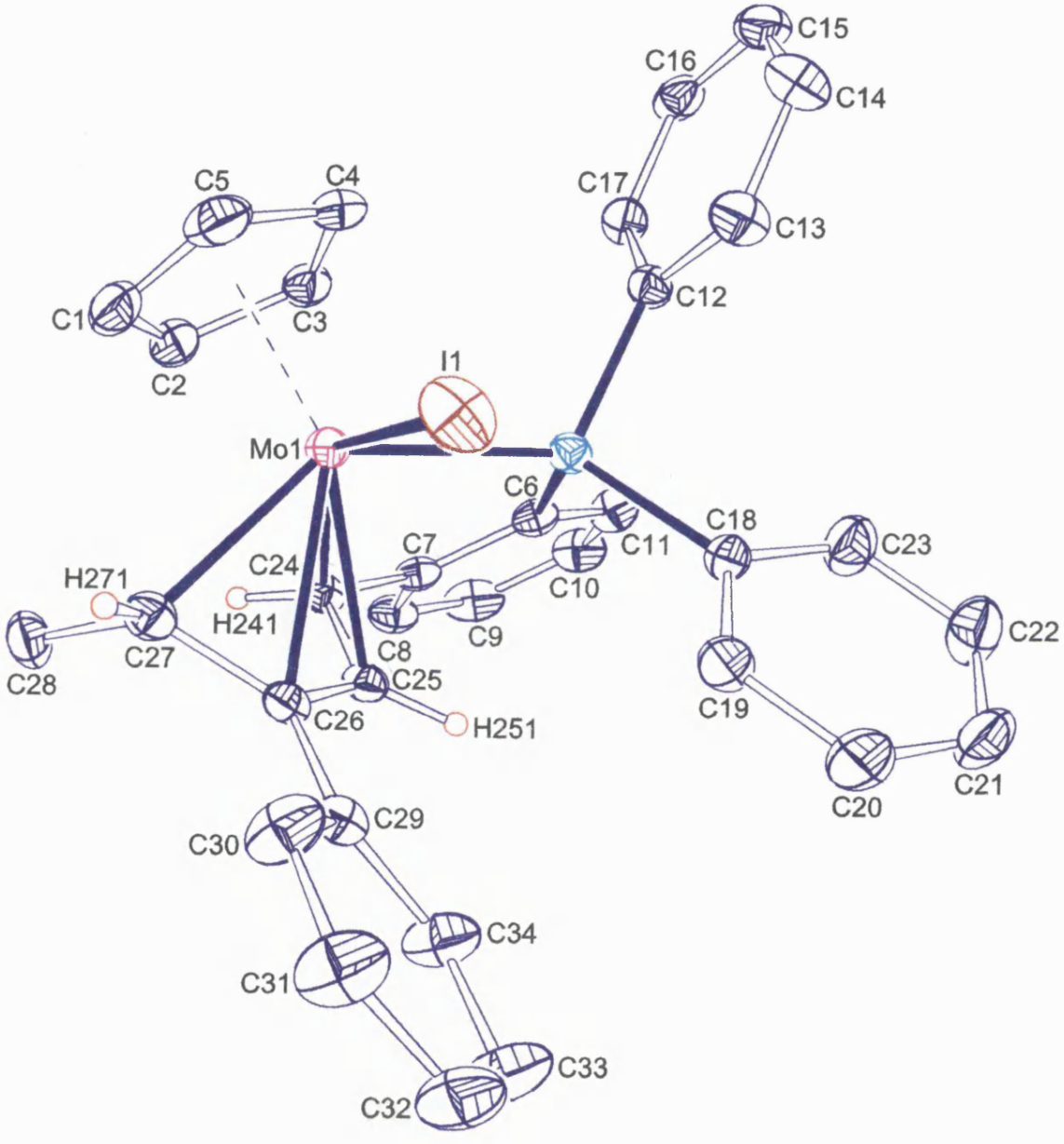

FIGURE 2.30 : ORTEP drawing of **6**

TABLE 2.7 : Selected Bond Lengths (Å) and Angles (°) for **6**

Atoms	Bond Length	Atoms	Bond Lengths
Mo1 -P1	2.490 (3)	Mo1 -I	2.845 (4)
Mo1 -C24	2.249 (6)	Mo1 -C25	2.341 (6)
Mo1 -C26	2.408 (6)	Mo1 -C27	2.291 (7)
C7 -C24	1.479 (7)	C24 -C25	1.448 (7)
C25 -C26	1.393 (7)	C26 -C27	1.439 (7)
C26 -C29	1.499 (7)	C27 -C28	1.521 (9)

Atoms	Angle	Atoms	Torsion Angle
P1-Mo1-I	88.1	H241-C24-C25-H251	134.90 (4.5)
C7-C24-C25	115.3(5)	C24-C25-C25-C27	-1.42 (0.7)
C24-C25-C26	123.2(5)	C28-C27-C26-C25	64.85(0.61)
C25-C26-C27	118.0(5)	C29-C26-C25-H251	-8.73(3.47)
C28-C27-C26	121.3(5)		

Conjugated dienes have delocalised π molecular orbitals (MO's) of differing energies and symmetries and, hence, offer a variety of combinations to interact with the metal atomic orbitals (AO's).[49] In an extension of the Dewar-Chatt-Duncanson[1] model, the bonding of the diene can be described by the components (σ) $\Psi_1 \rightarrow$ M, (π) $\Psi_2 \rightarrow$ M, (π) $\Psi_3 \leftarrow$ M and (δ) $\Psi_4 \leftarrow$ M (Figure 2.31). Both metal-ligand π interactions should result in a lengthening of the terminal C-C bonds and a shortening of the internal C-C bond.

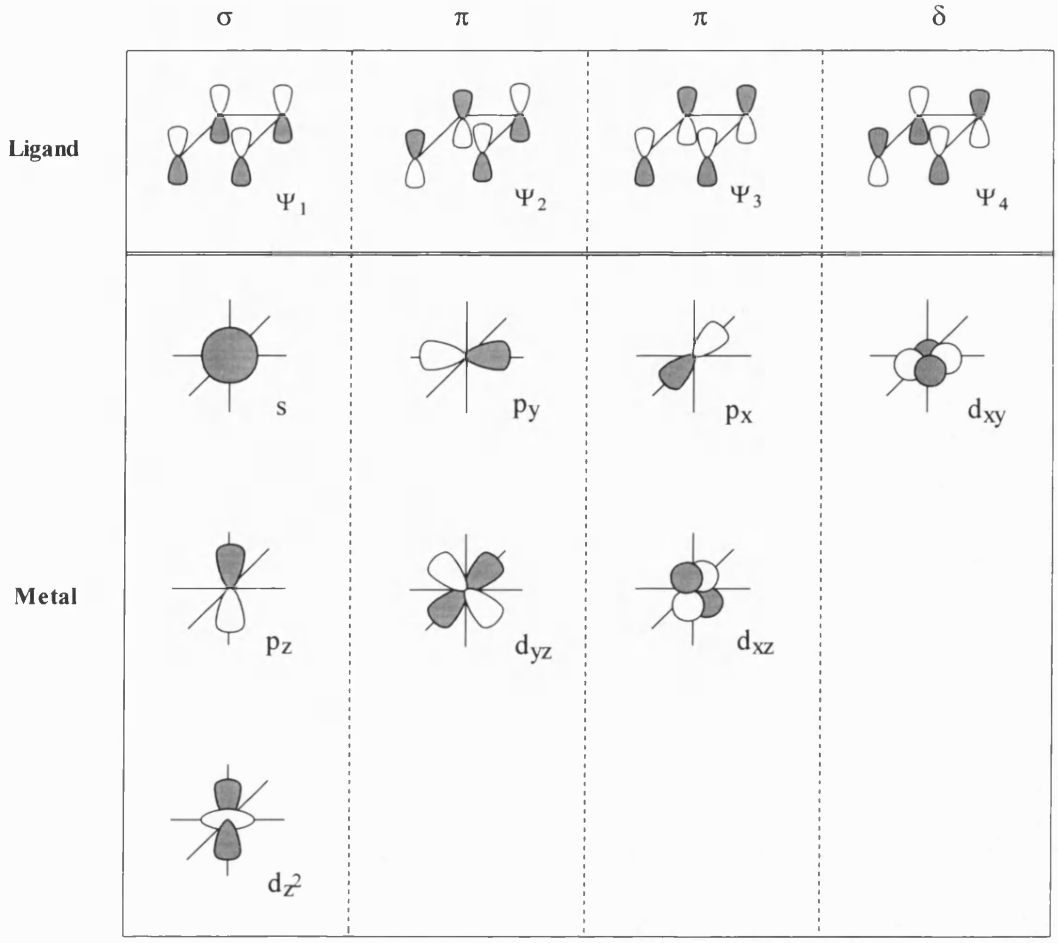

FIGURE 2.31 : Metal-Ligand Interactions.

Figure 2.32 illustrates how co-ordination of the diene to a transition metal influences the ligand's bond lengths. The free diene (**2.33**) has the expected short-long-short alternation of bond lengths, whereas upon co-ordination to a "late" transition metal such as iron[50] (**2.34**, Figure 2.32) the terminal bond lengths lengthen and the internal bond length shortens such that all the bond lengths appear approximately equal.

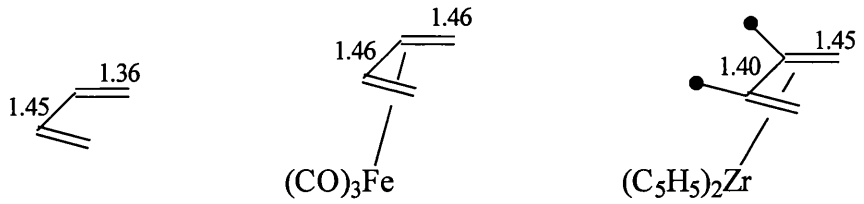

2.33 **2.34** **2.35**

FIGURE 2.32 : Bond Lengths of Butadienes (Å).

However, on co-ordination of the diene to an "early" transition metal such as zirconium[41] (**2.35**, Figure 2.32) the diene actually exhibits a long-short-long alternation of bond lengths. This is a consequence of the fact that the co-ordination of the diene to a metal centre can be described by two canonical forms **A** and **B** (Figure 2.33), where **A** can be described as a metallocyclopentene and **B** as a π-complex.

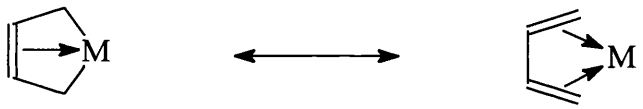

A **B**

FIGURE 2.33

The relative importance of these two canonical forms can be discussed in terms of the carbon-carbon and metal-carbon distances. Complexes of the "late" transition metals e.g. iron are generally described as form **B**, whereas, the corresponding complexes of the "early" transition metals e.g. zirconium are better described as canonical form **A** (Table 2.8 and Figure 2.33). Thus, by comparison of the structural parameters of [Zr(η^4-dimethylbutadiene)(η-C_5H_5)$_2$] **2.35**, [Fe(CO)(η^4-cyclohexadiene)$_2$] **2.34** and [MoI{η^2,η^2-CH_3CH=C(Ph)CH=CH-o-$C_6H_4PPh_2$}(η-C_5H_5)] **6**, it appears that **6** is similar to the "early" transition metal complexes with M-C27 [2.291(7) Å] and M-C24 [2.249(6) Å] being shorter than

the M-C26 [2.408(6) Å] and M-C25 [2.341(6) Å] bond distances. Also, C25-C26 [1.393(7) Å] is significantly shorter than the C27-C26 [1.439(7) Å] and C25-C24 [1.448(7) Å] bond distances, which is more consistent with the C25-C26 being an internal double bond.

Therefore, it appears that the agostic interaction observed in complex **3** can be displaced by good σ donors such as acetonitrile and co-ordinating anions (e.g. halides, CF_3COO^-). Also, it can be concluded that the *trans* orientation of the diene in complex **3** is "locked" in this conformation by the agostic interaction and once this is removed the diene rearranges to the more common *cis* conformer, as determined by the crystal structure of **6**.

TABLE 2.8 : Comparison of Structural Parameters of **2.35**, **2.34** and **6**.

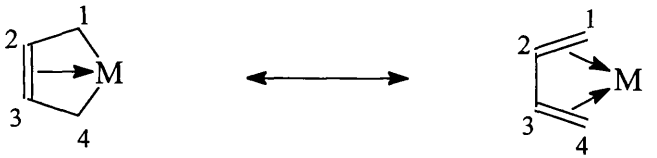

A **B**

[Zr(η^4-dimethylbutadiene)(η-C_5H_5)$_2$] **2.35** "***Metallocyclopentene***" **A**		[Fe(CO)(η^4-cyclohexadiene)$_2$] **2.34** "***π-Complex***" **B**		[MoI{η^2,η^2-CH_3CH=C(Ph)CH=CH-o-$C_6H_4PPh_2$}(η-C_5H_5)] **6**	
M-C1	= short 2.30 Å	M-C1	= long 2.12 Å	M-C24, M-C27	= 2.249(6), 2.291(7)
M-C2	= long 2.59 Å	M-C2	= short 2.03 Å	M-C25, M-C26	= 2.341(6), 2.408(6)
C1-C2	= 1.45 Å	C1-C2	= 1.39 Å	C25-C24, C27-C	= 1.448(7), 1.439(7)
C2-C3	= 1.40 Å	C2-C3	= 1.41 Å	C26-C25	= 1.393(7)

2.5 Reactivity of [MoI{η^2,η^2-CH_3CH=C(Ph)CH=CH-o-$C_6H_4PPh_2$}(η-C_5H_5)] 6

It has already been noted that the agostic interaction of **3** could not be displaced using carbon monoxide (Section 2.3) but could with good σ donors (Sections 2.4). Therefore, it was obviously of interest to determine whether there were steric reasons preventing the co-ordination of the CO molecule to the metal centre. Against this background the reaction of [MoI{η^2,η^2-CH_3CH=C(Ph) CH=CH-o-$C_6H_4PPh_2$}(η-C_5H_5)] **6** with thallium hexafluorophosphate in the presence of carbon monoxide was examined. with the intention of replacing the iodide with the carbon monoxide ligand to form a cationic carbonyl complex.

The reverse reaction i.e. **6** $\rightarrow$ **3** was unlikely to proceed in the absence of carbon monoxide, as the diene would have to undergo *cis* $\rightarrow$ *trans* isomerisation in order to allow the agostic interaction. Indeed, the reaction of **6** with thallium hexafluorophosphate did not yield any product. However, if the reaction was carried out in a stream of carbon monoxide, an orange, cationic product **9** was obtained. Infra-red spectroscopy [ν(CO) = 1977cm^{-1}], the mass spectrum [(M^+) 595, (M^+-CO) 567] and $^{13}C\{^1H\}$ NMR spectroscopy [δ 233.4, doublet, J(CP) 16.5 Hz] confirmed the presence of a co-ordinated CO molecule. The ^1H and $^{13}C\{^1H\}$ NMR spectra were similar to that observed for [Mo(NCMe){η^2,η^2-CH_3CH=C(Ph)CH=CH-o-$C_6H_4PPh_2$}(η-C_5H_5)][BF_4] **5**. In the ^1H NMR spectrum there was a doublet at δ 1.66 [methyl group, J(MeH^a) 6.7 Hz], a quartet at δ 4.03 [H^a, J(H^aMe) 6.7 Hz], a doublet of doublets at δ 4.48 [H^c, J(H^cH^b) 8.0 Hz, J(H^cP) 8.0 Hz], a singlet at δ 4.95 (η-C_5H_5) and a doublet of doublets at δ 5.45 [H^b, J(H^bP) 7.0 Hz, J(H^bH^c) 8.0 Hz]. The $^{13}C\{^1H\}$ NMR spectrum clearly showed that the methyl carbon resonated at δ 15.8 and the diene carbons, C_1, C_2, C_3 and C_4, at δ 58.1, 116.5, 105.4 and 68.4, respectively. These peak assignments were aided by H-H and C-H NMR correlation studies. Thus, it was concluded that the product of this reaction, **9**, was [Mo(CO){η^2,η^2-CH_3CH=C(Ph)CH=CH-o-$C_6H_4PPh_2$}(η-

C_5H_5)] (Figure 2.34), which conclusively showed that co-ordination of the carbon monoxide to complex **3** was not prevented purely on steric considerations.

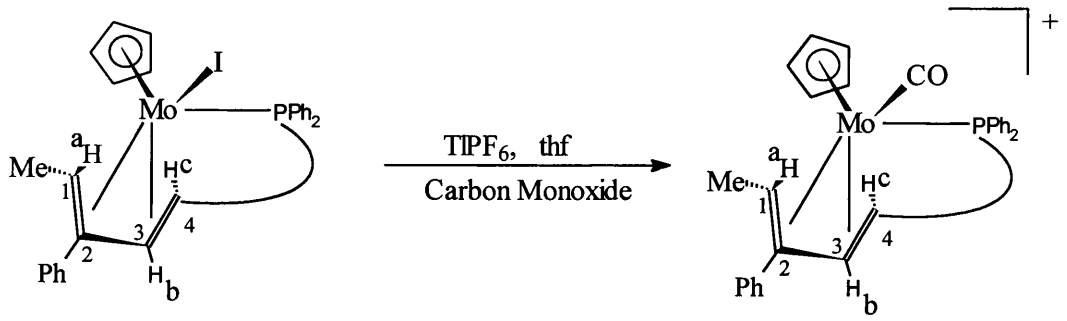

6 **9**

FIGURE 2.34

A comparison of the ^{1}H, $^{13}C\{^{1}H\}$ and $^{31}P\{^{1}H\}$ NMR spectra data of complexe **3**, $[Mo(NCMe)\{\eta^2,\eta^2\text{-}CH_3CH{=}C(Ph)CH{=}CH\text{-}o\text{-}C_6H_4PPh_2\}(\eta\text{-}C_5H_5)][BF_4]$ **5**, $[Mo(CO)\{\eta^2,\eta^2\text{-}CH_3CH{=}C(Ph)CH{=}CH\text{-}o\text{-}C_6H_4PPh_2\}(\eta\text{-}C_5H_5)][BF_4]$ **9**, $[Mo\{OC(O)CF_3\}\{\eta^2,\eta^2\text{-}CH_3CH{=}C(Ph)CH{=}CH\text{-}o\text{-}C_6H_4PPh_2\}(\eta\text{-}C_5H_5)]$ **4** and $[MoI\{\eta^2,\eta^2\text{-}CH_3CH{=}C(Ph)CH{=}CH\text{-}o\text{-}C_6H_4PPh_2\}(\eta\text{-}C_5H_5)]$ **6** (Table 2.9) clearly illustrates the similarities between **5**, **9**, **4** and **6**. Therefore, complexes **4**, **5** and **9** probably have the same orientation of the diene moiety as complex **6** i.e. *cis* as opposed to the *trans* conformation observed in complex **3**.

TABLE 2.9 : Comparison of ^{1}H, $^{13}C\{^{1}H\}$ and $^{31}P\{^{1}H\}$ NMR Spectra of Diene Complexes **3,4,5,6** and **9**.

Complex	**Room Temp ^{1}H NMR**					**$^{31}P\{^{1}H\}$ NMR**
	Me	**H^a**	**H^b**	**H^c**	**Cp**	**PPh_2**
3	-2.0	5.65	4.83	1.74	5.27	60.9
4	1.46	3.99	6.50	2.86	4.35	52.0
6	1.42	4.12	6.37	2.99	4.36	45.9
5	1.47	3.54	5.78	3.27	4.46	55.1
9	1.66	4.03	5.45	4.48	4.95	57.3

Complex	**$^{13}C\{^{1}H\}$ NMR**					
	Me	**C_1**	**C_2**	**C_3**	**C_4**	**η-C_5H_5**
3	1.1	67.6	90.5	75.9	81.8	95.2
4	14.9	60.1	112.6	113.1	64.3	93.2
6	17.0	54.8	89.5	109.4	63.2	92.1
5	14.8	57.1	119.2	110.9	63.9	92.1
9	15.8	58.1	116.5	105.4	68.4	92.6

Having shown that ligand substitution was possible, i.e. MeCN for iodide and iodide for carbon monoxide, attention was turned to the reactivity of the diene moiety of [MoI{η^2,η^2-CH_3CH=C(Ph)CH=CH-o-$C_6H_4PPh_2$}(η-C_5H_5)] **6**. Earlier work has shown that when a solution of a 1,3-diene complex **2.36** was treated at room temperature with a molar equivalent of trityl tetrafluoroborate the orange crystalline η^4(5e)-butadienyl complex **2.38** was obtained in good yield (Figure 2.35).[51] This reaction involved a formal hydride abstraction by the trityl cation from one of the terminal diene C-H bonds. Significantly, the hydride abstraction reaction was regioselective with the C-H bond of the 1,3-diene which was *trans* to the bromine ligand being preferentially activated and abstracted. It was proposed that in the reaction the trityl acted initially as a one-electron oxidant to form the radical cation intermediate complex **2.37**, which subsequently undergoes C-H bond cleavage to afford the final product **2.38**.

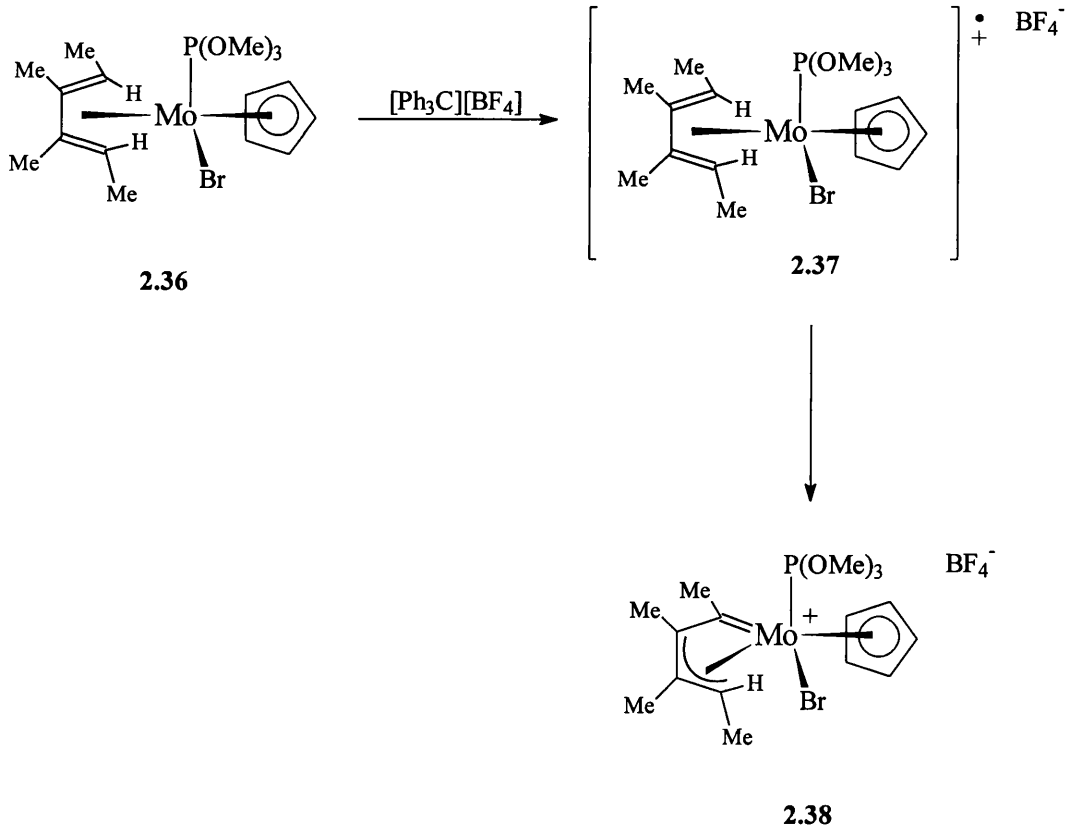

FIGURE 2.35

In light of this work the reaction of **6** towards trityl tetrafluoroborate was examined, with a view to transforming the 1,3-diene in **6** into a reactive η^4(5e)-butadienyl species. Addition of $[Ph_3C][BF_4]$ to a dichloromethane solution of **6** afforded a purple complex **10**, which was insoluble in hydrocarbon solvents and only sparingly soluble in polar solvents. Attempts to obtain ^1H and $^{31}P\{^1H\}$ NMR spectra were unsuccessful and suggested that the complex was possibly paramagnetic. A preliminary ESR study (g = 1.993) was, therefore, carried out and confirmed the paramagnetic nature of the complex. The elemental analysis (Found : 50.4% C, 3.8% H; Calc. : 50.2% C, 3.9% H) and mass spectrum [(M^+) 694, (BF_4^-) 87] suggested that the cation of **10** had the same molecular formula as **6** (i.e. $C_{34}H_{30}IMoP$). It is, therefore, proposed that the trityl tetrafluoroborate acted as a one-electron oxidant in the reaction with $[MoI\{\eta^2,\eta^2\text{-}CH_3CH{=}C(Ph)CH{=}CH\text{-}o\text{-}C_6H_4PPh_2\}(\eta\text{-}C_5H_5)]$ **6** to afford $[MoI\{\eta^2,\eta^2\text{-}CH_3CH{=}C(Ph)CH{=}CH\text{-}o\text{-}C_6H_4PPh_2\}(\eta\text{-}C_5H_5)][BF_4]$ **10**.

In order to test this theory **6** was reacted with one equivalent of ferrocenium tetrafluoroborate, a well known one-electron oxidising agent,[52] with the anticipation of forming the same product as in the trityl tetrafluoroborate reaction. Addition of ferrocenium tetrafluoroborate to a solution of **6** did also result in a paramagnetic, purple complex, which had the same elemental analysis, mass spectrum and preliminary ESR spectrum of $[MoI\{\eta^2,\eta^2\text{-}CH_3CH{=}C(Ph)CH{=}CH\text{-}o\text{-}C_6H_4PPh_2\}(\eta\text{-}C_5H_5)][BF_4]$ **10**. Thus, it is proposed that the product (**10**) is the cationic , 17-electron equivalent to **6** (Figure 2.36).

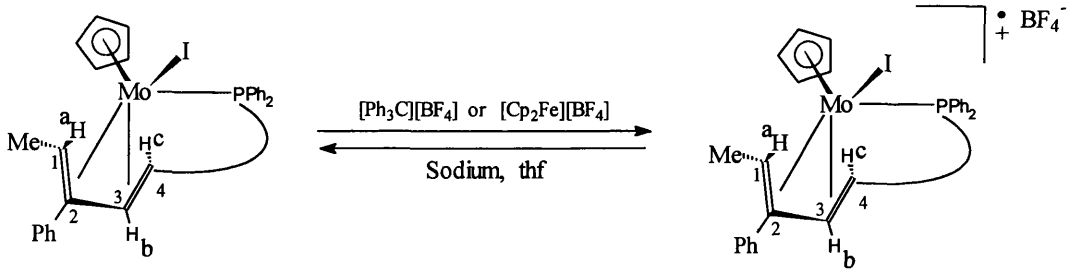

6 17e **10**

FIGURE 2.36

If the complex [MoI{η^2,η^2-CH_3CH=C(Ph)CH=CH-o-$C_6H_4PPh_2$}(η-C_5H_5)] [BF_4] **10** is the cationic equivalent to [MoI{η^2,η^2-CH_3CH=C(Ph)CH=CH-o-$C_6H_4PPh_2$}(η-C_5H_5)] **6**, an obvious reaction to attempt was the reverse reaction i.e. to reduce complex **10**. Stirring a solution of the purple complex **10** over excess sodium metal resulted in a green solution after three hours, which after column chromatography afforded the complex **6**. The successful regeneration of [MoI{η^2,η^2-CH_3CH=C(Ph)CH=CH-o-$C_6H_4PPh_2$}(η-C_5H_5)] **6** by the reduction of [MoI{η^2,η^2-CH_3CH=C(Ph)CH=CH-o-$C_6H_4PPh_2$}(η-C_5H_5)][BF_4] **10** was confirmed by ^1H and $^{31}P\{^1H\}$ NMR spectroscopy and, hence, supported the proposed structure of **10**.

Therefore, unlike **2.36** (Figure 2.35) the reaction of [MoI{η^2,η^2-CH_3CH=C(Ph)CH=CH-o-$C_6H_4PPh_2$}(η-C_5H_5)] **6** with trityl does not lead to an η^4-butadienyl complex. However, **10** is of interest in that it supports the proposed mechanism[51] for the formation of the η^4(5e)-butadienyl **2.38** from the buta-1,3-diene complex **2.36** *via* a radical cation.

Both trityl[53] and ferrocenium tetrafluoroborate are mild oxidising agents[52] and it was of interest to attempt the observation of the one-electron oxidation and reduction using electrochemistry. Therefore, a cyclic voltammetry experiment was carried out on complex **6** using a solution of degassed, dried dichloromethane (100ml) containing 0.67 mmol l^{-1} of **6** and 0.200 mol l^{-1} of the electrolyte tetrabutyl ammonium perchlorate (TBAP). The resulting voltammogram is illustrated in Figure 2.37 and shows that the complex easily undergoes a one-electron oxidation which is fully reversible and stable. Thus, the electrochemistry experiment reinforced the proposed structure of **10**.

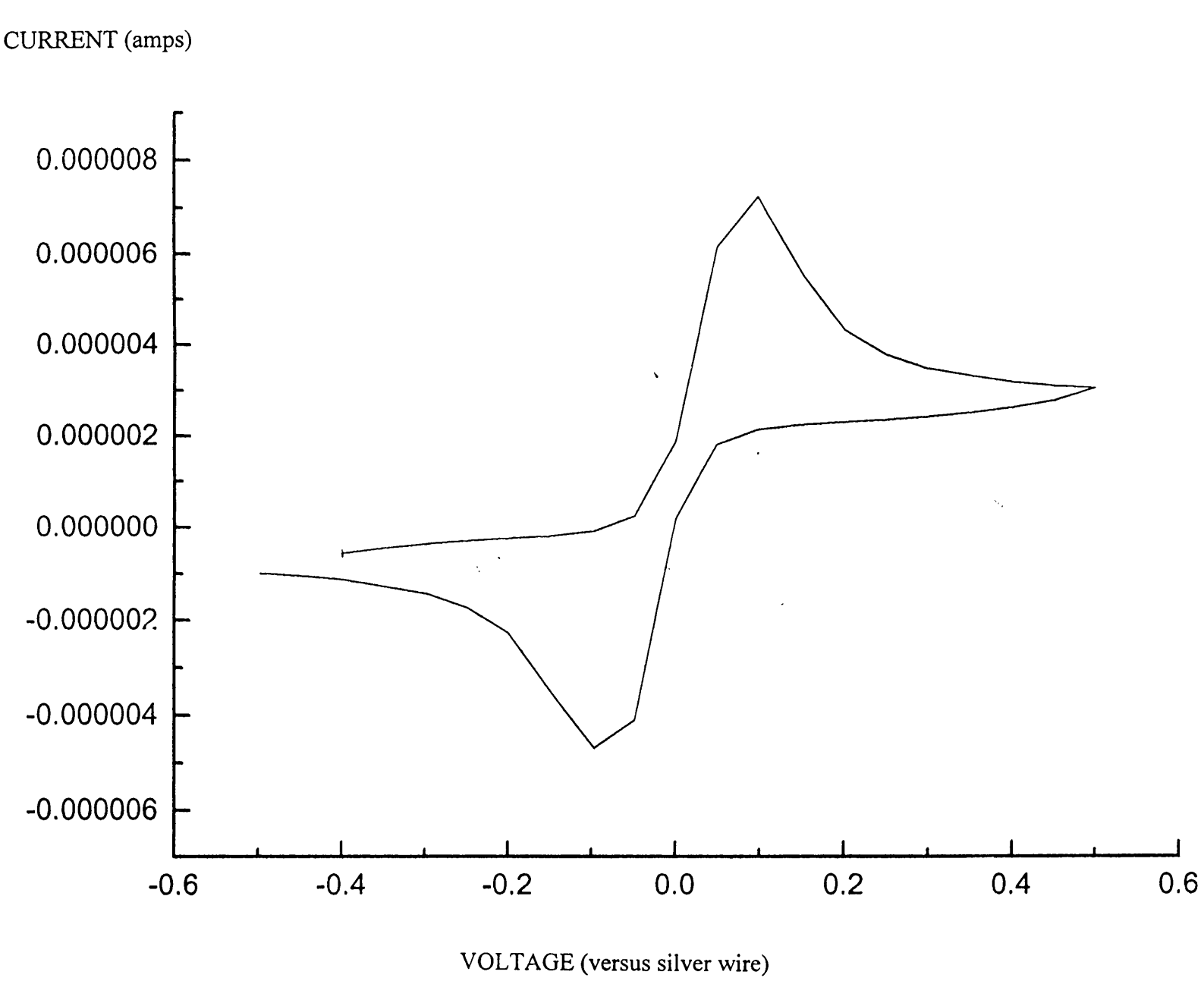

FIGURE 2.37. : Cyclic Voltammogram of **6**.

2.6 Synthesis and Reactivity of $[Mo(\eta^2\text{-}MeC_2Ph)(dpps)(\eta^5\text{-}C_9H_7)][BF_4]$ 11.

Having discovered the novel chemistry exhibited by $[Mo(\eta^2\text{-}MeC_2Ph)(dpps)\ (\eta\text{-}C_5H_5)][BF_4]$ **1** it was decided to attempt to widen the scope of this new chemistry to $\eta^5\text{-}C_9H_7$ (indenyl) and $\eta^5\text{-}C_5Me_5$ (pentamethylcyclopentadienyl) derivatives of **1** as the cationic, bis alkyne carbonyl complexes **2.39**[54] and **2.40**[54] (Figure 2.38) have both been synthesised within our group previously.

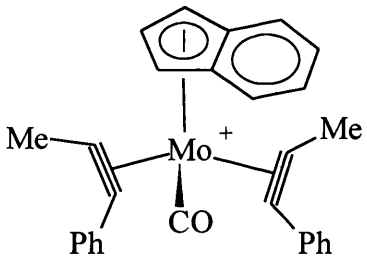

2.39

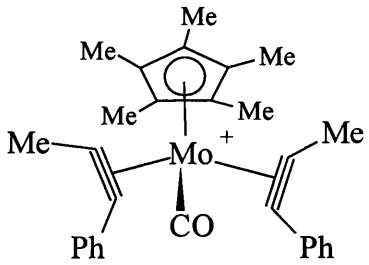

2.40

FIGURE 2.38

Complex **2.40** was refluxed in dichloromethane with excess *o*-dpps for 2-3 days, after which time there had been no detectable change in the infra-red spectrum. The solvent was then changed to thf but again there was no discernible change after approximately two days and only starting material was present. In a final attempt to displace the CO from **2.40** one equivalent of trimethyl amine N-oxide was added to the reaction vessel but unfortunately this only resulted in decomposition.

However, the same reaction with **2.39** was much more successful and refluxing **2.39** with *o*-dpps in dichloromethane for two days afforded the complex $[Mo(\eta^2\text{-}MeC_2Ph)(dpps)(\eta^5\text{-}C_9H_7)][BF_4]$ **11** (Figure 2.39) in excellent yield (91%). The NMR spectra were similar to those observed for the complex $[Mo(\eta^2\text{-}MeC_2Ph)(dpps)(\eta\text{-}C_5H_5)][BF_4]$ **1**. The presence of a co-ordinated dpps molecule

and the formation of only one isomer was confirmed by the presence of only one singlet in the $^{31}P\{^{1}H\}$ NMR spectrum at δ 83.2. Also, in a similar manner to **1**, the co-ordinated alkyne of **11** does not undergo "propeller rotation" about the metal alkyne axis, as variable temperature NMR studies showed that the methyl singlet at δ 2.13 in the ^{1}H NMR spectrum remained unchanged with temperature. The contact carbon resonances of the alkyne [δ 225.9 and 230.9] were typical of a four-electron donor alkyne.

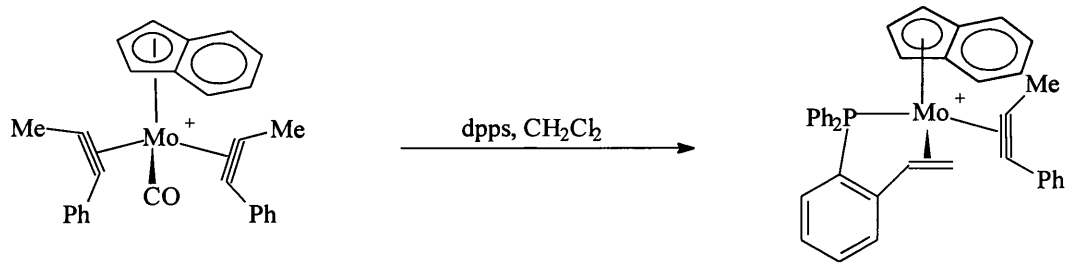

2.39 **11**

FIGURE 2.39

Having established that the indenyl alkene/alkyne complex **11** could be synthesised, it was obviously of interest to attempt to couple the alkene and alkyne moieties in a similar fashion to that observed for **1**. Treatment (-78° → +25°C) of a suspension of **11** in thf with a molar equivalent of $Li[N(SiMe_3)_2]$ led, on stirring, to the rapid dissolution of the solid and a colour change from red to yellow. Column chromatography of the reaction mixture and elution with a 4:1 hexane: dichloromethane mixture afforded the yellow complex $[Mo\{\eta^2,\eta^3(5e)\text{-}S\text{-}CH_2CHC(Ph)CH{=}CH\text{-}o\text{-}C_6H_4PPh_2\}(\eta^5\text{-}C_9H_7)]$ **12** (Figure 2.40). Elemental (Found : 74.0 %C, 5.1 %H; Calc. 74.01 %C, 5.07 %H) and mass spectrum analysis [(M^+) 616] of **12** showed that a molecule of HBF_4 had indeed been eliminated. Again, the phosphorus NMR spectrum confirmed the presence of only one isomer with one singlet at δ 83.2. Comparison of the ^{1}H and $^{13}C\{^{1}H\}$ NMR spectra of the neutral product **12** with that of **2** revealed, as expected, a proton had been abstracted from the methyl substituent of the η^2(4e)-bonded alkyne and that the alkyne and alkene

moieties had coupled to form an S-pentadienyl ligand. Complex **12** contained one quaternary carbon [δ 88.9], one CH_2 group [δ 41.2] and three CH groups [δ 62.4, 83.6 and 87.4] attributable to the C_5 pentadienyl chain.

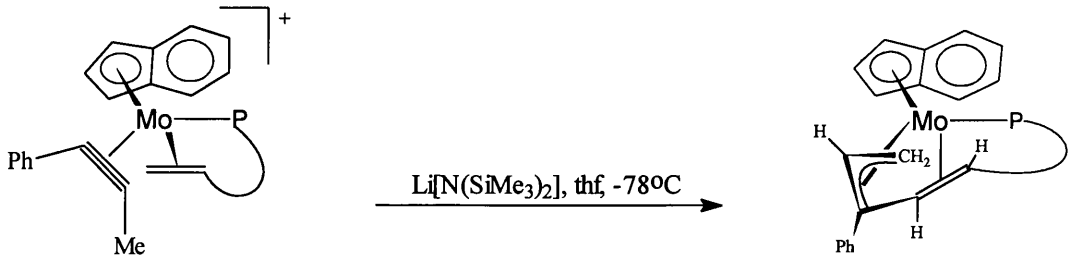

11 **12**

FIGURE 2.40

Therefore, it was established that the novel chemistry exhibited by **1** can be successfully extended to indenyl (η^5-C_9H_7) derivatives.

2.7 Synthesis of Rhenium η^4(5e)-Butadienyl Complexes

Having established the chemistry of molybdenum-(*o*-dpps) complexes, attention was then turned to another transition metal, namely rhenium of group 7. Recently, it has been found that the four-electron donor alkyne complexes $[ReBr_2(\eta^2\text{-}RC_2Ph)(\eta\text{-}C_5H_5)]$ **2.42** (R=Me) and **2.43** (R=Ph) can be readily accessed in good yield by heating a toluene solution of *cis/trans*-$[ReBr_2(CO)_2(\eta\text{-}C_5H_5)]$ **2.41** and the corresponding alkynes RC_2Ph (Figure 2.41).[55] Furthermore, reaction of **2.42** and **2.43** with bis(diphenylphosphino)ethane (dppe) and two equivalents of $AgBF_4$ in CH_2Cl_2, readily afforded the dications $[Re(\eta^2\text{-}RC_2Ph)(dppe)(\eta\text{-}C_5H_5)][BF_4]_2$ (R=Me **2.44**, R=Ph **2.45**) (Figure 2.41).[55]

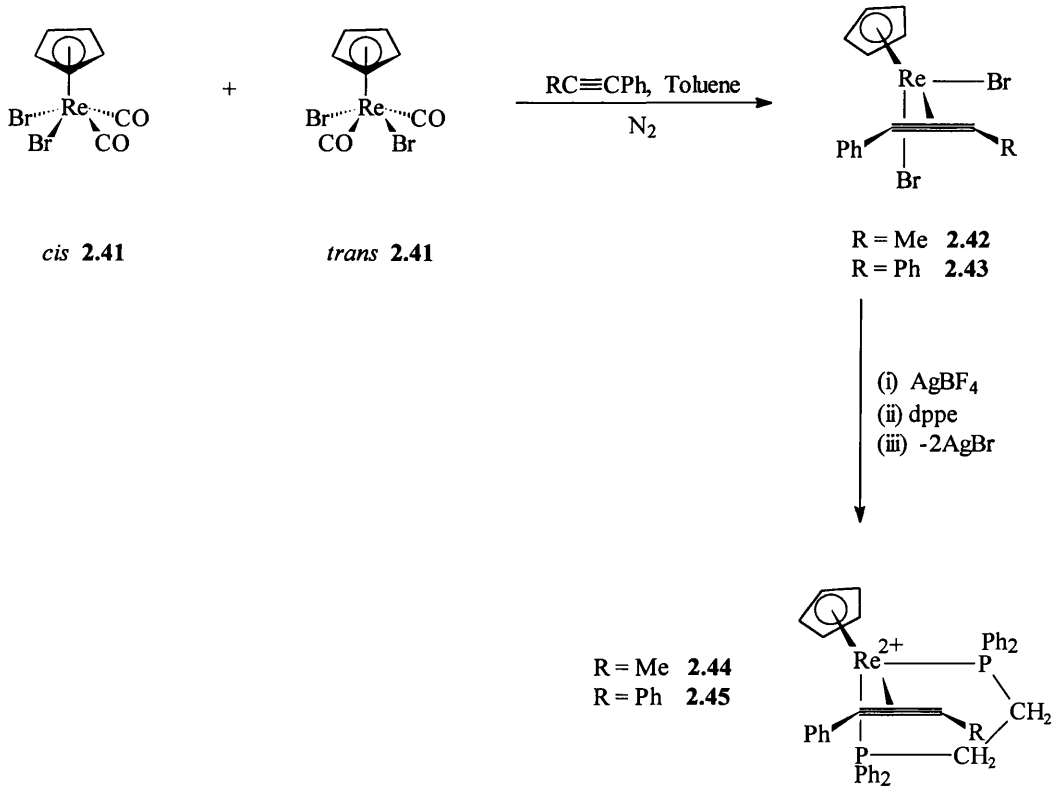

cis **2.41** *trans* **2.41** R = Me **2.42** R = Ph **2.43**

R = Me **2.44** R = Ph **2.45**

FIGURE 2.41

In view of the above and earlier work (Section 2.1 - 2.6) it was obviously of interest to examine the reaction of **2.42** and **2.43** with *o*-diphenylphosphinostyrene

in the presence of two equivalents of $AgBF_4$ with the expectation of forming reactive η^2(4e)-alkyne/η^2(2e)-alkene substituted dications **2.46** (Figure 2.42).

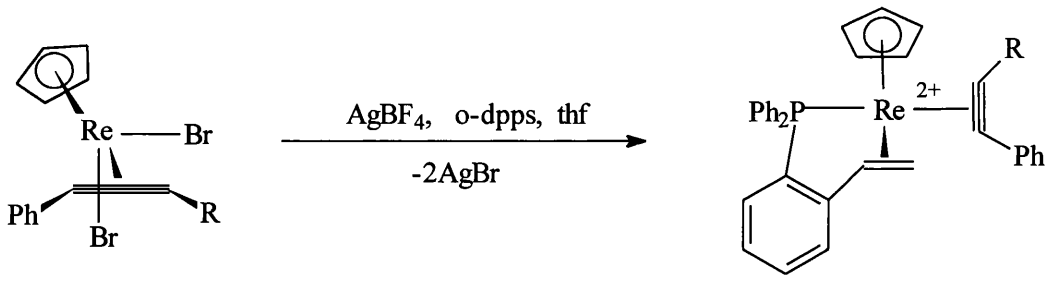

R = Me **2.42**
R = Ph **2.43**

2.46 R = Me or Ph

FIGURE 2.42

However, complex **2.46** was not the final product and an unexpected reaction occurred. Addition of $AgBF_4$ to a tetrahydrofuran solution of **2.42** and *o*-dpps led to the rapid precipitation of silver bromide (2 molar equivalents). After the solvent was removed *in vacuo*, the residue was extracted with dichloromethane and filtered through Celite. Addition of diethyl ether afforded a green, crystalline complex of $[Re{=}C(Ph)\text{-}\eta^3\text{-}\{C(Me)CHCHC_6H_4PPh_2\text{-}o\}(\eta\text{-}C_5H_5)][BF_4]$ **13** in 93% yield, which was insoluble in non-polar hydrocarbon solvents (Figure 2.43).

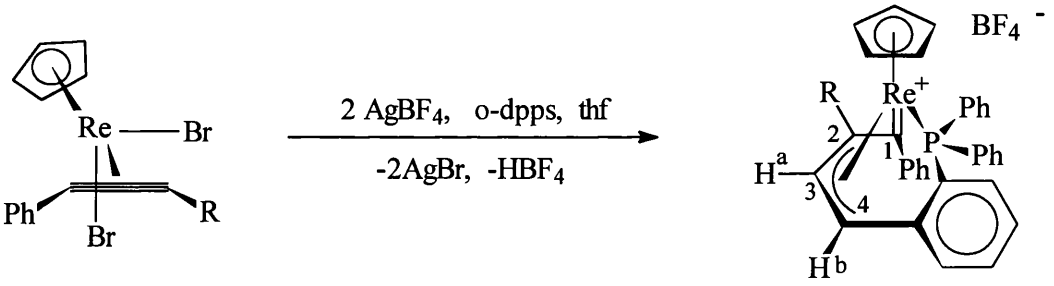

R = Me **2.42**
R = Ph **2.43**

R = Me **13**
R = Ph **14**

FIGURE 2.43

Interestingly, signals characteristic of a co-ordinated alkyne were absent from the $^{13}C\{^1H\}$ NMR spectrum. Instead there was one low field signal at δ 257.7, which was a doublet [J(CP) 16.3 Hz] and is characteristic of a rhenium alkylidene α-carbon. The mass spectrum [(M^+) 655, (BF_4^-) 87], and $^{31}P\{^1H\}$ NMR spectrum [δ 41.0] indicated that one dpps molecule was present. The protons H^a and H^b appear as an AB pattern [δ 6.59 and 6.55] in the ^1H NMR spectrum with a coupling constant, $J(H^aH^b)$ of 8.0 Hz. The AB pattern overlapped with the multiplet of signals attributable to the aryl protons but was clearly identified by C-H correlation NMR studies.

A similar reaction occurs with complex **2.43**, *o*-dpps and two equivalents of silver tetrafluoroborate to afford, in 90% yield, the corresponding green, cationic complex $[Re{=}C(Ph)\text{-}\eta^3\text{-}\{C(Ph)CHCHC_6H_4PPh_2\text{-}o\}(\eta\text{-}C_5H_5)][BF_4]$ **14** (Figure 2.43). The alkylidene α-carbon was clearly evident at δ 252.9 in the $^{13}C\{^1H\}$NMR spectrum as a doublet [J(CP) 14.9 Hz], due to coupling to the phosphorus atom originating from the dpps molecule, which resonated at δ 39.9 in the $^{31}P\{^1H\}$ NMR spectrum. The protons H^a and H^b appeared as an AB pattern [δ 6.70 and 6.81, $J(H^aH^b)$ 8.3 Hz] in the ^1H NMR spectrum, which overlapped with the multiplet of signals attributable to the aryl protons. Again, C-H correlation NMR studies were invaluable in identifying the signals of H^a and H^b from the aryl hydrogens.

A single crystal X-ray diffraction study with complex **13** was undertaken to elucidate the precise molecular geometry of the complex (Figure 2.44, selected bond lengths and angles are listed in Table 2.10). Interestingly, the study revealed that the complex was in fact a *mono*-cation, which contained an η^4(5e)-butadienyl ligand formed by the regioselective linking (C_2+C_2) of alkyne MeC_2Ph and alkene (dpps) ligands. The C_4 chain adopts an essentially *cisoid*-coplanar geometry with a torsion angle for C1-C2-C3-C4 (C9-C8-C7-C6 crystallographic numbering) of 11.42°. All the carbons of the C_4 chain are bonded to the rhenium centre but the Re-C9 bond distance is significantly shorter at 1.936(12) Å, whereas Re-C6, Re-C7

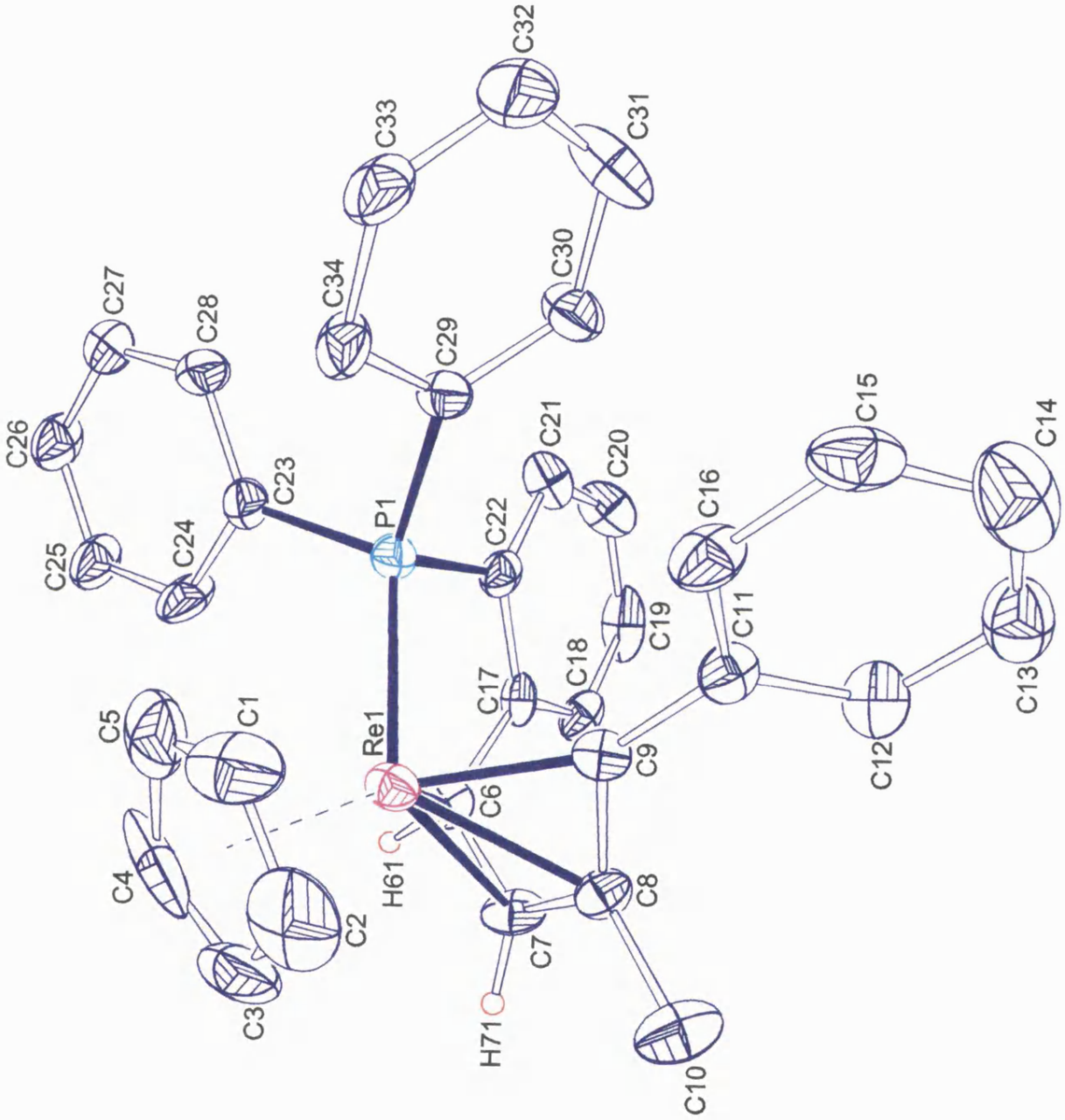

FIGURE 2.44 : ORTEP Drawing of the Cation of **13**.

and Re-C8 were at distances of 2.172(14) Å, 2.216(13) Å and 2.222(13) Å respectively. Thus, it is suggested that C9 is an alkylidene carbon doubly bonded to the rhenium centre, whereas the remaining three carbons of the butadienyl chain, C6, C7 and C8 are an η^3-allylic fragment (Figure 2.43). Therefore, the X-ray structure analysis determined that complex **13** contained an open chain butadienyl moiety, which was bonded to the rhenium as an η^4(5e) butadienyl fragment.

TABLE 2.10 : Selected Bond Lengths (Å) and Torsion Angles (°).

Atoms	Bond length	Atoms	Bond Length
Re-P1	2.375(5)	C6-C7	1.441(16)
Re-C6	2.172(14)	C7-C8	1.415(18)
Re-C7	2.216(13)	C8-C9	1.427(16)
Re-C8	2.222(13)	C8-C10	1.521(18)
Re-C9	1.936(12)		

Atoms	Angle	Atoms	Angle
C10-C8-C9-C11	43.99	C6-C7-C8-C9	11.42
C10-C8-C7-H71	9.60	C8-C7-C6-C17	60.16

Transition metal complexes containing butadienyl fragments, $C_4R_5^-$, have been known for many years and can bond to the metal in three different ways, **A**, **B**, or **C** (Figure 2.45). Formulation **A** represents an η^3(3e)-buta-1,2-dienyl and the attachment of this fragment to the metal is analogous to that found in the π allyl complexes except that one of the terminal carbon atoms is involved in an *exo*-allylic double bond. Representation **B** also has the butadienyl fragment acting as a three-electron donor in which the ligand formally σ-bonds to the metal with an additional π interaction from the alkene substituent. Finally, representation **C** contains a carbene carbon and an allyl moiety, which enables the ligand to donate five-electrons to the metal centre and is hence termed an η^4(5e) butadienyl fragment.

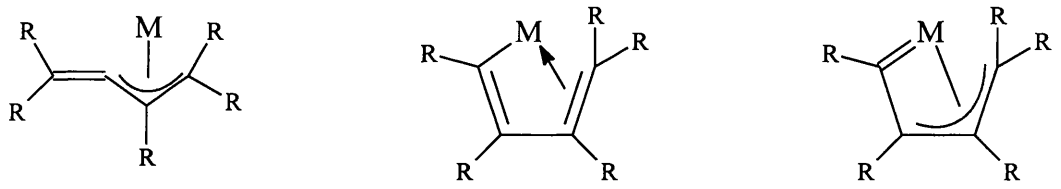

A **B** **C**

FIGURE 2.45

The η^3(3e) butadienyl complexes have been known longer than their η^4(5e) counterparts. As early as 1971, Stone reported the synthesis of [Ru(PPh_3){η^3(3e)-$C(CF_3)$=$C(CF_3)$-$C(CF_3)$=$CH(CF_3)$}(η-C_5H_5)] **2.48** by the reaction of [RuH(PPh_3)$_2$ (η-C_5H_5)] **2.47** with excess hexafluorobut-2-yne (Figure 2.46).[56] An X-ray crystallographic study of **2.48** confirmed the *cisoid* geometry of the butadienyl ligand and that the C_4 fragment was bonded to the ruthenium *via* a σ bond to C1 and a π-bond to the double bond of C3-C4. The interatomic distance for C3-C4 of 1.42 Å was longer than that exhibited for the non-ligated double bond C1-C2 (1.33 Å), therefore substantiating that C3-C4 was involved in bonding to the metal centre.

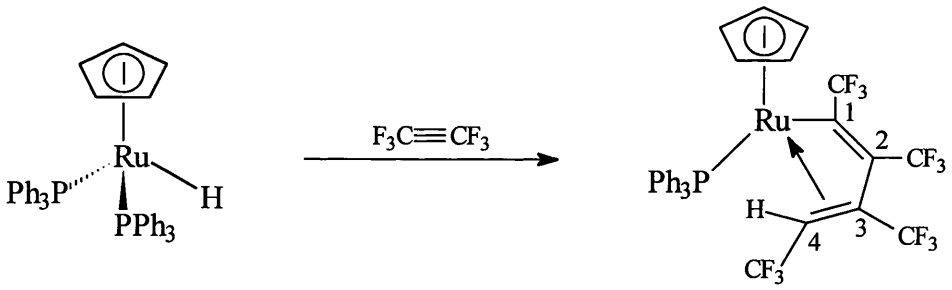

2.47 **2.48**

FIGURE 2.46

A similar bonding pattern was exhibited by the complex **2.49** (Figure 2.47), which was prepared by the reaction of [Rh(PPh_3)$_2$($PPh_2C_6H_4$)] with two equivalents of diphenylacetylene.[57] The X-ray structure indicated that the complex had a

distorted square planar conformation around the rhodium metal centre and that two alkyne molecules had coupled together to from a η^3-butadienyl fragment, which was also attached to a triphenyl phosphine ligand. Overall, the C_4 chain was acting as a three-electron donor *via* a σ and π bond.

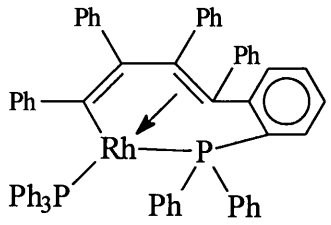

2.49

FIGURE 2.47

More recently, the formation of η^3(3e) butadienyl complexes by a coupling of an η^1-vinyl and alkyne moiety has been reported.[58] The niobocene hydrido complex **2.50** reacts with an alkyne to give the alkyne/η^1-vinyl complex **2.51**. These two ligands then undergo a C-C coupling reaction to afford the sixteen-electron intermediate **2.52** (Figure 2.48). Co-ordination of the terminal alkene bond to the niobium centre then affords the η^3(3e) butadienyl complex **2.53**.

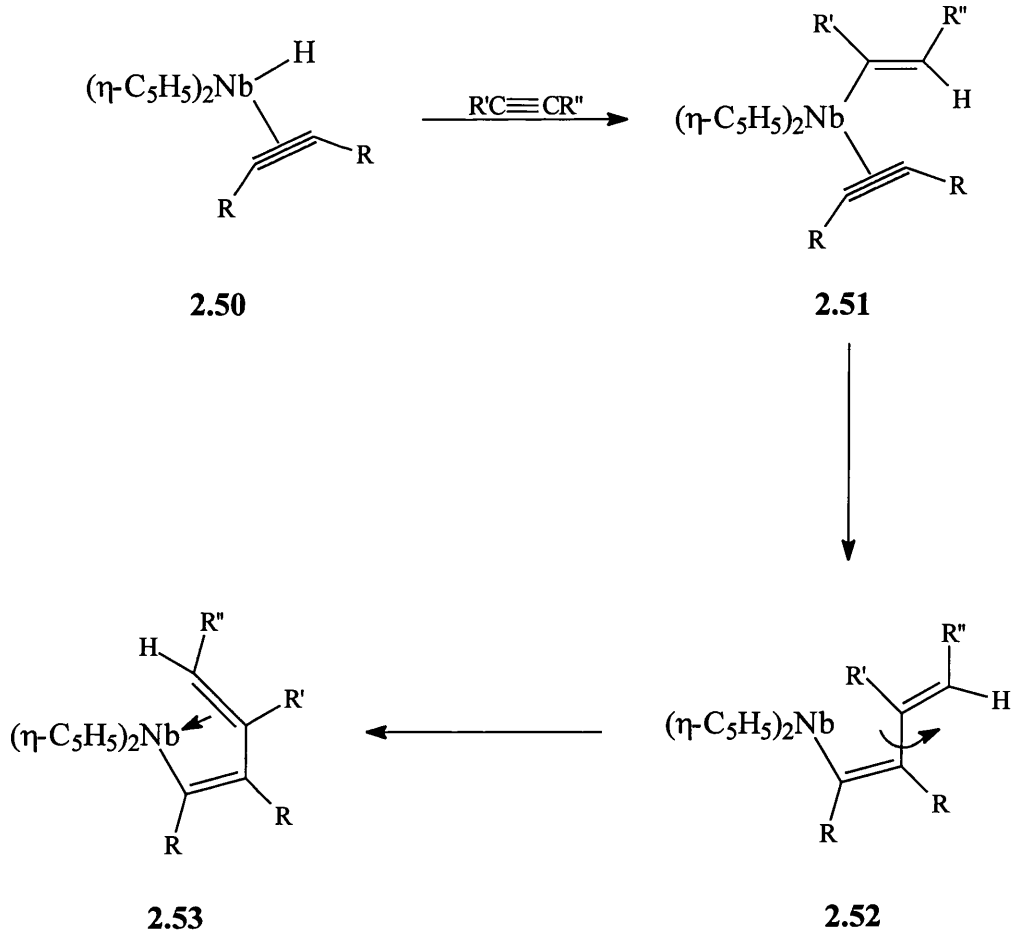

FIGURE 2.48

The first η^4(5e) butadienyl complex emerged in 1981 with the synthesis of [Ru=C(Ph)-η^3-{C(Ph)C(Ph)CH(Ph)}(η-C_5H_5)] **2.55**, which was formed by the conrotatory ring-opening reaction of an η^4-cyclobutadiene complex, [Ru(NCMe)(η^4-C_4Ph_4)(η-C_5H_5)][BF_4] **2.54**, upon treatment with H^- (Figure 2.49).[59] It was postulated that the immediate precursor to **2.55** was the sixteen-electron η^3(3e)-butadienyl complex, **A**, in which a geometrical and electronic redistribution occurs in order to allow the butadienyl fragment to function as a five-electron donor. In a sense, this switch in bonding mode from η^3(3e) $\rightarrow$ η^4(5e) stores the unsaturation at the metal centre. The ring-opening reaction of cyclobutadienes is discussed further in Section 3.4.

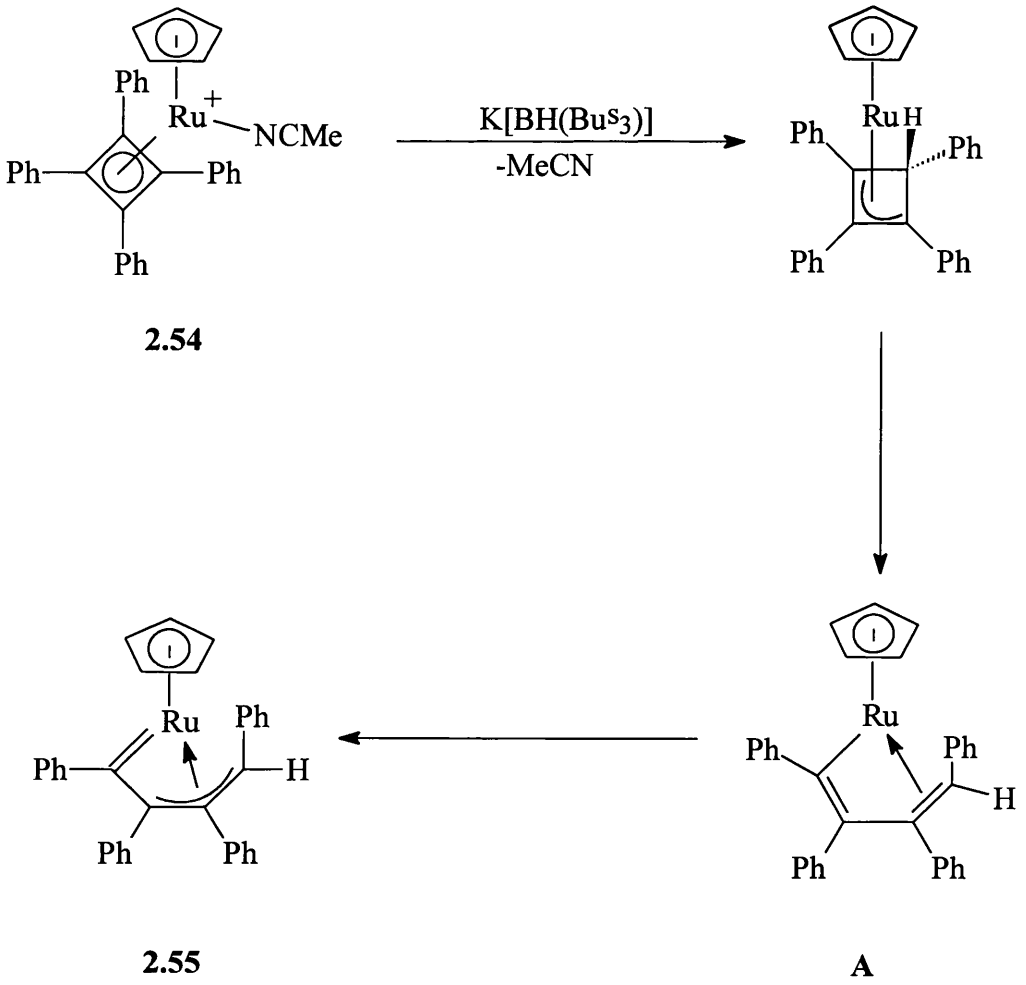

2.54

2.55 **A**

FIGURE 2.49

Complexes containing *cisoid*-η^4(5e)-butadienyl ligands can also be formed in three other ways. The first method is *via* the coupling (C_2+C_2) of alkyne and η^2-vinyl ligands. An η^2-vinyl/alkyne complex **A** (Figure 2.50) has been proposed as the initial product of H^+ attack on the bis-alkyne complex **2.56** (Figure 2.50).[51,60] The η^2-vinyl and alkyne then couple, with a concomitant take up of one water molecule, to afford the aqua-butadienyl complex [MoBr(OH_2){=C(Me)-η^3-{C(Me)C(Me)CHMe}(η-C_5H_5)][BF_4] **2.57**, which subsequently reacts with trimethylphosphite to displace the water molecule and afford the butadienyl complex [MoBr{$P(OMe)_3$}{=C(Me)-η^3-{C(Me)C(Me)CHMe}(η-C_5H_5)][BF_4] **2.58** (Figure 2.50). Both butadienyl complexes have been structurally characterised and

the presence of a short metal carbon double bond has been confirmed (see Table 2.12).

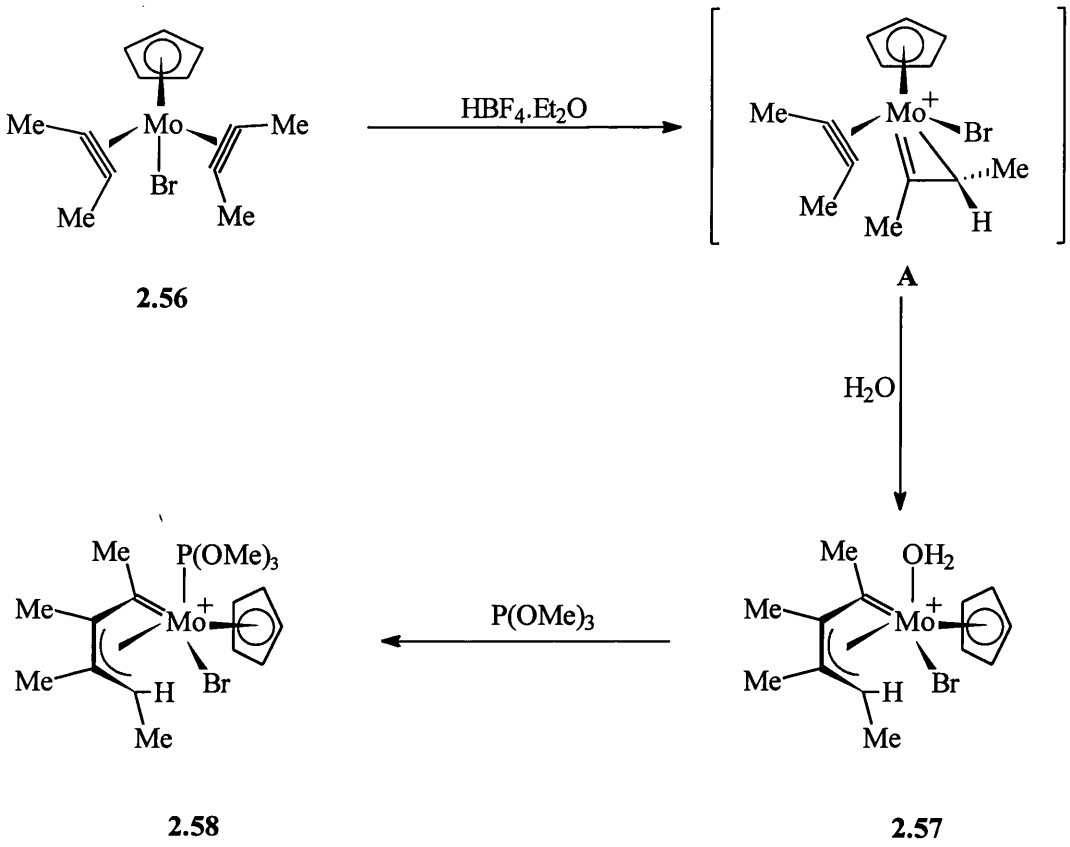

2.56 **2.58** **2.57**

FIGURE 2.50

Davidson[61] has also utilised η^2-vinyl precursors to form η^4-butadienyl complexes containing heteroatoms such as sulphur. Reaction of phosphines with the η^2-vinyl complex $[Mo\{\eta^3\text{-}C(CF_3)C(CF_3)SPr^i\}(CF_3C{\equiv}CCF_3)(\eta\text{-}C_5H_5)]$ **2.59** afforded the η^4-butadienyl derivatives $[Mo(PEt_3)\{C(CF_3){=}C(CF_3)C(CF_3)C{=}C(CF_3)\text{-}(SPr^i)\}(\eta\text{-}C_5H_5)]$ **2.60** (Figure 2.51), which was apparently as a result of insertion of the alkyne into the M=C bond of the η^2-C,C vinyl.

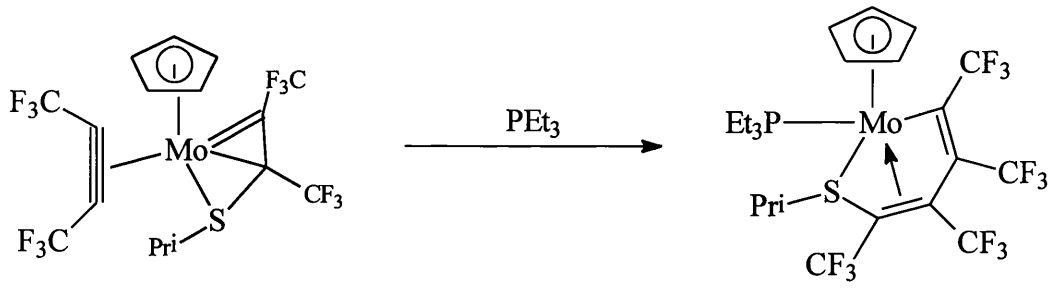

2.59 **2.60**

FIGURE 2.51

Alternatively, five-electron butadienyl complexes can be synthesised by the coupling of two alkyne ligands (Figure 2.52). Protonation of a metal-bound alkyne carbon in $[W(PhC_2Ph)_2(S_2CNR_2)_2]$ **2.61** with $HBF_4.Et_2O$ induces an oxidative coupling of the two C_2 moieties to form a complex containing an η^4-C_4R_4H ligand, which subsequently reacts with aqueous NEt_3 in dichloromethane to afford the neutral complex $[W(O)(\eta^4\text{-}C_4Ph_4H)(S_2CNEt_2)]$ **2.62**, which has been structurally characterised.[62]

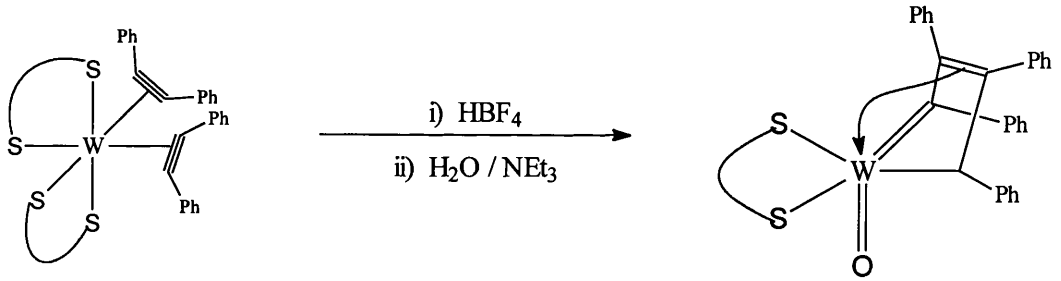

2.61 **2.62**

FIGURE 2.52

More recently, Etienne[63] reported that butadienyl ligands could be synthesised by the coupling of allyl and alkyne ligands (Figure 2.53). The coupling reaction to afford the niobium butadienyl complexes **2.65** and **2.66** arose from the addition of an allyl Grignard to the dichloro alkyne complex $[NbCl_2(PhC_2R)(Tp^*)]$, where R = Me **2.63** or Ph **2.64** and Tp^* = hydrotris(3,5-dimethylpyrazolyl)-borate.

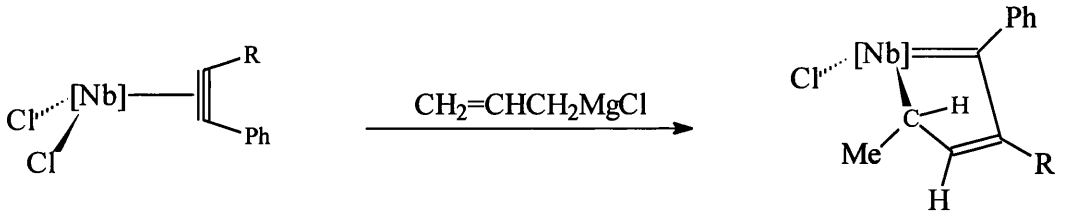

2.63, R = Me
2.64, R = Ph

2.65, R = Me
2.66, R = Ph

FIGURE 2.53 : [Nb] = Nb{hydrotris(3,5-dimethylpyrazolyl)-borate}

As indicated in the previous illustrations (Figures 2.49-2.53) the η^4(5e) butadienyls can adopt one of three possible resonance structures (**A**, **B**, or **C**, Figure 2.54). **A** is best described as an allyl substituted carbene, whereas **B** resembles a metallocyclopent-3-ene and, **C** a vinyl substituted η^2-vinyl complex.

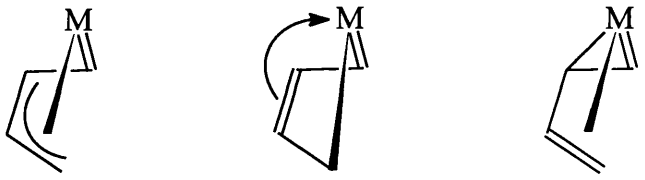

A **B** **C**

FIGURE 2.54

A comparison of the $^{13}C\{^1H\}$ NMR spectra data (Table 2.11) of compounds $[Re{=}C(Ph)\text{-}\eta^3\text{-}\{C(R)CHCHC_6H_4PPh_2\text{-}o\}(\eta\text{-}C_5H_5)][BF_4]$ (where R = Me **13** and Ph **14**), $[Ru{=}C(Ph)\text{-}\eta^3\text{-}\{C(Ph)C(Ph)CH(Ph)\}(\eta\text{-}C_5H_5)]$ **2.55**, $[MoBr\{P(OMe)_3\}\{{=}C(Me)\text{-}\eta^3\text{-}\{C(Me)C(Me)CHMe\}(\eta\text{-}C_5H_5)][BF_4]$ **2.58**, $[W(O)(\eta^4\text{-}C_4Ph_4H)(S_2CNEt_2)]$ **2.62**, and $[NbCl_2\{{=}C(Ph)C(Ph){=}C(H)CH(Me)\}(Tp^*)]$ **2.66** reveals that, in general, η^4(5e) butadienyl ligands show a low field resonance in the range of δ 230-280, which is attributable to the alklyidene carbon C1, while the other end of the C_4 chain, C4, is found at much higher field (*ca* δ 50 - 100). The two

intervening carbons, C2 and C3, are also bound to the metal and are found to resonate in the $^{13}C\{^1H\}$ NMR spectrum in the range δ 70 - 125 (Table 2.11). However, the carbon NMR data does not indicate which resonance structure, (**A**, **B** or **C** Figure 2.54) the butadienyl fragment has adopted.

TABLE 2.11 : Comparison of $^{13}C\{^1H\}$ NMR data of **13**, **14**, **2.55**, **2.58**, **2.62**, and **2.66** (Metal).

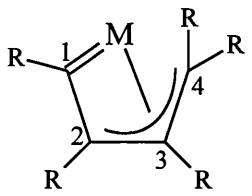

	13 (Re)	**14** (Re)	**2.55** (Ru)	**2.58** (Mo)	**2.62** (W)	**2.66** (Nb)
C1	257.7	252.9	246.0	305.5	266.5	235.7
C2	69.2	71.3	95.0	132.5	123.0	108.0
C3	78.3	73.5	97.5	108.4	119.1	114.2
C4	57.3	57.7	55.1	73.4	68.0	95.6

A similar comparison of the structural data (Table 2.12) of **13**, [Ru=C(Ph)-η^3-{C(Ph)C(Ph)CH(Ph)}(η-C_5H_5)] **2.55**, [MoBr{P(OMe)$_3$}{=C(Me)-η^3-{C(Me) C(Me)CHMe}(η-C_5H_5)][BF_4] **2.58**, [MoBr(OH_2){=C(Me)-η^3-{C(Me)C(Me) CHMe}(η-C_5H_5)][BF_4] **2.57**, [W(O)(η^4-C_4Ph_4H)(S_2CNEt_2)] **2.62**, [$NbCl_2${=C(Ph)C(Ph)=C(H)CH(Me)}(Tp^*)] **2.66** and [Ru(PPh_3){η^3(3e)-$C(CF_3)$=$C(CF_3)$-$C(CF_3)$=$CH(CF_3)$}(η-C_5H_5)] **2.48** reveals that, in general, η^4(5e) butadienyl complexes have approximately equal C1-C2, C2-C3and C3-C4 bond distances. A more interesting feature is the metal-carbon bond distances. In the tungsten complex **2.62**, the C_4 fragment shows slight asymmetry in its bonding to the tungsten. It appears to have a metal-carbon double bond to C_1 [1.96(1) Å cf. 1.94 Å for W=$CHCMe_3$],[62] a single bond to C_4 (2.25 Å cf. 2.26 Å for W-CH_2CMe_3)[62] and only a weak donation from C_2 and C_3 to the metal (2.52(1) and

2.61(1) Å), which is best represented as resonance structure **B** (Figure 2.54). By contrast, in the ruthenium complex **2.55** the carbons C2, C3 and C4 are symmetrically bound to the metal centre [2.204(5), 2.152(4) and 2.154(6) Å, respectively) and are best represented as resonance structure **A** in Figure 2.54. Thus, by comparison it is proposed that complex **13** is best described as an allyl-carbene **A** (Figure 2.54) because, like the ruthenium case **2.55**, the metal-carbon distances are approximately equal with M-C2, M-C3 and M-C4 distances of 2.222(13), 2.216(13) and 2.172(14), respectively.

TABLE 2.12 : Comparison of Bond Lengths of Complexes **13**, **2.55**, **2.58**, **2.57**, **2.62**, **2.66** and **2.48**.

COMPLEX [Metal]	**BOND LENGTH (Å)**						
	M-C1	**M-C2**	**M-C3**	**M-C4**	**C1-C2**	**C2-C3**	**C3-C4**
13 [Re]	1.936(12)	2.222(13)	2.216(13)	2.172(14)	1.427(16)	1.415(18)	1.441(16)
2.55 [Ru]	1.896(5)	2.204(5)	2.152(4)	2.154(6)	1.419(5)	1.435(7)	1.445(7)
2.58 [Mo]	1.94	2.33	2.48	2.31	1.40	1.40	1.34
2.57 [Mo]	1.93(1)	2.34(1)	2.41(1)	2.29(1)	1.46(1)	1.41(1)	1.45(1)
2.62 [W]	1.96(1)	2.52(1)	2.61(1)	2.25(1)	1.44(1)	1.43(1)	1.49(1)
2.67 [Nb]	1.993(4)	2.334(4)	2.370(5)	2.277(5)	1.439(7)	1.418(6)	1.392(7)
***2.48** [Ru]	2.05	2.65	2.16	2.19	1.33	1.51	1.42

* The η^3(3e)-butadienyl complex [Ru(PPh$_3$){η^3(3e)-C(CF$_3$)=C(CF$_3$)-C(CF$_3$)=CH(CF$_3$)}(η-C$_5$H$_5$)] **2.48** is included for comparison purposes.

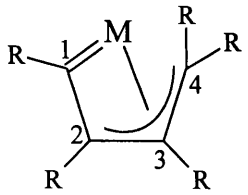

η^4(5e)

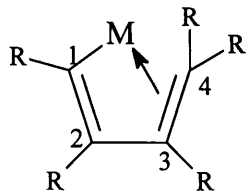

η^3(3e)

As regards the mechanism of formation of **13** and **14**, it was assumed that reaction of **2.42** and **2.43** with $AgBF_4$ and dpps does indeed form the η^2(4e)-alkyne/ η^2(2e)-alkene substituted dication **A** (Figure 2.55), then oxidative [Re(III)→Re(V)] carbon-carbon coupling provides access to the dicationic rhenacyclopent-2-ene **B**. Loss of a proton from **B**, and the synchronous formation of a strong rhenium to carbon double bond, would then lead to the intermediate **C**, which was an obvious precursor of the isolated products **13** and **14**. Clearly, because these products carry a positive charge they are protected from attack by the HBF_4 present in solution, which is generated as a by-product of the reaction along with two molar equivalents of silver bromide. Since HBF_4 was generated as a by-product, when the reaction was scaled up one molar equivalent of anhydrous sodium carbonate was added to the solution before the addition of the silver tetrafluoroborate in order to prevent the thf from polymerising.

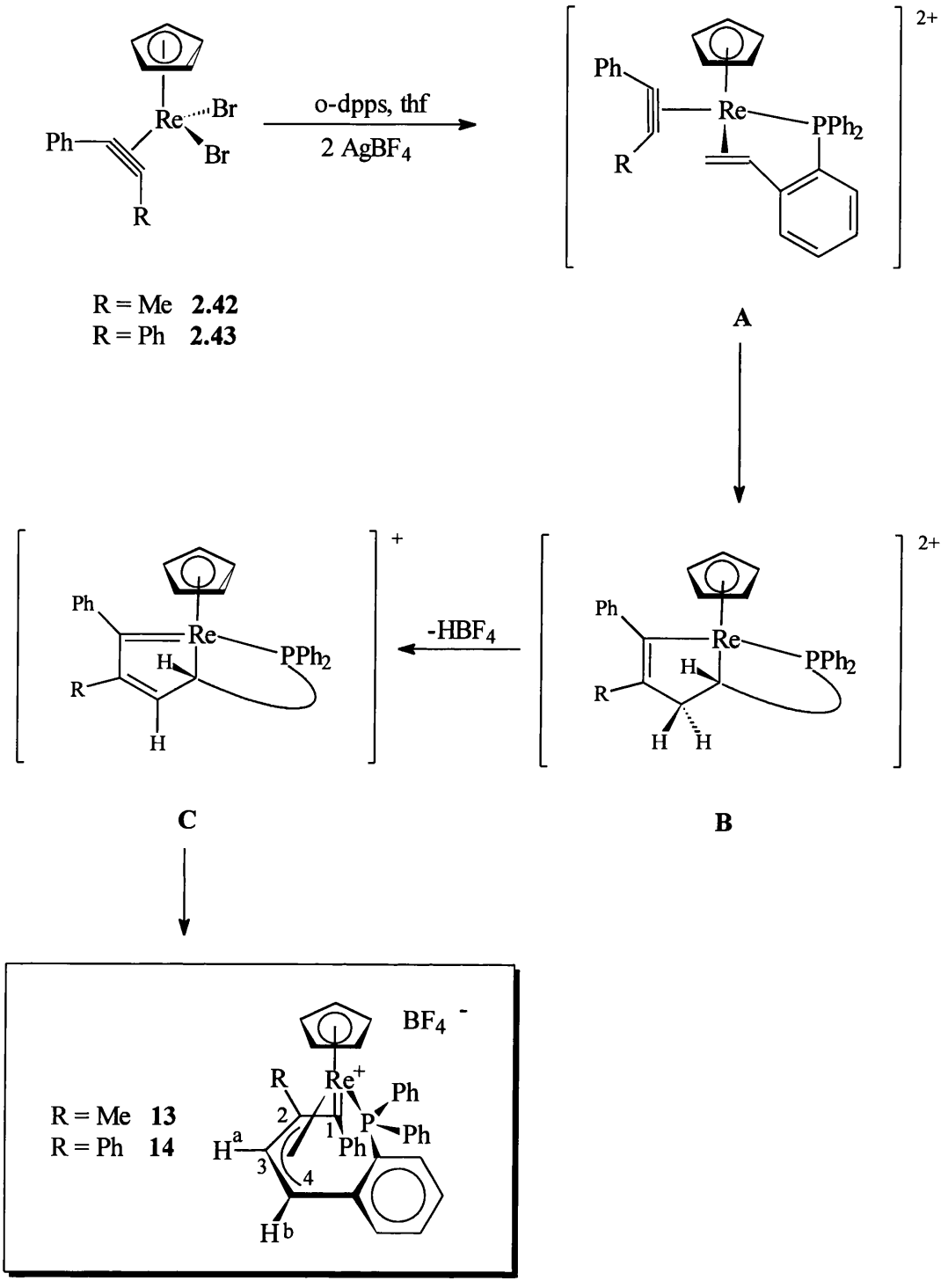

FIGURE 2.55

The formation of metallacyclopentenes *via* the coupling of alkenes and alkynes i.e. **B** (Figure 2.55) has been known for many years in the field of

cyclisation reactions of alkyne and alkenes promoted by zirconium complexes.[64] It is proposed that these cyclisation reactions occur through the formation of five-membered metallacycles (Figure 2.56).

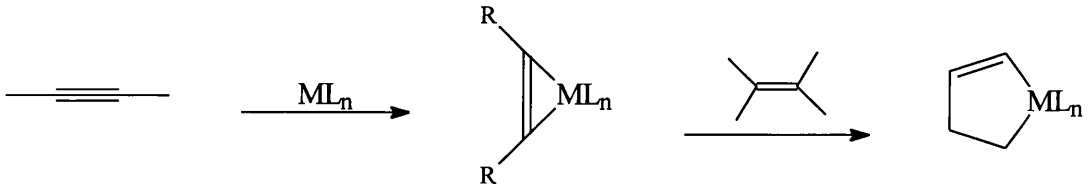

FIGURE 2.56

Of particular interest are the bi-cyclisation reactions of enynes (**A**, Figure 2.57), which result in metallacyclopentenes (**B**, Figure 2.57) that allow regio-selective transformations. Zirconium-promoted bi-cyclisation of enynes is applicable to a wide variety of monocyclic, bicyclic and polycyclic compounds, including terpenoids, although at present the number of such applications is still small.[64]

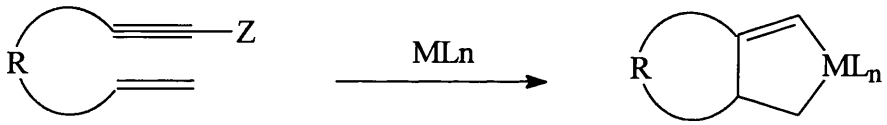

A **B**

FIGURE 2.57

Consideration of the molecular orbital interactions suggest that transition metal complexes having at least two empty and one filled nonbonding metal valence shell orbital would be ideal for facile bi-cyclisation reactions.[64] This was based on assumptions that effective π-complexation of an alkyne or an alkene with a metal complex requires the simultaneous availability of one empty and one filled non-bonding metal orbital as illustrated in Figure 2.58.

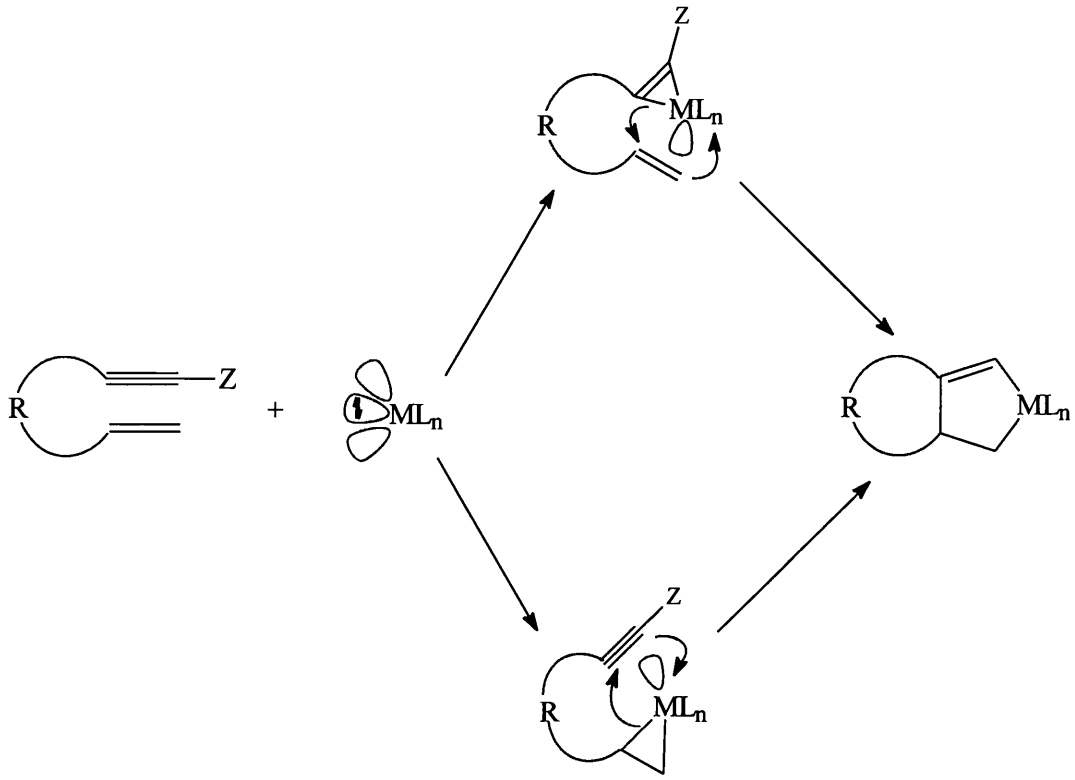

FIGURE 2.58

The formation of **13** and **14** was also of importance in that it provided an insight into Mo and Re mediated formation of 1,3-dienes *via* the coupling of alkynes and alkenes. Earlier studies of the chemistry of η^2(4e)-bonded molybdenum alkyne complexes observed that when the cation [Mo{η^2(4e)-MeC_2Me}(dpps)(η-C_5H_5)][BF_4] **2.67** was refluxed in acetonitrile solution, surprisingly a carbon-carbon coupling reaction and a 1,3-H-shift process occurred resulting in the formation of the 1,3-diene complex [Mo(NCMe){η^4-$MeCH{=}C(Me)CH{=}CHC_6H_4PPh_2$-o}($\eta$-$C_5H_5$)][$BF_4$] **2.68** (Figure 2.59).[19]

The initial step involves the co-ordination of the good σ donor acetonitrile, which was accommodated by a simultaneous 'switch' in the bonding mode of the but-2-yne ligand (4e to 2e). This was followed by a metallacyclopent-2-ene ring (**A**, Figure 2.59) formation similar to that observed in the zirconium bi-cyclisation

of enynes. A 1,3-hydrogen shift process generated the intermediate **B**, which then collapsed to give the final product **2.68**. Deuterium labelling studies using α-[^{2}H]-*o*-diphenylphosphinostyrene indicated that an α-elimination was not involved in the transformation of **2.67** to **2.68** and that the exact nature of the 1,3-shift process was not entirely clear.

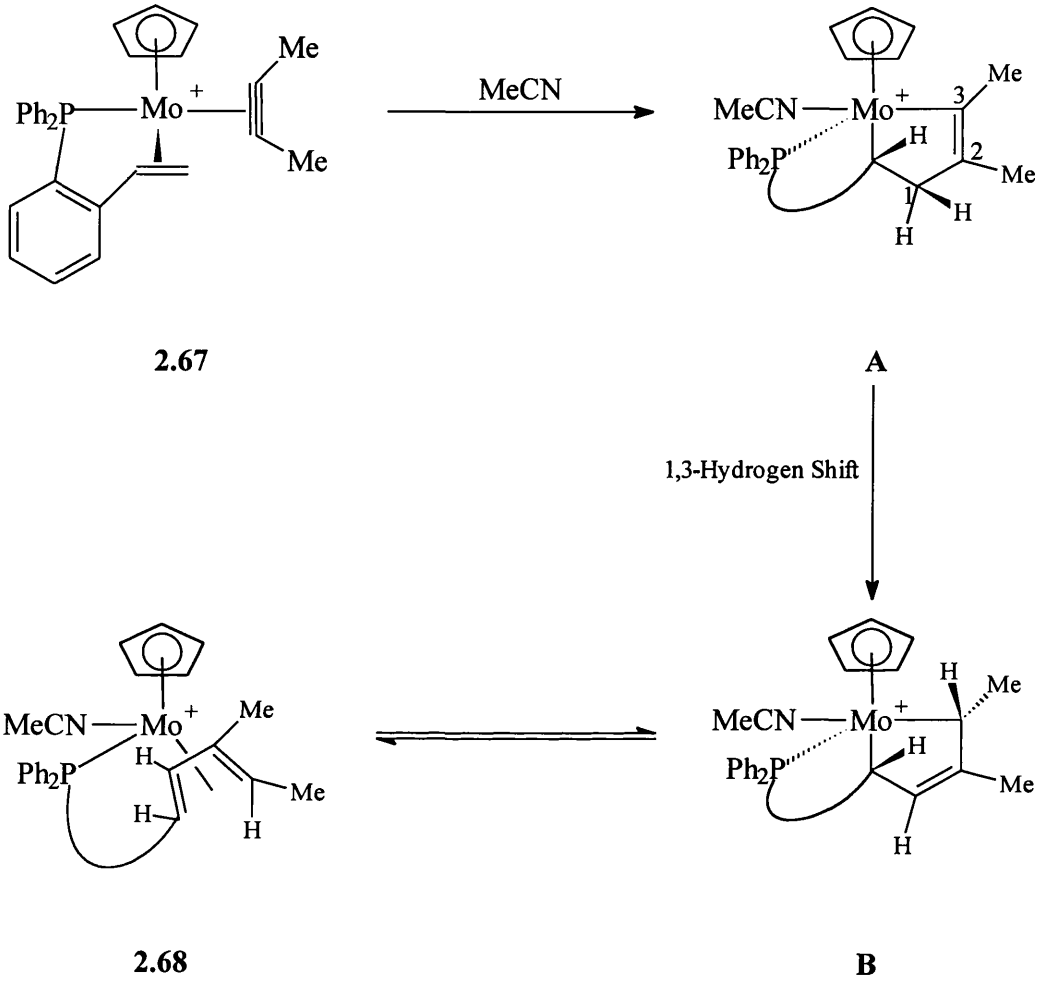

FIGURE 2.59

Later, in a related study, it was reported by Herrmann and co-workers[65] that treatment of [$ReCl_2(\eta^2\text{-}MeC_2Me)(\eta\text{-}C_5Me_5)$] **2.69** with an alkene and a catalytic amount of $HBF_4.Et_2O$ resulted in the formation of the 1,3-diene complexes [$ReCl_2(\eta^4\text{-}1,3\text{-diene})(\eta\text{-}C_5Me_5)$] **2.70** (Figure 2.60). Again, a suprafacial 1,3-hydrogen shift occurred but the exact nature of this process was not elucidated.

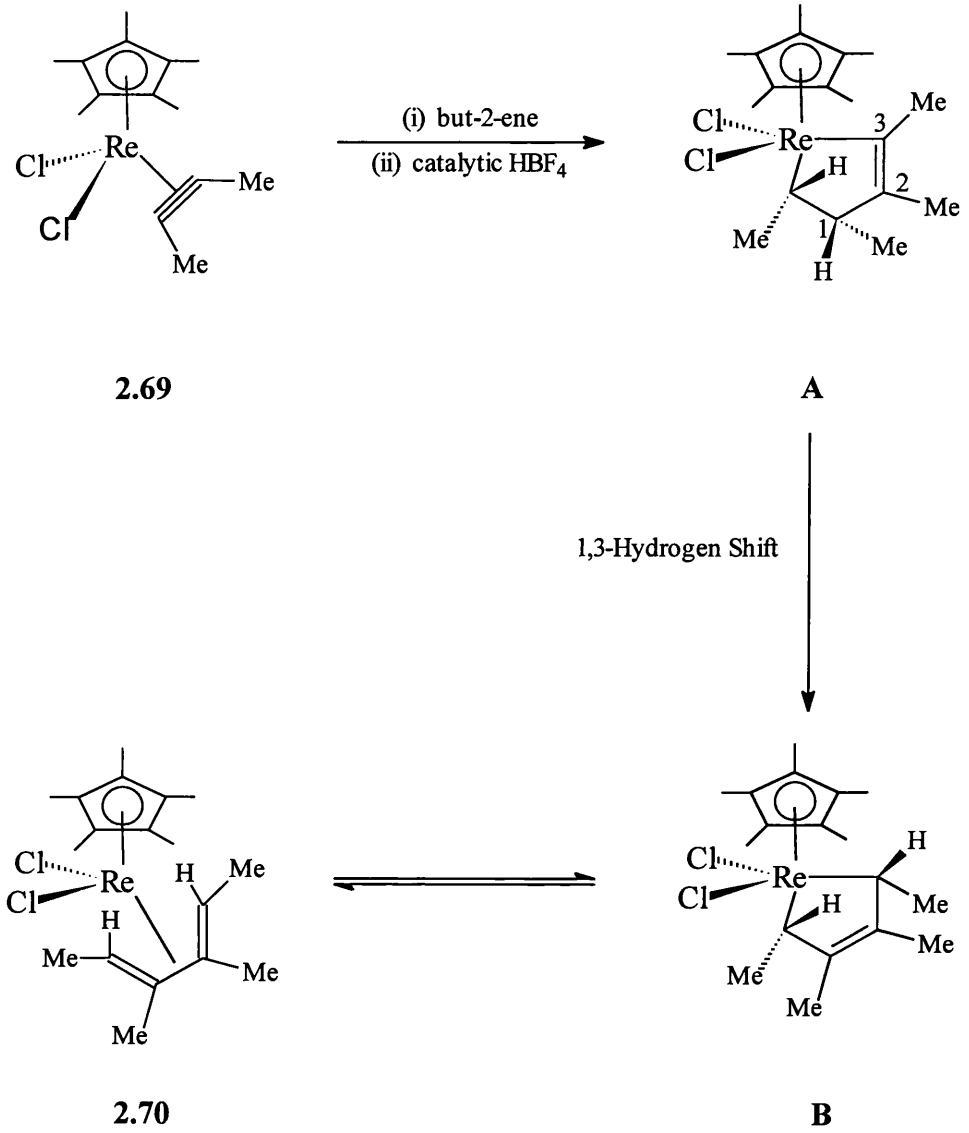

2.69 **A**

2.70 **B**

FIGURE 2.60

In both of the above reactions (Figures 2.59 and 2.60) metallacyclopent-2-enes were implicated as intermediates and it was suggested that the five-membered ring intermediates were formed by oxidative coupling of the co-ordinated alkyne and alkene ligands. However, in order to transform these species into a 1,3-diene, a 1,3-H-shift process is required This poses a major difficulty in that a β-H elimination is a most unlikely pathway as it requires a *cis*-coplanar transition state. Also, a suprafacial 1,3-shift is unlikely as it is generally disallowed on the principle

of symmetry conservation, although, it has been previously postulated[19] that the metal could assist in a suprafacial 1,3-hydrogen shift by donating electrons into the π^* orbital such that it became sufficiently populated to facilitate a 1,3-suprafacial shift. It is, therefore, clear that if the synthetic organic potential of the coupling of alkenes and alkynes is to be exploited a better understanding of the hydrogen-shift process is required.

The formation of **13** and **14** lends some insight into these 1,3-suprafacial shifts in that if proton loss occurred from the β-carbons of the metallacyclopent-2-enes implicated in the molybdenum chemistry (**C**, Figure 2.61) or in Herrmann's rhenium system (**E**, Figure 2.61), then the metallacyclopentadienes **D** and **F** would result, respectively. These intermediates would be analogous to **B** (Figure 2.61), which has been proposed as an intermediate in the formation of **13** and **14** (Figure 2.55). Unlike **B**, however, **D** and **F** do not carry a positive charge and, hence, would be liable to attack by a proton on the alkylidene α-carbon resulting in the formation of a 1,3-diene. Thus, it is suggested that the required suprafacial 1,3-H shift mentioned earlier is actually achieved by deprotonation followed by transfer of the resulting proton across the face of the five-membered ring to the electron-rich alkylidene carbon.

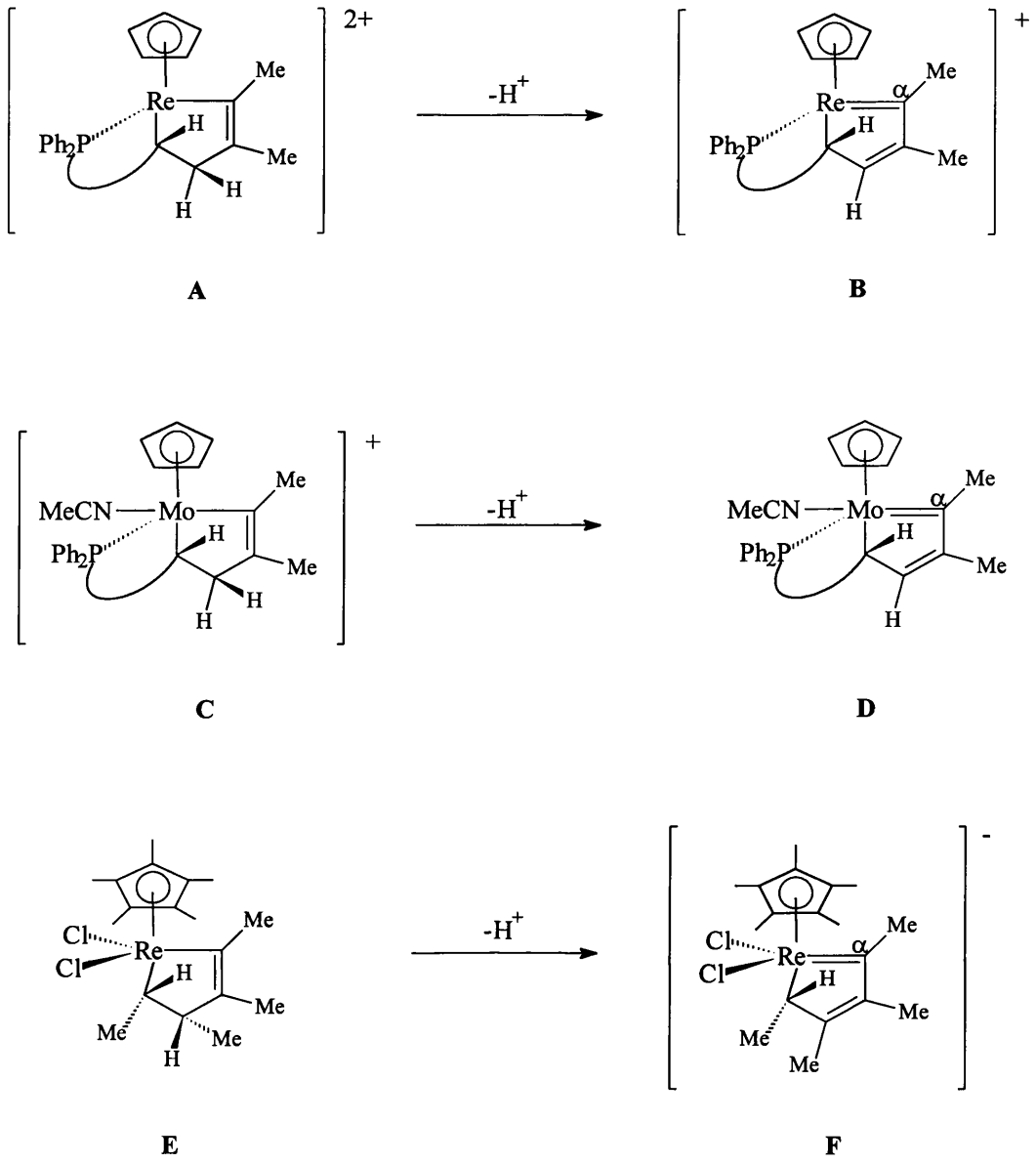

FIGURE 2.61

In summary, a new synthetic pathway to η^4(5e)-butadienyl ligands has been established, and a mechanistic insight gained into how 1,3-dienes can be formed from alkenes and alkynes.

2.8 Reactivity of Rhenium η^4(5e)-Butadienyl Complexes.

The reactivity of η^4(5e)-butadienyl complexes can be divided into three categories, the first of which involves the dechelation of the alkene tail to form η^2-vinyl complexes. For example, addition of dithiocarbamate to the cationic butadienyl tungsten complex $[W(S_2CNR_2)_2(\eta^4\text{-}C_4Ph_4H)][BF_4]$, results in dechelation of the alkene tail to form the neutral tris (dithiocarbamate) complex containing a vinyl-substituted η^2-vinyl ligand, $[W(S_2CNR_2)_3\{\eta^2\text{-}C(Ph)=C(Ph)C(Ph)=C(Ph)H\}]$ **2.71** (Figure 2.62).[66]

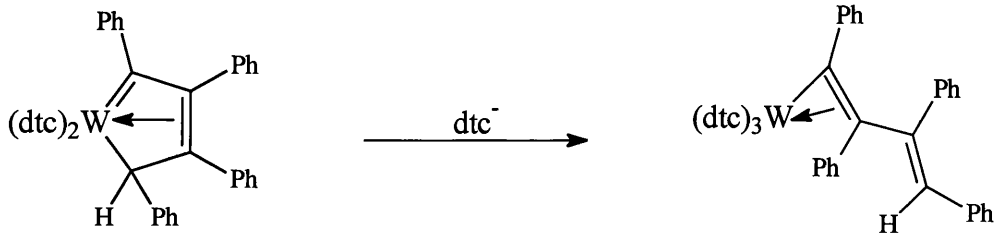

2.71

FIGURE 2.62

The reactivity of the η^4(5e)-butadienyl ligand can also be associated with the metal-carbon double bond or its potential ability to behave as a masked η^3(3e) butadienyl complex. Indeed, reaction of $[Ru{=}C(Ph)\text{-}\eta^3\text{-}\{C(Ph)C(Ph)CH(Ph)\}(\eta\text{-}C_5H_5)]$ **2.55** with $P(OMe)_3$ or PPh_3 affords the complexes $[RuL\{C(Ph){=}C(Ph)\text{-}\eta^2\text{-}C(Ph){=}CH(Ph)\}(\eta\text{-}C_5H_5)]$ L = $P(OMe)_3$ **2.72** and PPh_3 **2.73** (Figure 2.63). This reaction involved a change in the bonding mode of the butadienyl fragment from η^4(5e) to η^3(3e) in order to accommodate the attacking ligand at the ruthenium centre.[67]

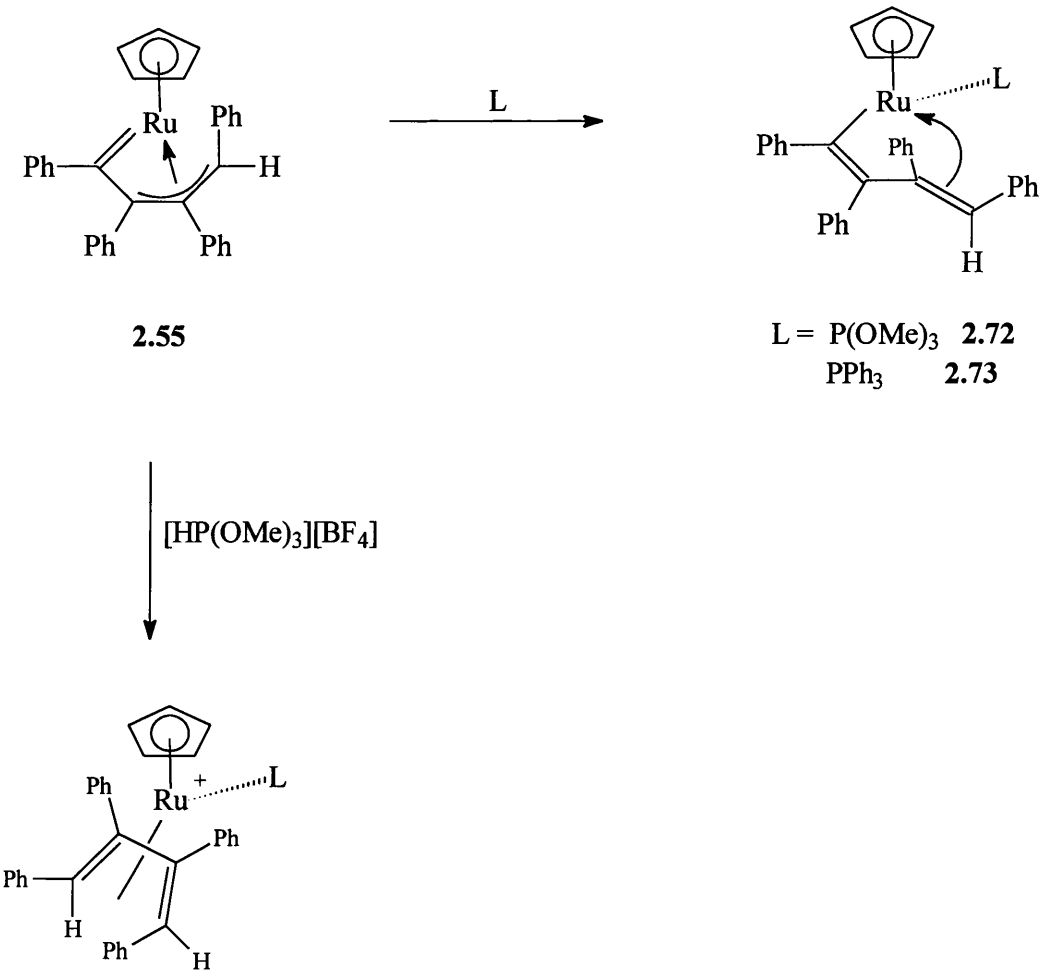

2.55

L = $P(OMe)_3$ **2.72**
PPh_3 **2.73**

2.74

FIGURE 2.63

The ruthenium species, $[Ru{=}C(Ph)\text{-}\eta^3\text{-}\{C(Ph)C(Ph)CH(Ph)\}(\eta\text{-}C_5H_5)]$ **2.55**, was also susceptible to attack at the α-alkylidene carbon by protons to form the substituted buta-1,3-diene complex **2.74** (Figure 2.63).[67] This propensity to form buta-1,3-dienes by attack of H^+ or H^- on the α-carbon also manifests itself in cationic $\eta^4(5e)$ butadienyl species, where complexes such as $[MoBr\{P(OMe)_3\}\{{=}C(Me)\text{-}\eta^3\text{-}\{C(Me)C(Me)CHMe\}(\eta^5\text{-}C_5H_5)][BF_4]$ **2.58** react with hydride sources to form the 1,3-diene complex $[MoBr\{P(OMe)_3\}\{\eta^4\text{-}\{CH(Me){=}C(Me)C(Me){=}C(H)Me\}(\eta^5\text{-}C_5H_5)]$ **2.75** (Figure 2.64).[51]

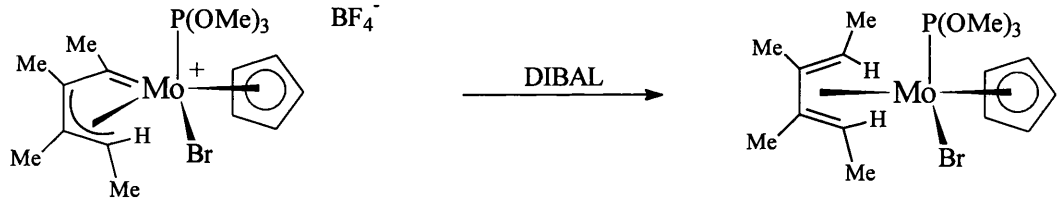

2.58 **2.75**

FIGURE 2.64 : DIBAL = Diisobutylaluminium hydride

In the light of these observations it was clearly of interest to examine the reactivity of the cationic η^5-butadienyl complex [Re=C(Ph)-η^3-{C(Ph)CHCH $C_6H_4PPh_2$-o}(η-C_5H_5)][BF_4] towards sources of H^-. First, however, an EHMO calculation was carried out based on the bond parameters derived form the X-ray crystallographic study of complex [Re=C(Ph)-η^3-{C(Me)CHCH$C_6H_4PPh_2$-o}(η-C_5H_5)][BF_4] **13**. This established that the LUMO (Lowest Unoccupied Molecular Orbital) resides, in the main, on the rhenium metal and on C1, the α-alkylidene carbon, (Figure 2.65). Examination of the relative charge distribution (Table 2.13) reveals that the rhenium centre carries a negative charge, whereas C1, C2 and C3 all have a positive charge. However, although C1, C2 and C3 carry positive charges, the LUMO of the complex resides mainly on C1 and not C2 or C3. Therefore, as hydride attack is generally frontier orbital controlled, H^- would be most likely to attack at the α-alkylidene carbon (C1).

TABLE 2.13 : Charge Distribution of Complex **13**.

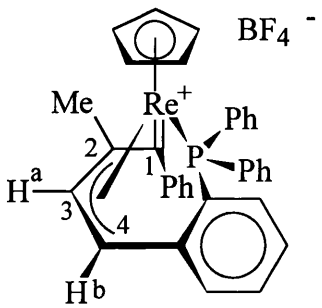

Re	C1	C2	C3	C4	P
-0.495	0.125	0.136	0.058	-0.037	0.719

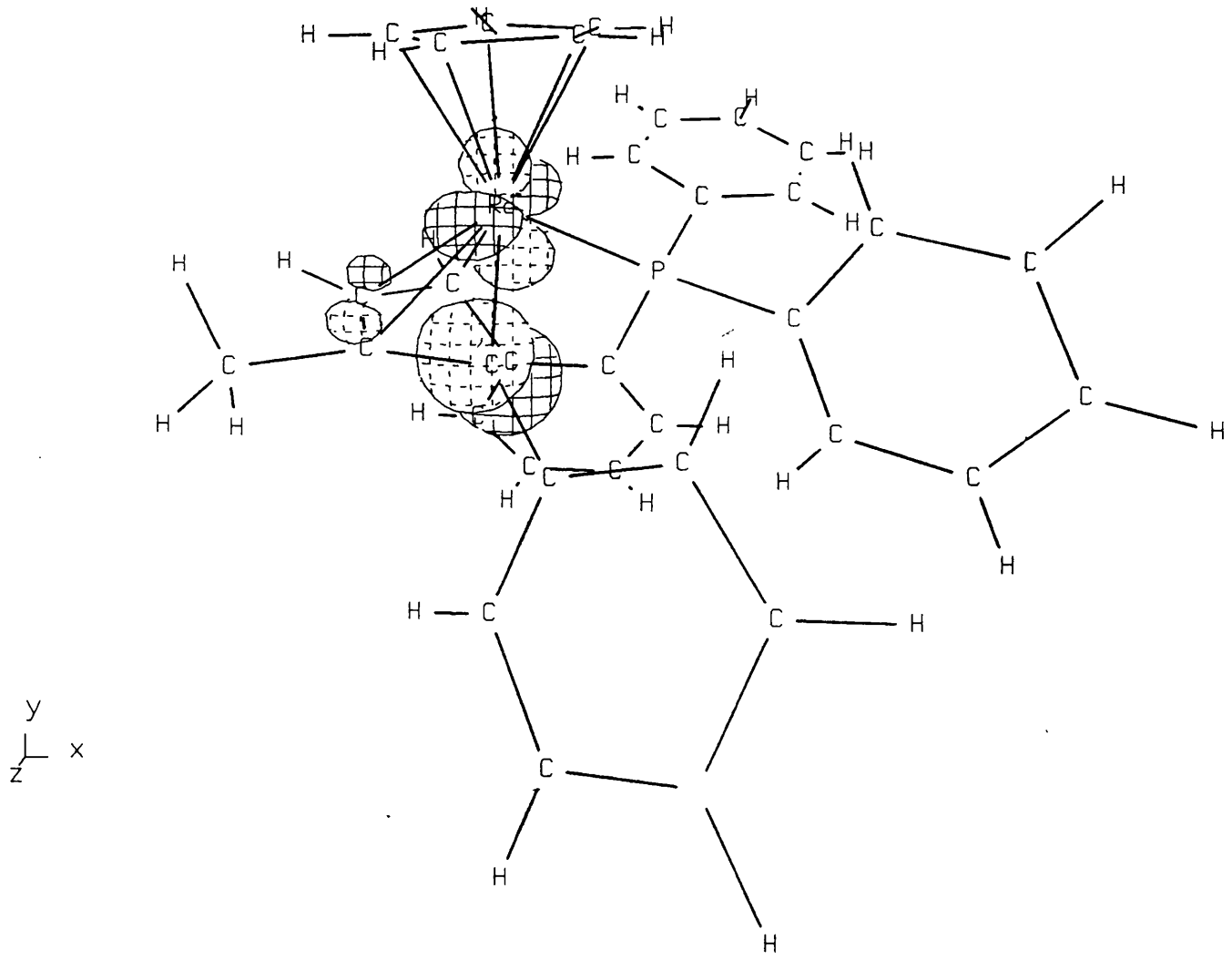

FIGURE 2.65 : LUMO of Complex **13**.

Addition of K-Selectride (-78°C) to a thf solution of complex [Re=C(Ph)-η^3-{C(Ph)CHCHC$_6$H$_4$PPh$_2$-o}(η-C$_5$H$_5$)][BF$_4$] **14** afforded the neutral, orange complex [Re{η^4-CH(Ph)=C(Ph)CH=CH(C$_6$H$_4$PPh$_2$-o)}(η-C$_5$H$_5$)] **15** (Figure 2.66), after column chromatography using a short alumina column and elution with a 4:1 dichloromethane:hexane mixture.

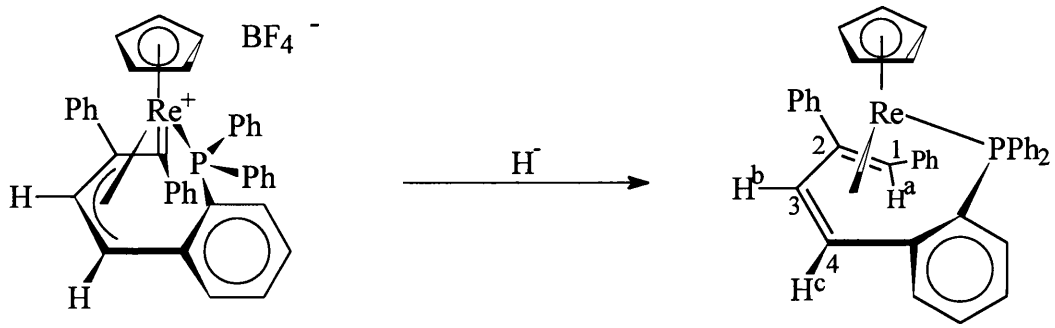

14 **15**

FIGURE 2.66

The phosphorus NMR spectrum of **15** clearly indicated that only one species was present with one singlet at δ 61.8. In the ^{1}H NMR spectrum, H^b and H^c appeared as an AB pattern [δ 5.02 and 5.14, 2H] with a similar coupling constant [J(H^{b}H^c) = 7.8 Hz] to that observed for complex [Re=C(Ph)-η^3-{C(Ph)CHCH C$_6$H$_4$PPh$_2$-o}(η-C$_5$H$_5$)][BF$_4$] **14**. The ^{13}C{^{1}H} NMR spectrum no longer displayed a low field signal characteristic of the α-alkylidene carbon suggesting that the hydride had attacked the carbene carbon. Furthermore, a C-H correlation NMR study revealed that H^b was attached to C$_3$ [δ 64.2], H^c to C$_4$ [δ 52.2] and H^a, which resonated as a singlet at δ 0.93 in the proton spectrum, was connected to C$_1$ [δ 43.2]. Therefore, it was concluded that hydride had attacked the α-alkylidene carbon to form the substituted buta-1,3-diene complex [Re{η^4-CH(Ph)=C(Ph)CH=CH(C$_6$H$_4$PPh$_2$-o)}(η-C$_5$H$_5$)] **15** (Figure 2.66).

The NMR spectra of complex **15** were similar to those previously observed for other buta-1,3-diene complexes such as [Mo(NCMe){η^4-MeCH=C(Me)CH=CH

$C_6H_4PPh_2$-o}(η-C_5H_5)][BF_4] **2.68** (Figure 2.59, Section 2.7), which was formed by the co-condensation of the alkene of *o*-dpps and a co-ordinated but-2-yne.[19] The acetonitrile ligand of **2.68** was very labile, hence allowing facile substitution reactions with carbon monoxide and trimethyl phosphite affording the complexes [Mo(CO){η^4-MeCH=C(Me)CH=$CHC_6H_4PPh_2$-o}(η-C_5H_5)][BF_4] **2.76** and [Mo{$P(OMe)_3$}{η^4-MeCH=C(Me)CH=$CHC_6H_4PPh_2$-o}(η-C_5H_5)][BF_4] **2.77**, respectively.[19] A comparison of the ^1H and $^{13}C\{^1H\}$ NMR spectra of **15**, **2.68**, **2.76** and **2.77** (Table 2.14), reveals that complex **15** exhibits similar characteristics to the previously observed buta-1,3-dienes **2.68**, **2.76** and **2.77**. All these buta-1,3-dienes exhibited resonances in the ^1H NMR spectra due to H^a at *ca* δ 1.0 and H^b and H^c in the range δ 3.6 - 6.0 with a coupling constant of approximately 8-9 Hz.

TABLE 2.14 : Comparison of the ^1H NMR of Complexes **15**, **2.68**, **2.76** and **2.77**.

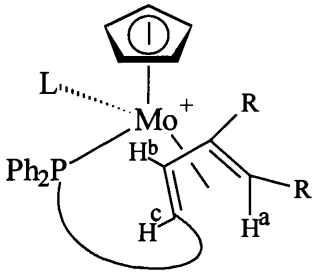

^1H NMR (δ) /Complex	**15**	**2.68** L = MeCN	**2.76** L = CO	**2.77** L = $P(OMe)_3$
H^a	0.93	1.80	1.78	1.20
H^b and H^c	5.02, 5.14	4.80, 3.59	5.98, 4.76	5.32, 4.32
$J(H^bH^c)$	7.8	9.8	8.5	8.9

The exact stereochemistry of C_1 in complex [Re{η^4-CH(Ph)=C(Ph) CH=$CH(C_6H_4PPh_2$-o)}(η-C_5H_5)] **15** could not be determined from NMR spectrum alone. Therefore, in order to elucidate the precise molecular structure, attempts were made to grow crystals of **15** suitable for a single crystal X-ray diffraction (Figure 2.67, selected bond lengths and angles are listed in Table 2.15).

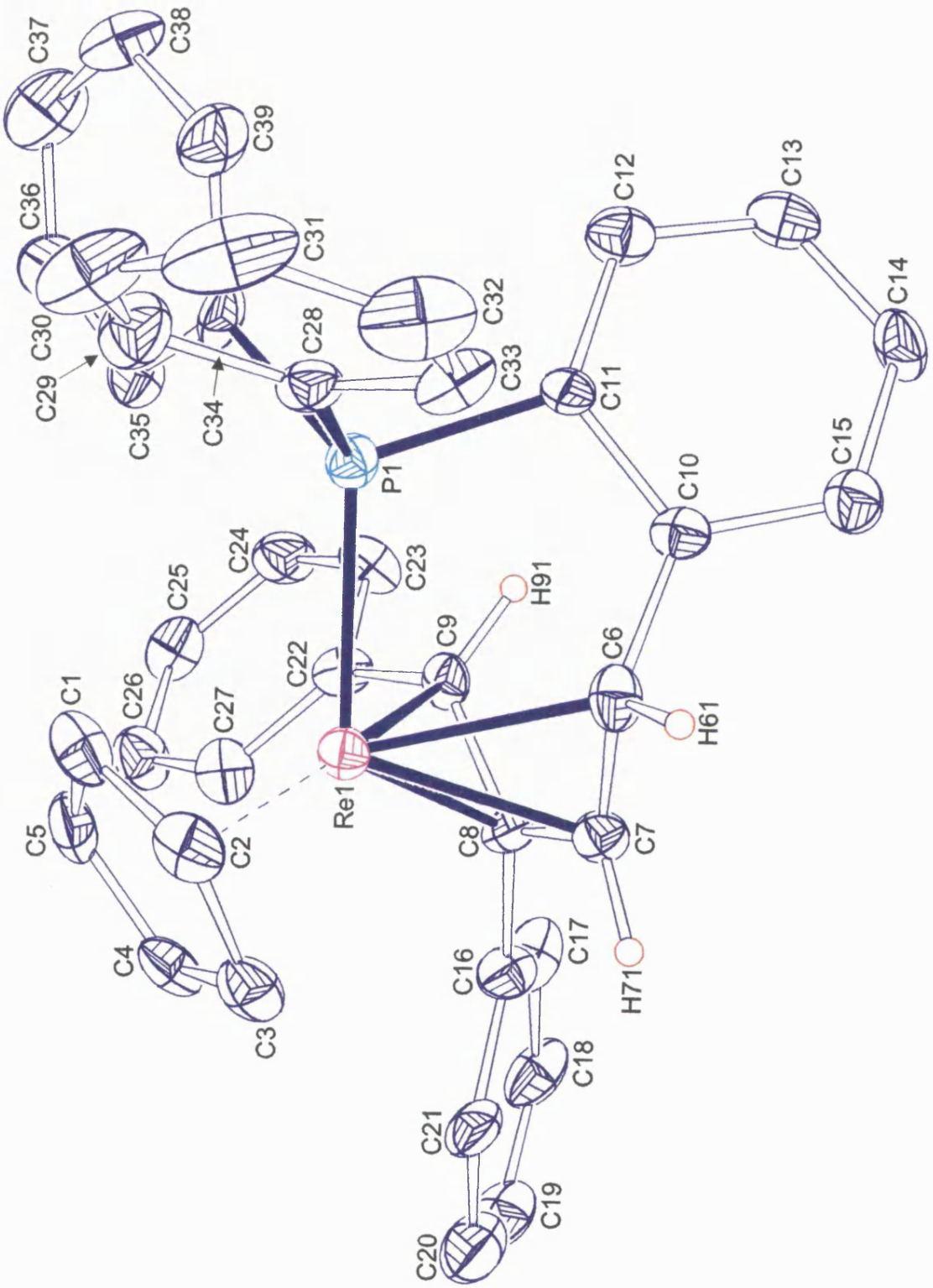

FIGURE 2.67 : ORTEP Drawing of **15**

TABLE 2.16 : Table of Selected Bond Lengths (Å) and Angles (°) of **15**.

Atoms	Bond Length	Atoms	Bond Length
Re-C9	2.264(9)	Re-P1	2.335(3)
Re-C8	2.199(10)	C9-C8	1.424(14)
Re-C7	2.184(11)	C8-C7	1.43(2)
Re-C6	2.229(11)	C7-C6	1.43(2)

Atoms	Torsion Angle	Atoms	Torsion Angle
C6-C7-C8-C9	6.37	H71-C7-C6-H61	10.68
C22-C9-C8-C16	14.44	C16-C8-C7-C6	-179.99

As predicted by the EHMO calculation the hydride had attacked the α-alkylidene carbon to form a substituted buta-1,3-diene complex. The diene of complex **15** adopts the expected *cisoid* geometry and is exemplified by the torsion angle of C6-C7-C8-C9 (6.37°). The hydride has attacked the α-carbon such that the two phenyl substituents are *cis* to each other (C22-C9-C8-C16 14.44°) and the hydrogen is in the *anti* position. As discussed previously in Section 2.4 when a *cis* buta-1,3-diene co-ordinates to a metal centre it can adopt one of two resonance structures (Figure 2.33, Section 2.4) i.e. a π complex or a metallacyclopentene. In complex **15** the C6-C7, C7-C8 and C8-C9 bond distances are very similar at *ca* 1.43 Å, with the internal diene carbons, C7 and C8, being slightly closer to the metal [2.184(11) and 2.199(10) Å, respectively] than C6 and C9 [2.229(11) and 2.264(9) Å]. This is indicative of π complexation of the diene (see Table 2.8, Section 2.4) rather than a metallacyclopentene co-ordination of the diene.

As mentioned previously, (Section 2.5) treatment of a co-ordinated buta-1,3-diene with trityl tetrafluoroborate can lead to the formation of η^4(5e)-butadienyls or seventeen-electron cations.[51] Therefore, it was obvious of interest to treat the orange complex [Re{η^4-CH(Ph)=C(Ph)CH=CH($C_6H_4PPh_2$-o)}(η-C_5H_5)] **15** with trityl tetrafluoroborate.

Addition of one equivalent of trityl tetrafluoroborate to a dichloromethane solution of complex **15** resulted in a colour change of orange to dark green over the period of one hour. The resulting green powder was recrystallised from dichloromethane/ether and was identified as complex [Re=C(Ph)-η^3-{C(Ph)CHCH $C_6H_4PPh_2$-o}(η-C_5H_5)][BF_4] **14** by ^1H and $^{31}P\{^1H\}$ NMR spectroscopy. (Figure 2.68).

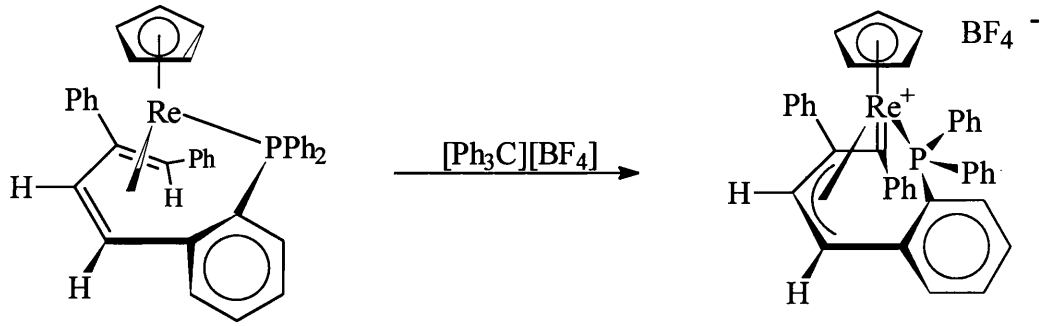

15 **14**

FIGURE 2.68

Interestingly, whilst chromatographing complex **15** using a longer column than before an unusual observation was noted. The orange band, initially, moved as before with a 4:1 hexane:dichloromethane mixture. However, as the orange band progressed down the column the orange coloration appeared to fade to pale yellow. The pale yellow fraction was collected and the solvent was removed *in vacuo* to afford a yellow powder (**16**), which surprisingly had the same mass spectrum [(M^+) 718] as complex **15**. The $^{31}P\{^1H\}$ NMR spectrum of complex **16** showed only one species was present at δ 56.5. The ^1H NMR spectrum of complex **16** also differed from that observed for **15** in that there were three resonances which each integrated for one hydrogen, one doublet at δ 2.86 (J = 14.5 Hz) and two singlets at δ 2.74 and 4.09. Unusually, an H-H COSY NMR study did not display any off diagonal peaks, therefore implying that the three hydrogens were not significantly coupled to any other hydrogens and so the doublet at δ 2.86 is probably due to phosphorus coupling. The $^{13}C\{^1H\}$ NMR spectrum of complex **16**

also differed from that observed for complex **15** in that the four carbons of the C_4 chain now resonated at δ 23.7, 31.6, 71.8 and 91.4.

TABLE 2.16 : Comparison of the ^1H, $^{13}C\{^1H\}$ and $^{31}P\{^1H\}$ NMR Spectra of Complexes **15** and **16**.

NMR (δ) / Complex	15	16
^1H		
H^a	0.93	2.74
H^b	5.02	4.09
H^c	5.14	2.86
$^{13}C\{^1H\}$		
C_1 and C_4	43.2, 52.2	23.7, 31.6
C_2 and C_3	64.2, 82.4	71.8, 91.4
$^{31}P\{^1H\}$	61.8	56.5

Comparison of the $^{13}C\{^1H\}$ NMR spectra (Table 2.16) of complexes **15** and **16** indicates that two carbons have become more sp^3- like, in that there are two upfield signals at δ 23.7 and δ 31.6. Also, a comparison of the ^1H NMR spectra (Table 2.16) suggests a similar trend in that in complex **15** H^a, H^b and H^c resonate at δ 0.93, 5.02 and 5.14, respectively, whereas, in complex **16** two hydrogens have similar shifts at *ca* δ 2.8 and one at δ 4.09. The signals at δ 2.74 and δ 2.86 indicate that these hydrogens are possibly attached to an sp^3 carbon, whereas the signal of δ 4.09 is more indicative of an sp^2 carbon.

Therefore, it is postulated that complex **16** contains a metallacyclopentene (Figure 2.68) in which C_1 and C_4 are σ bonded to the metal and C2-C3 is an internal double bond. This would result in H^a and H^c (δ 2.74 and δ 2.86) being attached to sp^3 carbons and H^b (δ 4.09) to an sp^2 carbon. The possible driving force for this rearrangement could be that in chromatographing the product on a longer alumina column the complex (**15**) picks up water, which co-ordinates to the rhenium metal altering the butadiene π complexation to that of a

metallacyclopentene in which the internal double bond does not co-ordinate to the metal centre (Figure 2.69).

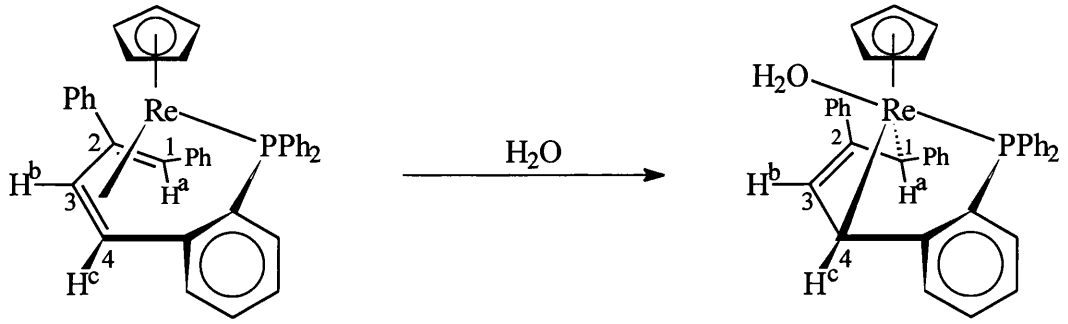

15 **16**

FIGURE 2.69

The fact that the co-ordinated water could not be detected in the ^{1}H NMR spectrum is not particularly unusual as co-ordinated water signals can be broad and very difficult to detect. For example, the butadienyl complex $[MoBr(OH_2)\{=C(Me)\text{-}\eta^3\text{-}\{C(Me)C(Me)CHMe\}(\eta\text{-}C_5H_5)][BF_4]$ **2.57** (Figure 2.50, Section 2.7) contains a co-ordinated water molecule which was not detected by ^{1}H NMR spectrum and was only discovered after a single crystal X-ray diffraction study.[60]

In the ^{1}H NMR spectrum of complex **16** H^b and H^c appear no longer to couple to each other. This is not as peculiar as it may first appear. In organic chemistry Karplus[68] predicted an approximate relationship between the torsion angle (Φ) and the vicinal coupling constant $J_{H\text{-}C\text{-}C\text{-}H'}$, which is usually expressed as the Karplus equation in the form :

$$J = J^0 \cos^2 \Phi - C \qquad [0° \leq \Phi \leq 90°]$$

$$J = J^{180} \cos^2 \Phi - C \qquad [90° \leq \Phi \leq 180°]$$

where, J^0, J^{180} and C are constants for which the values J^0 = 8.5 Hz, J^{180} = 9.5 Hz and C = -0.3 Hz were originally chosen. Thus, the Karplus equation shows that, for

unperturbed organic molecules, the coupling constant tends towards zero as the torsion angle tends towards 90°. A similar situation can be envisaged as occurring in complex **16**, where the torsion angle H^b-C_3-C_4-H^c is such that the coupling $J(H^bH^c)$ is at the minimum and, hence, appears to be zero.

The exact nature of this yellow complex **16** is still being investigated but it is envisaged that a single crystal X-ray diffraction study is required to elucidate conclusively the structure.

3. RHENIUM η^4-CYCLOBUTADIENE COMPLEXES.

3.1. Introduction.

The field of cyclobutadiene-metal chemistry emerged in 1956 with the theoretical prediction of its feasibility by Longuet-Higgins and Orgel,[69] and soon after (1959) the first substituted cyclobutadiene metal complex, $[NiCl_2(\eta^4\text{-}C_4Me_4)]_2$ **3.2** was reported.[70] This complex was prepared by Criegee and Schröder by the reaction of *trans*-3,4-dichloro-1,2,3,4-tetramethylcyclobutene **3.1** with nickel tetracarbonyl (Figure 3.1). This particular method of dehalogenation of 3,4-dihalocyclobutenes in the presence of metal carbonyls is potentially the most straightforward route. However, the main disadvantage of this synthetic approach is the limited availability of suitable dihalocyclobutenes. Modifications of this original synthesis have since been reported[71] and a significant development came in 1963 when Pettit[72] and co-workers reported the synthesis of cyclobutadiene iron tricarbonyl **3.3**, which contained an unsubstituted cyclobutadiene ring (Figure 3.1).

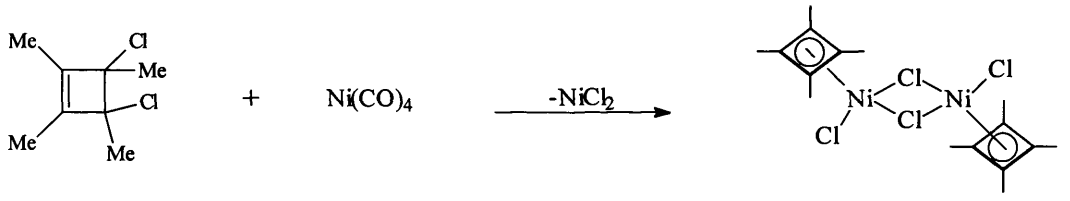

3.1 **3.2**

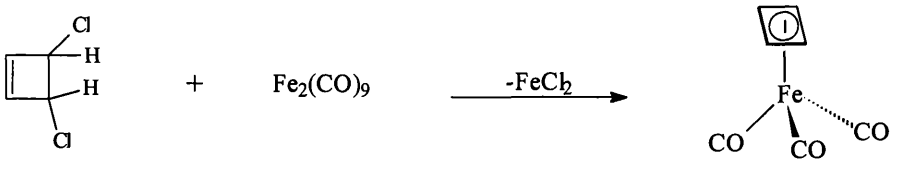

3.3

FIGURE 3.1 : Dehalogenation of Cyclobutene Dihalides

Since the initial discovery of metal cyclobutadiene complexes several alternative synthetic approaches to their synthesis have been reported,[73] including the use of photo-α-pyrone, which contains a cyclobutene unit and is obtained in near quantitative yield by photolysis of α-pyrone[74] **3.4** (Figure 3.2). In 1967[75] photo-α-pyrone was successfully employed in the synthesis of the cyclobutadiene iron complex $[Fe(CO)_3(\eta\text{-}C_4H_4)]$ **3.5** (Figure 3.2), which also generates α-pyrone iron tricarbonyl **3.6** as a by-product. The mechanism of this reaction was presumed to involve the substitution of one of the iron carbonyls by the photo-α-pyrone, followed by the loss of carbon dioxide.

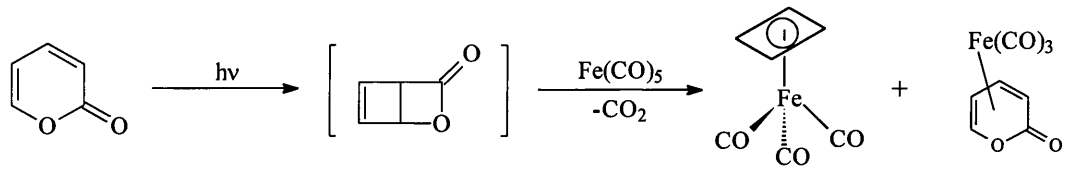

3.4 **3.5** **3.6**

FIGURE 3.2 : Decarboxylation of Photo-α-pyrone

Thus far, the synthetic routes described have involved the use of precursors which already contain a C_4 ring. However, a particularly useful synthetic approach involves the building of the C_4 ring at the metal centre *via* the cyclo-dimerisation of alkynes. This approach was successfully employed to synthesise the first reported cyclobutadiene cobalt complex, cyclopentadienyl tetraphenylcyclobutadiene cobalt **3.10**, by reaction of diphenylacetylene with various cyclopentadienyl precursors such as (cyclopentadienyl)(1,5-cyclooctadiene)cobalt[76] **3.7**, cobaltocene[77] **3.8** and cyclopentadienyl cobalt dicarbonyl[78] **3.9** (Figure 3.3).

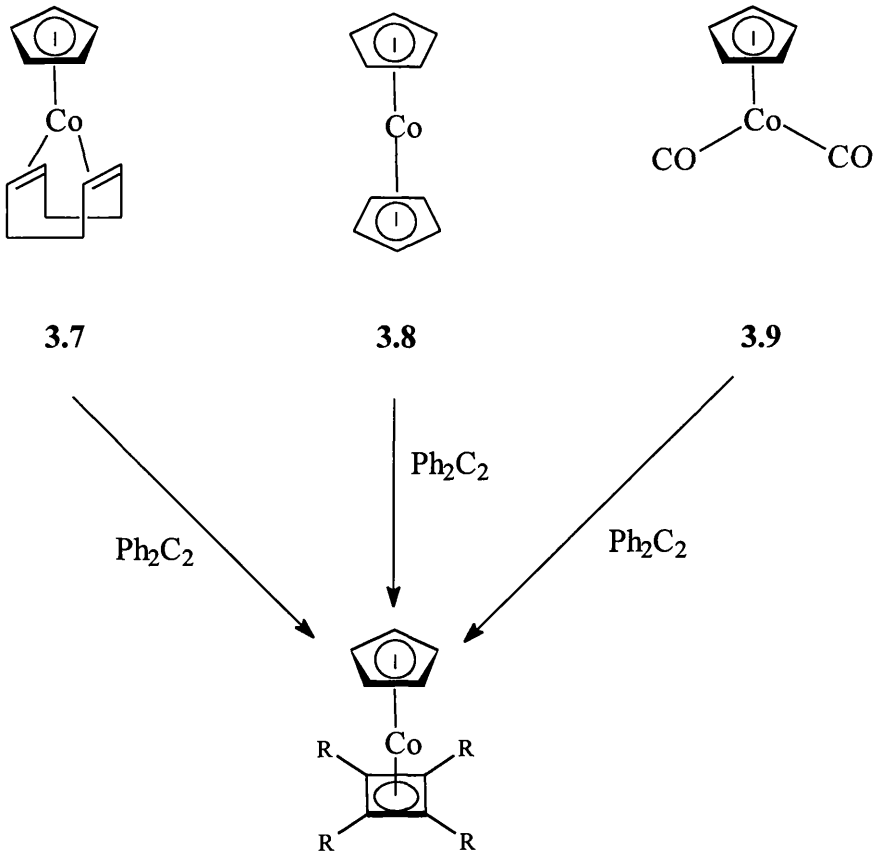

FIGURE 3.3 : Dimerisation of Alkynes at Metal Centre

In general, upon complexation to a transition metal centre the η^4-cyclobutadiene moiety adopts a square structure, which should posses two unpaired electrons. However, in the complex $[Ru(NCMe)(\eta^4\text{-}C_4Ph_4)(\eta\text{-}C_5H_5)][BF_4]$ **2.59** (Figure 3.4) the cyclobutadiene moiety was described as adopting a more rectangular shape, with C1-C2 and C3-C4 being shorter [1.44 and 1.46 Å, respectively] than the C2-C3 and C4-C1 distances [1.49 and 1.50 Å].[79]

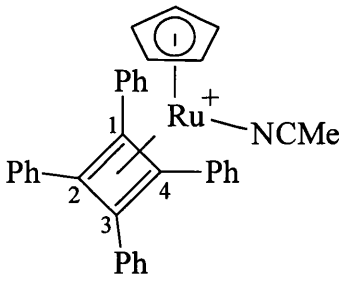

2.54

FIGURE 3.4

Since the initial discovery of these cyclobutadiene transition metal complexes their chemical properties have been extensively studied[73] and, in general, can be divided into four major categories. The first category involves reactions which do not affect the C_4R_4 ligand, such as carbonyl substitution by donor ligands, nucleophilic addition to ligands other than the cyclobutadiene moiety and introduction of σ- or π- ligands to a metal already containing a co-ordinated cyclobutadiene. The most extensive investigations in this area have been carried out on a variety of cyclobutadiene cobalt and iron complexes. Of particular note are the reactions of cyclobutadiene iron tricarbonyl complexes [**3.11** (R = H) and **3.12** (R = Ph), Figure 3.5], which react under irradiation with dimethyl fumarate,[80] dimethyl maleate[80] and *N*-carboethoxyazepine[81] to afford the cyclobutadiene derivatives **3.13**, **3.14** and **3.15**, respectively (Figure 3.5). Also, carbonyl substitution with tertiary phosphines[82] can be effected by the thermal reaction between **3.12** and triphenylphosphine to afford complex **3.16**.

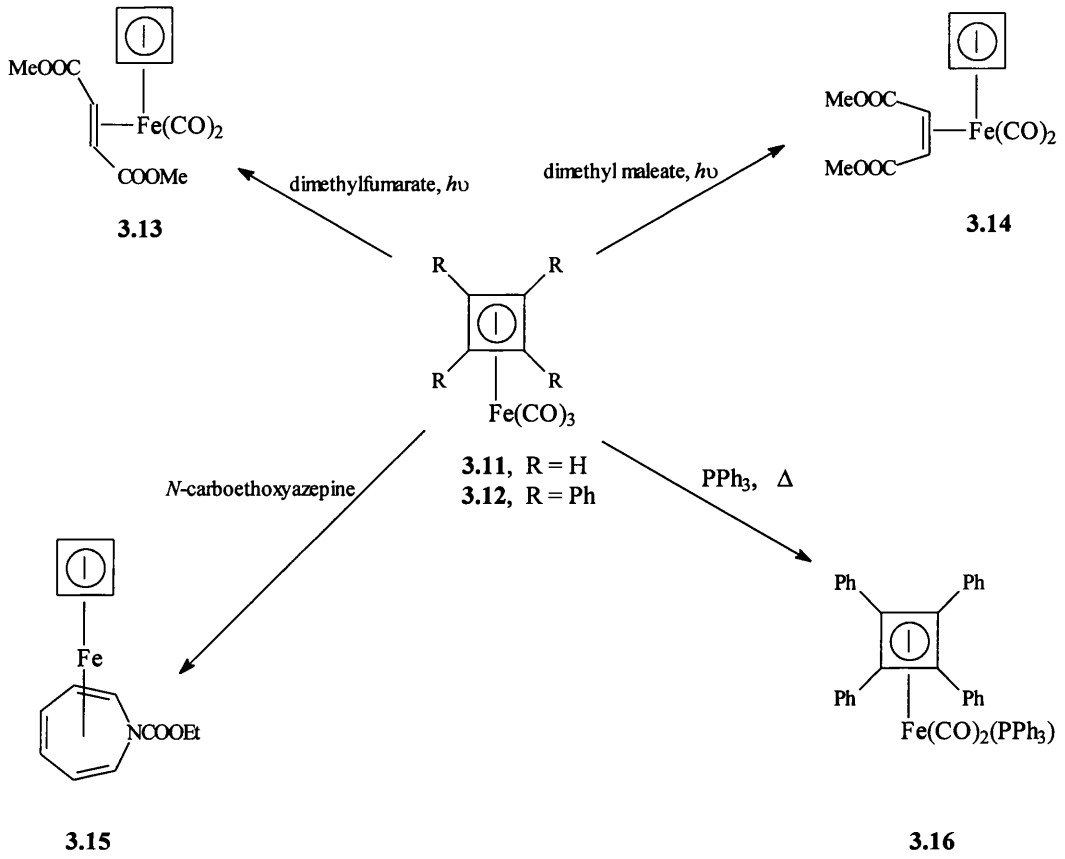

FIGURE 3.5

The second class of reactions involves the conversion of the co-ordinated cyclobutadiene to other ligands such as cyclobutenyl metal complexes. In particular, some unusual photochemical additions of unsaturated organic molecules with electron-withdrawing substituents to the cyclobutadiene ligand have been reported. For example, tetrafluoroethylene reacted upon irradiation with cyclobutadiene iron tricrabonyl **3.11** (R = H) and **3.17** (R = Me) to afford the cyclobutenyl derivatives **3.18** and **3.19** (Figure 3.6).[83] Also, a similar photochemical reaction between **3.17** and hexafluorobut-2-yne afforded the 1,2-insertion product **3.20** (Figure 3.6).[84]

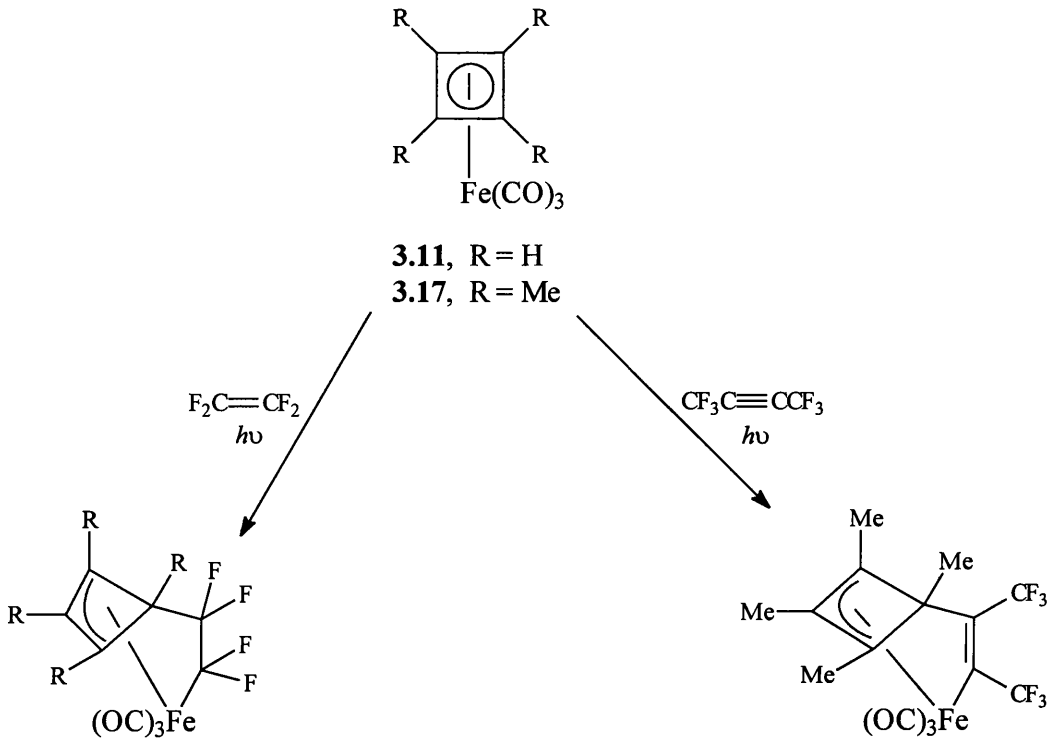

FIGURE 3.6

The third class of reactions involves organic transformations of the co-ordinated cyclobutadiene, which do not disrupt its bonding with the metal atom. Most of the studies in this area have been performed on the cyclobutadiene iron tricarbonyl systems. For example, in 1965, Pettit and co-workers demonstrated that the parent cyclobutadiene ligand in **3.11** readily underwent electrophilic substitution reactions similar to those of ferrocene. These included Friedel-Crafts acylation (**3.21**), Vilsmeier formylation (**3.22**), acetoxy mercuration (**3.23**) and deuteration (**3.24**) (Figure 3.7).[85]

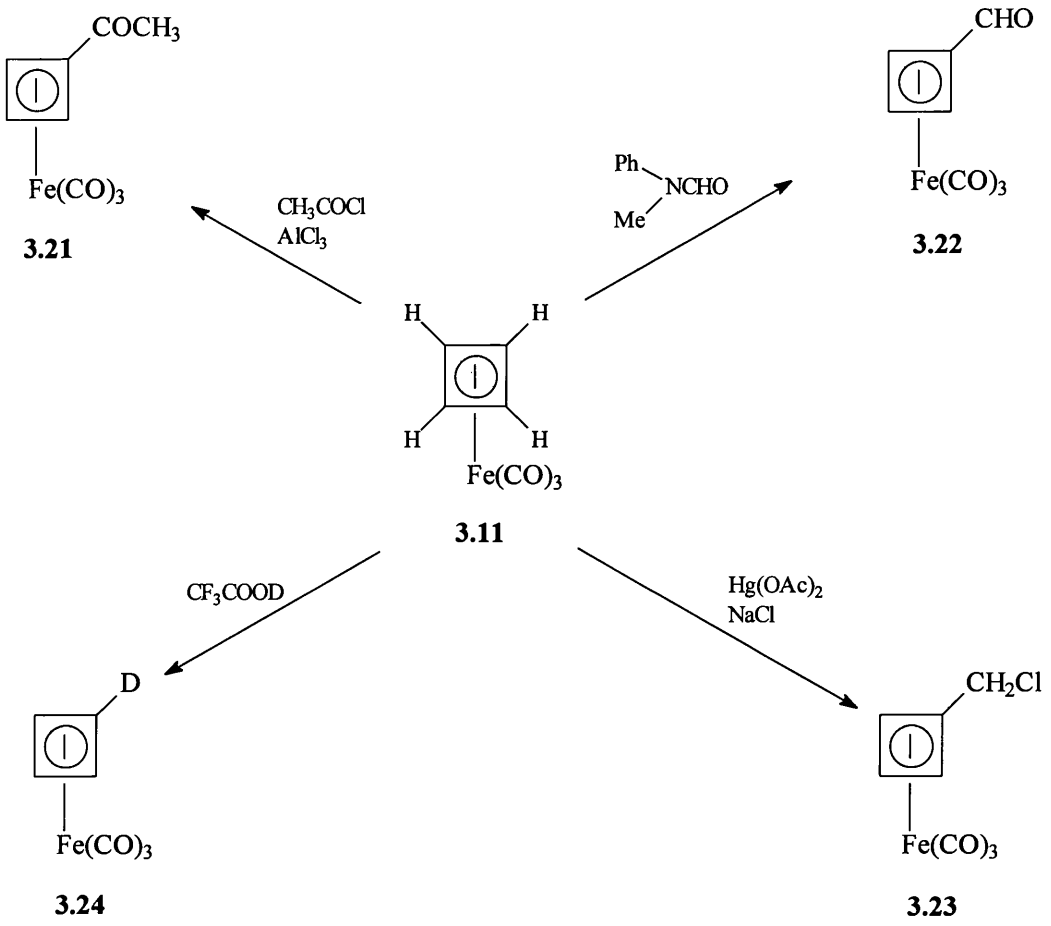

FIGURE 3.7

Mechanistically, the electrophilic substitution of **3.11** was rationalised in terms of an electrophilic addition of E^+ to give the cationic η^3-cyclobutenyl iron tricarbonyl (**3.26**) intermediate, followed by proton abstraction to afford the final product **3.27** (Figure 3.8). Although the intermediate **3.26** has not been isolated a closely related η^3-allyl iron tricarbonyl cation complex has been successfully synthesised and characterised[86] and hence supports the plausibility of the intermediate **3.26** in the electrophilic substitution of **3.11**.

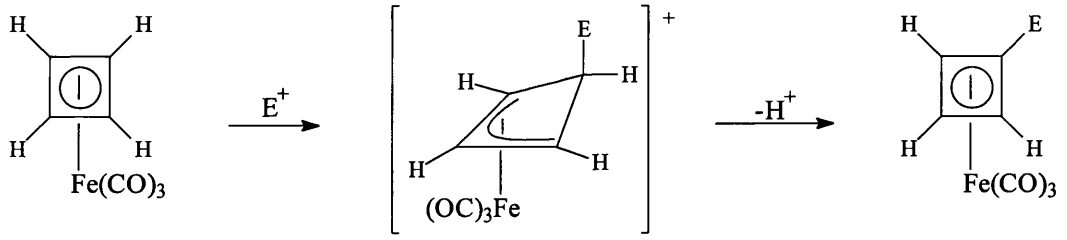

3.11 **3.26** **3.27**

FIGURE 3.8

The final class of reactions is that which causes the displacement of the co-ordinated cyclobutadiene. Cyclobutadiene iron tricarbonyl complexes have been previously shown to undergo facile oxidative decomposition when treated with Ce(IV) or Fe(III). If the oxidation is carried out in the presence of dienophiles or other substrates then a wide variety of products can be obtained. In the absence of such trapping agents oxidative decomposition of **3.11** with Ce(IV) resulted in a mixture of *syn-* and *anti-* tricyclooctadienes in a 5:1 ratio.[87] A few of the products obtained when trapping agents are employed in the oxidative decomposition of **3.11** are summarised in Figure 3.9.

Trapping Agent	Oxidising Agent	Products	Ref.
-----	Ce^{4+}	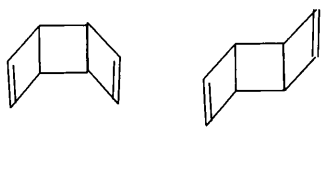 *syn* *anti*	87
CH≡CCOOMe	Ce^{4+}	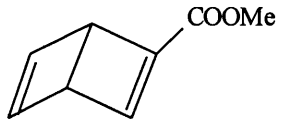	88
PhC≡CH	Ce^{4+}	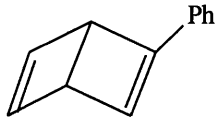	89
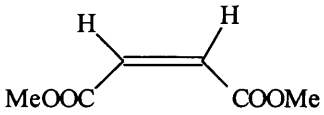	Ce^{4+}	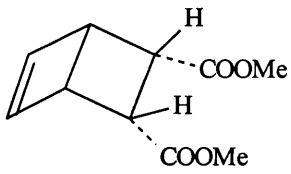	87
	Ce^{4+}	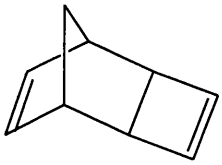	87

FIGURE 3.9

Thus, since the initial prediction by Longuet-Higgins and Orgel in 1956 the chemistry of transition metal cyclobutadiene complexes has proved to be wide and varied area.

3.2 Synthesis And Reactivity of $[ReBr(PPh_3)(\eta\text{-}C_5H_5)(\eta^4\text{-}C_4Ph_4)][BF_4]$ 17.

Recently, within our group the chemistry of the rhenium mono-alkyne complex $[ReBr_2(PhC{\equiv}CPh)(\eta\text{-}C_5H_5)]$ **2.43**, which was formed by refluxing *cis* and *trans* $[ReBr_2(CO)_2(\eta\text{-}C_5H_5)]$ **2.41** with excess diphenylacetylene in toluene under a nitrogen atmosphere for 6-8 hours (Figure 3.10), has been extensively studied.[55] However, it was discovered that if the reaction was refluxed in air for 2-4 hours the mono-alkyne complex was no longer formed and instead a second molecule of diphenylacetylene had been incorporated into the complex.[90] The co-ordination of the second molecule of diphenylacetylene resulted in a cyclodimerisation of the alkynes to form a co-ordinated tetraphenylcyclobutadiene ring $[ReBr_2(\eta^4\text{-}C_4Ph_4)(\eta\text{-}C_5H_5)]$ **3.28** (Figure 3.10). As mentioned previously, the dimerisation of alkynes at metal centres is an important route to cyclobutadiene complexes e.g. the synthesis of $[Co(\eta\text{-}C_4R_4)(\eta\text{-}C_5H_5)]$ **3.10**, which was also obtained by the thermal reaction of cyclopentadienyl cobalt dicarbonyl complex with an alkyne (Figure 3.3).

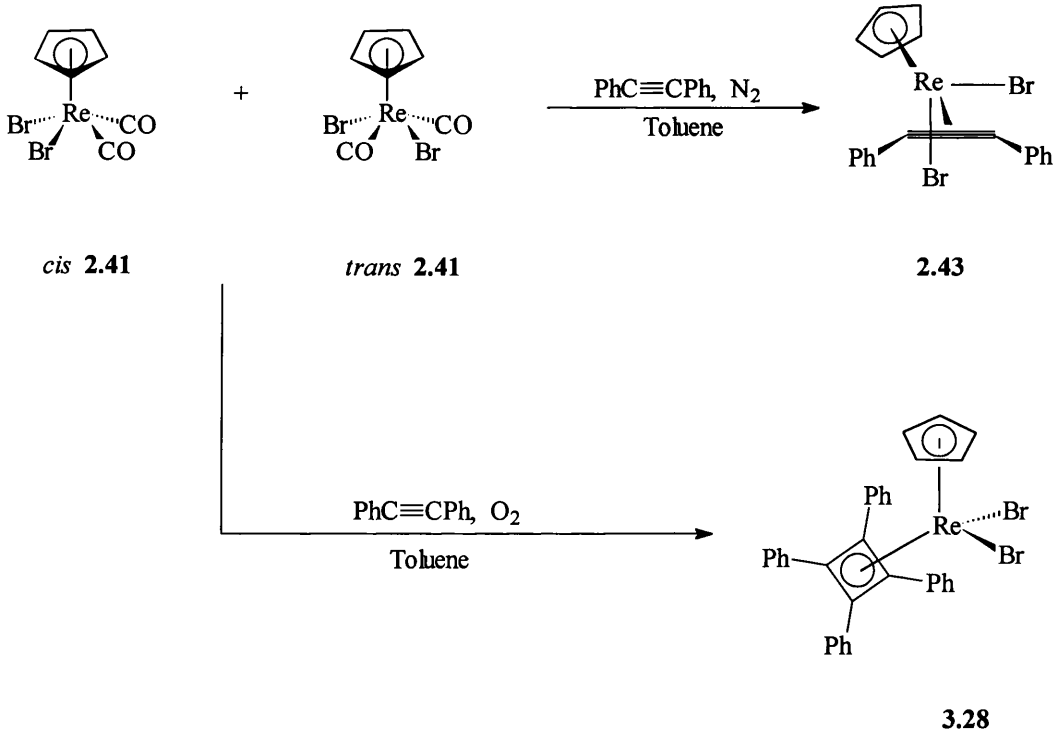

FIGURE 3.10

Therefore, having recently discovered the new cyclobutadiene metal complex, $[ReBr_2(\eta^4\text{-}C_4Ph_4)(\eta\text{-}C_5H_5)]$ **3.28**, it was obviously interesting and important to examine its reaction chemistry. The initial thrust of this investigation focused on bromide substitution reactions i.e. reactions which do not effect the C_4R_4 ligand. As mentioned above, the reaction chemistry of the mono-alkyne complex **2.43** has been extensively studied and it has been found that a common reaction was the substitution of one (or both) of the bromine ligands with a variety of donor ligands such as phosphines, phosphites and alkynes (Figure 3.11).[55]

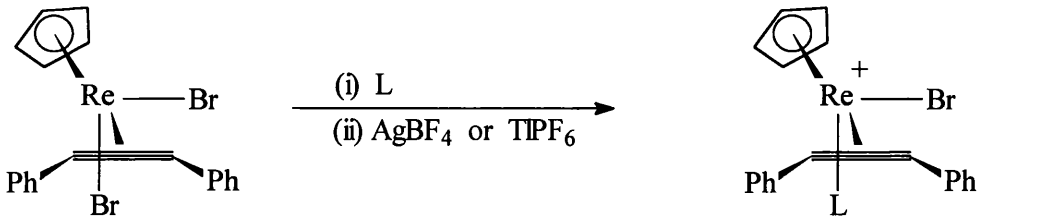

2.43

L = PR_3, $P(OMe)_3$, $RC{\equiv}CR$

FIGURE 3.11

The substitution of one of the bromide ligands in the complex $[ReBr_2(\eta^4\text{-}C_4Ph_4)(\eta\text{-}C_5H_5)]$ **3.28** with a tertiary phosphine was successfully effected using the halide abstracting agent silver tetrafluoroborate (Figure 3.12). When one equivalent of both silver tetrafluoroborate and triphenylphosphine were added to a dichloromethane solution of $[ReBr_2(\eta^4\text{-}C_4Ph_4)(\eta\text{-}C_5H_5)]$ **3.28** the orange, cationic, crystalline complex **17** was obtained in good yield (70%) (Figure 3.12). The presence of a co-ordinated triphenylphosphine group was established by a singlet at δ 15.0 in the $^{31}P\{^1H\}$ NMR spectrum. The aryl hydrogens of the phenyl groups appeared as overlapping multiplets in both the ^1H NMR [δ 6.25-7.55] and $^{13}C\{^1H\}$ NMR [δ 125.8-133.9] spectra, whereas, the $\eta^5\text{-}C_5H_5$ moiety resonated as a singlet in both the ^1H [δ 5.89] and $^{13}C\{^1H\}$ [δ 96.0] NMR spectra.

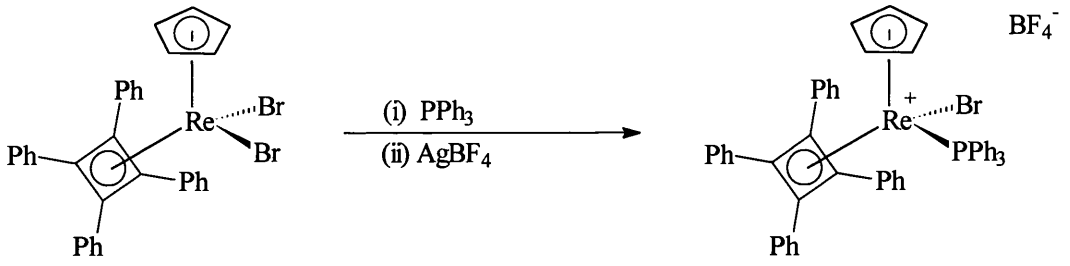

3.28 **17**

FIGURE 3.12

This new cationic π complex **17** was of interest from the standpoint of reactivity towards sources of H^-, as nucleophilic attack on such complexes can result in the conversion of η^n-bonded ligands to their corresponding η^{n-1} ligands. Unsaturated hydrocarbons like butadiene and benzene do not normally undergo nucleophilic attack but when they are co-ordinated to a transition metal they are readily attacked by H^-, CN^- or MeO^-. This enhanced reactivity is a result of transfer of electron density from the hydrocarbon to the positively charged metal atom. Davis, Green and Mingos[91] have proposed three general rules which allow the prediction of kinetically controlled nucleophilic attack at eighteen-electron cationic complexes containing unsaturated hydrocarbon ligands (DGM rules). Applications of these rules require the ligands to be classified as *even* (η^2, η^4, η^6 etc.) or *odd* (η^3, η^5, etc.), with a distinction between *closed* (cyclic conjugated) and *open* ligands (Figure 3.13).

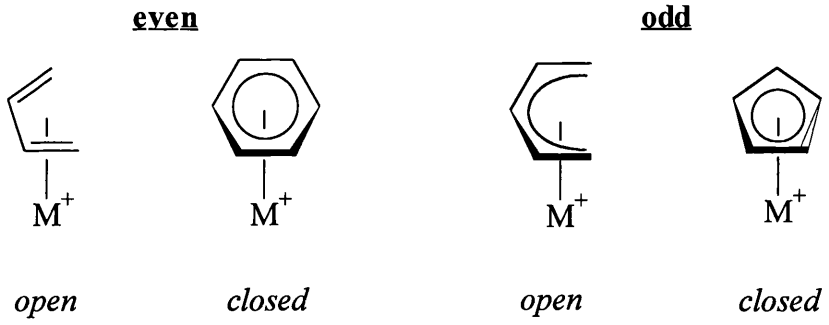

FIGURE 3.13

The proposed rules must be applied sequentially to determine the preferred site of attack and are :

1. Nucleophilic attack occurs preferentially at ***even*** co-ordinated polyenes.
2. Nucleophilic addition to ***open*** co-ordinated polyenes is preferred to addition to closed polyene ligands.
3. In the case of even open polyenes, nucleophilic attack always occurs at the ***terminal*** *carbon atom.*

In the case of complex **17** only the first rule need be applied as both the cyclopentadienyl and cyclobutadiene are "*closed*" co-ordinated polyenes. Thus, the DGM rules predict that H^- should attack the cyclobutadiene ring.

In practice, however, addition of Super Hydride to a thf suspension of **17** at -78°C resulted in two products in a ratio of approximately 20:1. Interestingly, the ^1H NMR spectrum of the major product, **18**, displayed a high field singlet at δ -12.14, which is very indicative of a metal hydride. The η-C_5H_5 moiety resonated as a singlet in both the ^1H and $^{13}C\{^1H\}$ NMR spectra [δ 5.19, δ 89.9 respectively]. However, in complex **19** (minor product) the high field signal at δ -11.81 resonated as a doublet with a coupling constant of J(HP) = 25.2 Hz. The η-C_5H_5 moiety of **19** also resonated as a doublet in the proton NMR spectrum at δ 5.07 [J(HP) = 1.4 Hz].

The minor product **19** was formed in such a small quantity that it was only observable in the ^1H and $^{31}P\{^1H\}$ [δ 27.3] NMR spectra. Unexpectedly, the phosphorus NMR spectrum of the mixture of the two products displayed only a large peak which corresponded to free triphenylphosphine at δ -3.9, the singlet at δ 27.3 and no other signals. This suggested that the major product (**18**) did not, in fact, contain a triphenylphosphine ligand but that this ligand has been displaced and hence a large free triphenyl phosphine signal is observed. It is, therefore, proposed that the hydride does not attack either of the ring systems but attacks the metal

centre, which is accommodated at the metal centre by ring slippage of the cyclopentadienyl moiety from η^5 to η^3 (**A**, Figure 3.14).

After the incoming hydride ligand has been accomodated by ring slippage, displacement of either the bromide or phosphine ligand occurs to afford the complexes $[ReBr(H)(\eta^4\text{-}C_4Ph_4)(\eta\text{-}C_5H_5)]$ **18** and $[Re(H)(PPh_3)(\eta^4\text{-}C_4Ph_4)(\eta\text{-}C_5H_5)][BF_4]$ **19**, respectively (Figure 3.14). The structure of **19** also helps rationalise the metal hydride-phosphorus coupling of 25 Hz, which is smaller than expected for *trans* coupling.

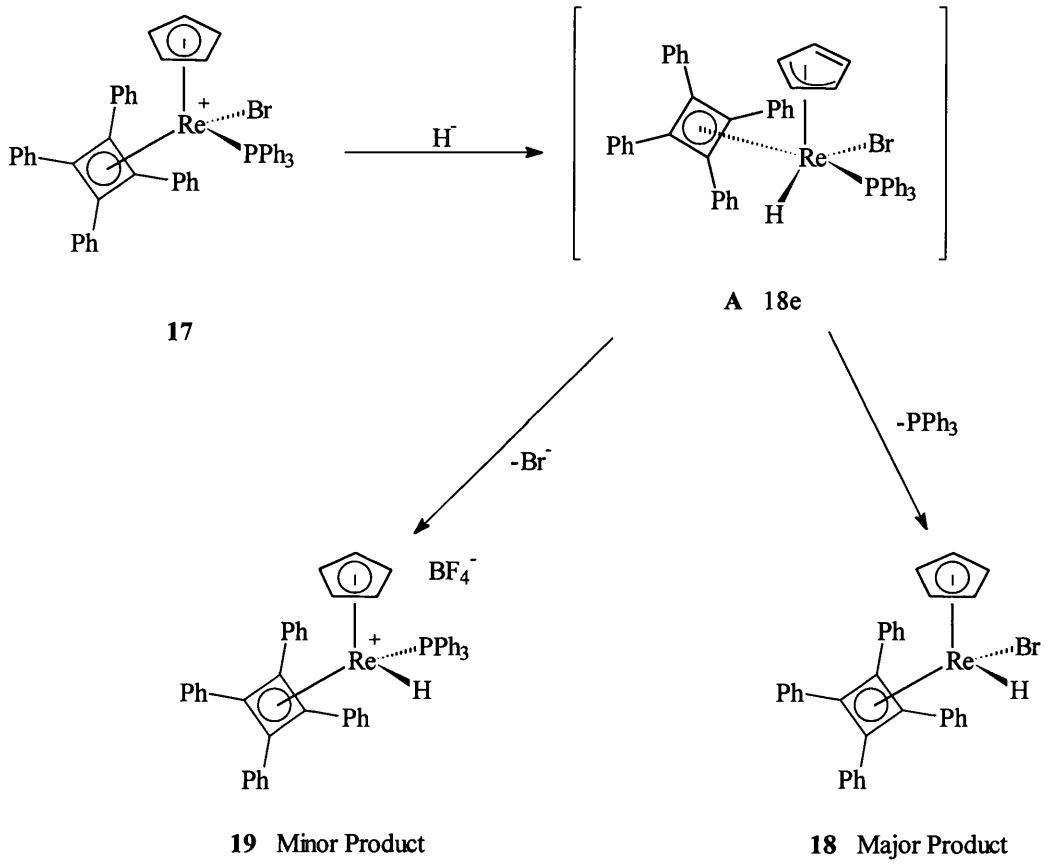

17

A 18e

19 Minor Product

18 Major Product

FIGURE 3.14

Ring slippage in transition metal complexes is a well known process. For example, molybdenum forms the stable eighteen-electron complex $[Mo(CO)(\eta\text{-}C_5H_5)_2]$, whereas the tungsten analogue **3.29** reacts with excess CO to give an

apparent twenty-electron species, $[W(CO)_2(\eta\text{-}C_5H_5)_2]$ **3.30**. Although the solution NMR spectra show that both the cyclopentadienyl ligands are identical in complex **3.30**, the solid state structure confirms that one of the cyclopentadienyl rings is, in fact, only η^3 and thus the eighteen-electron count is maintained (Figure 3.15). This phenomenon is also observed with mono-cyclopentadienyl complexes and in fact, $[Re(Me)(CO)(NO)(\eta^5\text{-}C_5H_5)]$ **3.31** reacts with the strong donor ligand PMe_3 to give the isolable η^3 species, $[Re(Me)(CO)(NO)(PMe_3)(\eta^3\text{-}C_5H_5)]$ **3.32** (Figure 3.15).

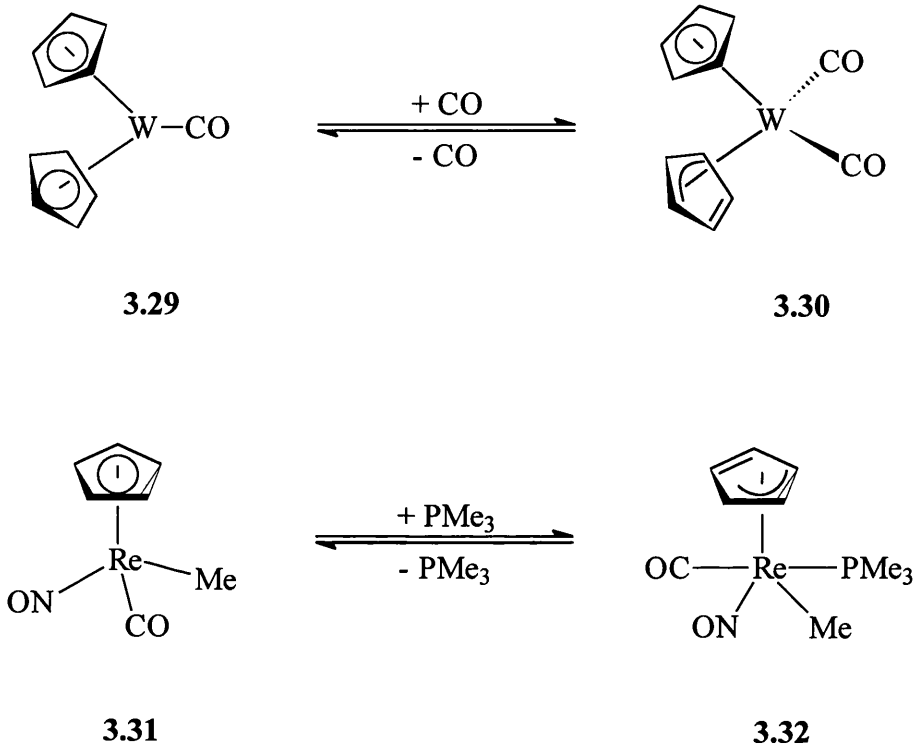

3.29 **3.30**

3.31 **3.32**

FIGURE 3.15 : $\eta^5 \rightarrow \eta^3$ Ring Slippage of Cyclopentadienyl Ligand

Confirmation of the proposed molecular structure of **18** was obtained by comparison of the ^1H and $^{13}C\{^1H\}$ NMR spectra of **18** prepared by a different route (hydride attack on the parent complex **3.28**) in a preliminary experiment by C. Vaughn (Figure 3.16).[92] When one molar equivalent of lithium aluminium hydride was added to a cooled solution of $[ReBr_2(\eta^4\text{-}C_4Ph_4)(\eta\text{-}C_5H_5)]$ **3.28** a swift colour change from red to orange was observed and after a chromatographic work-up the

orange complex [ReBr(H)(η^4-C_4Ph_4)(η-C_5H_5)] **18** was obtained in poor yield (20%).

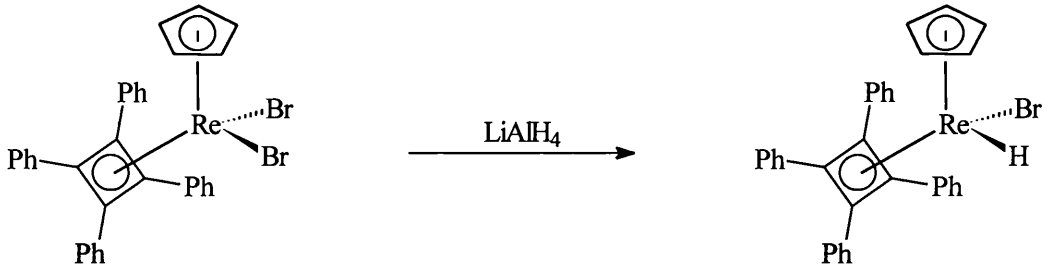

3.28 **18**

FIGURE 3.16

Therefore, having successfully synthesised the mono-hydrido complex it was obviously of interest to attempt to displace both bromo ligands of [$ReBr_2$(η^4-C_4Ph_4)(η-C_5H_5)] **3.28** with a hydride ligand and hopefully obtain a stable rhenium dihydride species.

3.3 Preparation of $[ReH_2(\eta^4\text{-}C_4Ph_4)(\eta\text{-}C_5H_5)]$ 20.

Metal hydrides in general are numerous and one important class is that of the cyclopentadienyl metal hydride complexes. These complexes are mainly encountered with second and third row transition metals e.g. $[MH_3(Cp_2)]$ (M = Nb, Ta),[93,94] $[MH_2(Cp_2)]$ (M = **3.33** Mo, W)[93] and $[MH(Cp)_2]$ (M = Tc, **3.34** Re)[93,95] (Figure 3.17) and in general the planes of the cyclopentadienyl rings are tilted back i.e. the normals to the planes of the cyclopentadienyl ligands are less than 180°.

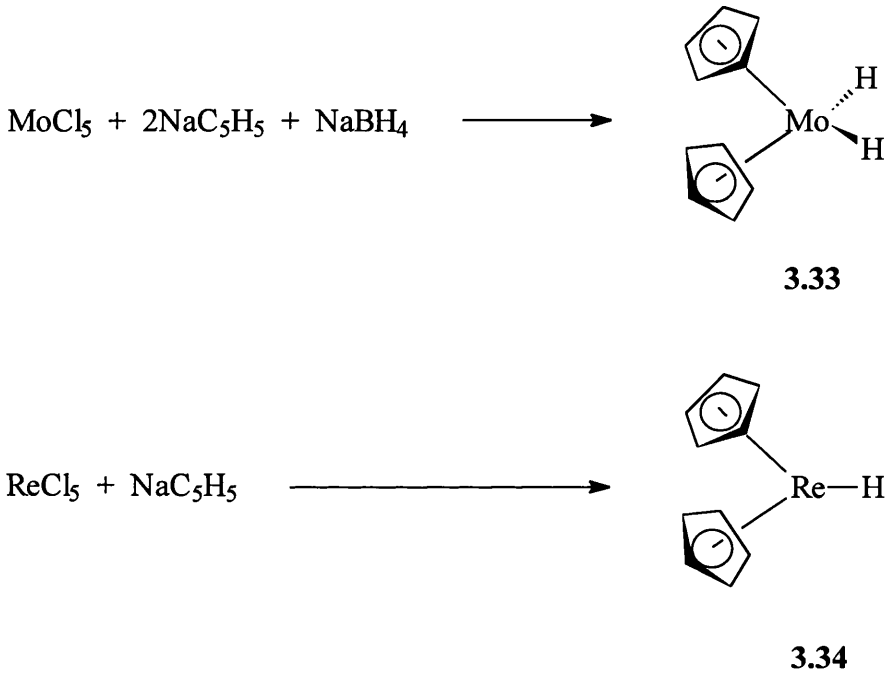

FIGURE 3.17

The ability of rhenium (VII) to accommodate a large number of hydride ligands in its co-ordination shell e.g. $K_2[ReH_9]$ also manifests itself in the cyclopentadienyl hydride complexes (**3.35**, Figure 3.18).

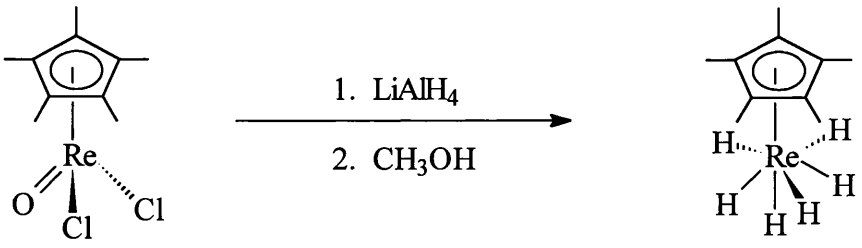

3.35

FIGURE 3.18

There have been numerous theoretical studies[96] carried out on a variety of bis(cyclopentadienyl) metal complexes and in general the frontier orbital (Figure 3.19) of the bis(cyclopentadienyl) metal fragments change very little in shape or symmetry from metal to metal. The simplest examples of bent $M(\eta\text{-}C_5H_5)_2$ are the metal hydride complexes because the hydride ligand can only bond to the metal in a σ fashion. Examples of this type of complex are $[ReH(\eta\text{-}C_5H_5)_2]$ and $[FeH(\eta\text{-}C_5H_5)_2]^+$, which are both d^4 systems.[93] The most symmetrical and presumably the most favoured structure for the $[MH(\eta\text{-}C_5H_5)_2]$ molecule is the one in which the H^- ligand is located on the z-axis. In this geometry the hydride ligand overlaps very well with the $2a_1$ fragment orbital and a little with the $1a_1$ orbital resulting in a strong bonding interaction between the $2a_1$ and the σ orbital of the hydride ligand (Figure 3.19). The b_2 and $1a_1$ orbitals can accommodate four-electrons. Thus, d^4 systems should be favoured.

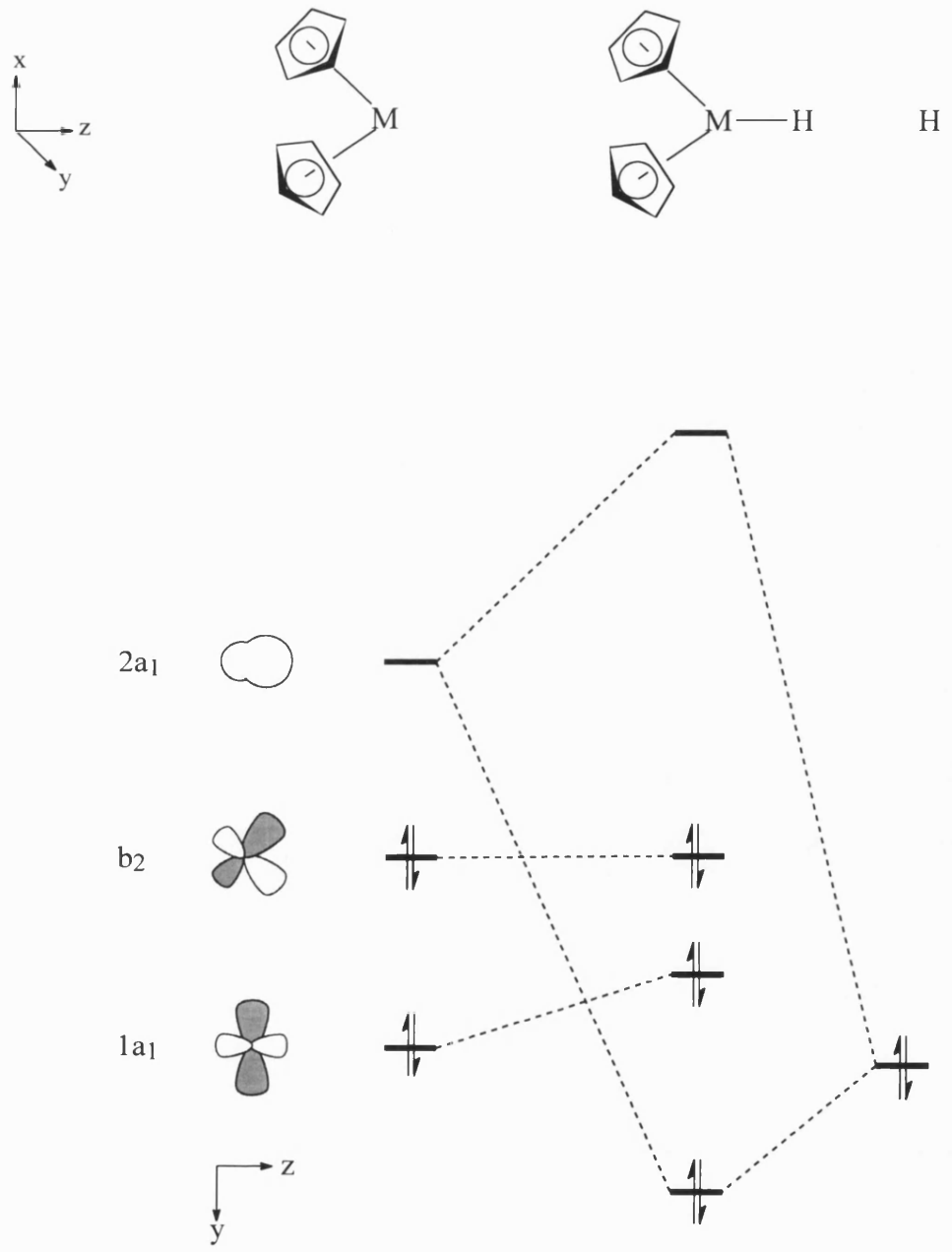

FIGURE 3.19

There are also numerous examples of bent metallocenes with 2 σ bonding ligands which could occupy two of the three low lying orbitals of the bent metallocene e.g. $[MoH_2(\eta\text{-}C_5H_5)_2]$ and $[ReH_2(\eta\text{-}C_5H_5)_2]^+$. The molecular structure[97] of several of these complexes (*ca.* 20) has been determined and, in general, they all have the same geometry (Figure 3.20), with varying angles of φ between the two X ligands.

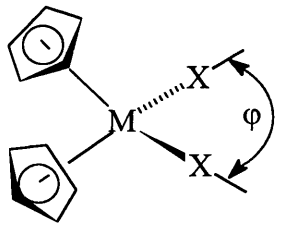

FIGURE 3.20

Recently, Curtis[98] compared $[ML_n(\eta\text{-}C_5H_5)_2]$ and $[ML_n(\eta^4\text{-}C_4Ph_4)(\eta\text{-}C_5H_5)]$ complexes and concluded that the $M(\eta\text{-}C_5H_5)_2$ and $M(\eta^4\text{-}C_4Ph_4)$ $(\eta\text{-}C_5H_5)$ fragments were very similar. The energies and forms of the frontier orbitals of both fragments are nearly identical except for a small shift in energies and a slight tilting of the b_2 and $2a_1$ orbitals as a result of the lower symmetry in the $Mo(\eta\text{-}C_5H_5)(\eta^4\text{-}C_4Ph_4)$. It was concluded that the bonding of bis(cyclopentadienyl) metal and cyclopentadienyl (cyclobutadiene) metal fragments will, for all practical purposes, be identical and so it would be reasonable to assume that the rhenium dihydride cyclobutadiene/cyclobutadiene analogue to **3.34** should exist.

Against this background it was therefore of interest to examine the reactivity of $[ReBr_2(\eta^4\text{-}C_4Ph_4)(\eta\text{-}C_5H_5)]$ **3.28** towards lithium aluminium hydride with a view to synthesising a cyclopentadienyl/cyclobutadiene dihydride species. Addition (-78°C) of lithium aluminium hydride to a thf solution of $[ReBr_2(\eta^4\text{-}C_4Ph_4)(\eta\text{-}C_5H_5)]$ **3.28** resulted in an immediate colour change from orange to bright yellow. After chromatography the yellow complex $[ReH_2(\eta^4\text{-}C_4Ph_4)(\eta\text{-}C_5H_5)]$ **19** was obtained in good yield (80%). The elemental analysis (Found : 64.9% C; 4.39% H. Calculated : 65.0 % C; 4.46 % H) suggested that both bromo-ligands had indeed been replaced by H^- (Figure 3.21).

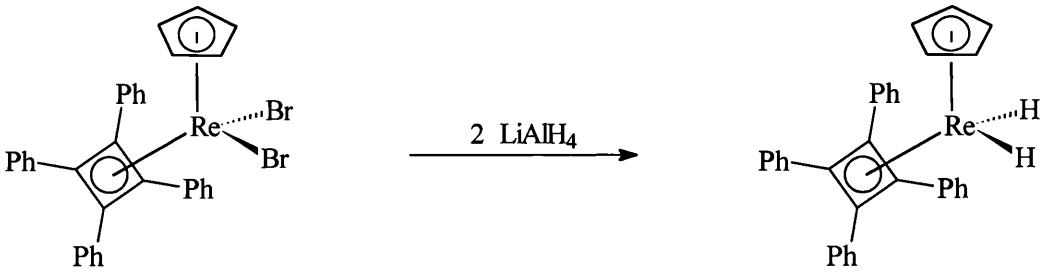

3.28 **20**

FIGURE 3.21

The ^{1}H NMR spectrum of complex **20** exhibited a high field singlet at δ -13.07, which was indicative of a metal hydride. This hydride signal integrated for two hydrogens with respect to the five hydrogens at δ 4.85, which were attributable to the cyclopentadienyl moiety. The only other signals in the ^{1}H NMR spectrum were the aryl hydrogens, which resonated as a group of multiplets between δ 7.14-7.36. The $^{13}C\{^{1}H\}$ NMR spectrum clearly displayed the cyclopentadienyl and the cyclobutadiene ring carbons at δ 89.3 and δ 66.9, respectively. The other signals in the $^{13}C\{^{1}H\}$ NMR spectrum were four singlets at δ 126.4, 128.0, 130.6 and 136.6, which were attributable to the *ipso*, *ortho*, *meta* and *para* carbons of the phenyl substituents of the cyclobutadiene ring.

In order to confirm the precise molecular structure a single crystal X-ray diffraction study was undertaken on **20** (Figure 3.22, selected bond lengths and angles are listed in Table 3.1). The crystal contained two molecules per unit cell and for clarity only the structural data of the complex containing Re2 will be discussed; all arguments are equally applicable to the second molecule of the unit cell. As predicted, the complex contained co-ordinated cyclopentadienyl and tetraphenylcyclobutadiene moieties which were tilted back in the usual fashion as described above. The hydride ligands were not located because there are so few electrons associated with this ligand and hence, they are difficult to locate accurately with single crystal X-ray diffraction techniques. The C_4Ph_4 ligand had

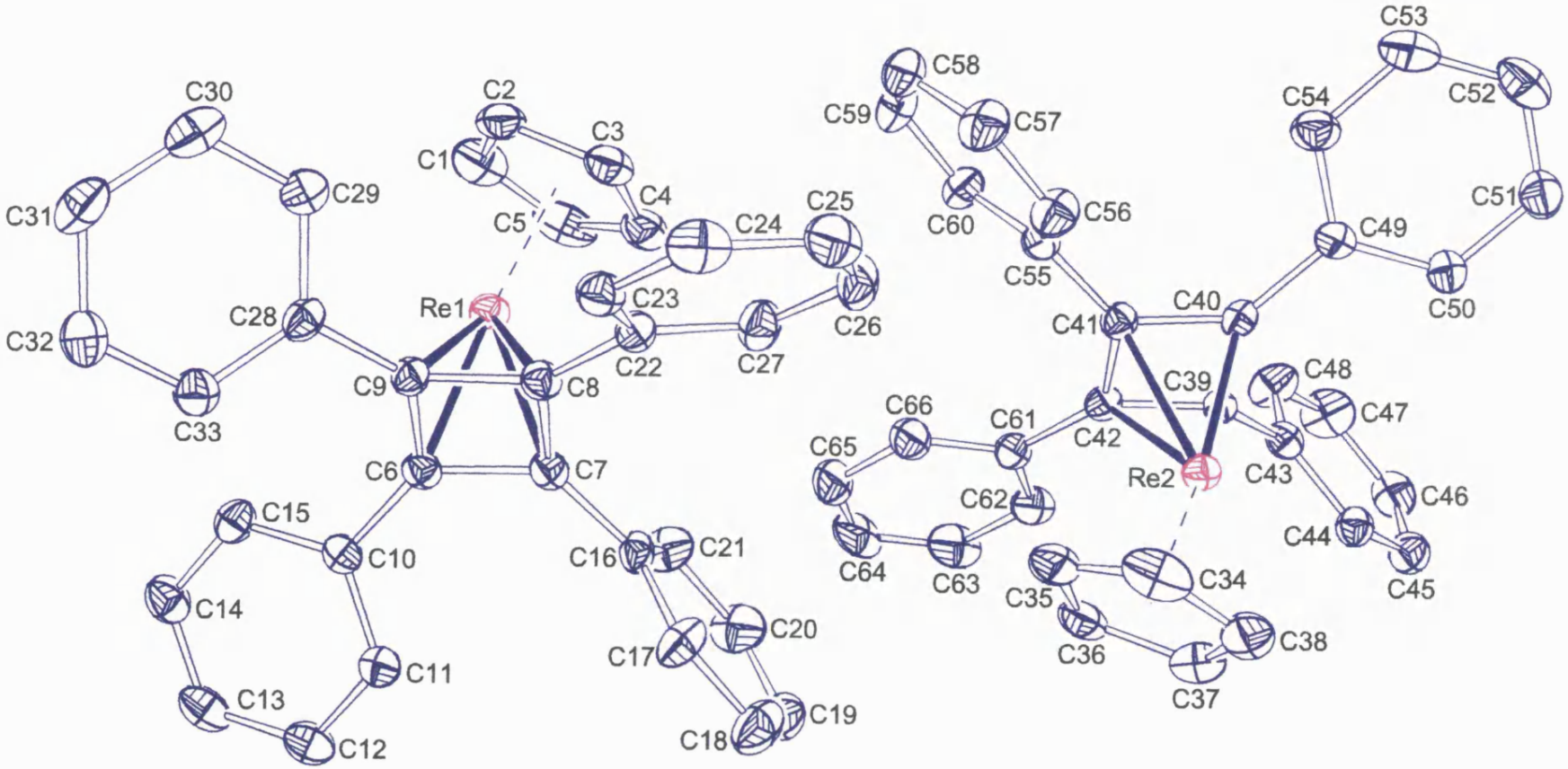

FIGURE 3.22 : ORTEP Drawing of **20**.

adopted a square structure with all four sides being of approximately equal length [C39-C40 1.479 Å, C40-C41 1.464 Å, C41-C42 1.468 Å and C42-C39 1.446 Å] and all four internal angles of *ca.* 90°. Three of the carbons of the C_4Ph_4 unit were equidistant from the rhenium centre [Re2-C39 2.156Å, Re2-C40 2.167Å and Re2-C41 2.166Å]. However, the close proximity of the phenyl group attached to C42 forces C42 further from the metal centre with a Re2-C42 distance of 2.233Å. Also, the phenyl groups attached to the C_4Ph_4 unit all lie below the C39-C40-C41-C42 plane and on the opposite side to the metal centre, which is presumably in order to relieve steric interactions.

Table 3.1 : Selected Bond Lengths (Å) and Angles (°) of **20**.

Atoms	Bond Length	Atoms	Bond Length
C6-C7	1.462(10)	C39-C40	1.479(10)
C7-C8	1.478(10)	C40-C41	1.464(10)
C8-C9	1.452(10)	C41-C42	1.468(10)
C9-C6	1.480(9)	C42-C39	1.446(10)
Re1-C6	2.164(8)	Re2-C39	2.156(9)
Re1-C7	2.164(9)	Re2-C40	2.167(8)
Re1-C8	2.219(8)	Re2-C41	2.166(9)
Re1-C9	2.181(8)	Re2-C42	2.233(9)

Atoms	Angle	Atoms	Angle
C6-C7-C8	88.5(6)	Re-C8-C22	129.5(5)
C7-C8-C9	91.5(6)	Re-C7-C16	130.5(4)
C8-C9-C6	88.0(6)	Re-C6-C10	130.5(4)
C9-C6-C7	91.0(6)	Re-C9-C28	126.9(5)
C39-C40-C41	89.5(6)	Re-C39-C43	133.1(4)
C40-C41-C42	89.7(6)	Re-C40-C49	136.6(6)
C41-C42-C39	90.6(6)	Re-C41-C55	129.2(5)
C42-C39-C40	89.9(6)	Re-C42-C61	125.5(5)

3.4 An EHMO Calculation and Reactivity of $[ReH_2(\eta^4\text{-}C_4Ph_4)(\eta\text{-}C_5H_5)]$ 20.

The reactivity of cyclopentadienyl metal hydride complexes, $[ML_n(\eta\text{-}C_5H_5)_2]$ (n = 1, 2) is largely governed by the Lewis-basicity of the central metal atom. Therefore, these complexes are readily protonated (Figure 3.23), presumably interacting with the HOMO (Highest Occupied Molecular Orbital), which has been shown to lie between the two L ligands.[98] However, bent metallocene complexes with three additional ligands[94,93] i.e. $[ML_3(\eta\text{-}C_5H_5)_2]$ are not as prevalent and examples such as $[MoH_3(\eta\text{-}C_5H_5)_2]^+$ **3.36** and $[TaH_3(\eta\text{-}C_5H_5)_2]$ are d^0 systems, since all three valence orbitals of the fragment are used to bond the three σ ligands. In $[TaH_3(\eta\text{-}C_5H_5)_2]$ all three hydrides lie in the *yz* plane similar to that illustrated for $[MoH_3(\eta\text{-}C_5H_5)_2]^+$ **3.36** in Figure 3.23.

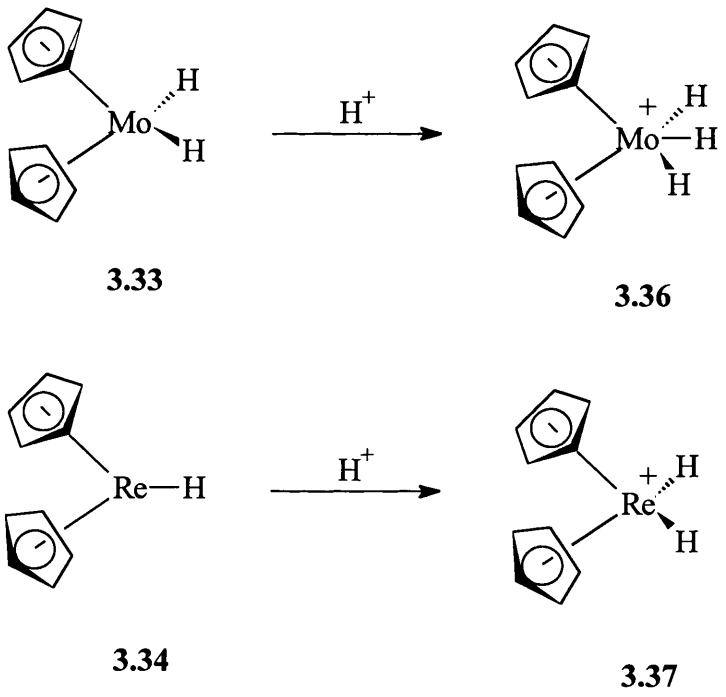

3.33 **3.36**

3.34 **3.37**

FIGURE 3.23

Therefore, having obtained a crystal structure of **20** (Figure 3.22) it was obviously of interest to carry out an EHMO calculation in order to attempt to predict the site of proton attack. As mentioned previously the hydride ligands were

not located in the X-ray diffraction study and therefore were idealised at 1.68Å from the metal, which is similar to previously observed rhenium-hydride distances.[99] The idealised H-Re-H angle of *ca.* 80-85° was found by varying this angle until the total energy of the molecule was minimised (Table 3.2).

TABLE 3.2 : Table of Atom Charges and E(Total) for Complex **20** at Various H-Re-H Angles.

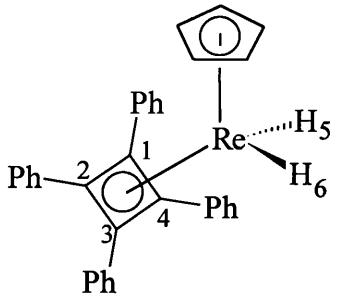

ATOM	**CHARGES** H-Re-H Angle (°)		
	80	70	100
Re	-0.225	-0.236	-0.240
C1	0.151	0.168	0.110
C2	0.063	0.051	0.088
C3	0.124	0.127	0.115
C4	0.040	0.029	0.063
H5	-0.212	-0.200	-0.209
H6	-0.233	-0.215	-0.246
E(TOTAL)	***-2930.25***	***-2930.10***	***-2930.09***

Figure 3.24 illustrates the HOMO of the complex and shows that it is mainly centred on the metal and the C_4 ring. Figure 3.25 illustrates the same HOMO except the four phenyl groups have been omitted for clarity. Protonation is generally a charge controlled process and so, although the HOMO is located both on the C_4 ring and the rhenium metal, further examination of the atom charges

located both on the C_4 ring and the rhenium metal, further examination of the atom charges reveals that the carbon atoms of the C_4 ring are all positive (0.151, 0.036, 0.124 and 0.040) and, in fact, the largest negative charge (-0.225) resides at the metal centre. Figure 3.25 also illustrates that part of the HOMO on the metal lies between the two hydride ligands, which is similar to that previously observed for $[M(\eta\text{-}C_5H_5)_2H_2]$ complexes by Lauher and Hoffmann.[96] Thus, the EHMO calculations predict that protonation should occur at the rhenium centre.

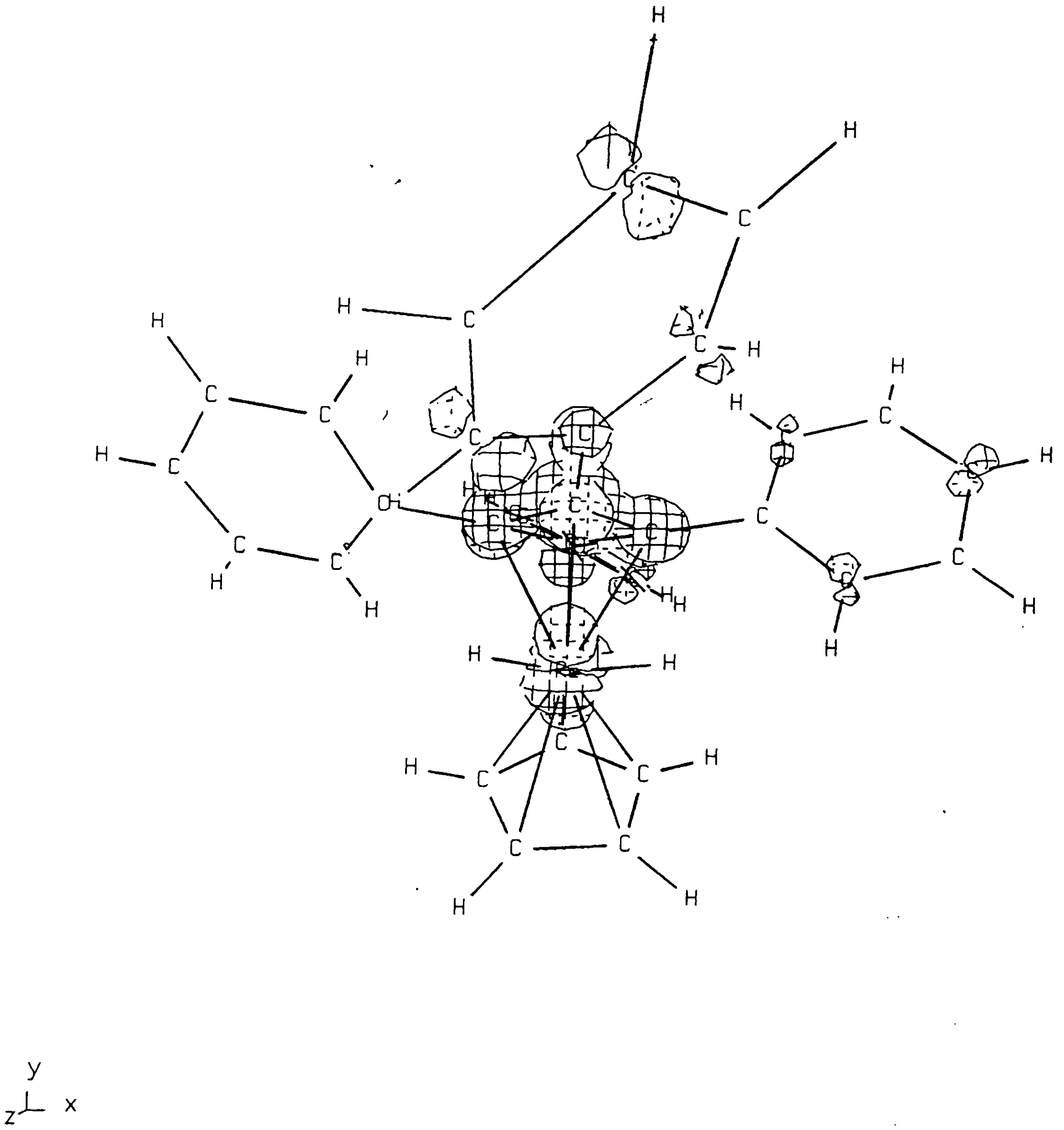

FIGURE 3.24

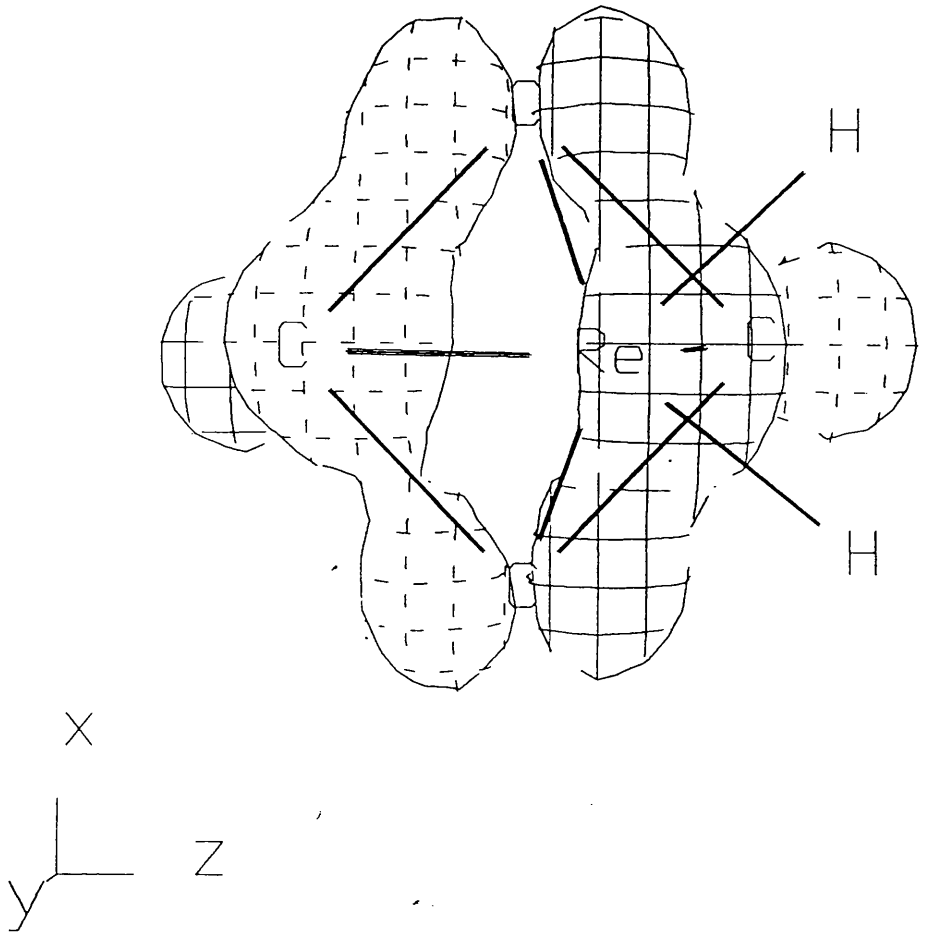

FIGURE 3.25

Addition of one equivalent of $HBF_4.Et_2O$ at -78°C to a solution of [ReH_2 (η^4-C_4Ph_4)(η-C_5H_5)] **20** resulted in the formation of complex **21**, which was extremely air amd moisture sensitive, so much so that the complex rapidly decomposed in solution. In fact, only a ^1H NMR spectrum could be obtained due to the sensitive nature of the complex. Surprisingly, the ^1H NMR spectrum displayed only one high field signal at δ -8.7 [multiplet], which integrated for one hydrogen with respect to the signal for the five hydrogens of the cyclopentadienyl moiety at δ 4.86, thus suggesting that the expected trihydride product **3.38** had not been formed (Figure 3.26).

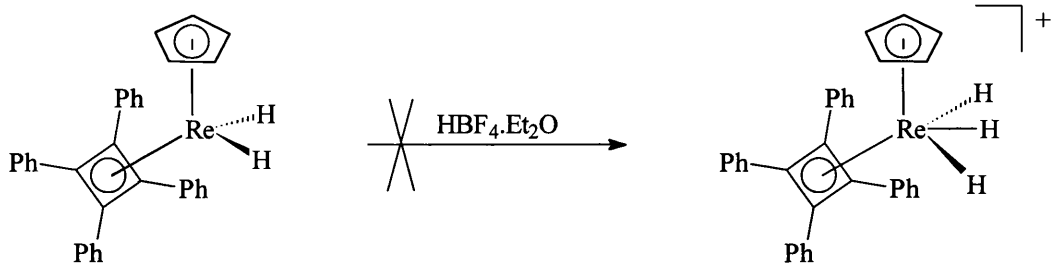

20 **3.38**

FIGURE 3.26

Upon further review of the literature, it was found that protonation of $[Re(CO)(H_2)(NO)(PMe_3)_2]$ **3.39** with stoichiometric or excess amounts of trifluoroacetic acid yielded the monohydrido trifluoroacetate compound $[ReH\{OC(O)CF_3\}(CO)(NO)(PMe_3)_2]$ **3.40** and the bis (trifluoroacetate) complex $[Re\{OC(O)CF_3\}(CO)(NO)(PMe_3)_2]$ **3.41**, respectively (Figure 3.27).[100] Both protonation reactions were presumed to proceed *via* the intermediacy of unstable non-classical dihydrogen species, $[ReH(CO)(H_2)(NO)(PMe_3)_2]^+$ and $[ReH\{OC(O)CF_3\}(CO)(H_2)(NO)(PMe_3)_2]^+$ respectively.

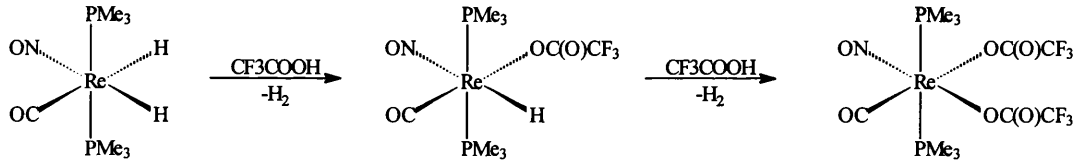

3.39 **3.40** **3.41**

FIGURE 3.27

In light of this work, it was initially postulated that possibly a similar reaction had occurred to afford the cationic sixteen-electron species **3.42** (Figure 3.28). This would explain the presence of only one metal hydride, one cyclopentadienyl ligand and four phenyl groups. Also, as the BF_4^- counterion is generally considered to be a non-co-ordinating (or at best a weakly co-ordinating)

anion, a sixteen-electron complex would result, which would account for the very sensitive nature of the complex.

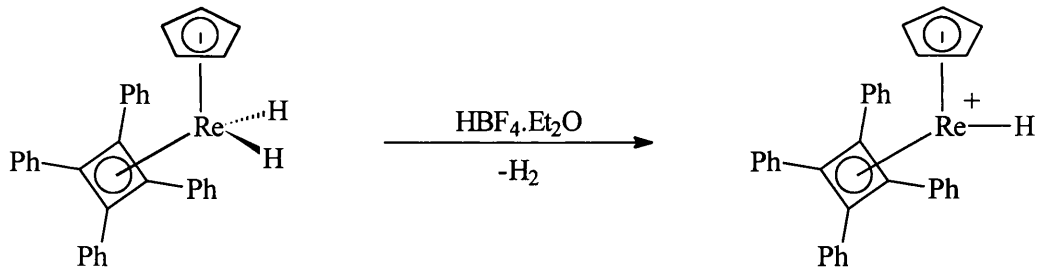

20 16 e **3.42**

FIGURE 3.28

In order to test this theory **20** was treated with excess trifluoroacetic acid, as the trifluoroacetate anion would help stabilise any electron-deficient product formed. Addition of CF_3COOH at -78°C to an ether solution of **20** resulted in a neutral, orange complex **22**, which could be chromatographed on alumina and eluted with neat dichloromethane. The elemental analysis [Found : 58.2% C; 4.0% H. Calculated : 58.08% C; 3.90% H.] and mass spectrum [(M^+) 723, (M^+-CF_3COO) 610] were consistent with a 1:1 adduct of **20** and CF_3COOH. The $^{13}C\{^1H\}$ NMR spectrum [quartet, CF_3, δ 112.3, $^1J(CF)$ 291Hz and quartet, CCF_3, δ 165.0, $^2J(CF)$ 36Hz] and ^{19}F NMR spectrum [δ -74.9] confirmed the presence of a trifuoroacetate group. In the $^{13}C\{^1H\}$ NMR spectrum there was the expected cyclopentadienyl signal at δ 88.7 and phenyl group signals at δ 126.5 - 143.1 [multiplet] but there were also three anomalous signals apparent at δ 57.8, δ 61.5 and δ 113.1. In the ^1H NMR spectrum there was a high field signal at δ -7.87 [H^a], which integrated for one proton with respect to the five hydrogens of the cyclopentadienyl ring at δ 4.52 and was similar to the observed high field signal for **21** (the protonation product of **20** with $HBF_4.Et_2O$). However, it was now evident that this high field signal was a doublet of doublets [J = 3.0 Hz and 5.6 Hz] and from a H-H COSY study it was apparent that H^a was coupled to H^b at δ 3.40 [H^b, 1H, $J(H^aH^b)$ = 5.6Hz] and H^c at δ 4.04 [H^c, 1H, $J(H^aH^c$ = 3.0Hz], thus resulting in

H^a appearing as a doublet of doublets. This suggested that an unexpected reaction had occurred and that possibly ring-opening of the tetraphenylcyclobutadiene moiety had actually taken place to afford the buta-1,3-diene complex $[ReH\{OC(O)CF_3\}\{\eta^2,\eta^2\text{-}PhC(H)=C(Ph)C(Ph)=C(Ph)H\}(\eta\text{-}C_5H_5)]$ **22** (Figure 3.29). A C-H correlation NMR study revealed that H^b was bonded to the carbon at δ 57.8 and H^c to the carbon at δ 61.5 and hence confirmed the presence of two CH groups within the molecule.

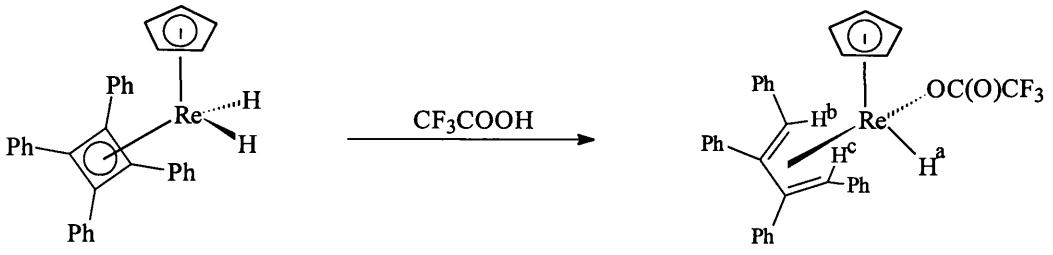

20 **22**

FIGURE 3.29

In order to elucidate the exact molecular geometry and confirm that a ring-opening reaction had indeed taken place a single crystal X-ray diffraction study was undertaken on complex $[ReH\{OC(O)CF_3\}\{\eta^2,\eta^2\text{-}PhC(H)=C(Ph)C(Ph)=C(Ph)H\}(\eta\text{-}C_5H_5)]$ **22** (Figure 3.30, selected bond lengths are listed in Table 3.3). The asymmetric unit consisted of three independent molecules (a, b, and c, Figures 3.30a, 3.30b and 3.30c, respectively) but, unfortunately, refinement of the structure was severely hampered by many factors. In the first instance, although the complex was relatively stable the crystals appeared to lose solvent very rapidly and cracks developed. The solvent loss from the crystals posed some difficult handling problems and the only remotely "suitable" sample was substandard. Although, the structure determination was carried out at low temperature (-196°C) poor quality was quickly manifested in broad scan widths during early search routines on the diffractometer. In addition, the diffracting ability of the sample fell off rapidly with increasing Bragg angle, and much of the higher angle data were flagged as weak

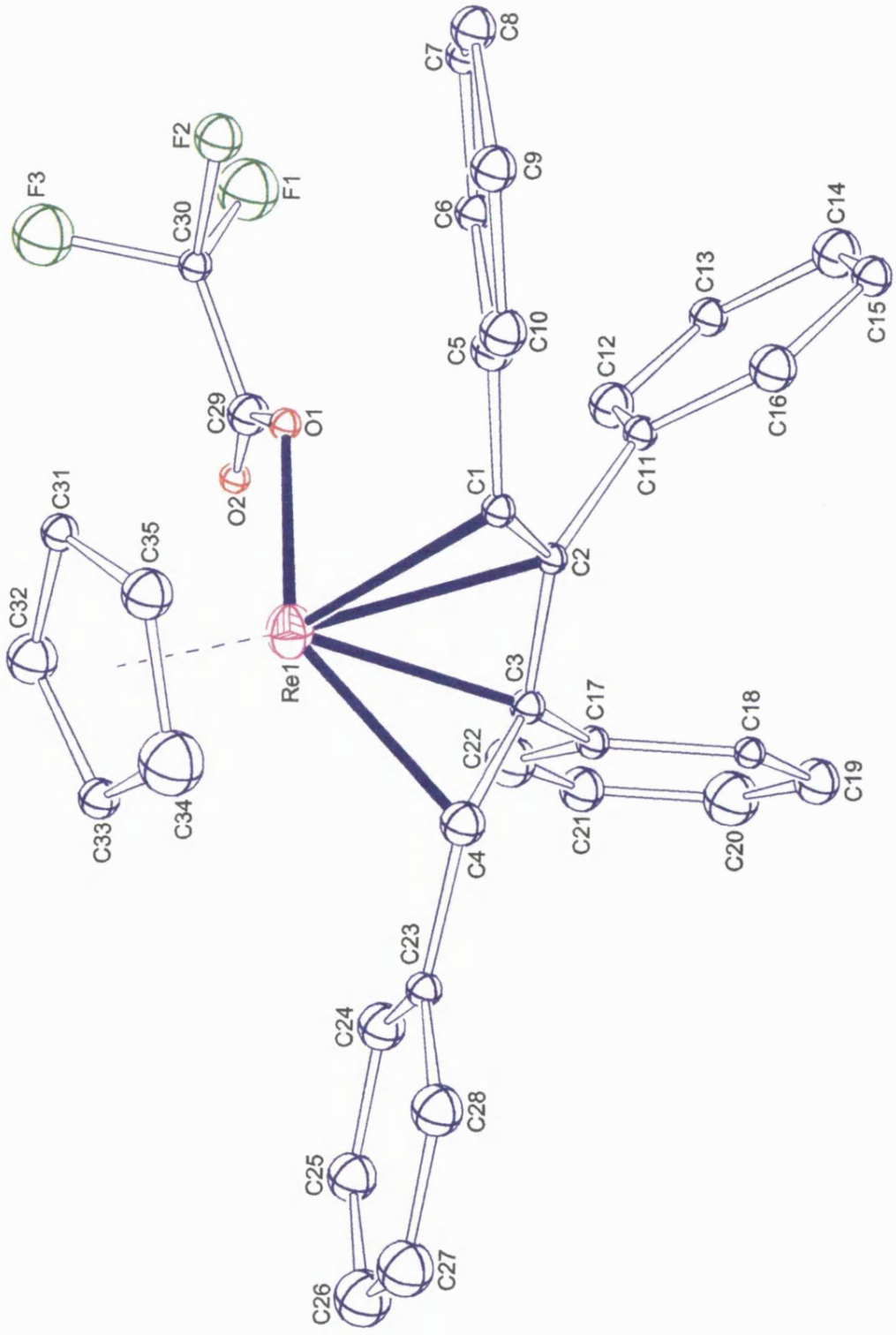

FIGURE 3.30a : ORTEP Drawing of Molecule (a) of Asymmetric Unit of **22**.

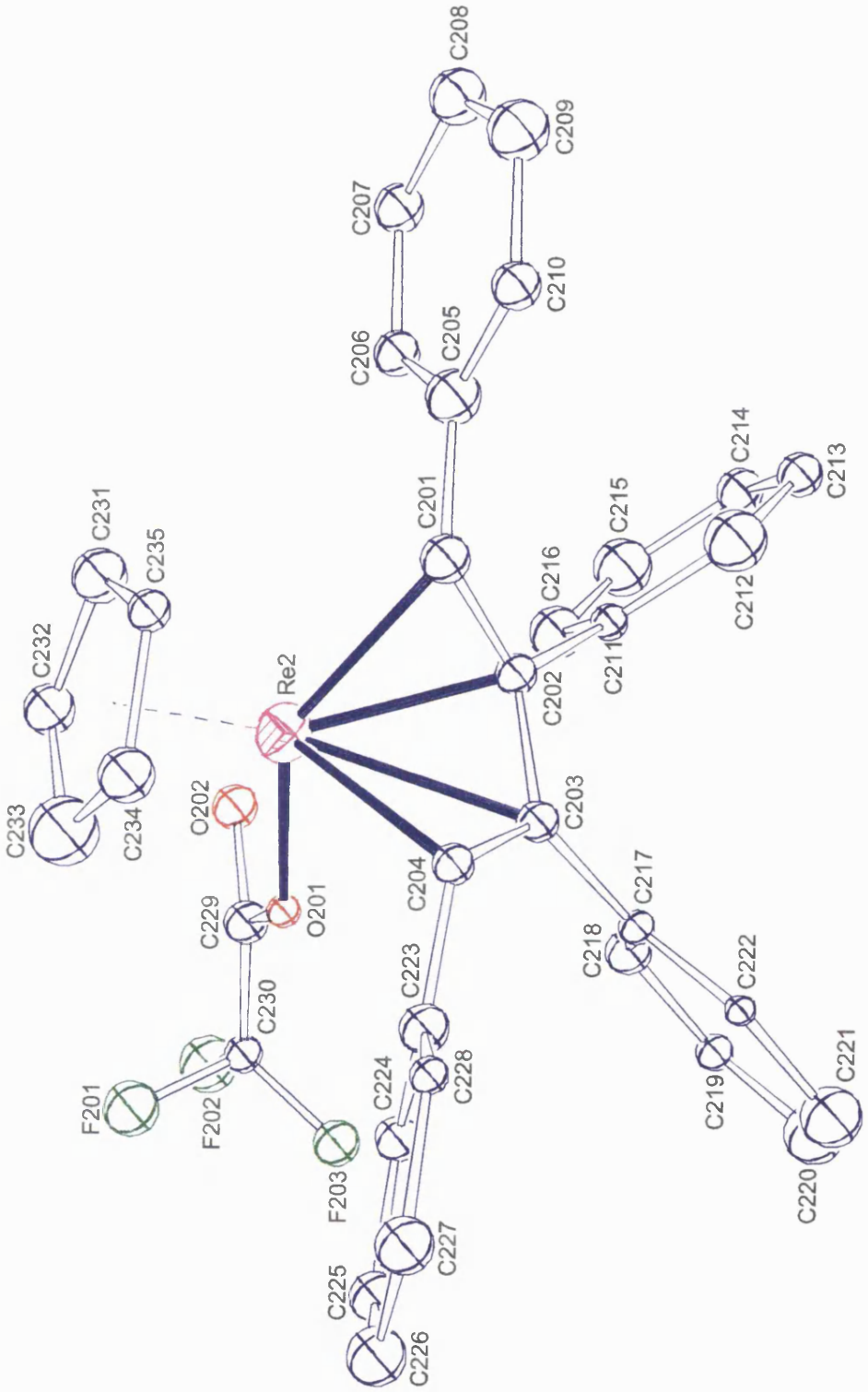

FIGURE 3.30b : ORTEP Drawing of Molecule (b) of Asymmetric Unit of **22**.

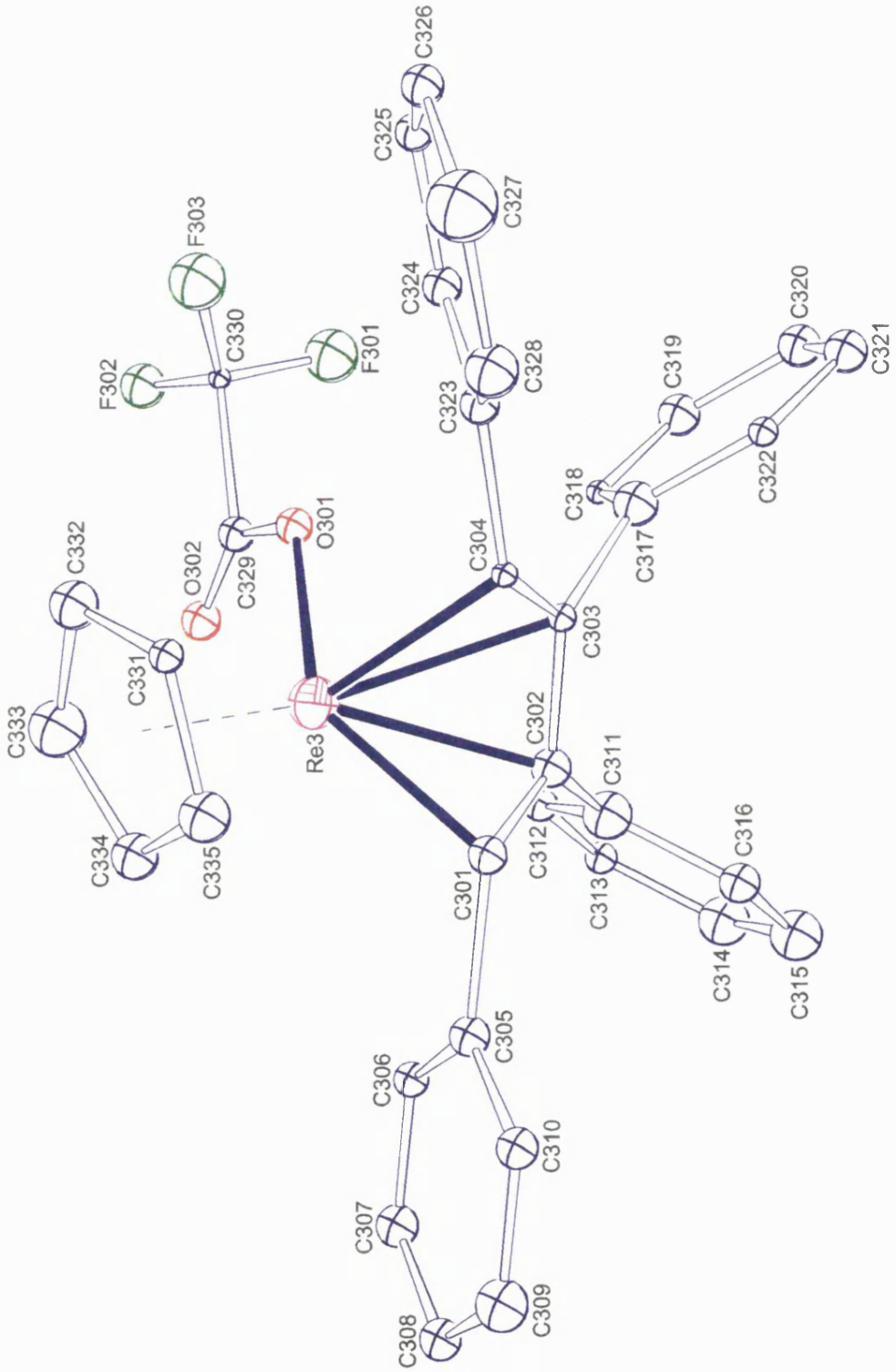

FIGURE 3.30c : ORTEP Drawing of Molecule (c) of Asymmetric Unit of **22**.

and as a consequence of a poor data set, convergence was inhibited. Therefore, bond distances and angles were not reliable for comparison purposes, but the structural analysis did attain some of its objectives by providing proof that a novel cyclobutadiene ring-opening reaction had occurred and that the butadiene had an *exo* configuration.

TABLE 3.4 : Selected Bond Lengths (Å) of **22**.

Atom	Bond Length	Atom	Bond Length
C1-C2	1.42(3)	Re-C2	2.31(4)
C2-C3	1.43(3)	Re-C3	2.24(4)
C3-C4	1.42(3)	Re-C4	2.20(7)
Re-C1	2.35(4)		

As previously mentioned, protonation of complex **20** was predicted to occur directly at the rhenium centre. In order to confirm this was occurring in practice, complex **20** was reacted with deuterated trifluoroacetic acid (Figure 3.31). A deuterium spectrum of the resulting complex [ReD{OC(O)CF_3}{η^2,η^2-PhC(H)=C(Ph)C(Ph)=C(Ph)H}(η-C_5H_5)] **23** revealed only one signal at *ca.* δ - 7.5, thus confirming that deuteration occurred solely at the metal centre.

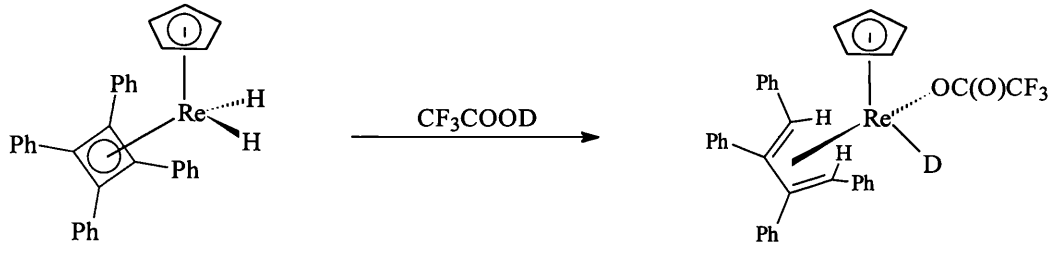

20 **23**

FIGURE 3.31

Therefore, proton attack at the metal centre must be the first step, which would result in the trihydride intermediate **3.38** (Figure 3.32). This was

presumably followed by the migration of one of the hydride ligands to the C_4 ring to form the butenyl species **A** which could be in equilibrium with **B**. It was initially postulated that the reaction then proceeded by a conrotatory ring-opening reaction **C** followed by a second hydride migration to give a sixteen-electron species **D**, which could then be stabilised by the co-ordinating trifluoroacetate anion. This postulated mechanism would result in one of the hydrogens in a *syn* position and one in the *anti* position **E** (Figure 3.32). This mechanism is not unreasonable in that previously, ring-opening reactions of η^3-cyclobutenylpalladium (II) complexes have been suggested to explain the formation of η^3(3e)-butadienyl species, and therefore it is reasonable to propose that a related reaction is involved in the formation of intermediate **C**.

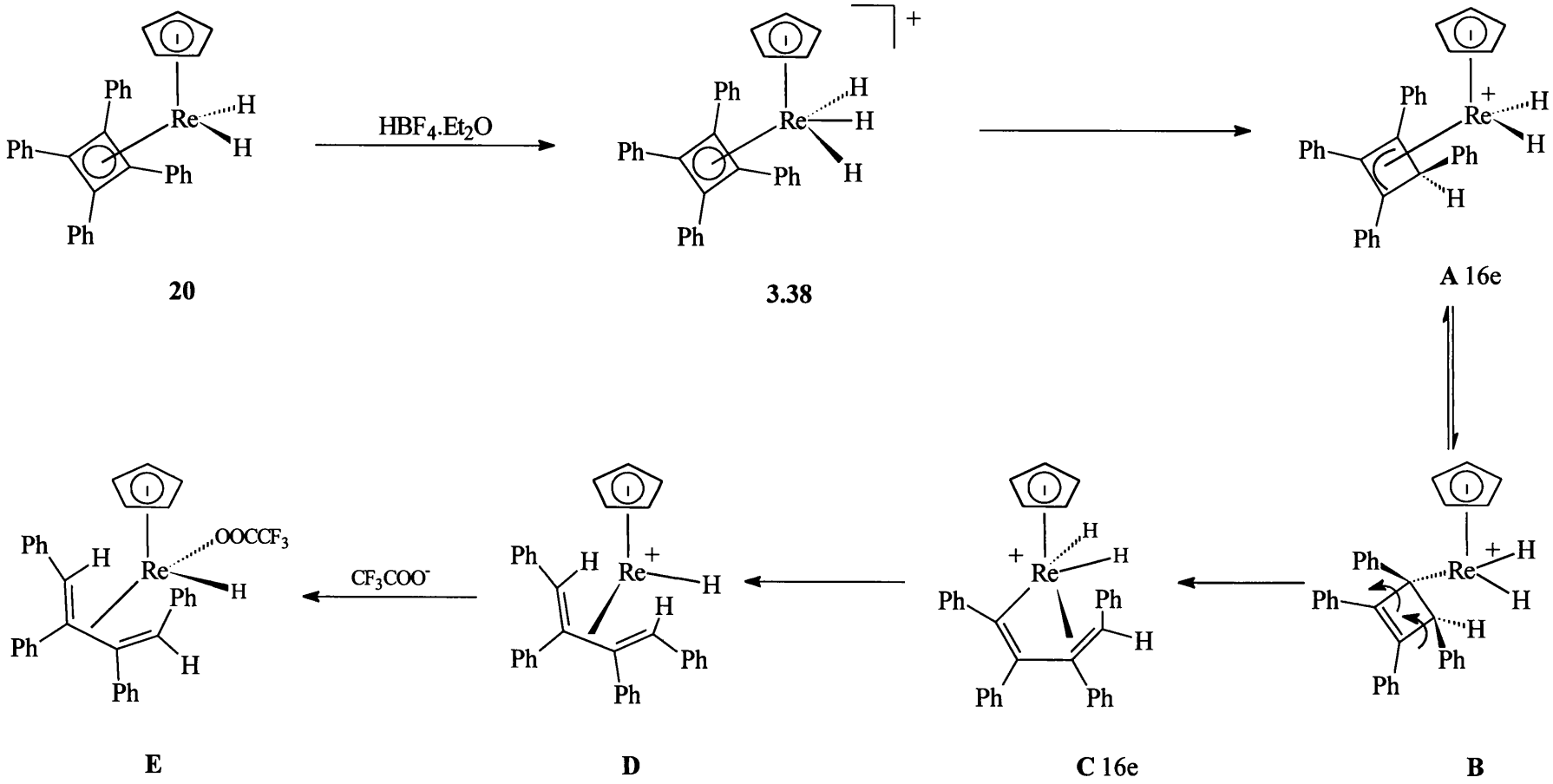

FIGURE 3.32

However, the crystal structure indicated that the hydrogens were, in fact, both in an *anti* position, which is inconsistent with the above mechanism as the ring-opening would have to proceed in a disrotatory manner, which usually only occurs in photochemical ring-opening reactions. Therefore, it is proposed that after the η^3-butenyl complex **A** undergoes a conrotatory ring-opening reaction to afford the η^3(3e) butadienyl fragment **C** (Figure 3.32) which then rearranges to a σ,η^3(5e) butadienyl species **F** (Figure 3.33). The trifluoroacetate anion reacts with the metal *via* an associative process to give the kinetically controlled product **G** (Figure 3.33). In this intermediate the hydrogen at the terminus of the C_4 chain is pointing away from the metal centre. Thus, it is proposed that stereomutation of this carbon occurs *via* a metallocycle flip process to generate the corresponding isomer **H**, where the hydrogen now points towards the metal centre and the phenyl group points away. Finally migration of the second hydride would result in the formation of the stable, neutral, eighteen-electron complex [ReH{OC(O)CF_3}{η^4-CH(PH)=C(Ph)-C(Ph)=CH(Ph)}] **22** with both hydrogens in the *anti* position.

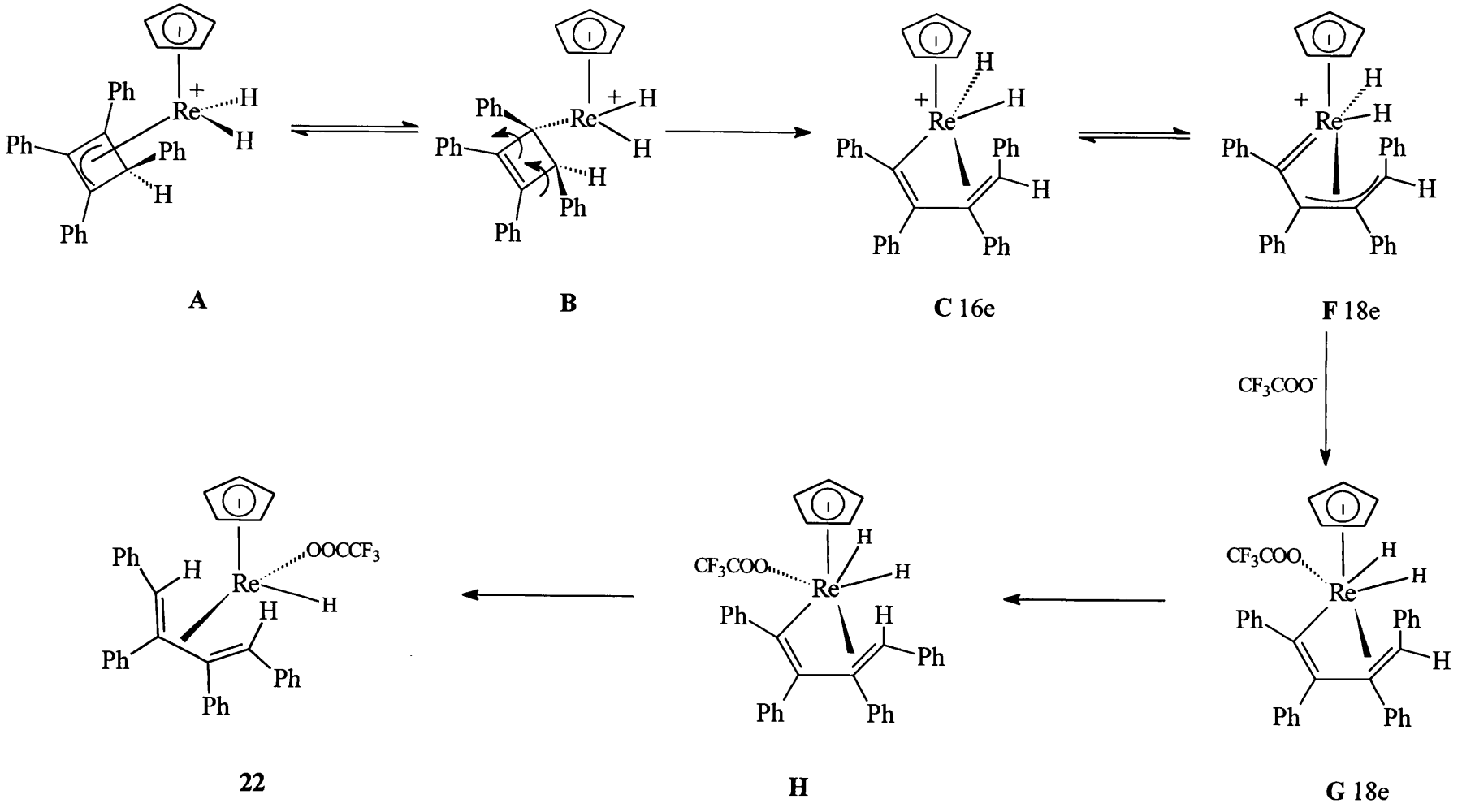

FIGURE 3.33

Maitlis[101] first proposed that a metallocycle ring flip process of η^3-butadienyls was responsible for the stereomutation of the substituents of the terminal carbon (C_4). It was postulated that the formation of a metallocyclopentenyl intermediate **C** (Figure 3.34) from the ground state **A** would require only a small amount of reorganisation. The metallocyclopentenyl **C** ring, which was close to planar would then allow C_3 and its substituents to move either back, giving **B** and hence **A**, or move in the opposite sense, giving **D** and hence **E**.

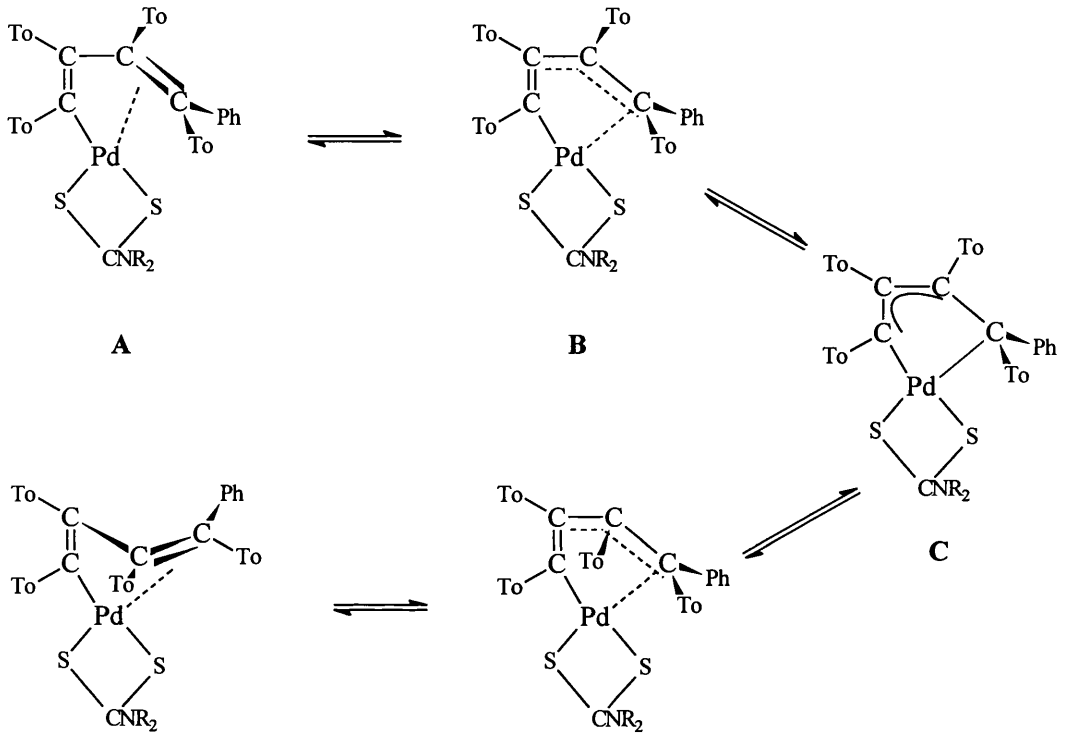

FIGURE 3.34

This particular ring flip process has previously been invoked to explain the formation of the acyl complex [Ru{P(OMe)$_3$}{C(O)C(Ph)=C(Ph)-η^2-(Z)-C(Ph)=CH(PH)}(η-C_5H_5)] **3.39** (Figure 3.35), which has been structurally characterised.[102] The ring flip process, **B** to **C**, (Figure 3.35) was followed by an oxidative addition reaction ($Ru^{II} \rightarrow Ru^{IV}$) of the proximal CHO group. A

subsequent reductive elimination afforded the complex [Ru{P(OMe)$_3$}{C(O)C(Ph)=C(Ph)-η^2-(Z)-C(Ph)=CH(Ph)}(η-C_5H_5)] **3.39**.

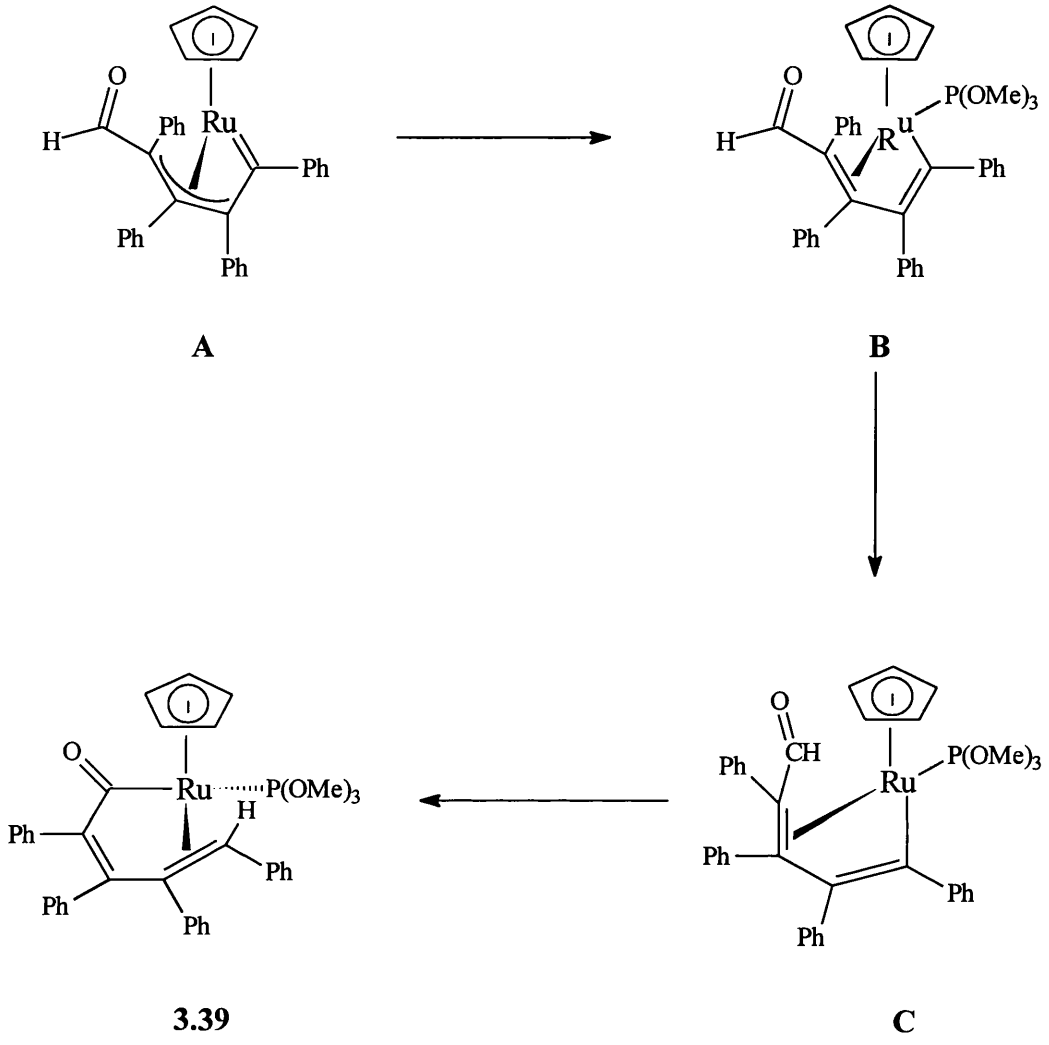

FIGURE 3.35

On re-examination of the ^{1}H NMR spectrum (Table 3.5) of **21** it was evident that the reactive species formed on reaction of **20** with $HBF_4.Et_2O$ is a sixteen-electron 1,3-butadiene complex (Figure 3.36), which is similar to the intermediate **D** in Figure 3.32. The butadiene protons were evident in the ^{1}H NMR spectrum as doublets at δ 3.78 [$J(H^bH^a)$ 3.0 Hz] and δ 4.04 [$J(H^cH^a)$ = 2.5 Hz]. However, because of the absence of a co-ordinating anion it is postulated that in

complex **21** the hydrogens of the terminal 1,3-diene are in *syn* and *anti* positions as the mechanism probably follows that illustrated in Figure 3.32 (**20** → **D**).

TABLE 3.5 : ^{1}H NMR data of **21** and **22**.

	M-H^a	CH^b	CH^c	η-C_5H_5	C_6H_5
22	-8.7	3.78	4.28	4.86	6.84-8.52
21	-7.87	3.40	4.04	4.52	6.74-8.42

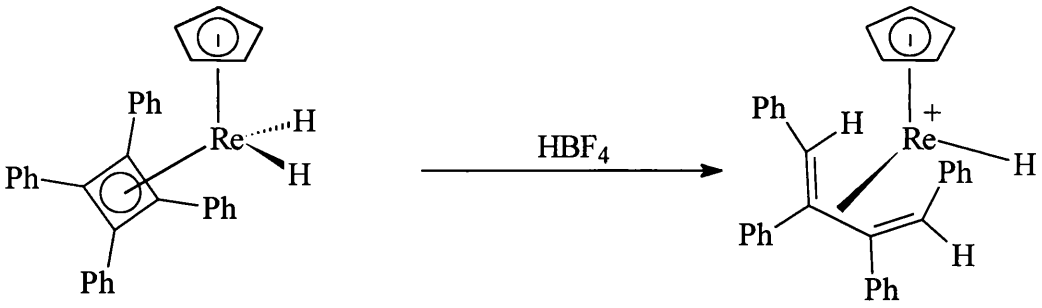

20 **21**

FIGURE 3.36

Thus, it has been successfully demonstrated that proton attack on the cyclobutadiene complex **20** results in a novel ring-opening reaction of the cyclobutadiene ligand to afford substituted buta-1,3-diene complexes.

4. STRUCTURE AND REACTIVITY OF MOLYBDENUM PROP-2-YNYL COMPLEXES.

4.1 Introduction

In Section 2.2 a prop-2-ynyl complex was postulated as an intermediate in the coupling reaction of an alkene and alkyne to afford the S-pentadienyl ligand (Figure 2.16). The chemistry of transition metal prop-2-ynyl and allenyl complexes in general has expanded recently, stimulated by intriguing structural features and the unusual reactivities of these complexes.[103-107]

The first prop-2-ynyl complex $[Os\{\sigma,\eta^2(3e)\text{-}HC{=}C{=}C(H)Ph\}(PMe_3)_4][PF_6]$ **4.1** (Figure 4.1) was reported by Werner[104] in 1985 and since that time there have been several related complexes containing various metals. However, until 1991 all reported complexes had a =CHR group attached to the prop-2-ynyl terminus. The first unsubstituted prop-2-ynyl complex was the cation $[Mo(CO)_2\{\sigma,\eta^2(3e)\text{-}CH_2C_2H\}(\eta^6\text{-}C_6Me_6)][BF_4]$ **4.2** (Figure 4.1) prepared by Krivykh[105] by photolysis of $[Mo(CO)_3(\eta^6\text{-}C_6Me_6)]$ and prop-2-ynyl alcohol in the presence of HBF_4.

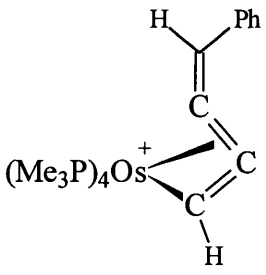

4.1

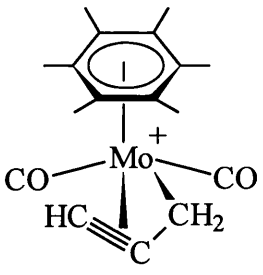

4.2

FIGURE 4.1

These cationic, prop-2-ynyl complexes are susceptible to nucleophilic attack either at the terminal carbons, which is the case with most open π-ligands[106],

or at the central carbon of the C_3H_3 moiety. In fact, Casey observed that $[Re(CO)_2\{\sigma,\eta^2(3e)\text{-}CH_2C_2Me\}(\eta\text{-}C_5Me_5)][PF_6]$ **4.3**, prepared by hydride abstraction with $[Ph_3C][PF_6]$ from the two-electron donor but-2-yne complex $[Re(CO)_2(\eta^2\text{-}MeC_2Me)(\eta\text{-}C_5Me_5)]$, reacted with a variety of soft nucleophiles exclusively at the central carbon atom (Figure 4.2).

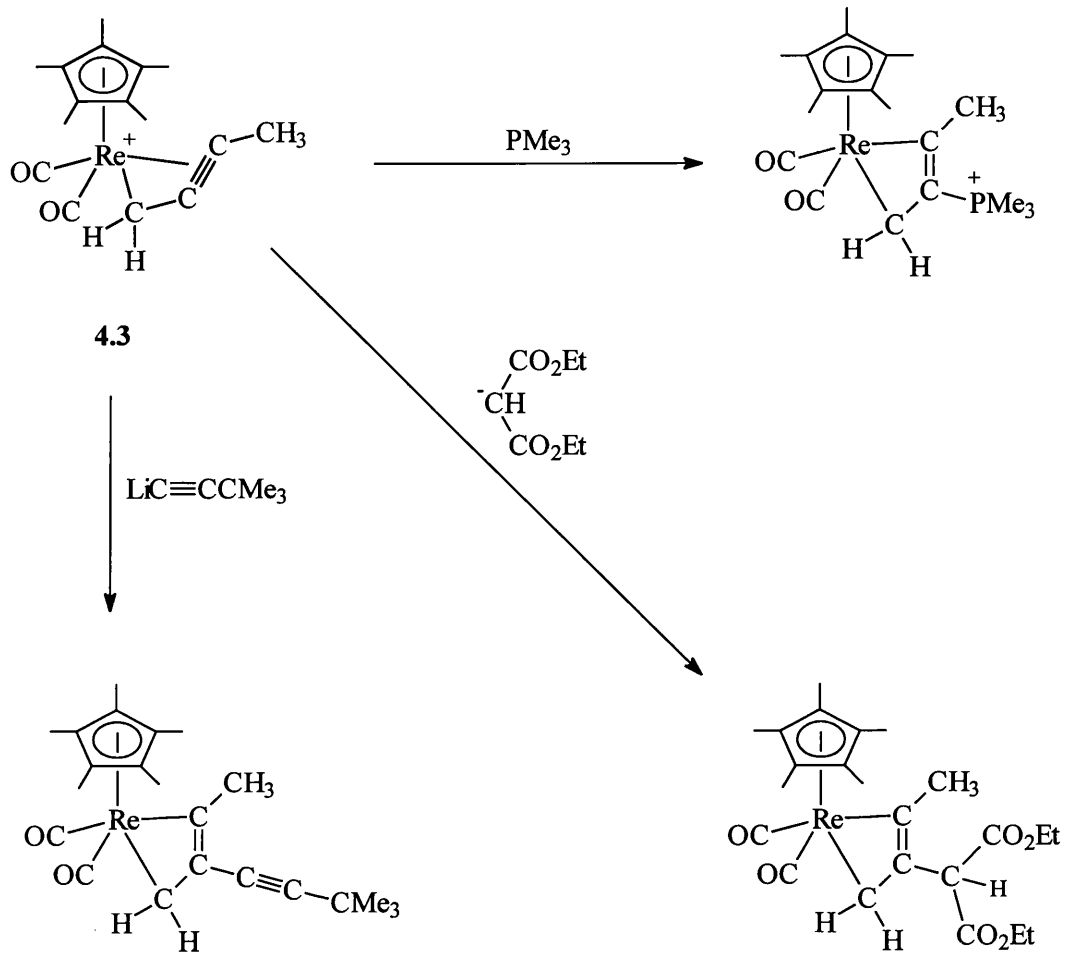

FIGURE 4.2

Cationic prop-2-ynyl complexes are more prevalent than their neutral counterparts, which were first prepared by Wojcicki[107] in 1993 by the reaction of $[ZrCl(Me)(\eta\text{-}C_5H_5)_2]$ **4.4** with the Grignard reagent PhC_2CH_2MgBr to afford $[Zr(Me)\{\sigma,\eta^2(3e)\text{-}CH_2C_2Ph\}(\eta\text{-}C_5H_5)_2]$ **4.5**.

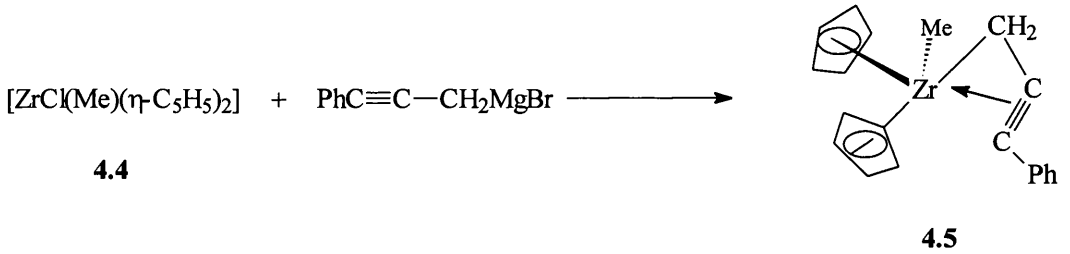

4.4 **4.5**

FIGURE 4.3

The bonding of the CH_2CCPh moiety was described as a combination of η^3-prop-2-ynyl (**A**) and η^3-allenyl (**B**) resonance structures (Figure 4.4), which are possible for these CR_2CCR ligands.

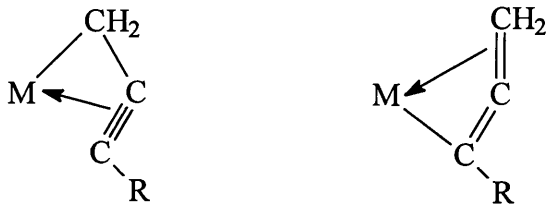

A **B**

FIGURE 4.4

Furthermore, Wojcicki[107] also reported that the reaction of $[ZrCl_2(\eta\text{-}C_5H_5)_2]$ **4.6** with $PhC{\equiv}CCH_2MgBr$ afforded $[Zr(\sigma\text{-}CH_2C_2Ph)\{\sigma,\eta^2(3e)\text{-}CH_2C_2Ph\}(\eta\text{-}C_5H_5)_2]$ **4.7** (Figure 4.5), the first example of a transition metal complex which contained both η^1-prop-2-ynyl and η^3-prop-2-ynyl/allenyl ligands. This complex (**4.7**) exhibited fluxional behaviour in solution and at ambient temperature the two ligands appeared to interconvert.

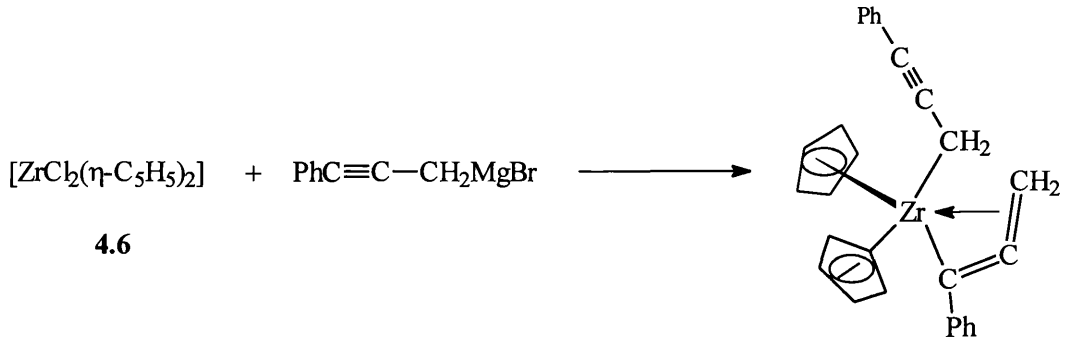

FIGURE 4.5

More recently, within our group, we have reported the synthesis of neutral molybdenum prop-2-ynyl species (**2.5** and **2.6**, see Section 2.1), *via* dehydrohalogenation of [MoBr(RC≡CMe)$_2$(η-C$_5$H$_5$)] complexes (R = Me **2.3** or Ph **2.4**) with lithium bis(trimethyl)silyl amide (Figure 4.6).

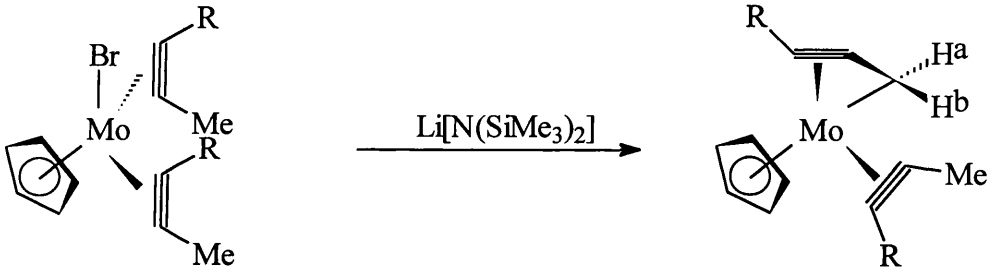

R = Me **2.3**
Ph **2.4**

R = Me **2.5**
Ph **2.6**

FIGURE 4.6

The preparation of **2.5** and **2.6** established a new synthetic pathway to these ligands and constituted the first synthesis of a three-electron σ,η^2-prop-2-ynyl complex by deprotonation of a four-electron donor η^2-alkyne ligand.

Although neutral prop-2-ynyl ligands have been known since 1993, very little has been reported on the reactivity of these species. Complexes **2.5** and **2.6**

offer an opportunity for reactivity studies because of the ability of both the η^2-alkyne (4e to 2e) and the η^3-prop-2-ynyl (3e to 1e) ligands to switch bonding modes, thus providing a co-ordination site for reactive molecules. It has already been reported that the neutral prop-2-ynyl complexes react with two molecules of carbon monoxide to form the complex $[Mo(CO)\{\eta^2,\eta^3\text{-}C(Me)C(O)C(Me)C\text{-}CH_2\}(\eta\text{-}C_5H_5)]$ **4.8** (Figure 4.7), which contained a novel alicyclic C_5 ligand with an exocyclic oxygen and CH_2 groups.[17a]

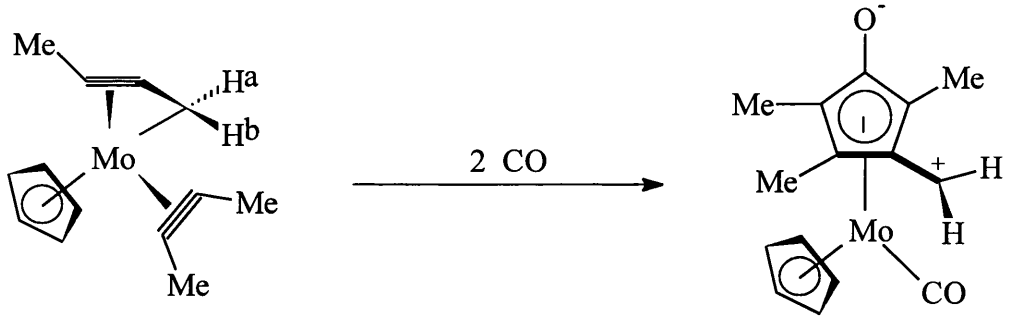

2.5 **4.8**

FIGURE 4.7

As an initial step towards understanding the reactivity and structure of transition metal prop-2-ynyl species a comparative Extended Hückel Molecular Orbital Calculation was carried out on three complexes, the cationic molybdenum complex $[Mo(CO)_2\{\sigma,\eta^2(3e)\text{-}CH_2C_2H\}(\eta^6\text{-}C_6Me_6)][BF_4]$ **4.2** (Figure 4.1), the zirconium complex $[Zr(Me)\{\sigma,\eta^2(3e)\text{-}CH_2C_2Ph\}(\eta\text{-}C_5H_5)_2]$ **4.5** (Figure 4.3) and $[Mo\{\sigma,\eta^2(3e)\text{-}CH_2C_2Ph\}(\eta^2\text{-}MeC_2Ph)(\eta\text{-}C_5H_5)]$ **2.6** (Figure 4.6), using the CACAO2 program.

4.2 An Extended Hückel Molecular Orbital Investigation of the Structure of Prop-2-ynyl Complexes.

The cationic molybdenum complex $[Mo(CO)_2\{\sigma,\eta^2(3e)\text{-}CH_2C_2H\}(\eta^6\text{-}C_6Me_6)][BF_4]$ **4.2** (Figure 4.1)[105], the zirconium complex $[Zr(Me)\{\sigma,\eta^2(3e)\text{-}CH_2C_2Ph\}(\eta\text{-}C_5H_5)_2]$ **4.5** (Figure 4.3)[107] and $[Mo\{\sigma,\eta^2(3e)\text{-}CH_2C_2Ph\}(\eta^2\text{-}MeC_2Ph)(\eta\text{-}C_5H_5)]$ **2.6** (Figure 4.6)[17] have all been structurally characterised by single crystal X-ray crystallography, and it was clearly interesting to compare the bond parameters of the prop-2-ynyl ligand reported for these three complexes. Until now, the bonding description of the prop-2-ynyl ligand has been described in terms of either an η^3-propargyl (**A**) or an η^3-allenyl (**B**) (Figure 4.4).

As is evident from examination of Table 4.1 there are major variations in the C1-C2-C3 angle, and in the M-C1, M-C2 and M-C3 bond lengths, suggesting that the $\sigma,\eta^2(3e)\text{-}C_3H_3$ ligand can adopt different bonding modes. In order to examine the nature of the metal C_3H_3 bonding, and its relationship to the structures observed for the three complexes, a comparative standard Extended Hückel Molecular Orbital (EHMO) study was carried out as implemented in the CACAO2 program using the published molecular parameters and with the simplification that the phenyl substituent in the zirconium complex **4.5** was replaced by a hydrogen atom.

Table 4.1 : Bond parameters of σ,η^2(3e)-prop-2-ynyl complexes

COMPLEX	**BOND LENGTHS(Å)**					**ANGLE (°)**
	C1-C2	**C2-C3**	**M-C1**	**M-C2**	**M-C3**	**C1-C2-C3**
$[Mo(\sigma,\eta^2\text{-}CH_2C_2Ph)(\eta^2\text{-}MeC_2Ph)(\eta\text{-}C_5H_5)]$ **2.6**	1.404(9)	1.281(8)[a]	2.278(6)	2.164(5)	2.105(5)	146.1(6)
$[Mo(CO)_2(\sigma,\eta^2\text{-}CH_2C_2H)(\eta^6\text{-}C_6Me_6][BF_4]$ **4.2**	1.380(4)	1.236(4)	2.340(3)	2.282(3)	2.319(3)	150.9(3)
$[Zr(Me)(\sigma,\eta^2\text{-}CH_2C_2Ph)(\eta\text{-}C_5H_5)_2]$ **4.5**	1.344(5)	1.259(4)	2.658(4)	2.438(3)	2.361(3)	155.4(3)

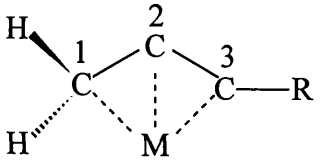

The isolated prop-2-ynyl fragments in all three complexes displayed similar geometries in the sense that they had shorter C2-C3 distances than C1-C2 and had C1-C2-C3 angles of *ca.* 150°. The Fragment Molecular Orbitals (FMOs) for the three prop-2-ynyl units are very similar and are displayed schematically in Figure 4.8. Focusing on the C-C π-type orbitals, the intraligand bonding appears at first sight to resemble allyl-like functions, which extend over the whole carbon framework, and an additional π-bond between C2 and C3 perpendicular to the "allyl" functions. However, the analogy with the η^3-allyl ligand cannot be taken too far since the relevant MO's lie in the plane of the prop-2-ynyl while in an η^3-allyl fragment, these functions are perpendicular to the ligand plane.

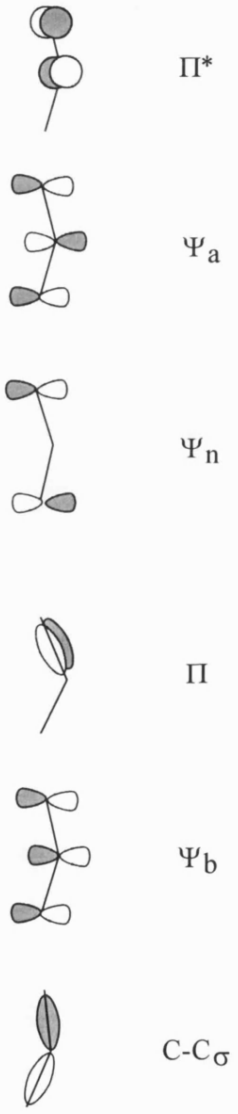

FIGURE 4.8

In all three complexes the metal-C_3H_3 interaction was dominated by a single interaction between the ligand HOMO and the metal fragment LUMO **A** (Figure 4.9). There was also strong evidence for a π-bond lying perpendicular to the ligand plane between C2 and C3 **B** (Figure 4.9).

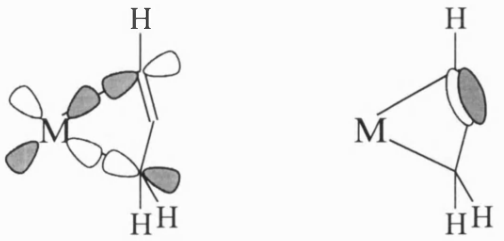

A **B**

FIGURE 4.9

Thus, in all three complexes the C_3H_3 ligand binds mainly through its terminal carbons C1 and C3, while the C2-C3 π-bond does not interact significantly with the metal fragment. In addition to these, there are a number of secondary orbital interactions, which vary from complex to complex (Figures 4.10, 4.11 and 4.12). The most important one for each complex is highlighted and gives an insight into the differences between the bonding modes. Both complex $[Mo\{\sigma,\eta^2(3e)\text{-}CH_2C_2Ph\}(\eta^2\text{-}MeC_2Ph)(\eta\text{-}C_5H_5)]$ **2.6** and $[Zr(Me)\{\sigma,\eta^2(3e)\text{-}CH_2C_2Ph\}(\eta\text{-}C_5H_5)_2]$ **4.5** contain a very asymmetrically bonded C_3H_3 ligand with the M-C1 distance significantly longer than the M-C3 contact. The orbital interactions shown in Figures 4.10 and 4.12 illustrate how C3 is rather more firmly held than C1. In contrast, the extra orbital interaction for the cation $[Mo(CO)_2\{\sigma,\eta^2(3e)\text{-}CH_2C_2H\}(\eta^6\text{-}C_6Me_6)][BF_4]$ **4.2** was concentrated in a C_3H_3 function, which extended more or less equally over the whole ligand, and therefore tended to favour a more symmetrical binding. Hence, the Mo-C1 and Mo-C3 distances for complex **4.2** are almost identical.

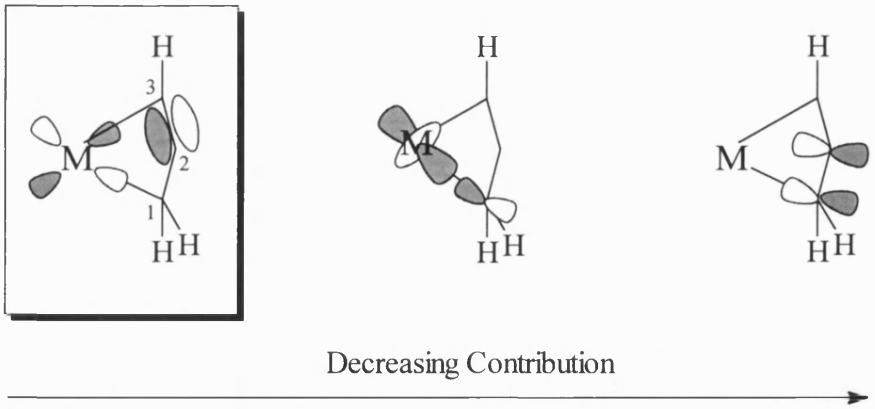

FIGURE 4.10 : Secondary Orbital Interactions of [Zr(Me){σ,η^2(3e)-CH_2C_2Ph}(η-$C_5H_5)_2$] **4.5**

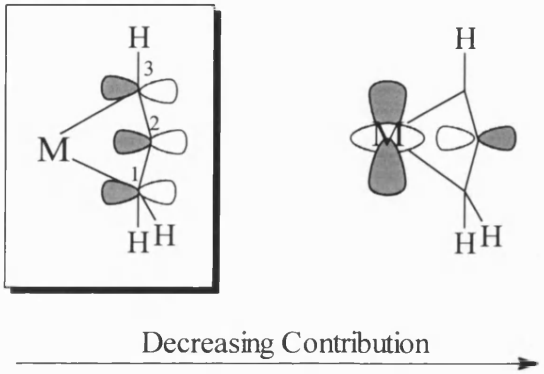

FIGURE 4.11 : Secondary Orbital Interactions of [$Mo(CO)_2$}{σ,η^2(3e)-CH_2C_2H} (η^6-C_6Me_6)][BF_4] **4.2**

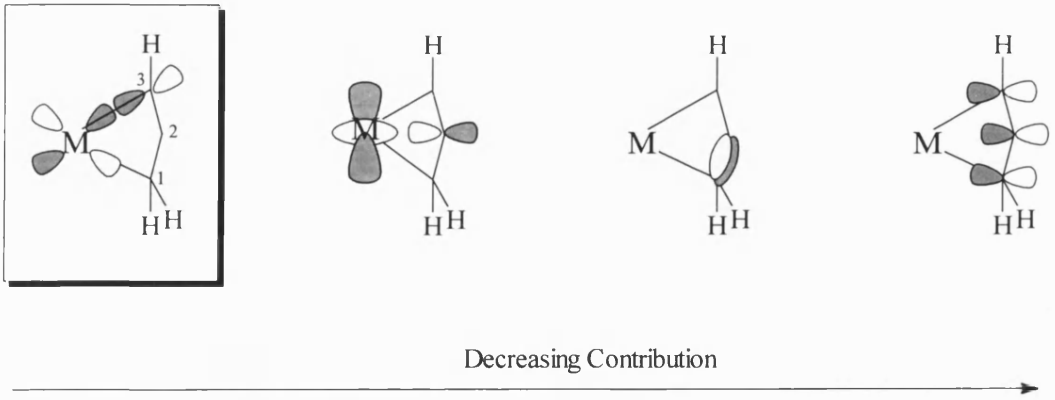

FIGURE 4.12 : Secondary Orbital Interactions of [Mo{σ,η^2(3e)-CH_2C_2Ph}(η^2-MeC_2Ph)(η-C_5H_5)] **2.6**

Although these secondary interactions rationalise why the C_3H_3 ligand is unsymmetrically bonded in the complexes $[Zr(Me)\{\sigma,\eta^2(3e)\text{-}CH_2C_2Ph\}(\eta\text{-}C_5H_5)_2]$ **4.5** and $[Mo\{\sigma,\eta^2(3e)\text{-}CH_2C_2Ph\}(\eta^2\text{-}MeC_2Ph)(\eta\text{-}C_5H_5)]$ **2.6**, they also highlight the variations in the M-C_3H_3 bonding. Valence bond representations provide an alternative view and Figure 4.13 shows schematic representations of the formal valence bond canonical structures for M-C_3H_3 binding. Indeed, it is interesting that the structures of such complexes have previously only been described usually in terms of one or other of the outer two forms (**A** and **C**). However, the present EHMO calculations suggest that a third canonical structure is also relevant **B** (Figure 4.13). Taking all of the theoretical data together, it was clear that the cation $[Mo(CO)_2\{\sigma,\eta^2(3e)\text{-}CH_2C_2H\}(\eta^6\text{-}C_6Me_6)][BF_4]$ **4.2** conformed more to canonical form **B**, whilst complexes **4.5** and **2.6** lie towards the two extremes (**A** and **C**, respectively). Hence, despite the qualitatively similar asymmetric bonding mode for the latter two species, the bonding was better described by different canonical forms.

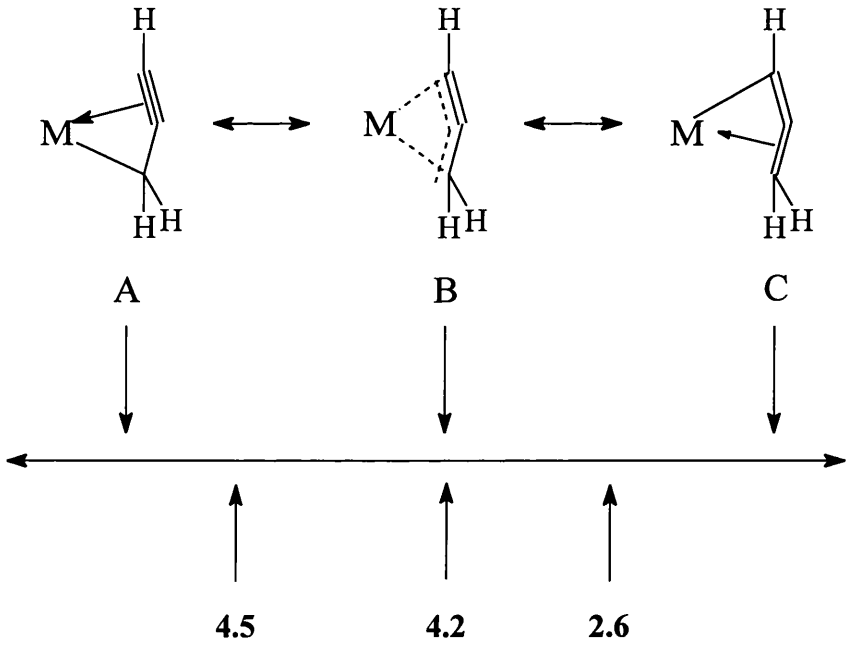

FIGURE 4.13

4.3 Reactivity of $[Mo\{\sigma,\eta^2(3e)\text{-}CH_2C_2R\}(\eta^2\text{-}MeC_2R)(\eta\text{-}C_5H_5)]$ with Trifluoroacetic Acid.

The complexes $[Mo\{\sigma,\eta^2(3e)\text{-}CH_2C_2Ph\}(\eta^2\text{-}MeC_2Ph)(\eta\text{-}C_5H_5)]$ **2.5** and $[Mo\{\sigma,\eta^2(3e)\text{-}CH_2C_2Ph\}(\eta^2\text{-}MeC_2Me)(\eta\text{-}C_5H_5)]$ **2.6** are obviously also of interest from the standpoint of reactivity. As mentioned previously, it has already been established that these complexes react with carbon monoxide to form a cyclic C_5 ring (Figure 4.8).

As complexes **2.5** and **2.6** are formed by deprotonation (see Section 4.1) their reactivity towards protonic acids HA was examined. Treatment (-78°C → +25°C) of **2.6** with trifluoroacetic acid in dichloromethane solution resulted in a change in colour from red to yellow, and workup by recrystallisation afforded the bis-alkyne complex $[Mo\{OC(O)CF_3\}(\eta^2\text{-}MeC_2Ph)_2(\eta\text{-}C_5H_5)]$ **24** (Figure 4.14), which was characterised by elemental analysis and nmr spectroscopy. The $^{13}C\{^1H\}$ NMR spectrum clearly showed the presence of three electron donor alkynes by the contact carbon resonances at δ 168.2 and δ 186.8. It also indicated the presence of a trifluoroacetate group by the two quartets at δ 116.3 [$^1J(CF)$ 292] and δ 163.3 [$^2J(CF)$ 37.5]. A similar reaction between **2.5** and CF_3CO_2H resulted in the formation of $[Mo\{OC(O)CF_3\}(\eta^2\text{-}MeC_2Me)_2(\eta\text{-}C_5H_5)]$ **25** (Figure 4.14), which was similarly characterised to complex **24**.

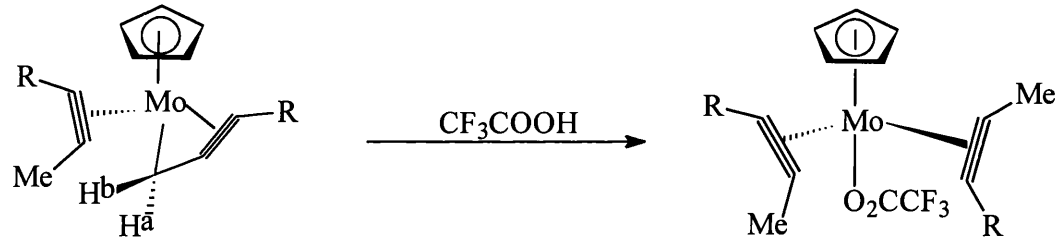

R = Me **2.5**
Ph **2.6**

24 R = Ph, X = CF_3CO_2
25 R = Me, X = CF_3CO_2

FIGURE 4.14

These reactions are especially interesting because a Z-shaped $\sigma,\eta^2(3e)$-prop-2-ynyl fragment is transformed on protonation into a U-shaped η^2-alkyne ligand. As a first step towards understanding this process it was clearly important to examine the charge distribution within molecules of the type represented by **2.5** and **2.6**, as it was a reasonable assumption that the protonation reaction was charge controlled. From an EHMO calculation using the bond parameters established for complex **2.5** the charge distribution within the molecule was obtained, with the alkyl substituents being replaced by hydrogen atoms for simplicity (Table 4.2).

TABLE 4.2 : Charge Distribution of Complex $[Mo\{\sigma,\eta^2(3e)\text{-}CH_2C_2H\}(\eta^2\text{-}HC_2H)(\eta\text{-}C_5H_5)]$ **2.5**.

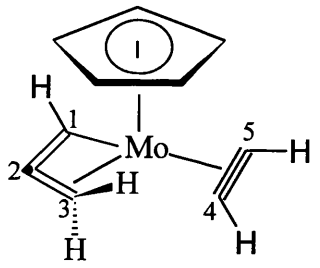

Mo	C1	C2	C3	C4	C5
0.739	-0.316	0.102	-0.165	-0.304	-0.240

This indicated that direct protonation of the prop-2-ynyl methylene group, i.e. C3, Table 4.2, was unlikely, and that if the C_3H_3 fragment was actually the site of an initial charge controlled attack by a proton then this was more likely to occur on the opposite end (C1, Table 4.2) of the prop-2-ynyl ligand. This would, however, lead to the formation of the $\eta^2(2e)$-allene/$\eta^2(4e)$-alkyne substituted species $[Mo\{OC(O)CF_3\}\{\eta^2\text{-}CH(Me)=C=CH_2\}(\eta^2\text{-}MeC_2Me)(\eta\text{-}C_5H_5)]$, which would be expected to be stable and not likely to rearrange *via* a H-shift process into the isolated product $[Mo\{OC(O)CF_3\}(\eta^2\text{-}MeC_2Me)_2(\eta\text{-}C_5H_5)]$ **25**. This mechanistic difficulty was avoided if, as illustrated in Figure 4.15 and in agreement

with the calculations (Table 4.2), protonation occurred on the alkyne contact carbon *cis* to the prop-2-ynyl methylene group thus affording the η^2(3e)-vinyl substituted intermediate **A** (Figure 4.15). There is, in fact, precedent for the formation of an η^2-vinyl ligand by the protonation of an η^2(4e)-alkyne, and for the transformation of an η^2(3e)-vinyl into a η^1(1e)-vinyl as is required by the step **A** $\rightarrow$ **B**. A β-hydrogen elimination reaction **B** $\rightarrow$ **C**, followed by migration of the Mo-H hydrogen onto the methylene end of the prop-2-ynyl ligand, thus provides access to the conformationally unstable η^2-U-alkyne/η^2-Z-alkyne substituted species **D**, which is an obvious precursor of the isolated products $[Mo\{OC(O)CF_3\}(\eta^2\text{-}MeC_2Ph)_2(\eta\text{-}C_5H_5)]$ **24** and $[Mo\{OC(O)CF_3\}(\eta^2\text{-}MeC_2Me)_2(\eta\text{-}C_5H_5)]$ **25**.

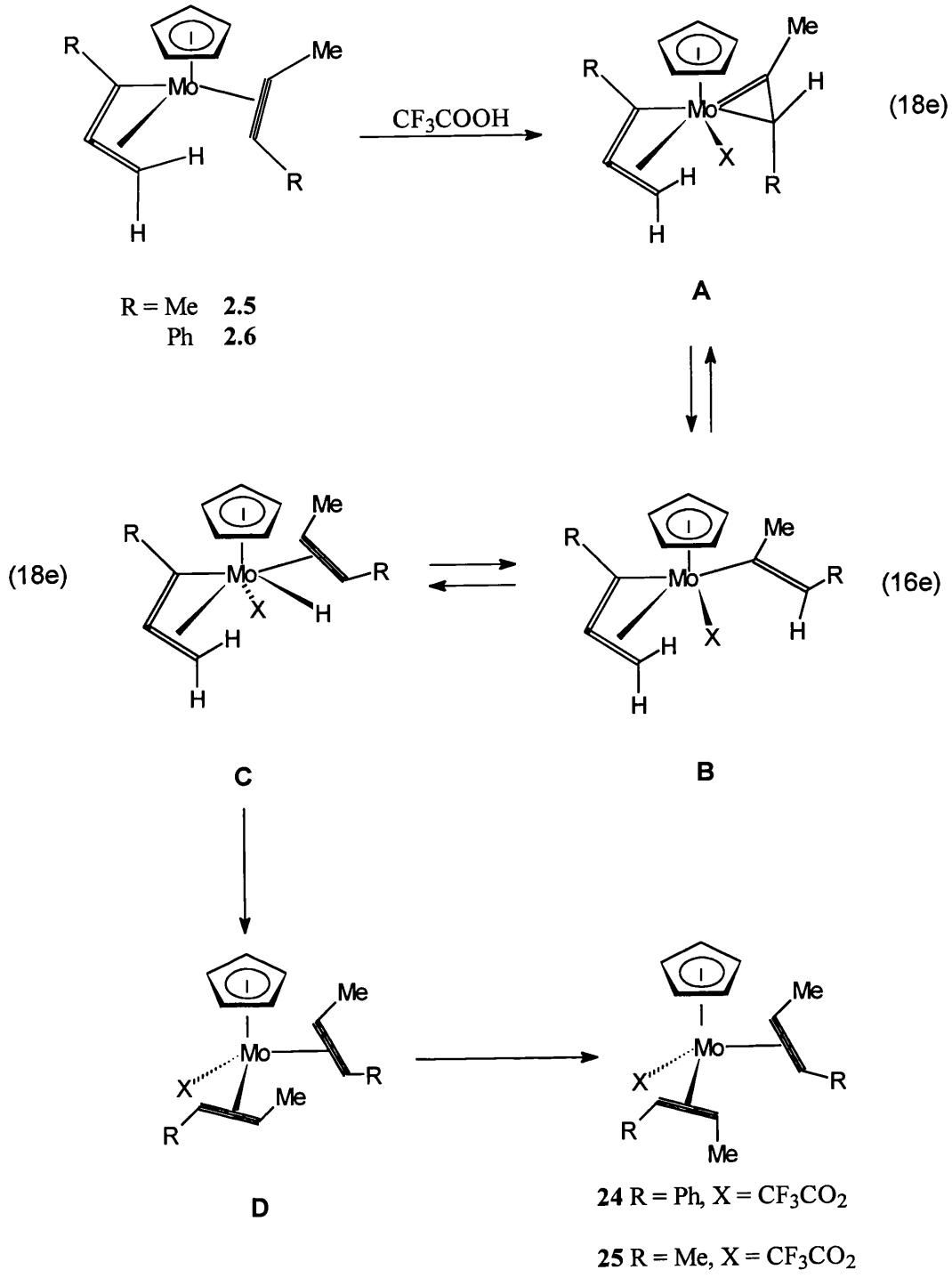
R
Mo
Me
H
R
H
CF_3COOH
(18e)
R = Me 2.5
Ph 2.6
A
(18e)
C
B
(16e)
D
24 R = Ph, X = CF_3CO_2
25 R = Me, X = CF_3CO_2

FIGURE 4.15

4.4. Reactivity of [Mo{σ,η^2(3e)-CH_2C_2Me}(η^2-MeC_2Me)(η-C_5H_5)] with Hexafluorobut-2-yne.

As mentioned previously, complex [Mo{σ,η^2(3e)-CH_2C_2Me}(η^2-MeC_2Me)(η-C_5H_5)] **2.5** contains η^2-alkyne and η^2(3e)-prop-2-ynyl ligands, which both have the ability to switch bonding modes and, hence, provide a co-ordination site for reactive molecules. Thus, following the finding commented on in Section 4.1 that [Mo{σ,η^2(3e)-CH_2C_2Me}(η^2-MeC_2Me)(η-C_5H_5)] **2.5** reacts with carbon monoxide to afford the alicyclic complex **4.8** (Figure 4.7), it was clearly interesting to examine the reactivity of complex **2.5** towards the good π-acceptor hexafluorobut-2-yne.

Excess hexafluorobut-2-yne gas was condensed at -196°C into a reinforced Schlenk tube, under vacuum, containing a toluene solution of [Mo{σ,η^2(3e)-CH_2C_2Me}(η^2-MeC_2Me)(η-C_5H_5)] **2.5**. After leaving the solution in the sealed tube at room temperature for 4-5 hours, with occasional agitation, the solution was filtered through a canula. The solvent was then removed *in vacuo* and the residue chromatographed (Florisil) using toluene as the eluant to afford a yellow/orange complex **26** (Yield 15%). An elemental analysis (Found : C, 42.8 ; H, 2.8%. Calc. C, 42.59; H, 2.72%) and mass spectrum (M^+ = 593) suggested that two molecules of hexafluorobut-2-yne had been incorporated. This was supported by the ^{19}F NMR spectrum, which displayed four different CF_3 resonances at δ - 49.2 (multiplet), δ -53.81 (quartet), δ -57.1 (multiplet) and δ 72.6 (multiplet). Four quartets in the $^{13}C\{^1H\}$ NMR spectrum corresponded to the four inequivalent carbons of the trifluoromethyl groups at δ 122.3, 124.9, 125.5 and 128.7, all with a $^1J(CF)$ coupling of 270-280 Hz.

The ^1H and $^{13}C\{^1H\}$ NMR spectra displayed resonances characteristic of a co-ordinated cyclopentadienyl ring at δ 4.46 and δ 94.0, respectively. However, particularly interesting was the absence of alkyne contact carbons in the $^{13}C\{^1H\}$ NMR spectrum, and the presence of three different methyl carbon environments at

δ 13.6, 18.4 and 19.4. These three inequivalent methyl groups were also clearly evident in the ^{1}H NMR spectrum at δ 1.4 (singlet), 1.73 (quartet) and 2.0(quartet). A second interesting feature of the ^{1}H NMR spectrum was the presence of a quartet and a singlet resonance at δ 2.68 and δ 4.69, respectively, both of which integrated for one proton.

Thus, the NMR spectrocopic evidence suggested that an unusual reaction had occurred between the methyl substituted prop-2-ynyl fragment, the co-ordinated but-2-yne and two molecules of hexafluorobut-2-yne.

Earlier work has shown that two and three molecules of hexafluorobut-2-yne can couple or cyclise at a metal centre. For example, the reaction of the ruthenium hydride complex $[RuH(PPh_3)_2(\eta\text{-}C_5H_5)]$[56] **2.47** with hexafluorobut-2-yne afforded the σ-vinyl complex **4.9** (Figure 4.16) and an η^3(3e)-butadienyl complex **2.48** (See Figure 2.46, section 2.7). The loss of a phosphine from **2.47** provides a vacant co-ordination site for the hexafluorobut-2-yne molecule, which then provides access to the intermediate **A**. This can then undergo a form of ring-opening to afford the intermediate **B**, which can either react with the free phosphine to form the σ-vinyl product **4.9**, or with a second molecule of hexafluorobut-2-yne to afford the η^3(3e)-butadienyl complex **2.48** (Figure 4.16).

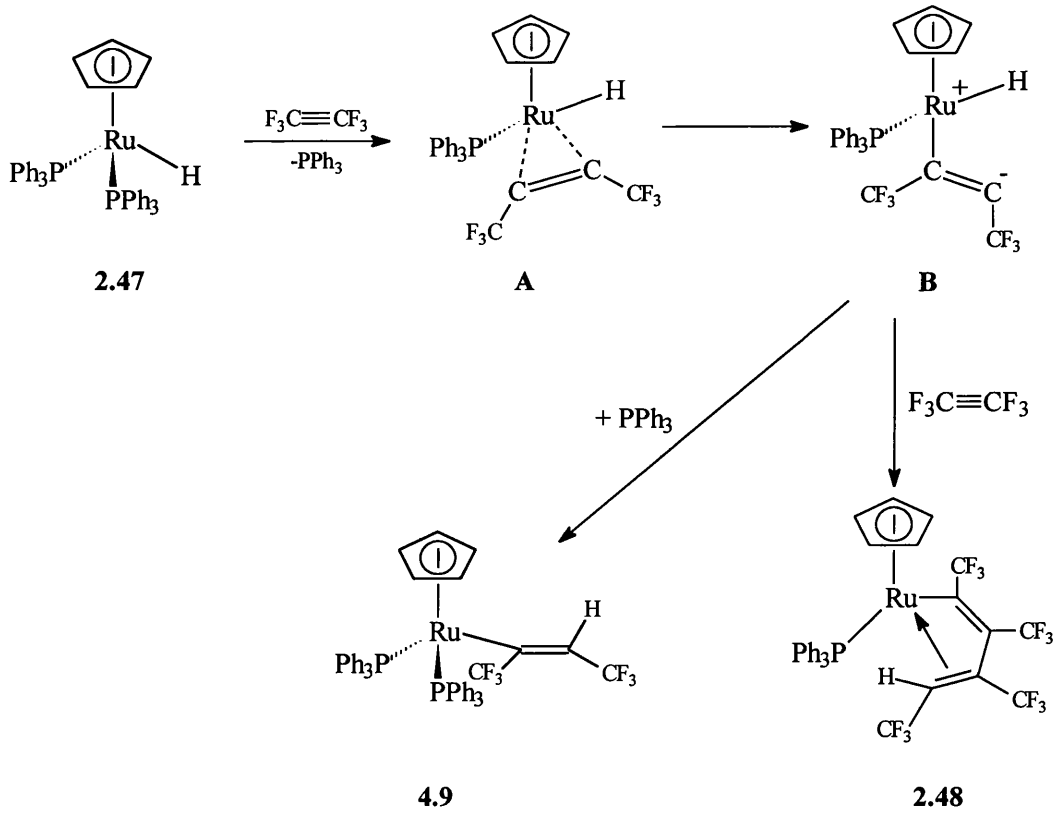

2.47 **A** **B**

4.9 **2.48**

FIGURE 4.16

In order to elucidate the exact nature of complex **26** a single crystal X-ray diffraction study was undertaken on crystals grown from an toluene/hexane mixture at -10°C (Figure 4.17, selected bond lengths and angles are listed in Table 4.4). Complex **26** was shown to contain an (η^5-C_5H_5)Mo fragment as expected and an η^3,η^4-bicyclo[4,3,0]nonyl ring system which exhibited a torsion angle for C2-C1-C5-C6 of 154.0° and for C9-C1-C5-C4 of -114.39° with an angle between the planes of C1-C2-C3-C4 and C1-C9-C8-C7 of 52.42°.

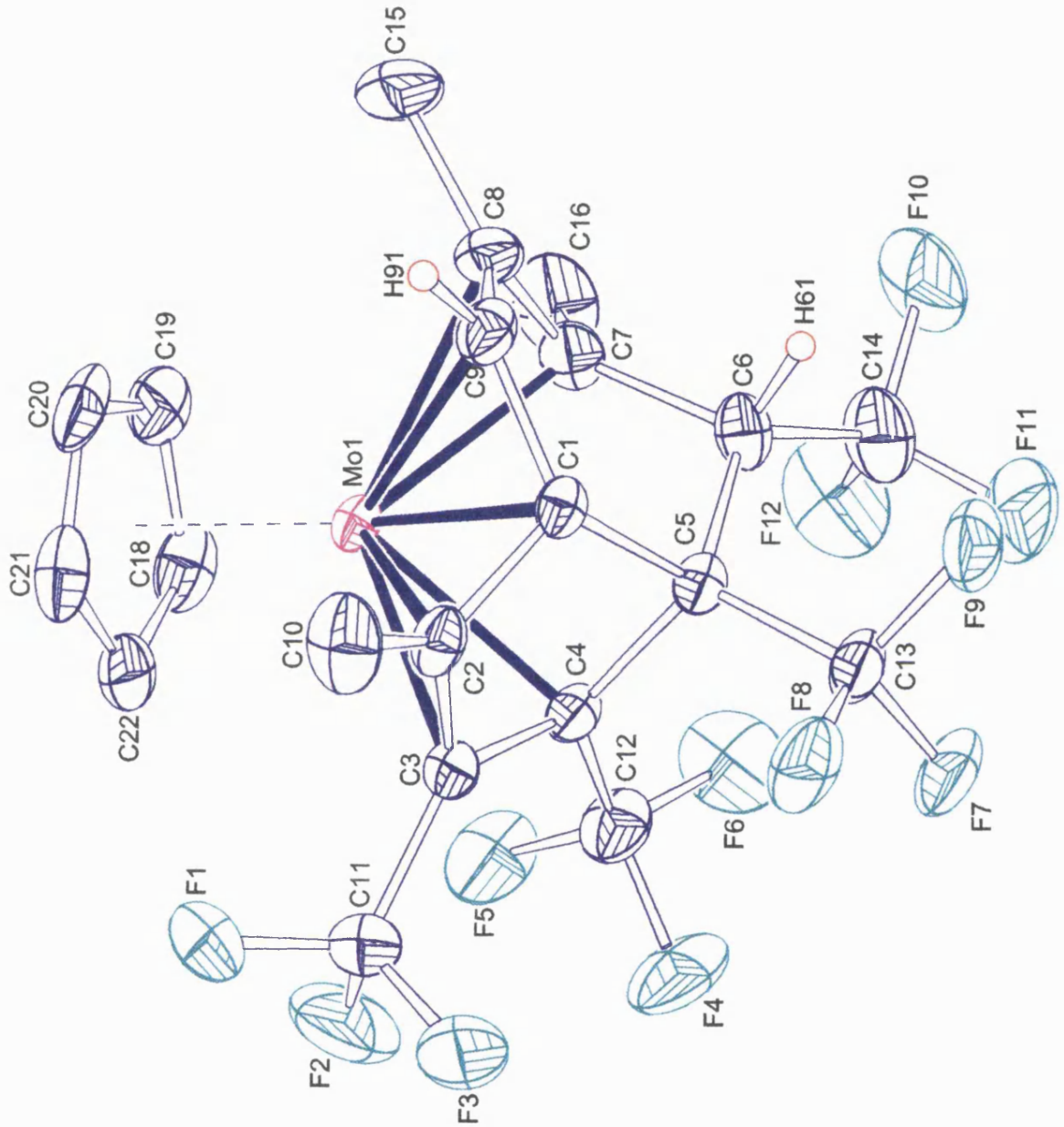

FIGURE 4.17 : ORTEP of Complex **26**.

TABLE 4.4 : Selected Bond Lengths(Å) and Angles (°) for complex **26**.

Atom	Bond Length	Atom	Bond Length
C1-C2	1.447(6)	C1-C5	1.543(5)
C2-C3	1.424(6)	Mo-C1	2.119(4)
C3-C4	1.465(6)	Mo-C2	2.196(4)
C4-C5	1.541(6)	Mo-C3	2.239(4)
C5-C6	1.525(6)	Mo-C4	2.269(4)
C6-C7	1.563(7)	Mo-C7	2.343(4)
C7-C8	1.423(7)	Mo-C8	2.337(4)
C8-C9	1.399(7)	Mo-C9	2.241(4)
C9-C1	1.451(6)		

Atom	Angle	Atom	Angle
C1-C2-C3	103.1(3)	C3-C4-C5	107.9(4)
C1-C9-C8	115.9(4)	C5-C6-C7	106.6(3)
C9-C1-C5	127.6(4)	C6-C7-C8	111.9(4)

The bonding between the molybdenum and the C_9 ring can be described as an asymmetric η^3-allylic interaction from the C_6 ring with Mo-C9 and Mo-C7 distances of 2.241(4) and 2.343(4) Å, respectively, along with an asymmetric η^4-1,3-diene interaction from the C_5 ring with Mo-C1, Mo-C2, Mo-C3 and Mo-C4 distances of 2.119(4), 2.196(4), 2.239(4) and 2.269(4) Å.

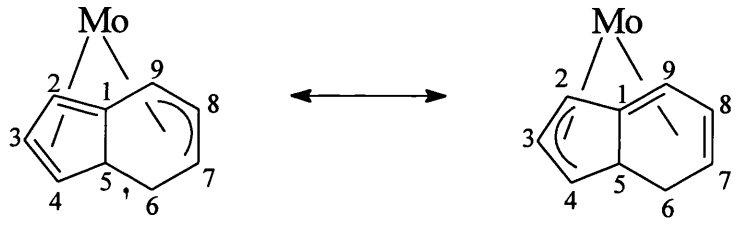

FIGURE 4.18

However, a more accurate picture of the bonding is provided by the two canonical forms illustrated in Figure 4.18. Pyramidalisation is evident on carbon C1 as measured by the fact that this carbon is 0.213Å out of the plane defined by

C2, C9 and C5. Pyramidalisation has also been observed in η^4-trimethylenemethane metal complexes[108] and the reason for this effect has been discussed by Hoffmann and co-workers.[109]

With the establishment of the structure of complex **26** by X-ray crystallography the ^{1}H NMR spectrum was re-examined. It was clear that the methyl resonance at δ1.4, which was a singlet, was attributable to the methyl (Me^a) attached to C8 (Figure 4.19) and that the other two methyl resonances (δ 1.73 and 2.0) were quartets as a result of coupling to a trifluoromethyl group. H^b resonated at δ 2.68 as a quartet, again due to coupling to a trifluoromethyl group, and was therefore readily distinguishable from the H^c at δ 4.69, which resonated as a singlet.

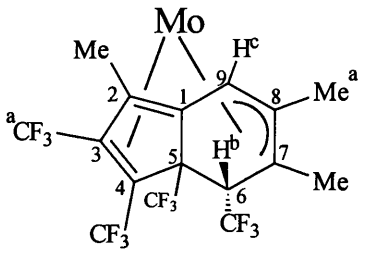

FIGURE 4.19

Although the linking of alkynes at one or two metal centres has attracted considerable attention, there is no precedent for a reaction of the type involved in the formation of complex **26**. A mechanism which can explain its formation must show how the bicyclic system is formed, and also explain how a hydrogen atom, which has its origin on a prop-2-ynyl methylene group ends up on the opposite face of the C_6 ring to which the molybdenum is co-ordinated. The well established reaction paths for hydrogen-shift processes would all place the hydrogen i.e. H61 in Figure 4.17, on the same face as the metal. Interestingly, these special stereochemical requirements are accommodated by the reaction pathway illustrated in Figure 4.20.

Initially in the reaction of [Mo{σ,η^2(3e)-CH_2C_2Me}(η^2-MeC_2Me)(η-C_5H_5)] **2.5** with excess hexafluorobut-2-yne, one hexafluorobut-2-yne molecule might reasonably be expected to co-ordinate onto the molybdenum centre with a concomitant switch (3e → 1e) in the bonding mode of the prop-2-ynyl fragment. Migration (**A** → **B**, Figure 4.20) of the resulting σ-allenyl group onto the co-ordinated hexafluorobut-2-yne then provides access to the intermediate **B** carrying a co-ordinated allene and η^2(4e)-bonded but-2-yne. Reaction of **B** with a second molecule of hexafluorobut-2-yne could then lead to the coupling of the co-ordinated allene and but-2-yne to form the metalla-bicyclo[3,3,0]octyl ring system present in **C**. Ring expansion (5 → 7) *via* migration of the dimethyl substituted σ-vinyl group and the co-ordinated hexafluorobut-2-yne then provides access to the metalla-bicyclo[5,3,0]nonyl intermediate **D**, which carries all of the substituents in the correct positions except for the hydrogen attached to C6. Of course, not only must a hydrogen atom be moved, but also a final carbon-carbon bond needs to be formed. This latter step can be achieved *via* a reductive elimination reaction **D** → **E** which gives the cyclonona-tetraene complex **E**. Since a suprafacial 1,7 hydrogen shift process within **E** would be disallowed such a reaction cannot be used to relocate the hydrogen atom. This can, however, be achieved by first forming **F** by a ring closure reaction, i.e. migration of the Mo-vinyl onto a co-ordinated alkene and then *via* a molybdenum assisted step to form the molybdenum-hydrido complex **G**. It is suggested that the trifluoromethyl substituents present in this molecule will then assist ionisation of the acidic Mo-H bond to give **H**, which can either be attack by H^+ to reform **G** or the stabilised anion could be protonated on the face opposite to which the metal is co-ordinated to the isolated product **26**. Thus, it is suggested that it is the stability of the anion present in **H** which allows for the placement of a hydrogen on C6 (crystallographic numbering) *trans* to the molybdenum.

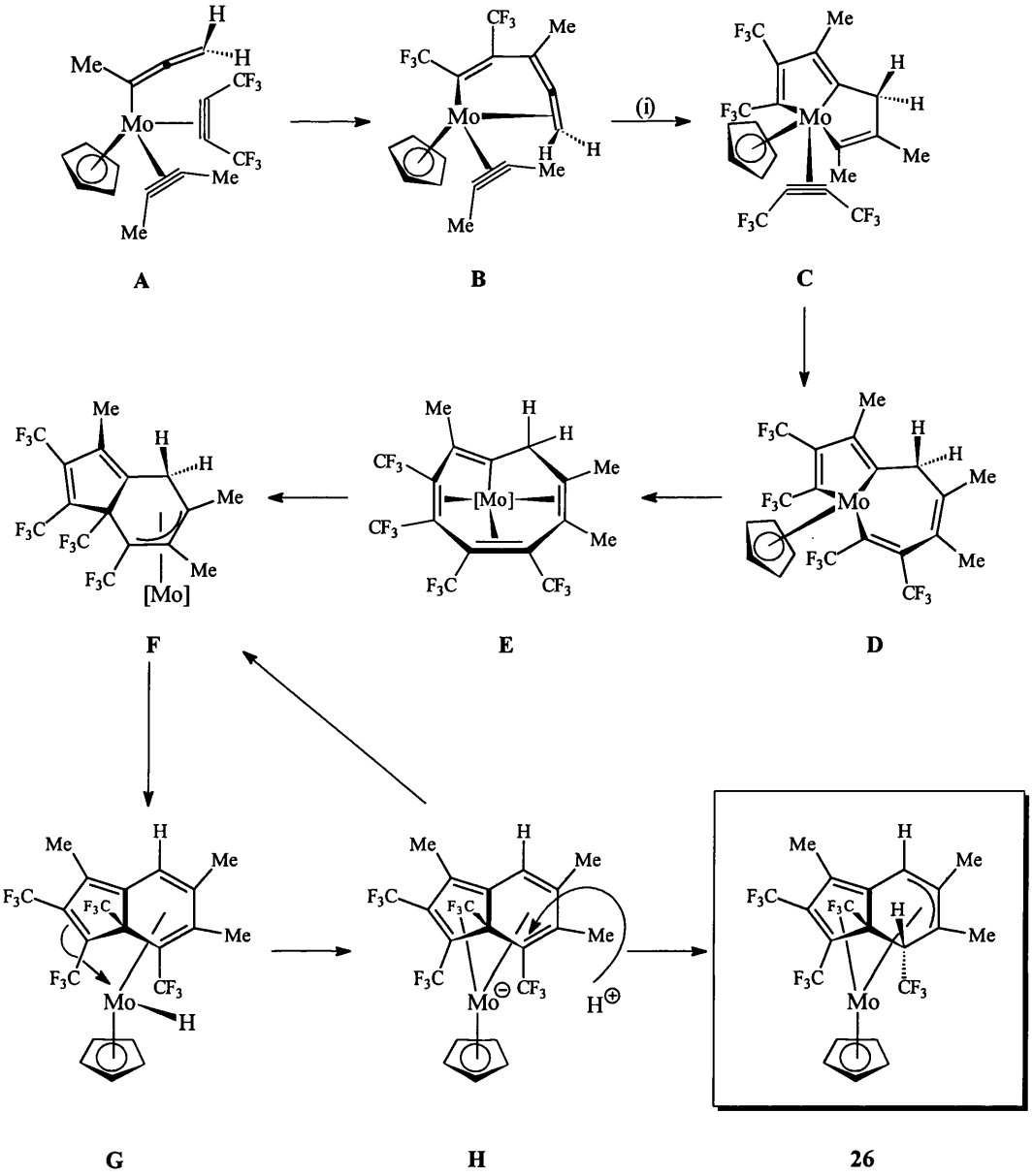

FIGURE 4.20 : [Mo] = (η-C_5H_5)Mo, (i) + $CF_3C{\equiv}CCF_3$.

Thus, it has been demonstrated that complex **2.5** undergoes an unusual cyclisation reaction not only in the presence of carbon monoxide but also in the presence of excess hexafluoro-but-2-yne.

5. EXPERIMENTAL

The ^{1}H, $^{13}C\{^{1}H\}$, $^{31}P\{^{1}H\}$ and ^{19}F NMR spectra were recorded on JEOL GX270 and EX400 spectrometers. Data are given for room temperature (20°C) measurements unless otherwise stated. Chemical shifts are referenced relative to tetramethylsilane, external H_3PO_4 and CCl_3F respectively. Coupling constants are in Hz. IR spectra were recorded on a Nicolet 580P FT-IR spectrometer. The EPR spectra were recorded on a Varian E3-EPR spectrometer at room temperature. All reactions were carried out in Schlenk tubes under an atmosphere of dry oxygen-free nitrogen, using freshly distilled and degassed solvents. Column chromatography was performed using BDH alumina, Brockmann activity II unless otherwise stated, as the solid support. The complexes *o*-diphenylphosphinostyrene (dpps),[110] $[Mo(CO)(\eta^2\text{-}MeC_2Ph)_2(\eta\text{-}C_5H_5)][BF_4]$,[111] $[Mo(CO)(\eta^2\text{-}MeC_2Ph)_2(\eta^5\text{-}C_9H_7)][BF_4]$,[54] $[Mo(CO)(\eta^2\text{-}MeC_2Ph)_2(\eta^5\text{-}C_5Me_5)][BF_4]$,[54] $[ReBr_2(\eta^2\text{-}MeC_2Ph)(\eta\text{-}C_5H_5)]$,[55] $[ReBr_2(\eta^2\text{-}PhC_2Ph)(\eta\text{-}C_5H_5)]$,[55] $[Fe(\eta\text{-}C_5H_5)_2][BF_4]$,[112] $[Mo\{\sigma,\eta^2(3e)\text{-}CH_2C_2Ph\}(\eta^2\text{-}MeC_2Ph)(\eta\text{-}C_5H_5)]$[17] and $[Mo\{\sigma,\eta^2(3e)\text{-}CH_2C_2Me\}(\eta^2\text{-}MeC_2Me)(\eta\text{-}C_5H_5)]$,[17] were prepared by published procedures. All other chemicals were commercially obtained and used as received, unless otherwise stated.

Extended Hückel MO calculations were performed using the CACAO2 program package of Mealli and Proserpio.[113] In general, unless otherwise stated all C-H distances were idealised to 1.10Å. EHMO parameters for molybenum and rhenium were as supplied with the CACAO program while those for the zirconium complex **4.5** (Section 4.2) were obtained from the literature.[114]

The cyclic voltammetry was performed using a-three electrode system with a platinum working electrode, a platinum gauze counter (secondary) electrode and a silver wire reference on an Oxford Electrodes potentiostat. The solution was degassed with argon prior to use.

5.1 Preparation of $[Mo(\eta^2\text{-}MeC_2Ph)(dpps)(\eta\text{-}C_5H_5)][BF_4]$ 1.

A solution of $[Mo(CO)(\eta^2\text{-}MeC_2Ph)_2(\eta\text{-}C_5H_5)][BF_4]$ (0.51g, 1mmol) and dpps (0.29g, 1mmol) in dichloromethane (20ml) was refluxed for 24 hours. On cooling and addition of diethyl ether (20ml) a red solid was precipitated. Recrystallisation from dichloromethane/ether afforded red solvated *crystals* of **1** (0.64g, Yield 98%) (Found : C, 60.4 ; H, 4.5%. Calc. for $C_{34}H_{30}BF_4MoP.\ 0.5CH_2Cl_2$: C, 59.6 ; H, 4.5%).

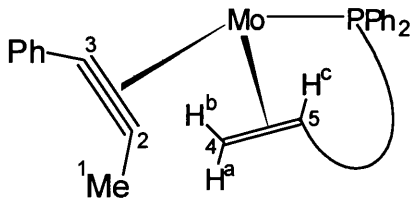

^{1}H ($CDCl_3$) : δ 1.00 [br.d, 1H, H^a, J(H^aH^c) 14.1], 1.75 (s, 3H, Me), 2.86 [br.d, 1H, H^b, J(H^bH^c) 8.6], 4.41 (m, 1H, H^c), 5.33 (s, CH_2Cl_2), 5.52 (s, 5H, Cp), 7.0-8.0 (m, 19H, Ph).

^{13}C{^{1}H} (CD_2Cl_2) : δ 20.5 [d, ≡C*Me*, J(CP) 8.1], 35.6 (s, C_4), 61.7 (s, C_5), 100.4 (s, Cp), 127.9-150.4 (m, Ph), 220.5 [d, ≡*C*Me, J(CP) 5.5], 229.6 [d, ≡*C*Ph, J(CP) 22.6].

^{31}P{^{1}H} ($CDCl_3$) : δ 80.2 (s).

Mass Spectrum : m/z 567 (M^+), 87 (BF_4^-).

5.2 Deprotonation of 1 to form [Mo{η^2,η^3(5e)-S-CH_2CHC(Ph)CH=CH-o-$C_6H_4PPh_2$}(η-C_5H_5)] 2.

Lithium bis(trimethylsilyl)amide (0.9ml of 1M solution in thf, 0.9 mmol) was added at -78°C to a stirred solution of **1** (0.50g, 0.79mmol) in tetrahydrofuran (20ml). After warming to room temperature and stirring for 1½ hr, the volatiles were removed *in vacuo*, and then preadsorbed on alumina. Column chromatography and elution with a 4:1 hexane/dichloromethane mixture afforded a yellow band, which on collection and recrystallisation from toluene/hexane gave yellow *crystals* of [Mo{η^2,η^3(5e)-S-CH_2CHC(Ph)CH=CH-o-$C_6H_4PPh_2$}(η-C_5H_5)] **2** (0.31g, Yield 70%) (Found : C, 71.3 ; H, 5.0%. Calc. for $C_{34}H_{29}PMo$ C, 72.0 ; H, 5.2%).

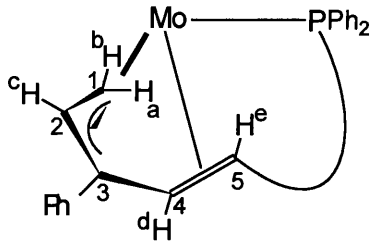

^{1}H (CD_2Cl_2) : δ -0.27 [ddd, 1H, H^a, J(H^aH^c) 8.1 J(H^aH^b) 2.9, J(H^aP) 11.0], 0.44 [dd, 1H, H^e, J(H^eH^d) 4.1, J(H^eP) 14.0], 2.31[dd, 1H, H^b, J(H^bH^c) 8.1, J(H^bH^a) 2.9], 3.76 [dd, 1H, H^d, J(H^dH^e) 4.1, J(H^dP) 4.8], 4.62 [dd, 1H, H^c, J(H^cH^b) 8.1, J(H^cH^a) 8.1], 5.28 [d, 5H, Cp, J(HP) 1.3], 7.0-7.7 (m, 19H, Ph).

^{13}C{^{1}H} (CD_2Cl_2) : δ 37.0 [d, C_1, J(CP) 5.0], 55.7 (s, C_2), 77.5-77.9 (m, C_3, C_4, C_5), 89.4 (s, Cp), 124.0-161.7 (m, Ph).

^{31}P{^{1}H}(CD_2Cl_2) : δ 78.5 (s).

Mass Spectrum : m/z 566 (M^+).

Peak assignments aided by H-H and C-H 2D correlation studies.

5.3 Protonation of [Mo{η^2,η^3(5e)-S-$CH_2CHC(Ph)CH{=}CH$-o-$C_6H_4PPh_2$}(η-C_5H_5)] 2 with $HBF_4.Et_2O$.

$HBF_4.Et_2O$ (261 µl, 85% solution, 1.5mmol) was added (-78°→ +25°C) to a stirred solution of **2** (0.74g, 1.3mmol) in dichloromethane (20ml). The reaction mixture was allowed to warm to room temperature and stirred for 2hr. The volatiles were removed *in vacuo* and the resulting solid recrystallised three times from CH_2Cl_2/Et_2O to afford orange solvated *crystals* of the *trans* diene complex Mo{η^2,η^2($\mu_{Mo,C}$-H)-$CH_3CH{=}C(Ph)CH{=}CH$-o-$C_6H_4PPh_2$}(η-C_5H_5)][BF_4] **3** (0.57g, Yield 77%) (Found : C, 59.2 ; H, 4.5%. Calc. for $C_{34}H_{30}BF_4MoP.\ 0.5CH_2Cl_2$: C, 59.6 ; H, 4.5%).

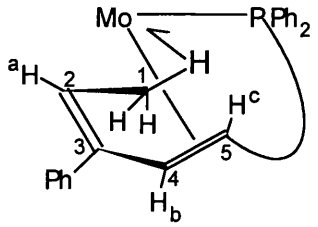

^{1}H [$(CD_3)_2CO$] : δ -2.0 (br.s, 3H, Me), 1.74 [dd, 1H, H^c, J(H^cH^b) 5.5, J(H^cP) 9.4], 4.83 [dd, 1H, H^b, J(H^bH^c) 5.5, J(H^bP) 3.3], 5.27 [d, 5H, C_5H_5, J(HP) 1.1], 5.65 [q, 1H, H^a, J(H^aMe) 6.4], 6.5-8.0 (m, 19H, Ph).

^{1}H (CD_2Cl_2, -80°C) : δ -7.56 (br.s, 1H), -1.13 (br.s, 1H), 2.33 (br.s, 1H), [$\Delta G^{\ddagger}_{(Tc)}$ = 43 kJ mol^{-1}, T_c 253K].

^{13}C{^{1}H} (CD_2Cl_2) : δ 1.1 (s, C_1), 67.6 (s, C_2), 75.9 (s, C_4 or C_5), 81.8 (s, C_4 or C_5), 90.5 (s, C_3), 95.2 (s, Cp), 126.0-154.6 (m, Ph).

^{31}P{^{1}H} (CD_2Cl_2) : δ 60.9 (s).

^{19}F (CD_2Cl_2) : δ -156.0 (s).

Mass Spectrum : m/z 567 (M^+), 87 (BF_4^-).

Peak assignments aided by H-H and C-H 2D correlation studies.

5.4 Reaction of 2 with Tetrafluoroboric Acid in the Presence of Carbon Monoxide.

Carbon monoxide was bubbled through a solution of **2** (100mg, 0.18mmol) in dichloromethane (20ml). Tetrafluoroboric acid (30μl, 85% solution, 0.20 mmol) was added at -78°C and the solution was stirred at room temperature for two hours in a continuous stream of carbon monoxide. The solvent was then removed *in vacuo* and the residue was recrystallised twice from dichloromethane/ether to give an orange microcrystalline solid (70mg, Yield 70%) The ^{1}H, ^{13}C and ^{31}P NMR spectra identified the product as the *trans*-diene complex **3**.

5.5 Reaction of 3 with Li[$N(SiMe_3)_2$] to Regenerate [$Mo\{\eta^2,\eta^3(5e)$-S-$CH_2CHC(Ph)CH{=}CH$-o-$C_6H_4PPh_2\}(\eta$-$C_5H_5)$] 2.

Addition (-78°C) of lithium bis(trimethylsilyl)amide (20μl of 1M solution in thf, 0.20mmol) to a stirred solution of **3** (0.10g, 018mmol) in thf (10ml) resulted in a colour change of orange to yellow. Column chromatography afforded yellow *crystals* from [$Mo\{\eta^2,\eta^3(5e)$-S-$CH_2CHC(Ph)CH{=}CH$-o-$C_6H_4PPh_2\}(\eta$-$C_5H_5)$] **2** (0.82g, Yield 80%), identified by ^{1}H and $^{31}P\{^{1}H\}$ NMR spectroscopy.

5.6 Reaction of [Mo{η^2,η^3(5e)-S-$CH_2CHC(Ph)CH{=}CH$-o-$C_6H_4PPh_2$}(η-C_5H_5)] 2 with Trifluoroacetic Acid.

Trifluoroacetic acid (40µl, 0.52mmol) was added to a yellow solution (CH_2Cl_2, 20ml) of **2** (165mg, 0.29mmol) at -78°C. After stirring at room temperature for 4-5 hours the solution became dark green. The solvent was removed *in vacuo* and the resulting powder chromatographed on alumina. A green band was collected by initially eluting with 2:1 hexane/dichloromethane mixture and finally neat dichloromethane. The solvent was removed *in vacuo* to afford the microcrystalline green *cis* diene complex, [Mo{$OC(O)CF_3$}{η^2,η^2,$CH_3CH{=}C(Ph)CH{=}CH$-o-$C_6H_4PPh_2$}(η-C_5H_5)] **4** (157mg, Yield 80%). (Found : C, 63.6; H, 4.57%. Calc. for $C_{36}H_{30}F_3MoO_2P$: C, 63.72; H, 4.46%).

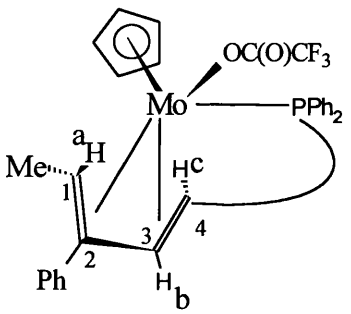

^{1}H (CD_2Cl_2) : δ 1.46 [d, 3H, Me, J(MeH^a) 6.9], 2.86 (br.s, 1H, H^c), 3.99 (br.s,1H, H^a), 4.35 (d, 5H, Cp, J(HP) 1.6), 6.50 [ddd, 1H, H^b, J(H^bH^c) 9.4, J(H^bP) 5.6, J(H^bH^a) 2.2], 6.94 - 8.03 (m, 19H, Ph).

^{1}H (CD_2Cl_2, -50°C) : δ 2.86 [dd, H^c, J(H^cP) 5.4, J(H^bH^c) 9.4], 3.99 [q.d, H^a, J(H^aMe) 6.9, J(H^aH^b) 1.9].

^{13}C{^{1}H} (CD_2Cl_2) : δ 14.9 (s, Me), 60.1 (s, C_1), 64.3 (s, C_4), 93.2 (s, Cp), 112.6 (s , C_2), 113.1 (s, C_3), 115.3 [q, CCF_3, ^{1}J(CF) 294], 163.1 [q, CCF_3, ^{2}J(CF) 24], 125.3 - 138.3 (m, Ph).

^{31}P{^{1}H}(CD_2Cl_2) : δ 52.0 (s).

^{19}F (CD_2Cl_2) : δ -74.5 (s, CF_3CO_2).

Mass Spectrum : m/z 680 (M^+), 565 (M^+-CF_3CO_2), 113 ($CF_3CO_2^-$).

Peak assignments aided by H-H and C-H 2D correlation studies.

5.7 Reaction of $Mo\{\eta^2,\eta^2(\mu_{Mo,C}\text{-}H)\text{-}CH_3CHC(Ph)CH{=}CH\text{-}o\text{-}C_6H_4PPh_2\}(\eta\text{-}C_5H_5)][BF_4]$ 3 with Acetonitrile.

Acetonitrile (10ml) was added to a dark orange solution (CH_2Cl_2, 20ml) of **3** (100mg, 0.15mmol) at room temperature, with stirring. Over a period of 12 hours the solution changed colour from orange to purple. The volatiles were then removed *in vacuo* and the resulting purple powder was recrystallised three times from dichloromethane and ether to afford purple *crystals* of the *cis* diene complex $[Mo(NCMe)\{\eta^2,\eta^2,CH_3CH{=}C(Ph)CH{=}CH\text{-}o\text{-}C_6H_4PPh_2\}(\eta\text{-}C_5H_5)][BF_4]$ **5** (84mg,Yield 80%). (Found : C, 62.3; H, 4.79; N, 1.98%. Calc. for $C_{36}H_{33}BF_4MoNP$: C, 62.35; H, 4.80; N, 2.02%).

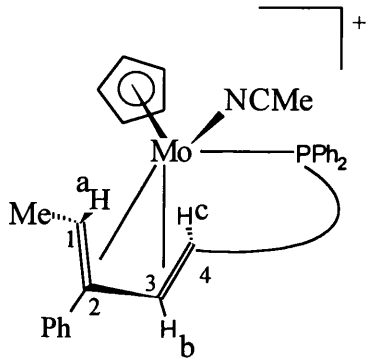

^{1}H (CD_2Cl_2, -60°C) : δ 1.47 [d, 3H, Me, J(MeH^a) 7.0], 1.56 (s, 3H, *Me*CN), 3.27 [dd, 1H, H^c, J(H^{c}H^b) 5.9, J(H^{c}P) 10.2], 3.54 [dq, 1H, H^a, J(H^{a}Me) 7.0, J(H^{a}H^b) 1.9], 4.46 [d, 5H, Cp, J(HP) 0.8], 5.78 [ddd, 1H, H^b, J(H^{b}H^c) 5.9, J(H^{b}P) 8.0, J(H^{b}H^a) 1.9], 7.27-7.74 (m, 19H, Ph).

^{13}C{^{1}H} (CD_2Cl_2) : δ 3.5 (br.s, *Me*CN), 14.8 (br.s, Me), 57.1 (br.s, *C*H, C_1), 63.9 (br.s, *C*H, C_4), 92.1 (s, Cp), 99.9 (s, *C*N), 110.9 (s, *C*H^b, C_3), 119.2 (s, C_2), 124.1 - 137.9 (m, Ph).

^{31}P{^{1}H} (CD_2Cl_2, -60°C) : δ 55.1 (s).

Mass Spectrum : m/z (M^+) 607, (M^+-MeCN) 567, (BF_4^-) 87.

Peak assignments aided by low temperature H-H and C-H 2D correlation studies.

5.8 Reaction of [Mo{η^2,η^2($\mu_{Mo,C}$-H)-$CH_3CHC(Ph)CH{=}CH$-o-$C_6H_4PPh_2$}(η-C_5H_5)][BF_4] 3 with Lithium Iodide.

Addition of lithium iodide (21mg, 0.16mmol) to a solution (thf, 20ml) of **3** (73mg, 0.12mmol) resulted in an immediate colour change from orange to dark green. After stirring at room temperature for 2-3 hours the solvent was removed *in vacuo* and the residue chromatographed on an alumina column. The product was eluted as a green band with a 3:1 hexane/dichloromethane mixture to afford green *crystals* of the *cis* diene complex [MoI{η^2,η^2-$CH_3CH{=}C(Ph)CH{=}CH$-o-$C_6H_4PPh_2$}(η-C_5H_5)] **6** (58mg, Yield 70%). (Found : C, 59.0; H, 4.4%. Calc. for $C_{34}H_{30}IMoP$: C, 58.79; H, 4.36%).

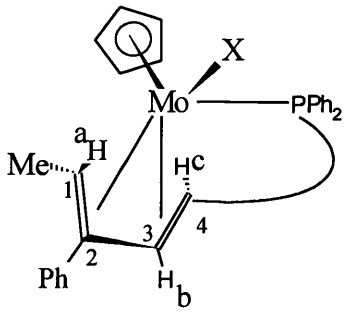

^{1}H (C_6D_6) : δ 1.42 [d, 3H, *Me*, J(HP) 7.3], 2.99 (br, 1H, H^c), 4.12 (br, 1H, H^a), 4.36 [d, 5H, Cp, J(HP) 1.0], 6.37 [ddd, 1H, H^b, J(H^bH^c) 7.8, J(H^bP) 5.4, J(H^bH^a) 2.0], 7.12 - 8.43 (m, Ph).

^{13}C{^{1}H} (C_6D_6) : δ 17.0 (s, Me), 54.8 (br, C_1), 63.2 (br, C_4), 89.5 (s, C_2, quaternary), 92.1 (s, Cp), 109.4 (s, CH, C_3), 122.3 - 138.6 (m, Ph).

^{31}P{^{1}H} (C_6D_6) : δ 45.9 (s).

Mass Spectrum : m/z (M^+) 694, (M^+-I) 565.

Peak assignments aided by H-H and C-H 2D correlation studies.

5.9 Reaction of 3 with a) Lithium Bromide and b) Lithium Chloride.

Similarly, reaction of $[Mo\{\eta^2,\eta^2(\mu_{Mo,C}\text{-}H)\text{-}CH_3CHC(Ph)CH{=}CH\text{-}o\text{-}C_6H_4PPh_2\}(\eta\text{-}C_5H_5)][BF_4]$ **3** with either a) lithium bromide or b) lithium chloride afforded the green *cis* diene complexes $[MoBr\{\eta^2,\eta^2\text{-}CH_3CH{=}C(Ph)CH{=}CH\text{-}o\text{-}C_6H_4PPh_2\}(\eta\text{-}C_5H_5)]$ **7** and $[MoCl\{\eta^2,\eta^2\text{-}CH_3CH{=}C(Ph)CH{=}CH\text{-}o\text{-}C_6H_4PPh_2\}(\eta\text{-}C_5H_5)]$ **8** respectively.

a) $[MoBr\{\eta^2,\eta^2\text{-}CH_3CH{=}C(Ph)CH{=}CH\text{-}o\text{-}C_6H_4PPh_2\}(\eta\text{-}C_5H_5)]$ **7**
(Yield 70%). (Found : 63.6, C ; 4.7, H %. Calc. for $C_{34}H_{30}BrMoP$: C, 63.27 ; H, 4.68%).

^{1}H (CD_2Cl_2) : δ 1.23 (br, 3H, Me), 3.21 (br, 1H, H^c), 4.42 (br, 1H, H^a), 5.40 (br, 5H, Cp), 6.21 (br, 1H, H^b), 6.70-8.15 (m, 19H, Ph).
$^{31}P\{^1H\}$ (C_6D_6) : δ 46.2 (s).
Mass Spectrum : m/z, (M^+) 646, (M^+-Br) 565.

b) $[MoCl\{\eta^2,\eta^2\text{-}CH_3CH{=}C(Ph)CH{=}CH\text{-}o\text{-}C_6H_4PPh_2\}(\eta\text{-}C_5H_5)]$ **8**
(Yield 65%). (Found : C, 68.0; H, 5.1 %. Calc. for $C_{34}H_{30}ClMoP$: C, 67.95; H, 5.03%).

^{1}H (CD_2Cl_2) : δ 1.40 (br, 3H, Me), 2.28 (br, 1H, H^c), 3.85 (br, 1H, H^a), 4.26 (br, 5H, Cp), 6.18 (br, 1H, H^b), 6.79-8.18 (m, Ph).
$^{31}P\{^1H\}$ (C_6D_6) : δ 45.4 (s).
Mass Spectrum : m/z, (M^+) 602, (M^+-Cl) 565.

5.10 Reaction of [MoI{η^2,η^2-CH_3CH=C(Ph)CH=CH-o-$C_6H_4PPh_2$}(η-C_5H_5)] 6 with Thallium Hexafluorophosphate in the presence of Carbon Monoxide.

Thallium hexafluorophosphate (270mg, 0.77 mmol) was added at room temperature to a dark green solution (thf, 20 ml) of **6** (514mg, 0.74 mmol) in the presence of a stream of carbon monoxide. After stirring for 2-3 days the volatiles were removed *in vacuo* and the resulting orange powder recrystallised three times from dichloromethane/ether to afford orange *crystals* of [Mo(CO){η^2,η^2-CH_3CH=C(Ph)CH=CH-o-$C_6H_4PPh_2$}(η-C_5H_5)][PF_6] **9** (410mg, Yield 75%). (Found : C, 56.5; H, 4.0%. Calc. for $C_{35}H_{30}MoP_2F_6O$: C, 56.92; H, 4.09%).

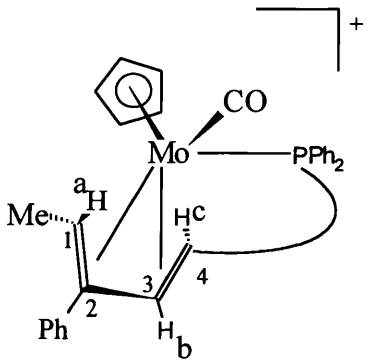

Infra-red (CH_2Cl_2) : ν (CO) 1977 cm^{-1}.

^{1}H (CD_2Cl_2) : δ 1.66 (d, 3H, Me, J(MeH^a) 6.7), 4.03 (q, 1H, H^a, J(H^aMe) 6.7), 4.48 (dd, 1H, H^c, J(H^cH^b) 8.0, J(HP) 8.0), 4.95 (s, 5H, Cp), 5.45 (dd, 1H, H^b, J(HP) 7.0, J(H^bH^c) 8.0), 7.04-7.71 (m, 19H, Ph).

^{13}C{^{1}H} (CD_2Cl_2) : 15.8 (s, Me), 58.1 (s, C_1), 68.4 (s, C_4), 92.6 (s, Cp), 105.4 (s, C_3), 116.5 (s, C_2), 126.7-154.6 (m, Ph), 233.4 [d, CO, J(CP) 16.5].

^{31}P{^{1}H} (CD_2Cl_2) : δ 57.3 (s, PPh_2), -144 [septet, PF_6, J(PF) 711].

Mass Spectrum : m/z, (M^+) 595, (M^+-CO) 567, (PF_6^-) 145.

Peak assignments aided by H-H and C-H 2D correlation studies.

5.11 Reaction of $[Mo\{\eta^2,\eta^2\text{-}CH_3CH{=}C(Ph)CH{=}CH\text{-}o\text{-}C_6H_4PPh_2\}(NCMe)(\eta\text{-}C_5H_5)][BF_4]$ 5 with Lithium Iodide.

Addition of lithium iodide (15mg, 0.11mmol) to a stirred solution of **5** (80mg, 0.11mmol) in tetrahydrofuran (10ml) resulted in a change of colour from orange to green. After four hours, column chromatography afforded green crystals of $[MoI\{\eta^2,\eta^2\text{-}CH_3CH{=}C(Ph)CH{=}CH\text{-}o\text{-}C_6H_4PPh_2\}(\eta\text{-}C_5H_5)]$ **6** (53mg, Yield 70%), identified by ^1H and $^{31}P\{^1H\}$ NMR spectroscopy.

5.12 Reaction of $[MoI\{\eta^2,\eta^2\text{-}CH_3CH{=}C(Ph)CH{=}CH\text{-}o\text{-}C_6H_4PPh_2\}(\eta\text{-}C_5H_5)]$ 6 with Ferrocenium Tetrafluoroborate.

Addition of ferrocenium tetrafluoroborate (80mg, 0.29mmol) to a solution of **6** (210mg, 0.30mmol) in dichloromethane (20ml) resulted in a colour change from green to dark purple. After stirring at room temperature for two hours, the solvent was removed *in vacuo* and recrystallisation twice from dichloromethane/ether afforded the purple, paramagnetic complex $[MoI\{\eta^2,\eta^2\text{-}CH_3CH{=}C(Ph)CH{=}CH\text{-}o\text{-}C_6H_4PPh_2\}(\eta\text{-}C_5H_5)][BF_4]$ **10** in 80% yield (187mg). (Found : C, 50.2; H, 3.9%. Calc. for $C_{34}H_{30}BF_4IMoP.\ 0.5CH_2Cl_2$: C, 50.4; H, 3.80%).

Mass Spectrum : m/z, (M^+) 694, (BF_4^-) 87.

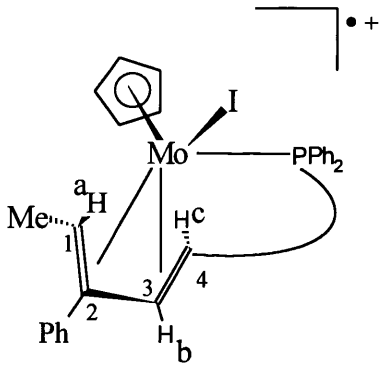

5.13 Reaction of [MoI{η^2,η^2-CH_3CH=C(Ph)CH=CH-o-$C_6H_4PPh_2$}(η-C_5H_5)] 6 with Trityl Tetrafluoroborate.

Similarly, reaction of **6** (120mg, 0.173mmol) with trityl tetrafluoroborate (57mg, 0.173mmol) in dichloromethane (20ml) also afforded the purple complex **10** (108mg, Yield 80%). The trityl tetrafluoroborate was recrystallised from dichloromethane/ether before use.

5.14 Reaction of 10 with Sodium Metal to Regenerate 6.

Complex [MoI{η^2,η^2-CH_3CH=C(Ph)CH=CH-o-$C_6H_4PPh_2$}(η-C_5H_5)][BF_4] **10** (60mg, 0.08mmol) was stirred in solution (thf, 20ml) over excess sodium metal at room temperature. The reaction was followed by tlc and after 3 hours the solution had changed colour from purple to green. The solvent was removed *in vacuo* and the product chromatographed on an alumina column. A green complex was eluted using a 3:1 hexane/dichloromethane mixture, which ^1H and $^{31}P\{^1H\}$ NMR spectra confirmed was [MoI{η^2,η^2-CH_3CH=C(Ph)CH=CH-o-$C_6H_4PPh_2$}(η-C_5H_5)] **6** (44mg, Yield 80%).

5.15 Preparation of [Mo(MeC≡CPh)(o-dpps)(η^5-C_9H_7)][BF_4] 11.

Similar to the cyclopentadienyl derivative (section 5.1.), a solution of [Mo(η^2-$MeC_2Ph)_2$(CO)(η^5-C_9H_7)][BF_4] (0.45g, 0.81mmol) and dpps (0.25g, 0.87mmol) in dichloromethane (40ml) was refluxed for 48 hours. On cooling, the volume was reduced to *ca.* 10ml and on addition of diethyl ether (20ml) a red solid was precipitated. Recrystallisation from dichloromethane/ether afforded the red complex [Mo(η^2-MeC_2Ph)(dpps)(η^5-C_9H_7)][BF_4] **11** (0.50g, Yield 91%) (Found : C, 64.9 ; H, 4.6 %. Calc. for $C_{38}H_{32}BF_4MoP$: C, 64.76; H, 4.58%).

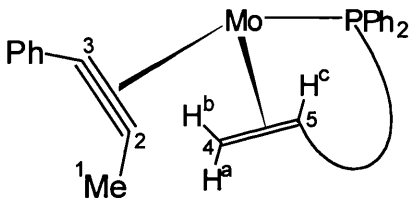

^{1}H (CD_2Cl_2) : δ 0.31 [dd, 1H, H^b, J(H^bH^a) 3.2, J(H^bH^c) 11.0], 1.49 [dd, 1H, H^a, J(H^aH^b) 3.2, J(H^aH^c) 11.6], 2.13 (s, 3H, Me), 2.91 [dd, 1H, H^c, J(H^cH^a) 11.6, J(H^cH^b) 11.0], 5.70-6.28 (m, 3H, indenyl), 7.46-8.25 (m, 23H, Ph).

^{13}C{^{1}H} (CD_2Cl_2) : δ 21.6 (s, Me), 49.0 (s, CH_2), 70.0 (s, C_5), 87.9, 89.1, 96.6 (s, indenyl), 117.8-150.2 (m, Ph and indenyl), 225.9 (s, *C*≡Me), 230.9 [d, *C*≡Ph, J(CP) 5.5]

^{31}P{^{1}H} (CD_2Cl_2) : δ 83.2 (s).

Mass Spectrum : m/z, (M^+) 617, (BF_4^-) 87.

Peak assignments aided by H-H and C-H 2D correlation studies.

5.16 Preparation of [Mo{η^2,η^3(5e)-S-$CH_2CHC(Ph)CH{=}CH$-o-$C_6H_4PPh_2$}(η^5-C_9H_7)] 12.

Lithium bis(trimethylsilyl)amide (0.35ml, 1M solution in thf, 0.35mmol) was added at -78°C to a stirred solution of **11** (190mg, 0.28mmol) in tetrahydrofuran (20ml). After warming to room temperature and stirring for 1½ hr, the volatiles were removed *in vacuo*, and then preadsorbed on alumina. Column chromatography and elution with a 4:1 hexane/dichloromethane mixture afforded a yellow band, which on collection and recrystallisation from toluene/pentane gave the yellow complex [Mo{η^2,η^3(5e)-S-$CH_2CHC(Ph)CH{=}CH$-o-$C_6H_4PPh_2$}(η^5-C_9H_7)] **12** (95mg, Yield 55%) (Found : C, 74.0 ; H, 5.1 %. Calc. for $C_{38}H_{31}PMo$: C, 74.01 ; H, 5.07%).

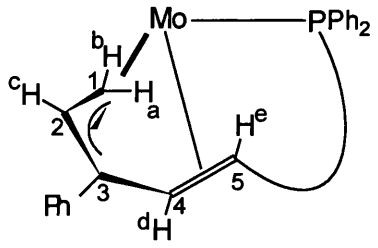

^{1}H (CD_2Cl_2) : δ -0.45 [ddd, 1H, H^a, J(H^aH^c) 8.1 J(H^aH^b) 2.7, J(H^aP) 11.0], 0.14 [dd, 1H, H^e, J(H^eH^d) 4.6, J(H^eP) 12.0], 1.74 [dd, 1H, H^b, J(H^bH^c) 7.5, J(H^bH^a) 2.7], 3.02 [dd, 1H, H^d, J(H^dH^e) 4.6, J(H^dP) 4.3], 4.31 [dd, 1H, H^c, J(H^cH^b) 7.5, J(H^cH^a) 8.1], 4.22, 4.71, 5.92, 6.30-7.93 (m, 26H, indenyl and Ph).

^{13}C{^{1}H} (CD_2Cl_2) : δ 41.2 (s, CH_2), 62.4 (s,C_2), 78.4, 79.2, 79.8 (s, indenyl), 83.6, 87.4, 88.9, (s, C_3, C_4, C_5), 110.1-155.6 (m, Ph).

^{31}P{^{1}H}(CD_2Cl_2) : δ 80.3 (s).

Mass Spectrum : m/z (M^+) 616.

Peak assignments aided by H-H and C-H 2D correlation studies.

5.17 Reaction of $[Mo(MeC{\equiv}CPh)_2(CO)(\eta^5\text{-}C_5Me_5)][BF_4]$ and *o*-dpps.

After refluxing $[Mo(CO)(MeC{\equiv}CPh)_2(\eta^5\text{-}C_5Me_5)][BF_4]$ (550mg, 0.95mmol) with dpps (290mg, 1.01mmol) in dichloromethane (25ml) for 48 hours no reaction had occurred. Therefore, one equivalent of trimethyl amine-*N*-oxide (108mg, 0.95mmol) was added, which only resulted in decomposition.

$[Mo(CO)(MeC{\equiv}CPh)_2(\eta^5\text{-}C_5Me_5)][BF_4]$ Infra red (CH_2Cl_2) : ν(CO) 2048 cm^{-1}

5.18 Preparation of [Re=C(Ph)-η^3-{C(Me)CHCHC$_6$H$_4$PPh$_2$-o}(η-C$_5$H$_5$)][BF$_4$] 13.

Silver tetrafluoroborate (210mg, 1.1mmol) was added to a solution (thf, 20ml) of dpps (160mg, 0.55mmol) and [ReBr$_2$(PhC≡CMe)(η-C$_5$H$_5$)] (294mg, 0.54mmol). After stirring at room temperature for four hours, the solvent was removed *in vacuo* and the product extracted with dichloromethane and filtered through Celite. Recrystallisation from dichloromethane/ether resulted in green *crystals* of [Re=C(Ph)-η^3-{C(Me)CHCHC$_6$H$_4$PPh$_2$-*o*}(η-C$_5$H$_5$)][BF$_4$] **13** (356mg, Yield 93%). (Found : C, 55.1; H, 3.8%. Calc. for C$_{34}$H$_{29}$BF$_4$PRe : C, 55.06; H, 3.94%).

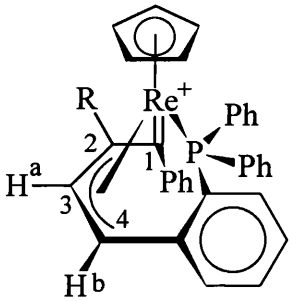

R = Me **13**
R = Ph **14**

^{1}H (CD$_2$Cl$_2$) : δ 2.17 (s, 3H, Me), 5.46 [d, 5H, Cp, J(HP) 1.65], 6.55 and 6.59 [AB, 2H, H^a and H^b, J(H^{a}H^b) 8.0], 6.46-7.65 (m, 19H, Ph).

^{13}C{^{1}H} (CD$_2$Cl$_2$) : δ 17.0 (s, Me), 57.3 (s, C$_3$ or C$_4$), 69.2 (s, C$_2$), 78.3 (s, C$_3$ or C$_4$), 88.1 (s, Cp), 126.7-152.0 (m, Ph), 257.7 [d, Re=C$_1$, J(CP) 16.3].

^{31}P{^{1}H} (CD$_2$Cl$_2$) : δ 41.0 (s).

Mass Spectrum : m/z, (M$^+$) 655, (BF$_4^-$) 87.

Peak assignments aided by H-H and C-H 2D correlation studies.

5.19 Preparation of $[Re{=}C(Ph)\text{-}\eta^3\text{-}\{C(Ph)CHCHC_6H_4PPh_2\text{-}o\}(\eta\text{-}C_5H_5)][BF_4]$ 14.

Similarly, reaction of $[ReBr_2(PhC{\equiv}CPh)(\eta\text{-}C_5H_5)]$ (250mg, 0.42mmol) with dpps (127mg, 0.4 mmol) and $AgBF_4$ (166mg, 0.85mmol) in tetrahydrofuran (20ml) affords the analogous green complex $[Re{=}C(Ph)\text{-}\eta^3\text{-}\{C(Ph)CHCHC_6H_4PPh_2\text{-}o\}(\eta\text{-}C_5H_5)][BF_4]$ **14** (304mg, 90% Yield). (Found : C, 58.3 ; H, 3.9 %. Calc. for $C_{39}H_{31}BF_4PRe$: C, 58.28; H, 3.89%).

^{1}H (CD_2Cl_2) : δ 5.42 [d, 5H, Cp, J(HP) 1.65], 6.69 and 6.81 [AB, 2H, H^a and H^b, J(H^aH^b) 8.3], 6.51-7.70 (m, 24H, Ph).

$^{13}C\{^1H\}$ (CD_2Cl_2) : δ 57.7 (s, C_3or C_4), 71.3 (s, C_2), 73.5 (s, C_3 or C_4), 89.3 (s, Cp), 125.8-151.5 (m, Ph), 252.9 [d, Re=C_1, J(CP) 14.9].

$^{31}P\{^1H\}$ (CD_2Cl_2) : δ 39.9 (s).

Mass Spectrum : m/z, (M^+) 717, (BF_4^-) 87.

Peak assignments aided by H-H and C-H 2D correlation studies.

Note : If the reaction is scaled up, one equivalent of anhydrous sodium carbonate should also be added to act as a proton trap for the HBF_4 generated, which could polymerise the thf.

5.20 Reaction of [Re=C(Ph)-η^3-{C(Ph)CHCHC$_6$H$_4$PPh$_2$-o}(η-C$_5$H$_5$)][BF$_4$] 14 with K-Selectride®.

K-Selectride® (0.38ml, 1M thf solution, 0.38mmol) was added at -78°C to a green solution (thf, 30ml) of **14** (300mg, 0.37mmol) and stirred at room temperature for 12 hours. The resulting orange solution was preadsorbed onto alumina and chromatographed on a short column (4cm x 1cm). An orange band was eluted with a (3:1) hexane/dichloromethane mixture to afford, after removing volatiles *in vacuo*, an orange powder, which was identified as [Re{η^4-CH(Ph)=C(Ph)CH=CH (C$_6$H$_4$PPh$_2$-o)}(η-C$_5$H$_5$)] **15** (160mg, Yield 60%).

K-Selectride® is the registered trade name of potassium tri-*sec*-butylborohydride.

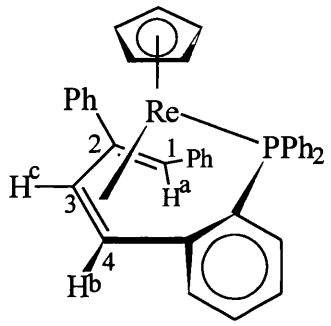

^{1}H (C$_6$D$_6$) : δ 0.93 (s, 1H, H^a), 4.34 (s, 5H, Cp), 5.02 and 5.14 [AB, 2H, H^b and H^C, J(H^{b}H^c) 7.8], 6.51-7.70 (m, Ph).

^{13}C{^{1}H} (C$_6$D$_6$) : δ 43.2 [d, *C*H^a, J(CP) 7.7], 52.2 [d, C$_4$, J(CP) 3.3], 64.2 (s, C$_3$), 80.5 (s, Cp), 82.4 (s, C$_2$) 122.8-153.4 (m, Ph).

^{31}P{^{1}H} (C$_6$D$_6$) : δ 61.8 (s).

Mass Spectrum : m/z, (M$^+$) 718.

Peak assignments aided by H-H and C-H 2D correlation studies.

5.21 Reaction of 15 with $[Ph_3C][BF_4]$ to Regenerate $[Re{=}C(Ph)\text{-}\eta^3\text{-}\{C(Ph)CHCHC_6H_4PPh_2\text{-}o\}(\eta\text{-}C_5H_5)][BF_4]$ 14.

Addition of trityl tetrafluoroborate (26mg, 0.08mmol) to a stirred solution of $[Re\{\eta^4\text{-}CH(Ph){=}C(Ph)CH{=}CH(C_6H_4PPh_2\text{-}o)\}(\eta\text{-}C_5H_5)]$ **15** (58mg, 0.08mmol) in dichloromethane (10ml) resulted in a colour change of orange to dark green. Recrystallisation from dichloromethane and ether afforded the green complex $[Re{=}C(Ph)\text{-}\eta^3\text{-}\{C(Ph)CHCHC_6H_4PPh_2\text{-}o\}(\eta\text{-}C_5H_5)][BF_4]$ **14** (50mg, Yield 80%), identified by ^1H and $^{31}P\{^1H\}$ NMR spectroscopy.

5.22 Conversion of [Re{η^4-CH(Ph)=C(Ph)CH=CH($C_6H_4PPh_2$-o)}(η-C_5H_5)] 15 to Complex 16.

Chromatographing complex **15** (100mg, 0.14mmol) with a longer column (25cm x 1cm) and elution with a (3:1) hexane/dichloromethane mixture to afforded the pale yellow complex [Re(OH_2){η^4-CH(Ph)=C(Ph)CH=CH($C_6H_4PPh_2$-*o*)}(η-C_5H_5)] **16** in 70% yield (70mg).

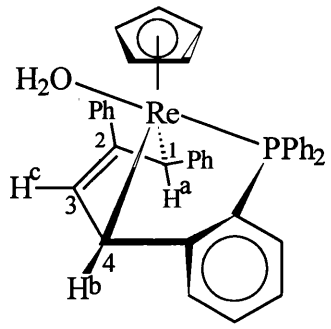

^{1}H (C_6D_6) : δ 2.74 (s, 1H, H^a), 2.86 [d, 1H, H^c, J(H^cP) 14.5], 4.09 (s, 1H, H^b), 4.57 (s, 5H, Cp), 6.66-7.86 (m, Ph).

^{13}C{^{1}H} (C_6D_6) : δ 23.7 (s, CH^a), 31.6 [d, C_4, J(CP) 4.0], 71.8 (s, C_2 or C_3), 82.7 (s, Cp), 91.4 (s, C_2 or C_3), 121.4-151.8 (m, Ph).

^{31}P{^{1}H} (C_6D_6) : δ 56.5 (s).

Mass Spectrum : m/z, (M^+) 718

Peak assignments aided by an H-H correlation study.

5.23 Preparation of $[ReBr(PPh_3)(\eta^4\text{-}C_4Ph_4)(\eta\text{-}C_5H_5)][BF_4]$ 17.

Addition of triphenylphosphine (363mg, 1.38mmol) and silver tetrafluoroborate (346mg, 1.8mmol) to a stirred red solution (CH_2Cl_2, 30ml) of $[ReBr_2(\eta^4\text{-}C_4Ph_4)(\eta\text{-}C_5H_5)]$ resulted in the immediate precipitation of silver bromide. After stirring for 12 hours the solution was filtered through Celite and the solvent removed *in vacuo*. An orange microcrystalline complex **17** (615mg, Yield 70%) was obtained after recrystallisation three times from dichloromethane/ether. (Found : C, 59.2 ; H, 4.0 %. Calc. for $C_{51}H_{40}BBrF_4PRe$: C, 59.06; H, 3.89%).

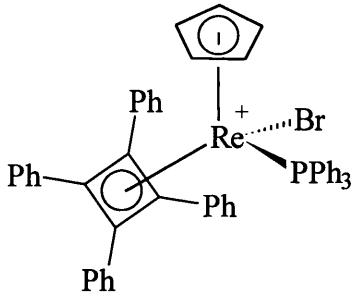

^{1}H (CD_2Cl_2) : δ 5.89 (s, 5H, Cp), 6.25-7.55 (m, 35H, Ph).

^{13}C{^{1}H} (CD_2Cl_2) : δ 96.0 (s, Cp), 125.8-133.9 (m, Ph).

^{19}F (CD_2Cl_2) : δ -154 (s, BF_4^-).

^{31}P{^{1}H} (CD_2Cl_2) : δ 15.0 (s, PPh_3).

Resonances for the C_4Ph_4 ring carbons were not observed in the ^{13}C{^{1}H} NMR spectrum.

5.24 Reaction of $[ReBr(PPh_3)(\eta^4\text{-}C_4Ph_4)(\eta\text{-}C_5H_5)][BF_4]$ 17 with Super Hydride®.

On addition of Super Hydride (160μl, 1M solution in thf, 0.16mmol) to a stirred orange suspension (thf, 20ml) of **17** (156mg, 0.151mmol) at -78°C the colour changed to black. The solution was stirred for 2 hours and then filtered through a plug of silica. The volatiles were removed *in vacuo* from the resulting orange solution and recrystallisation from thf/ether afforded the two complexes $[ReH(Br)(\eta^4\text{-}C_4Ph_4)(\eta^5\text{-}C_5H_5)]$ **18** and $[ReH(PPh_3)(\eta^4\text{-}C_4Ph_4)(\eta^5\text{-}C_5H_5)][BF_4]$ **19** in a ratio of 20:1 (58mg, Yield 40%).

The small amount of the minor product **19** was only observable in the ^1H and $^{31}P\{^1H\}$ NMR spectra.

Super Hydride® is the registered trade name of lithium triethylborohydride.

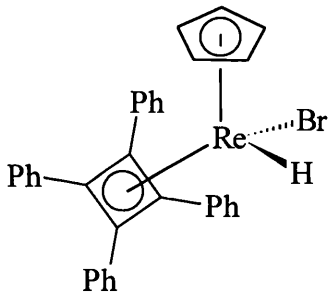

18 Major Product

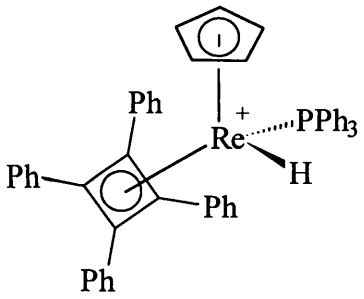

19 Minor Product

^1H (CD_2Cl_2) : δ -12.14 (s, 1H, Re-*H*, major), -11.81 [d, 1H, Re-*H*, minor, J(HP) = 25.2], 5.07 [d, 5H, Cp, minor, J(HP) 1.4], 5.19 (s, 5H, Cp, major), 7.14-7.48 (m, Ph).

$^{13}C\{^1H\}$ (CD_2Cl_2) : δ 89.9 (s, Cp), 127.7-134.1 (m, Ph).

$^{31}P\{^1H\}$ (CD_2Cl_2) : δ -3.9 (s, free *P*Ph_3), 27.3 (s, *P*Ph_3 of **19**)

Resonances for the C_4Ph_4 ring carbons were not observed in the $^{13}C\{^1H\}$ NMR spectrum.

5.25 Preparation of $[ReH_2(\eta^4\text{-}C_4Ph_4)(\eta\text{-}C_5H_5)]$ 20.

Addition (-78°C) of lithium aluminium hydride (3.2ml of 1M solution in thf, 3.2mmol) to a stirred solution of $[ReBr_2(\eta^4\text{-}C_4Ph_4)(\eta\text{-}C_5H_5)]$ (1.23g, 1.61mmol) in thf (20ml) resulted in a change of colour from red to yellow. Volatiles were removed *in vacuo* and the resulting yellow oil chromatographed. A pale yellow complex was eluted with thf and after recrystallisation from dichloromethane: hexane, yellow *crystals* of $[ReH_2(\eta^4\text{-}C_4Ph_4)(\eta\text{-}C_5H_5)]$ **20** were obtained (785mg, Yield 80%). (Found : C, 64.9; H, 4.39%. Calc. for $C_{33}H_{27}Re$: C, 65.0; H, 4.46%).

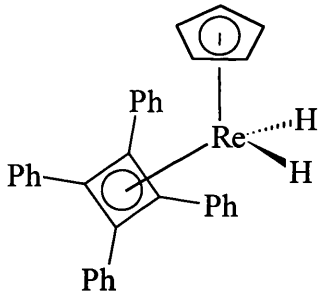

^{1}H (CD_2Cl_2) : δ -13.07 (s, 2H, Re-H), 4.85 (s, 5H, Cp), 7.14-7.36 (m, 20H, Ph).

$^{13}C\{^1H\}$ (CD_2Cl_2) : δ 66.9 (s, *C*Ph), 89.3 (s, Cp), 126.4, 128.0, 130.6 and 136.6 (s, Ph).

5.26 Reaction of $[ReH_2(\eta^4\text{-}C_4Ph_4)(\eta\text{-}C_5H_5)]$ 20 with Tetrafluoroboric Acid.

Addition of $HBF_4.Et_20$ (26µl, 0.17mmol) at -78°C to a yellow solution (ether, 20ml) of $[ReH_2(\eta^4\text{-}C_4Ph_4)(\eta\text{-}C_5H_5)]$ **20** (100mg, 0.16mmol) resulted in a dark yellow/green solution. Recrystallisation (O°C) from dichloromethane/ether afforded the very air and moisture sensitive complex $[ReH\{\eta^2,\eta^2\text{-}PhC(H)=C(Ph)C(Ph)=C(Ph)H\}(\eta\text{-}C_5H_5)][BF_4]$ **21** (65mg, Yield 55%).

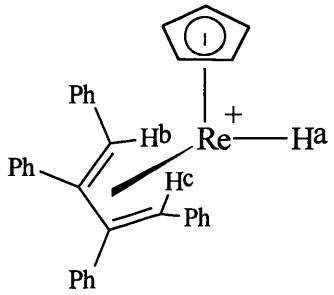

^{1}H (CD_2Cl_2) : δ -8.62 [dd, 1H, M-H^a, J(H^aH^c) 3.0, J(H^aH^b) 3.6], 3.78 [d, 1H, H^b, J(H^aH^b) 3.6], 4.22 [d, 1H, H^c, J(H^cH^a) 3.0], 4.95 (s, 5H, Cp), 6.82-8.46 (m, 20H, Ph).

Mass Spectrum : m/z, (M^+) 609, (BF_4^-) 87.

5.27 Reaction of $[ReH_2(\eta^4\text{-}C_4Ph_4)(\eta\text{-}C_5H_5)]$ 20 with Trifluoroacetic Acid.

Excess trifluoroacetic acid (84μl, 1.09mmol) was added at -78°C to a yellow solution (CH_2Cl_2, 20ml) of **20** (220mg, 0.36mmol) and stirred for 12 hours. The resulting dark orange solution was preadsorbed on alumina and chromatographed using a short column. An orange band was eluted with dichloromethane and the volatiles removed *in vacuo*. Recrystallisation (O°C) from toluene/hexane afforded orange *crystals* of $[ReH\{OC(O)CF_3\}\{\eta^2,\eta^2\text{-}PhC(H)=C(Ph)C(Ph)=C(Ph)H\}(\eta\text{-}C_5H_5)]$ **22** (222mg, Yield 85%). (Found : C, 58.2; H, 4.0%. Calc. for $C_{35}H_{28}F_3O_2Re$: C, 58.08; H, 3.90%).

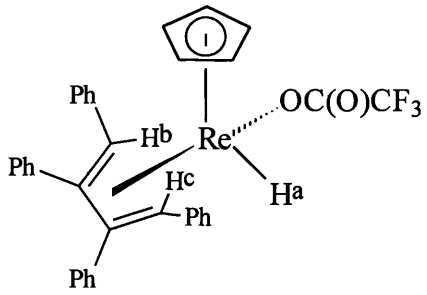

^{1}H (CD_2Cl_2) : δ -7.87 [dd, 1H, Re-H^a, J(H^aH^c) 3.0, J(H^aH^b) 5.6], 3.40 [d, 1H, H^b, J(H^aH^b) 5.6], 4.04 [d, 1H, H^c, J(H^cH^a) 3.0], 4.52 (s, 5H, Cp), 6.74-8.42 (m, 20H, Ph).

^{13}C{^{1}H} (CD_2Cl_2) : δ 57.8 (s, CH, C_1 or C_4), 61.5 (s, CH, C_4or C_1), 88.7 (s, Cp), 112.3 [q, CF_3, J^1(CF) 291], 113.1 (s, C_2 or C_3), 126.5-143.1 (m, Ph), 165.0 [q, CCF_3, J^2(CF) 36].

^{19}F (CD_2Cl_2) : δ -74.9 (s, CF_3).

Mass Spectrum : m/z, (M^+) 723, (M^+-CF_3CO_2) 610.

Peak assignments aided by H-H and C-H 2D correlation studies.

5.28 Reaction of $[ReH_2(\eta^4\text{-}C_4Ph_4)(\eta\text{-}C_5H_5)]$ 20 with CF_3COOD.

Deuterated trifluoroacetic acid (69μl, 0.9 mmol) was added at -78°C to a yellow solution (CH_2Cl_2, 20ml) of **20** (100mg, 0.9 mmol) and stirred for 12 hours. The resulting dark orange solution was preadsorbed on alumina and chromatographed using a short column. An orange band was eluted with dichloromethane and the volatiles removed *in vacuo*. Recrystallisation from toluene/hexane afforded the orange complex $[ReD\{OC(O)CF_3\}\{\eta^2,\eta^2\text{-}PhC(H)=C(Ph)C(Ph)=C(Ph)H\}(\eta\text{-}C_5H_5)]$ **23** (420 mg, Yield 80%).

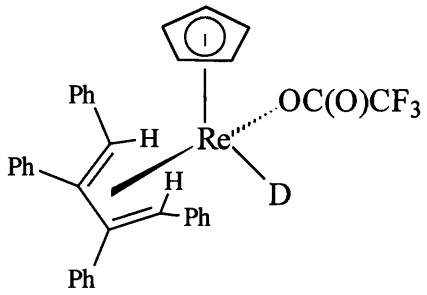

$^2\underline{H\,(CH_2Cl_2)}$: δ -7.5 (s).

5.29 Reaction of [Mo{σ,η²(3e)-CH_2C_2Ph}(η²-MeC_2Ph)(η-C_5H_5)] with Trifluoroacetic Acid.

Addition (-78° → +25°C) of CF_3CO_2H (29μl, 0.37mmol) to a solution of [Mo{σ,η²(3e)-CH_2C_2Ph}(η²-MeC_2Ph)(η-C_5H_5)] (0.17g, 0.30mmol) in dichloromethane (10ml) resulted in a change of colour from red to yellow. After 1.5 hours the volatiles were removed *in vacuo* and the resulting yellow solid recrystallised (-20°C) from toluene/hexane to give the yellow complex [Mo{$OC(O)CF_3$}(η²-MeC_2Ph)$_2$(η-C_5H_5)] **24** (0.10g, 60%) (Found: C, 60.1 ; H, 4.3 %. Calc. for $C_{25}H_{21}F_3MoO_2$; C, 59.2; H, 4.18%).

^{1}H (CD_2Cl_2) : δ 2.4-3.2 (br.s, 6H, Me), 5.65 (s, 5H, Cp), 7.00-7.80 (m, 10H, Ph).
^{13}C{^{1}H}(CD_2Cl_2) : δ 21.5 (s, Me), 102.9 (s, Cp), 116.3 [q, CF_3, ^{1}J(CF) 292], 128.4-130.1 (m, Ph), 163.3 [q, *C*CF_3, ^{2}J(CF) 37.5], 168.2 (br.s, C≡C), 186.8 (br.s, C≡C).
^{19}F(C_6D_6) : δ -75.6 (s).

5.30 Reaction of [Mo{σ,η²(3e)-CH_2C_2 Me}(η² -MeC_2Me)(η-C_5H_5)] with Trifluoroacetic Acid.

Similarly, reaction (-78°→ +25°C) of CF_3CO_2H (39 μl, 0.50mmol) with [Mo{σ,η²(3e)-CH_2C_2Me}(η²-MeC_2Me)(η-C_5H_5)] (0.14g, 0.50mmol) in dichloromethane (10ml) gave, after recrystallisation (-20°C) from toluene/hexane, the yellow complex [Mo{$OC(O)CF_3$}(η²-MeC_2Me)$_2$(η-C_5H_5)] **25** (0.89g, 55%) (Found : C, 46.9; H, 4.5%. Calc. for $C_{15}H_{17}F_3MoO_2$: C, 46.8; H,4.4%).

^{1}H (C_6D_6) : δ 2.37 (s, 12H, Me), 5.06 (s, 5H, Cp).
^{13}C{^{1}H} (C_6D_6) : δ 20.9 (br.s, Me), 101.5 (s, Cp), 117.8 [q, CF_3, ^{1}J(CF) 292.3], 164.1 [q, *C*CF_3, ^{2}J(CF) 35.0], 169.8 (br.s, *C*≡C), 183.4 (br.s, *C*≡C).
^{19}F (C_6D_6) : δ -74.2 (s).

5.32. Reaction of [Mo{σ,η²(3e)-CH_2C_2 Me}(η²-MeC_2Me)(η-C_5H_5)] with Hexafluorobut-2-yne.

Hexafluorobut-2-yne gas (1.059 g, 6.5mmol) was condensed at -196°C into a reinforced Schlenk tube under vacuum containing a frozen solution of [Mo{σ,η²(3e)-CH_2C_2 Me}(η²-MeC_2Me)(η-C_5H_5)] (330 mg, 1.23mmol) in toluene (30 ml.). After leaving the sealed tube at room temperature for 4-5 hours, the solution was filtered and the solvent removed *in vacuo*. After, chromatographing (florisil) the compound twice using toluene as eluant the yellow/orange complex **26** was obtained (110mg, Yield 15%). (Found : C, 42.8 ; H, 2.8%. Calc. for $C_{21}H_{16}F_{12}Mo$: C, 42.59; H, 2.72%).

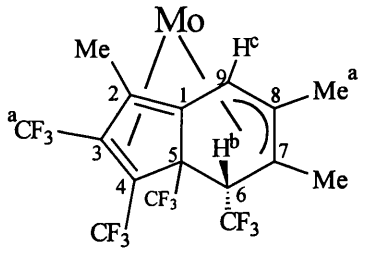

^{1}H (C_6D_6) : δ 1.4 (s, 3H, Me^a), 1.73 [q, 3H, Me, ^{5}J(HF) 2.38], 2.0 [q, 3H, Me, ^{5}J(HF) 1.47], 2.68 [q, 1H, H^b, ^{3}J(HF) 12.5], 4.46 (s, 5H, Cp), 4.69 (s, 1H, H^c).

^{19}F (C_6D_6) : δ -49.14/-49.25 (m, CF_3), -53.81 [q, $^aCF_3$, J(FF) 11.6], -57.01/-57.23 (m, CF_3), -72.55/-72.68 (m, CF_3).

^{13}C{^{1}H} (C_6D_6) : δ 13.6, 18.4 and 19.4 (s, Me), 56.4 [q, *C*CF_3, ^{2}J(CF) 30], 94.0 (s, Cp), 81.0 (s, CH), 118.0-131.4 (m, *C*F_3, and C_6D_6).

^{13}C{^{1}H} (CD_2Cl_2) : δ 122.3 [q, *C*F_3, ^{1}J(CF) 270], 124.9 [q, *C*F_3, ^{1}J(CF) 270], 125.5 [q, *C*F_3, ^{1}J(CF) 280], 128.7 [q, *C*F_3, ^{1}J(CF) 270].

Mass Spectrum : m/z, (M^+) 593

6. REFERENCES

1 a) M.J.S. Dewar, *Bull. Soc. Chim. France,* C79, 18, **1951**;
b) J. Chatt and L.A. Duncanson, *J. Chem. Soc.,* 2939, **1953**.

2 D.P. Tate and J.M. Augl, *J. Am. Chem. Soc.,* 2174, 85, **1963**.

3 R.M. Laine, R.E. Moriarty and R. Bau, *J. Am. Chem. Soc.,* 1402, 94, **1972**.

4 For a general review of four-electron alkyne complexes see J.L. Templeton, *Advances in Organometallic Chemistry,* 1, 29, **1989**.

5 J.L. Davidson and D.W.A. Sharp, *J.Chem. Soc., Dalton Trans.,* 2531, **1975**.

6 M. Green, K.R. Nagle, C.M. Woolhouse and D.J. Williams, *J. Chem. Soc. Chem. Commun.,* 1793, **1987**.

7 S.R. Allen, T.H. Glauert, M. Green, K.A. Mead, N.C. Norman, A.G. Orpen, C.J. Schaverien and P. Woodward, *J. Chem. Soc., Dalton Trans.,* 2747, **1984**.

8 W. Beck and K.Schloter, *Z. Naturforsch,* 1214, 33B, **1978**.

9 J.L. Templeton and B.C. Ward, *J. Am. Chem. Soc.,* 3288, 102, **1980**.

10 a) J.L. Davidson and D.W.A. Sharp, *J. Chem. Soc. Dalton Trans.,* 2531, **1975**;
b) J.L. Davidson and D.W.A. Sharp, *J. Chem. Soc. Dalton Trans.,* 241, **1976**;

11 a) P.L. Watson and R.G. Bergman, *J. Am. Chem. Soc.,* 2698, 102, **1980**;
b) K.A. Mead, H. Morgan and P. Woodward, *J. Chem. Soc., Dalton Trans.,* 271, **1983**.

12 S.R. Allen, P.K. Baker, S.G. Barnes, M. Green, L. Trollope, L. Manojlovic-Muir and K.W. Muir, *J. Chem. Soc. Dalton Trans.,* 171, **1979**.

13 R.S. Herrick, S.J. Burgmayer and J.L. Templeton, *Inorg. Chem.,* 3275, 22, **1983**.

14 J.L. Davidson, M. Green, D.W.A. Sharp, F.G.A. Stone and A.J. Welch, *J. Chem. Soc., Chem Commun.,* 706, **1974**.

15 M. Bamber, G.C. Conole, R.J. Deeth, S.F.T. Froom and M. Green, *J.Chem.Soc., Dalton Trans.,* 3569, **1994**.

16 F.J. Feher, M. Green and R.A. Rodrigues, *J.Chem.Soc., Chem. Commun.,* 1206, **1987**.

17 a) C. Carfagna, M. Green, M.F. Mahon, S. Rumble and C.M. Woolhouse, *J. Chem. Soc., Chem. Commun.*, 879, **1993**;

b) C. Carfagna, M. Green, M.F. Mahon, J.M. McInnes, S. Pellegrini and C.M. Woolhouse, *J. Chem. Soc., Dalton Trans.*, in press.

18 A.S. Gamble, K.R. Birdwhistell and J.L. Templeton, *J.Am.Chem.Soc.*, 1818, 112, **1990**.

19 S.R. Allen, M. Green, G. Moran, A.G. Orpen and G.E. Taylor, *J.Chem.Soc., Dalton Trans.*, 441, **1984**.

20 G.R. Clark, A.J. Nielson, A.D. Rae and C.E.F. Rickard, *J. Chem. Soc. Chem. Commun.*, 1069, **1992**.

21 C. Carfagna, M. Green, K.R. Nagle, D.J. Williams and C.M. Woolhouse, *J. Chem. Soc. Dalton Trans.*, 1761, **1993**.

22 For reviews of acyclic pentadienyl complexes see a) R. D. Ernst, *Chem. Res.*, 56, 18, **1985**;

b) H. Yasuda, A.J. Nakamura, *J. Organomet. Chem.*, 15, 285, **1985**.

23 a) S-F Lush, R-S Liu, *Organometallics*, 1908, 5, **1986**

b) G-H Lee, S-M Peng, S-F Lush, M-Y Liao and R-S Liu, *Organometallics,* 2094, 6, **1987**;

c) D. Seyferth, E.W. Goldman and J. Pornet, *J. Organomet. Chem.*, 189, 208, **1981**;

d) M.A. Paz-Sandoval, P. Powell, *J. Organomet Chem.*, 81, 219, **1981**;

e) M.A. Paz-Sandoval, P. Powell. M.G.B. Drew and R.N. Perutz, *Organometallics*, 1026, 3, **1984**;

f) G-H Lee, S-M Peng, F-C Liu, D. Mu, R-S Liu, *Organometallics*, 402, 8, **1989**;

g) J.R. Bleeke, M.K. Hays, *Organometallics*, 506, 3, **1984**.

24 L. Stahl, J.P. Hutchinson, D.R. Wilson and R.D. Ernst, *J. Am. Chem. Soc.*, 5017, 107, **1985**.

25 T.M. Sivavec, T.J. Katz, M.Y. Chiang and X-Q Yang, *Organometallics*, 1620, 8, **1989**.

26 J.W. Freeman, N.C. Hallinan, A.M. Arif, R.W. Gedridge, R.D. Ernst and F. Basolo, *J. Am. Chem. Soc.*, 6509, 113, **1991**.

27 A.D. Horton and A.G. Orpen, *Organometallics*, 8, 11, **1992**.

28 S.R. Allen, M. Green, N.C. Norman, K.E. Paddick and A.G. Orpen, *J. Chem. Soc. Dalton Trans.*, 1625, **1983**.

29 Pentadienyl iron carbonyl cations have been made in the sickle form but unless sterically encumbering substituents destablises the U form the sickle form quickly isomerises to the more common U configuration see :

a) T.S. Sorenson, C.P. Jablonski, *J. Organomet. Chem.*, C62, 25, **1970**;

b) M. Brookhart, D.L. Harris, *J. Organomet. Chem.*, 441, 42, **1972**;

c) C.P. Lillya, R.A. Sahajian, *J. Organomet. Chem.*, C67, 25, **1970**;

d) N.A. Clinton and C.P. Lillya, *J. Chem. Soc. Chem. Commun.*, 579, **1968**.

30 a) O. Eisenstein, R. Hoffmann and A.R. Rossi, *J.Am.Chem.Soc.*, 5582, 103, **1981**;

b) J. Kress and J.A. Osborn, *Angew. Chem., Int.Ed.Engl.*, 1585, 31, **1992**;

c) M.T. Youinou, J.Kress, J. Fischer, A. Aguero and J. A. Osborn, *J.Am.Chem.Soc.*, 1488, 110, **1988**.

31 M.D. Fryzuk, X. Gao and S.J. Rettig, *J.Am.Chem.Soc.*, 3106, 117, **1995**.

32 M. Brookhart and M.L.H. Green, *J. Organomet. Chem.*, 395, 250, **1983**.

33 J.R. Bleeke, J.J. Kottyk, D.A. Moore and D.J. Rauscher, *J. Am. Chem. Soc.*, 417, 109, **1987**.

34 G. Michael, J. Kaub and C.G. Kreiter, *Chem. Ber.*, 3994, 118, **1985**.

35 H.W. Bosch, H-U Hund, D. Nietlispach and A. Salzer, *Organometallics*, 2087, 11, **1992**.

36 M.A. Bennett, I.J. McMahon, S. Pelliing, M. Brookhart and D.M. Lincoln, *Organometallics,* 127, 11, **1992**.

37 B. Buchmann, U. Piantini, W. von Philipsborn and A. Salzer, *Helvetica Chimica Acta.*, 1487, 70, **1987**.

38 For general reviews of C-H activation see a) G.W. Parshall, *Acc. Chem. Res.*, 113, 8, **1975**;

b) D.E. Webster, *Adv. Organomet. Chem.*, 73, 16, **1977**;

c) M.I. Bruce, *Angew. Chem. Int. Ed. Engl.*, 63, 16, **1977**;

d) R.H. Crabtree, *Chem. Rev.*, 845, 85, **1985**;

e) A.D. Ryabov, *Chem. Rev.*, 403, 90, **1990**.

39 J.P. Collman, L.S. Hegedus, J.R. Norton, L.S. Finke, *Principles and Applications of Organotransition Chemistry*, Univ. Science Books, CA-Mill Valley, **1987**.

40 See for example a) G. Erker, K. Engel, C. Krüger and G. Müller, *Organometallics*, 28, 3, **1984**;

b) J.W. Chinn Jr., M.B. Hall, *Organometallics*, 284, 3, **1984** and references therein.

41 a) G. Erker, C. Krüger and G. Müller, *Adv. Organomet. Chem.*, 1, 24, **1985**

b) H. Yasuda, K. Tatsumi and A. Nakamura, *Acc. Chem. Res.*, 120, 18, **1985** and references therein.

42 H. Yasuda, *J. Am. Chem. Soc.*, 5008, 110, **1988**.

43 S.A. Benyunes, J.P. Day, M. Green, A.W. Al-Saadoon and T.L. Waring, *Angew. Chem. Int. Ed. Engl.*, 1416, **1990**.

44 R.D. Ernst, E. Melendez, L. Stahl and M.L. Ziegler, *Organometallics*, 3635, 10, **1991**.

45 a) N.J. Christensen, A.D. Hunter and P. Legzdins, *Organometallics*, 930, 8, **1988**;

b) N.J. Christensen, P. Legzdins, F.W.B. Einstein and R.H. Jones, *Organometallics*, 3070, 10, **1991**.

46 R.D. Ernst, E. Melendez, L. Stahl and M.L. Ziegler, *Organometallics*, 3635, 10, **1991**.

47 a) M.E. Squillacote, R.S. Sheridan, O.L. Chapman and F.A. Anet, *J. Am. Chem. Soc.*, 3657, 101, **1979**;

b) P.W. Mui and E. Grunwald, *J. Am. Chem. Soc.*, 6562, 104, **1982**.

48 A.D. Hunter, P. Legzdins, C.R. Nurse, F.W.B. Einstein and A.C. Willis, *J.Am.Chem.Soc.*, 1791, 107, **1985**.

49 Ch. Elschenbroich and A. Salzer, *Organometallics. A Concise Introduction*, 2nd Ed, **1992**.

50 F.A. Cotton, V.W. Day, B.A. Frenz, K.I. Hardcastle and J.M. Troup, *J. Am. Chem. Soc.*, 6645, 99, **1973**.

51 M. Green, M.F. Mahon, K.C. Molloy, C.B.M. Nation and C.M. Woolhouse, *J. Chem Soc. Chem. Commun.*, 1587, **1991**.

52 N.G. Connelly, *Chem. Soc. Rev.*, 153, 18, **1989**.

53 L. Brammer, B.J. Dunne, M. Green, G. Moran, A.G. Orpen, C. Reeve and C.J. Schaverien, *J. Chem. Soc. Dalton Trans.*, 1747, **1993**.

54 a) M. Green and A.P. Walker, *unpublished results*;
b) C. Butters, *PhD. Thesis*, University of Bath, **1995**.

55 C. Carfagna, N. Carr, R.J. Deeth, S.J. Dossett, M. Green, M.F. Mahon and C. Vaughan, *J. Chem. Soc. Dalton Trans.*, in press.

56 T. Blackmore, M.I. Bruce and F.G.A. Stone, *J. Chem. Soc. Chem. Commun.*, 852, **1971**.

57 J. S. Ricci and J.A. Ibers, *J. Organomet. Chem.*, 261, 27, **1971**.

58 G.E. Herberich and H. Mayer, *Organometallics*, 2655, 9, **1990**.

59 a) M. Crocker, M. Green, A.G. Orpen, H-P Neumann and C.J. Schaverien, *J. Chem. Soc. Chem. Commun.*, 1351, **1984**.
b) M. Crocker, M. Green, K.R. Nagle, A.G. Orpen, H-P. Neumann, C.E. Morton and C.J. Schaverien, *Organometallics*, 1422, 9, **1990**.

60 M. Green, M.F. Mahon and A.P. Walker, *unpublished results*.

61 a) N.M. Agh-Atabay, J.L. Davidson and K.W. Muir, *J. Chem. Soc. Chem Commun.*, 1399, **1990**;
b) N.M. Agh-Atabay, L.J. Canoira, L. Carlton and J.L. Davidson, *J. Chem. Soc. Dalton Trans.*, 1175, **1991**;
c) J.L. Davidson, *J. Chem. Soc. Dalton Trans.*, 2715, **1987**.

62 J.R. Morrow, T.L. Tonker and J.L. Templeton, *J. Am. Chem. Soc.*, 5004, 107, **1985**.

63 F. Biasotto, M. Etienne and F. Dahan, *Organometallics*, 1870, 14, **1995**.

64 E-I Negishi, *Comprehensive Organometallics*, 1163, 5, CHP 9.5.

65 W.A. Herrmann, R.A. Fischer and E. Herdtweck, *Organometallics*, 2821, 8, **1989**.

66 S.G. Feng, A.S. Gamble and J.L. Templeton, *Organometallics*, 2024, 8, **1989**.

67 a) L. Brammer, M. Crocker, B.J. Dunne, M. Green, C.E. Morton, K.R. Nagle and A.G. Orpen, *J. Chem. Soc. Chem. Commun.*, 1226, **1986**;
b) M. Crocker, B.J. Dunne, M. Green and A.G. Orpen, *J. Chem. Soc. Dalton Trans.*, 1589, **1991**.

68 L.M. Jackman and S. Sternell, *Applications of Nuclear Magnetic Resonance Spectroscopy in Organic Chemistry 2nd Ed.*, chp 4-2, Pergamon Press, **1978**.

69 H.C. Longuet-Higgins and L.E. Orgel, *J. Chem. Soc.*, 1969, **1956**.

70 R. Criegee and G. Schröder, *Justus Liebigs Ann. Che.*, 1, 623, **1959**.

71 G. Henrici-Olivé and S. Olivé, *Angew. Chem.*, 897, 79, **1967**.

72 a) G.F. Emerson, L. Watts and R. Pettit, *J. Am. Chem. Soc.*, 131, 87, **1965**;
b) R. Pettit and J. Henry, *Org. Synth.*, 21, 50, **1966**.

73 For a general review of transition metal cyclobutadiene complexes see A. Efraty, *Chem. Rev.*, 691, 77, **1977**, and references therein.

74 H.E. Zimmerman, G.L. Grunewald and R.M. Paufler, *Org. Synth.*, 101, 46, **1966**.

75 M. Rosenblum and C. Gatsonis, *J. Am. Chem. Soc.*, 5079, 89, **1967**.

76 A. Nakumura and N. Hagihara, *Bull. Chem. Soc. Jpn.*, 452, 34, **1961**.

77 J.L. Boston, D.W. Sharpe and G. Wilkinson, *J. Chem. Soc.*, 3488, **1962**.

78 M.D. Rausch and R.A. Genetti, *J. Am. Chem. Soc.*, 5502, 89, **1967**.

79 M. Crocker, M. Green, A.G. Orpen and D. M. Thomas, *J.Chem. Soc. Chem. Commun.*, 1141, **1984**.

80 P. Reeves, J. Henry and R. Pettit, *J. Am. Chem. Soc.*, 5888, 91, **1969**.

81 J.S. Ward and R. Pettit, *J. Am. Chem. Soc.*, 262, 93, **1971**.

82 F.M. Chaudhari and P.L. Pauson, *J. Organomet. Chem.*, 73, 5, **1966**.

83 A. Bond, M. Green and S.H. Taylor, *J. Chem. Soc. Chem. Commun.*, 112, **1973**.

84 a) A. Bond and M. Green, *J. Chem. Soc. Chem. Commun.*, 12, **1971**.
b) A. Bond and M. Green, *J. Chem. Soc. Dalton Trans.*, 763, **1972**.

85 J.D. Fitzpatrick, L. Watts, G.F. Emerson and R. Pettit, *J. Am. Chem. Soc.*, 3254, 87, **1965**.

86 G.F. Emerson and R. Pettit, *J. Am. Chem. Soc.*, 4591, 84, **1962**.

87 L. Watts, J.D. Fitzpatrick and R. Pettit, *J.Am. Chem. Soc.*, 623, 88, **1966**.

88 L. Watts, J.D. Fitzpatrick and R. Pettit, *J. Am. Chem. Soc.*, 3253, 87, **1965**.

89 G.D. Burt and R. Pettit, *J. Chem. Soc. Chem. Commun.*, 517, **1965**.

90 N.C. Carr, M. Green, J.M. McInnes and C. Vaughn, *unpublished results*.

91 S.G. Davies, M.L.H. Green and D.M.P. Mingos, *Tetrahedron*, 3047, 34, **1978**.

92 M. Green and C. Vaughn, *unpublished results*.

93 For a summary of the chemistry and synthesis of bis(cyclopentadienyl) metallocenes see M.L.H. Green, *"Organometallic Compounds" 3rd Ed.*, 90, 2, **1968**.

94 P.C. Wailes, S.P. Coutts and H. Weigold, *"Organometallic Chemistry of Titanium, Zirconium and Hafnium"*, Academic Press, New York, **1974**.

95 M. Dubeck and R.A. Schell, *Inorg. Chem.*, 1757, 3, **1967**.

96 J.W. Lauher and R. Hoffmann, *J. Am. Chem. Soc.*, 1729, 98, **1976** and references therein.

97 For a summary of structures of some $[MX_2(Cp)_2]$ complexes see K. Prout, T.S. Cameron, R.A. Forder, S.R. Critchley, B. Denton and G.V. Rees, *Acta. Crystallogr., Sect B*, 2290, 30, **1974**.

98 O.J. Curnow, W. Hirpo, W.M. Butler and M.D. Curtis, *Organometallics*, 4479, 12, **1993**.

99 F.A. Cotton and R.L. Luck, *Inorg Chem.*, 2182, 28, **1985**.

100 a) S, Feracin, T. Bürgi, V.L. Bakhmutov, I. Eremenko, E.V. Voronstov, A.B. Vimenits and H. Berke, *Organometallics,* 4194, 13, **1994**;
b) V. Bakhumutov, T. Bürgi, P. Burger, U. Ruppli and H. Berke, *Organometallics*, 4203, 13, **1994**.

101 S.H. Taylor and P.M. Maitlis, *J. Am. Chem. Soc.,* 4701, 100, **1978**.

102 M. Crocker, B.J. Dunne, M. Green and A.G. Orpen, *J. Chem. Soc. Dalton Trans.,* 1589, **1991**.

103 M-C. Chen, R-S. Keng, Y-C. Lin, Y. Wang, M-C. Cheng, G-H. Lee, *J. Chem. Soc. Chem. Commun.,* 1138, **1990**.

104 J. Gotzig, H. Otto and H. Werner, *J. Organomet. Chem.,* 247, 287, **1985**.

105 V.V. Krivykh, E.S. Taits, P.V. Petrovskii, Y.T. Struchkov and A.I. Yanovskii, *Mendeleev Commun.,* 103, **1991**.

106 S.G. Davies, M.L.H. Green and D.M.P. Mingos, *Tetrahedron*, 3047, 34, **1978**.

107 P.W. Blosser, J.C. Gallucci and A. Wojcicki, *J.Am.Chem.Soc.,* 2994, 115, **1993**.

108 S.R. Allen, S.G. Barnes, M. Green, G. Moran, L. Trollope, N.W. Murrall, A.G. Welch and D.M. Sharaiha, *J. Chem. Soc. Dalton Trans.,* 1157, **1984**.

109 T.A. Albright, P. Hoffmann and R. Hoffmann, *J. Am. Chem. Soc.,* 7546, 99, **1977**.

110 Modification of the synthesis of *p*-diphenylphosphinostyrene, R. Rabinowitz and R. Marcus, *J. Org. Chem.,* 4157, 26, **1961**.

111 a) M. Bottrill and M. Green, *J. Chem. Soc. Dalton Trans.,* 2365, **1977**;
b) C. Reeve, *PhD. Thesis*, University of Bristol, **1989**.

112 D.N. Hendrickson, Y.S. Sohn and H.B. Gray, *Inorg. Chem.,* 1559, 10, **1971**.

113 C. Mealli and D. Proserpio, *J. Chem Ed.,* 399, 67, **1990**.

114 Y.W. Aleyunas, N.C. Baenziger, P.K. Bradley and R.F. Jordan, *Organometallics*, 156, 13, **1994**.

7. APPENDIX.

7.1 Crystal Structure Determination of [Mo(η^2-MeC$_2$Ph)(dpps)(η-C$_5$H$_5$)][BF$_4$] 1.

A crystal of approximate dimensions 0.2x0.2x0.1 mm was used for data collection.

Crystal Data : $C_{34}H_{30}PBF_4Mo$, M = 622.3, monoclinic, a = 12.636(1), b = 13.467(2), c = 17.559(2) Å, β = 90.02(1)°, U = 2983.9 Å^3, space group $P2_1/c$, Z = 4, D_c = 1.39 gcm^{-3}, μ(Mo-K_α) = 5.20 cm^{-1}, $F(000)$ = 1268. Data were measured at room temperature on a CAD4 automatic four-circle diffractometer in the range $2 \leq \theta \leq 24°$. 5149 reflections were collected of which 2539 were unique with $I \geq 2\sigma(I)$. Data were corrected for Lorentz and polarisation effects but not for X-ray absorption effects. The structure was solved by Direct methods and refined using the SHELX[i,ii] suite of programs. The fluoroborate anion exhibited some disorder between F1, F2 and F3 (69% occupancy) and staggered partial atoms F12, F23 and F13 (31% occupancy). In the final least squares cycles all atoms except the minor disordered fluorines were allowed to vibrate anisotropically. Hydrogen atoms were included at calculated positions except in the case of those hydrogens attached to C6 and C7, which were located in the penultimate Difference Fourier and refined at a distance of 0.96Å from the relevant parent atoms. Final residues after 12 cycles of least squares were R = 0.0474, R_w =0.0363, for a weighting scheme of w = 2.7450/[σ^2(F) + 0.000136(F)^2]. Max. final shift/esd was 0.004. The max. and min. residual densities were 0.24 and -0.16 eÅ^{-3}, respectively. Final fractional atomic coordinates and isotropic thermal parameters, bond distances and angles are listed in Tables 7.1/7.2, 7.3 and 7.4, respectively. The asymmetric unit is shown in Figure 2.6 (Section 2.2), along with the labelling scheme employed.

---

i G.M. Sheldrick, SHELX86, a computer program for crystal structure determination, University of Göttingen, **1986**.

ii G.M. Sheldrick, SHELX76, a computer program for crystal structure determination, University of Cambridge, **1976**.

6. REFERENCES

1 a) M.J.S. Dewar, *Bull. Soc. Chim. France,* C79, 18, **1951**;
b) J. Chatt and L.A. Duncanson, *J. Chem. Soc.,* 2939, **1953**.

2 D.P. Tate and J.M. Augl, *J. Am. Chem. Soc.,* 2174, 85, **1963**.

3 R.M. Laine, R.E. Moriarty and R. Bau, *J. Am. Chem. Soc.,* 1402, 94, **1972**.

4 For a general review of four-electron alkyne complexes see J.L. Templeton, *Advances in Organometallic Chemistry,* 1, 29, **1989**.

5 J.L. Davidson and D.W.A. Sharp, *J.Chem. Soc., Dalton Trans.,* 2531, **1975**.

6 M. Green, K.R. Nagle, C.M. Woolhouse and D.J. Williams, *J. Chem. Soc. Chem. Commun.,* 1793, **1987**.

7 S.R. Allen, T.H. Glauert, M. Green, K.A. Mead, N.C. Norman, A.G. Orpen, C.J. Schaverien and P. Woodward, *J. Chem. Soc., Dalton Trans.,* 2747, **1984**.

8 W. Beck and K.Schloter, *Z. Naturforsch,* 1214, 33B, **1978**.

9 J.L. Templeton and B.C. Ward, *J. Am. Chem. Soc.,* 3288, 102, **1980**.

10 a) J.L. Davidson and D.W.A. Sharp, *J. Chem. Soc. Dalton Trans.,* 2531, **1975**;
b) J.L. Davidson and D.W.A. Sharp, *J. Chem. Soc. Dalton Trans.,* 241, **1976**;

11 a) P.L. Watson and R.G. Bergman, *J. Am. Chem. Soc.,* 2698, 102, **1980**;
b) K.A. Mead, H. Morgan and P. Woodward, *J. Chem. Soc., Dalton Trans.,* 271, **1983**.

12 S.R. Allen, P.K. Baker, S.G. Barnes, M. Green, L. Trollope, L. Manojlovic-Muir and K.W. Muir, *J. Chem. Soc. Dalton Trans.,* 171, **1979**.

13 R.S. Herrick, S.J. Burgmayer and J.L. Templeton, *Inorg. Chem.,* 3275, 22, **1983**.

14 J.L. Davidson, M. Green, D.W.A. Sharp, F.G.A. Stone and A.J. Welch, *J. Chem. Soc., Chem Commun.,* 706, **1974**.

15 M. Bamber, G.C. Conole, R.J. Deeth, S.F.T. Froom and M. Green, *J.Chem.Soc., Dalton Trans.,* 3569, **1994**.

16 F.J. Feher, M. Green and R.A. Rodrigues, *J.Chem.Soc., Chem. Commun.,* 1206, **1987**.

17 a) C. Carfagna, M. Green, M.F. Mahon, S. Rumble and C.M. Woolhouse, *J. Chem. Soc., Chem. Commun.*, 879, **1993**;

b) C. Carfagna, M. Green, M.F. Mahon, J.M. McInnes, S. Pellegrini and C.M. Woolhouse, *J. Chem. Soc., Dalton Trans.*, in press.

18 A.S. Gamble, K.R. Birdwhistell and J.L. Templeton, *J.Am.Chem.Soc.*, 1818, 112, **1990**.

19 S.R. Allen, M. Green, G. Moran, A.G. Orpen and G.E. Taylor, *J.Chem.Soc., Dalton Trans.*, 441, **1984**.

20 G.R. Clark, A.J. Nielson, A.D. Rae and C.E.F. Rickard, *J. Chem. Soc. Chem. Commun.*, 1069, **1992**.

21 C. Carfagna, M. Green, K.R. Nagle, D.J. Williams and C.M. Woolhouse, *J. Chem. Soc. Dalton Trans.*, 1761, **1993**.

22 For reviews of acyclic pentadienyl complexes see a) R. D. Ernst, *Chem. Res.*, 56, 18, **1985**;

b) H. Yasuda, A.J. Nakamura, *J. Organomet. Chem.*, 15, 285, **1985**.

23 a) S-F Lush, R-S Liu, *Organometallics*, 1908, 5, **1986**

b) G-H Lee, S-M Peng, S-F Lush, M-Y Liao and R-S Liu, *Organometallics,* 2094, 6, **1987**;

c) D. Seyferth, E.W. Goldman and J. Pornet, *J. Organomet. Chem.*, 189, 208, **1981**;

d) M.A. Paz-Sandoval, P. Powell, *J. Organomet Chem.*, 81, 219, **1981**;

e) M.A. Paz-Sandoval, P. Powell. M.G.B. Drew and R.N. Perutz, *Organometallics*, 1026, 3, **1984**;

f) G-H Lee, S-M Peng, F-C Liu, D. Mu, R-S Liu, *Organometallics*, 402, 8, **1989**;

g) J.R. Bleeke, M.K. Hays, *Organometallics*, 506, 3, **1984**.

24 L. Stahl, J.P. Hutchinson, D.R. Wilson and R.D. Ernst, *J. Am. Chem. Soc.*, 5017, 107, **1985**.

25 T.M. Sivavec, T.J. Katz, M.Y. Chiang and X-Q Yang, *Organometallics*, 1620, 8, **1989**.

26 J.W. Freeman, N.C. Hallinan, A.M. Arif, R.W. Gedridge, R.D. Ernst and F. Basolo, *J. Am. Chem. Soc.*, 6509, 113, **1991**.

27 A.D. Horton and A.G. Orpen, *Organometallics*, 8, 11, **1992**.

28 S.R. Allen, M. Green, N.C. Norman, K.E. Paddick and A.G. Orpen, *J. Chem. Soc. Dalton Trans.*, 1625, **1983**.

29 Pentadienyl iron carbonyl cations have been made in the sickle form but unless sterically encumbering substituents destablises the U form the sickle form quickly isomerises to the more common U configuration see :

a) T.S. Sorenson, C.R. Jablonski, *J. Organomet. Chem.*, C62, 25, **1970**;

b) M. Brookhart, D.L. Harris, *J. Organomet. Chem.*, 441, 42, **1972**;

c) C.P. Lillya, R.A. Sahajian, *J. Organomet. Chem.*, C67, 25, **1970**;

d) N.A. Clinton and C.P. Lillya, *J. Chem. Soc. Chem. Commun.*, 579, **1968**.

30 a) O. Eisenstein, R. Hoffmann and A.R. Rossi, *J.Am.Chem.Soc.*, 5582, 103, **1981**;

b) J. Kress and J.A. Osborn, *Angew. Chem., Int.Ed.Engl.*, 1585, 31, **1992**;

c) M.T. Youinou, J.Kress, J. Fischer, A. Aguero and J. A. Osborn, *J.Am.Chem.Soc.*, 1488, 110, **1988**.

31 M.D. Fryzuk, X. Gao and S.J. Rettig, *J.Am.Chem.Soc.*, 3106, 117, **1995**.

32 M. Brookhart and M.L.H. Green, *J. Organomet. Chem.*, 395, 250, **1983**.

33 J.R. Bleeke, J.J. Kottyk, D.A. Moore and D.J. Rauscher, *J. Am. Chem. Soc.*, 417, 109, **1987**.

34 G. Michael, J. Kaub and C.G. Kreiter, *Chem. Ber.*, 3994, 118, **1985**.

35 H.W. Bosch, H-U Hund, D. Nietlispach and A. Salzer, *Organometallics*, 2087, 11, **1992**.

36 M.A. Bennett, I.J. McMahon, S. Pelliing, M. Brookhart and D.M. Lincoln, *Organometallics*, 127, 11, **1992**.

37 B. Buchmann, U. Piantini, W. von Philipsborn and A. Salzer, *Helvetica Chimica Acta.*, 1487, 70, **1987**.

38 For general reviews of C-H activation see a) G.W. Parshall, *Acc. Chem. Res.*, 113, 8, **1975**;

b) D.E. Webster, *Adv. Organomet. Chem.*, 73, 16, **1977**;

c) M.I. Bruce, *Angew. Chem. Int. Ed. Engl.*, 63, 16, **1977**;

d) R.H. Crabtree, *Chem. Rev.*, 845, 85, **1985**;

e) A.D. Ryabov, *Chem. Rev.*, 403, 90, **1990**.

39 J.P. Collman, L.S. Hegedus, J.R. Norton, L.S. Finke, *Principles and Applications of Organotransition Chemistry*, Univ. Science Books, CA-Mill Valley, **1987**.

40 See for example a) G. Erker, K. Engel, C. Krüger and G. Müller, *Organometallics*, 28, 3, **1984**;

b) J.W. Chinn Jr., M.B. Hall, *Organometallics*, 284, 3, **1984** and references therein.

41 a) G. Erker, C. Krüger and G. Müller, *Adv. Organomet. Chem.*, 1, 24, **1985**

b) H. Yasuda, K. Tatsumi and A. Nakamura, *Acc. Chem. Res.*, 120, 18, **1985** and references therein.

42 H. Yasuda, *J. Am. Chem. Soc.*, 5008, 110, **1988**.

43 S.A. Benyunes, J.P. Day, M. Green, A.W. Al-Saadoon and T.L. Waring, *Angew. Chem. Int. Ed. Engl.*, 1416, **1990**.

44 R.D. Ernst, E. Melendez, L. Stahl and M.L. Ziegler, *Organometallics*, 3635, 10, **1991**.

45 a) N.J. Christensen, A.D. Hunter and P. Legzdins, *Organometallics*, 930, 8, **1988**;

b) N.J. Christensen, P. Legzdins, F.W.B. Einstein and R.H. Jones, *Organometallics*, 3070, 10, **1991**.

46 R.D. Ernst, E. Melendez, L. Stahl and M.L. Ziegler, *Organometallics*, 3635, 10, **1991**.

47 a) M.E. Squillacote, R.S. Sheridan, O.L. Chapman and F.A. Anet, *J. Am. Chem. Soc.*, 3657, 101, **1979**;

b) P.W. Mui and E. Grunwald, *J. Am. Chem. Soc.*, 6562, 104, **1982**.

48 A.D. Hunter, P. Legzdins, C.R. Nurse, F.W.B. Einstein and A.C. Willis, *J.Am.Chem.Soc.*, 1791, 107, **1985**.

49 Ch. Elschenbroich and A. Salzer, *Organometallics. A Concise Introduction*, 2nd Ed, **1992**.

50 F.A. Cotton, V.W. Day, B.A. Frenz, K.I. Hardcastle and J.M. Troup, *J. Am. Chem. Soc.*, 6645, 99, **1973**.

51 M. Green, M.F. Mahon, K.C. Molloy, C.B.M. Nation and C.M. Woolhouse, *J. Chem Soc. Chem. Commun.*, 1587, **1991**.

52 N.G. Connelly, *Chem. Soc. Rev.*, 153, 18, **1989**.

53 L. Brammer, B.J. Dunne, M. Green, G. Moran, A.G. Orpen, C. Reeve and C.J. Schaverien, *J. Chem. Soc. Dalton Trans.*, 1747, **1993**.

54 a) M. Green and A.P. Walker, *unpublished results*;
b) C. Butters, *PhD. Thesis*, University of Bath, **1995**.

55 C. Carfagna, N. Carr, R.J. Deeth, S.J. Dossett, M. Green, M.F. Mahon and C. Vaughan, *J. Chem. Soc. Dalton Trans.*, in press.

56 T. Blackmore, M.I. Bruce and F.G.A. Stone, *J. Chem. Soc. Chem. Commun.*, 852, **1971**.

57 J. S. Ricci and J.A. Ibers, *J. Organomet. Chem.*, 261, 27, **1971**.

58 G.E. Herberich and H. Mayer, *Organometallics*, 2655, 9, **1990**.

59 a) M. Crocker, M. Green, A.G. Orpen, H-P Neumann and C.J. Schaverien, *J. Chem. Soc. Chem. Commun.*, 1351, **1984**.
b) M. Crocker, M. Green, K.R. Nagle, A.G. Orpen, H-P. Neumann, C.E. Morton and C.J. Schaverien, *Organometallics*, 1422, 9, **1990**.

60 M. Green, M.F. Mahon and A.P. Walker, *unpublished results*.

61 a) N.M. Agh-Atabay, J.L. Davidson and K.W. Muir, *J. Chem. Soc. Chem Commun.*, 1399, **1990**;
b) N.M. Agh-Atabay, L.J. Canoira, L. Carlton and J.L. Davidson, *J. Chem. Soc. Dalton Trans.*, 1175, **1991**;
c) J.L. Davidson, *J. Chem. Soc. Dalton Trans.*, 2715, **1987**.

62 J.R. Morrow, T.L. Tonker and J.L. Templeton, *J. Am. Chem. Soc.*, 5004, 107, **1985**.

63 F. Biasotto, M. Etienne and F. Dahan, *Organometallics*, 1870, 14, **1995**.

64 E-I Negishi, *Comprehensive Organometallics*, 1163, 5, CHP 9.5.

65 W.A. Herrmann, R.A. Fischer and E. Herdtweck, *Organometallics*, 2821, 8, **1989**.

66 S.G. Feng, A.S. Gamble and J.L. Templeton, *Organometallics*, 2024, 8, **1989**.

67 a) L. Brammer, M. Crocker, B.J. Dunne, M. Green, C.E. Morton, K.R. Nagle and A.G. Orpen, *J. Chem. Soc. Chem. Commun.*, 1226, **1986**;
b) M. Crocker, B.J. Dunne, M. Green and A.G. Orpen, *J. Chem. Soc. Dalton Trans.*, 1589, **1991**.

68 L.M. Jackman and S. Sternell, *Applications of Nuclear Magnetic Resonance Spectroscopy in Organic Chemistry 2nd Ed.*, chp 4-2, Pergamon Press, **1978**.

69 H.C. Longuet-Higgins and L.E. Orgel, *J. Chem. Soc.*, 1969, **1956**.

70 R. Criegee and G. Schröder, *Justus Liebigs Ann. Che.*, 1, 623, **1959**.

71 G. Henrici-Olivé and S. Olivé, *Angew. Chem.*, 897, 79, **1967**.

72 a) G.F. Emerson, L. Watts and R. Pettit, *J. Am. Chem. Soc.*, 131, 87, **1965**;
b) R. Pettit and J. Henry, *Org. Synth.*, 21, 50, **1966**.

73 For a general review of transition metal cyclobutadiene complexes see A. Efraty, *Chem. Rev.*, 691, 77, **1977**, and references therein.

74 H.E. Zimmerman, G.L. Grunewald and R.M. Paufler, *Org. Synth.*, 101, 46, **1966**.

75 M. Rosenblum and C. Gatsonis, *J. Am. Chem. Soc.*, 5079, 89, **1967**.

76 A. Nakumura and N. Hagihara, *Bull. Chem. Soc. Jpn.*, 452, 34, **1961**.

77 J.L. Boston, D.W. Sharpe and G. Wilkinson, *J. Chem. Soc.*, 3488, **1962**.

78 M.D. Rausch and R.A. Genetti, *J. Am. Chem. Soc.*, 5502, 89, **1967**.

79 M. Crocker, M. Green, A.G. Orpen and D. M. Thomas, *J.Chem. Soc. Chem. Commun.*, 1141, **1984**.

80 P. Reeves, J. Henry and R. Pettit, *J. Am. Chem. Soc.*, 5888, 91, **1969**.

81 J.S. Ward and R. Pettit, *J. Am. Chem. Soc.*, 262, 93, **1971**.

82 F.M. Chaudhari and P.L. Pauson, *J. Organomet. Chem.*, 73, 5, **1966**.

83 A. Bond, M. Green and S.H. Taylor, *J. Chem. Soc. Chem. Commun.*, 112, **1973**.

84 a) A. Bond and M. Green, *J. Chem. Soc. Chem. Commun.*, 12, **1971**.
b) A. Bond and M. Green, *J. Chem. Soc. Dalton Trans.*, 763, **1972**.

85 J.D. Fitzpatrick, L. Watts, G.F. Emerson and R. Pettit, *J. Am. Chem. Soc.*, 3254, 87, **1965**.

86 G.F. Emerson and R. Pettit, *J. Am. Chem. Soc.*, 4591, 84, **1962**.

87 L. Watts, J.D. Fitzpatrick and R. Pettit, *J.Am. Chem. Soc.*, 623, 88, **1966**.

88 L. Watts, J.D. Fitzpatrick and R. Pettit, *J. Am. Chem. Soc.*, 3253, 87, **1965**.

89 G.D. Burt and R. Pettit, *J. Chem. Soc. Chem. Commun.*, 517, **1965**.

90 N.C. Carr, M. Green, J.M. McInnes and C. Vaughn, *unpublished results.*

91 S.G. Davies, M.L.H. Green and D.M.P. Mingos, *Tetrahedron*, 3047, 34, **1978**.

92 M. Green and C. Vaughn, *unpublished results.*

93 For a summary of the chemistry and synthesis of bis(cyclopentadienyl) metallocenes see M.L.H. Green, *"Organometallic Compounds" 3rd Ed.*, 90, 2, **1968**.

94 P.C. Wailes, S.P. Coutts and H. Weigold, *"Organometallic Chemistry of Titanium, Zirconium and Hafnium"*, Academic Press, New York, **1974**.

95 M. Dubeck and R.A. Schell, *Inorg. Chem.*, 1757, 3, **1967**.

96 J.W. Lauher and R. Hoffmann, *J. Am. Chem. Soc.*, 1729, 98, **1976** and references therein.

97 For a summary of structures of some $[MX_2(Cp)_2]$ complexes see K. Prout, T.S. Cameron, R.A. Forder, S.R. Critchley, B. Denton and G.V. Rees, *Acta. Crystallogr., Sect B,* 2290, 30, **1974**.

98 O.J. Curnow, W. Hirpo, W.M. Butler and M.D. Curtis, *Organometallics*, 4479, 12, **1993**.

99 F.A. Cotton and R.L. Luck, *Inorg Chem.*, 2182, 28, **1985**.

100 a) S, Feracin, T. Bürgi, V.L. Bakhmutov, I. Eremenko, E.V. Voronstov, A.B. Vimenits and H. Berke, *Organometallics,* 4194, 13, **1994**;
b) V. Bakhumutov, T. Bürgi, P. Burger, U. Ruppli and H. Berke, *Organometallics*, 4203, 13, **1994**.

101 S.H. Taylor and P.M. Maitlis, *J. Am. Chem. Soc.,* 4701, 100, **1978**.

102 M. Crocker, B.J. Dunne, M. Green and A.G. Orpen, *J. Chem. Soc. Dalton Trans.,* 1589, **1991**.

103 M-C. Chen, R-S. Keng, Y-C. Lin, Y. Wang, M-C. Cheng, G-H. Lee, *J. Chem. Soc. Chem. Commun.,* 1138, **1990**.

104 J. Gotzig, H. Otto and H. Werner, *J. Organomet. Chem.,* 247, 287, **1985**.

105 V.V. Krivykh, E.S. Taits, P.V. Petrovskii, Y.T. Struchkov and A.I. Yanovskii, *Mendeleev Commun.,* 103, **1991**.

106 S.G. Davies, M.L.H. Green and D.M.P. Mingos, *Tetrahedron*, 3047, 34, **1978**.

107 P.W. Blosser, J.C. Gallucci and A. Wojcicki, *J.Am.Chem.Soc.,* 2994, 115, **1993**.

108 S.R. Allen, S.G. Barnes, M. Green, G. Moran, L. Trollope, N.W. Murrall, A.G. Welch and D.M. Sharaiha, *J. Chem. Soc. Dalton Trans.,* 1157, **1984**.

109 T.A. Albright, P. Hoffmann and R. Hoffmann, *J. Am. Chem. Soc.,* 7546, 99, **1977**.

110 Modification of the synthesis of *p*-diphenylphosphinostyrene, R. Rabinowitz and R. Marcus, *J. Org. Chem.,* 4157, 26, **1961**.

111 a) M. Bottrill and M. Green, *J. Chem. Soc. Dalton Trans.,* 2365, **1977**;
b) C. Reeve, *PhD. Thesis*, University of Bristol, **1989**.

112 D.N. Hendrickson, Y.S. Sohn and H.B. Gray, *Inorg. Chem.,* 1559, 10, **1971**.

113 C. Mealli and D. Proserpio, *J. Chem Ed.,* 399, 67, **1990**.

114 Y.W. Aleyunas, N.C. Baenziger, P.K. Bradley and R.F. Jordan, *Organometallics*, 156, 13, **1994**.

7. APPENDIX.

7.1 Crystal Structure Determination of [Mo(η^2-MeC$_2$Ph)(dpps)(η-C$_5$H$_5$)][BF$_4$] 1.

A crystal of approximate dimensions 0.2x0.2x0.1 mm was used for data collection.

Crystal Data : $C_{34}H_{30}PBF_4Mo$, M = 622.3, monoclinic, a = 12.636(1), b = 13.467(2), c = 17.559(2) Å, β = 90.02(1)°, U = 2983.9 Å^3, space group $P2_1/c$, Z = 4, D_c = 1.39 gcm^{-3}, μ(Mo-K_α) = 5.20 cm^{-1}, $F(000)$ = 1268. Data were measured at room temperature on a CAD4 automatic four-circle diffractometer in the range $2\leq\theta\leq24°$. 5149 reflections were collected of which 2539 were unique with $I\geq2\sigma(I)$. Data were corrected for Lorentz and polarisation effects but not for X-ray absorption effects. The structure was solved by Direct methods and refined using the SHELX[i,ii] suite of programs. The fluoroborate anion exhibited some disorder between F1, F2 and F3 (69% occupancy) and staggered partial atoms F12, F23 and F13 (31% occupancy). In the final least squares cycles all atoms except the minor disordered fluorines were allowed to vibrate anisotropically. Hydrogen atoms were included at calculated positions except in the case of those hydrogens attached to C6 and C7, which were located in the penultimate Difference Fourier and refined at a distance of 0.96Å from the relevant parent atoms. Final residues after 12 cycles of least squares were R = 0.0474, R_w =0.0363, for a weighting scheme of w = 2.7450/[σ^2(F) + 0.000136(F)^2]. Max. final shift/esd was 0.004. The max. and min. residual densities were 0.24 and -0.16 eÅ^{-3}, respectively. Final fractional atomic coordinates and isotropic thermal parameters, bond distances and angles are listed in Tables 7.1/7.2, 7.3 and 7.4, respectively. The asymmetric unit is shown in Figure 2.6 (Section 2.2), along with the labelling scheme employed.

---

i G.M. Sheldrick, SHELX86, a computer program for crystal structure determination, University of Göttingen, **1986**.

ii G.M. Sheldrick, SHELX76, a computer program for crystal structure determination, University of Cambridge, **1976**.

TABLE 7.1 : Fractional atomic co-ordinates ($x10^4$) and equivalent isotropic temperature factors ($Å^2 \times 10^3$) for $[Mo(\eta^2\text{-}MeC_2Ph)(dpps)(\eta\text{-}C_5H_5)][BF_4]$ **1**.

Atom	x	y	z	U
Mo(1)	3478(1)	1873	1860	41
P(1)	1878(1)	1383(1)	1100(1)	44(1)
C(1)	2586(7)	1747(8)	3005(4)	72(4)
C(2)	2456(8)	2670(8)	2709(4)	80(4)
C(3)	3446(11)	3154(7)	2734(4)	95(4)
C(4)	4169(7)	2463(9)	3050(4)	81(4)
C(5)	3620(8)	1608(6)	3218(3)	72(4)
C(6)	4515(6)	497(5)	1916(4)	55(3)
C(7)	3490(6)	200(5)	1671(3)	49(3)
C(8)	3176(5)	-99(5)	864(4)	50(3)
C(9)	3627(6)	-886(6)	505(4)	82(3)
C(10)	3281(7)	-1127(7)	-233(5)	110(5)
C(11)	2478(7)	-609(7)	-607(5)	89(4)
C(12)	2007(6)	164(6)	-255(4)	66(3)
C(13)	2346(5)	416(5)	492(3)	47(2)
C(14)	842(5)	779(5)	1624(3)	45(2)
C(15)	785(5)	-239(5)	1696(4)	61(3)
C(16)	34(6)	-669(6)	2133(5)	81(3)
C(17)	-656(6)	-82(7)	2520(5)	84(4)
C(18)	-609(6)	934(7)	2454(4)	76(4)
C(19)	122(6)	1359(5)	2008(4)	65(3)
C(20)	1104(5)	2256(5)	517(4)	50(3)
C(21)	162(6)	1945(6)	128(4)	72(3)
C(22)	-428(7)	2597(8)	-324(5)	89(4)
C(23)	-83(8)	3567(8)	-394(5)	96(4)
C(24)	834(6)	3887(6)	-15(5)	80(4)
C(25)	1422(5)	3220(6)	448(3)	59(3)
C(26)	3887(5)	2340(5)	819(3)	49(2)
C(27)	4627(5)	2587(5)	1335(3)	44(2)
C(28)	5648(5)	3077(5)	1391(3)	50(2)
C(29)	6425(6)	2801(5)	1937(4)	61(3)
C(30)	7421(6)	3210(7)	1946(5)	78(3)
C(31)	7664(7)	3885(7)	1405(6)	96(5)
C(32)	6921(8)	4181(7)	866(5)	94(4)
C(33)	5913(6)	3786(5)	854(4)	65(3)
C(34)	3776(6)	2398(6)	-37(3)	79(3)
B(1)	3215(9)	5725(10)	1368(7)	83(5)
F(1)	2452(9)	5205(9)	993(5)	130(5)
F(2)	4152(7)	5692(15)	1120(6)	175(7)
F(3)	2798(12)	6695(7)	1368(5)	159(6)
F(4)	3243(4)	5498(5)	2117(3)	138(3)

TABLE 7.2 : Hydrogen fractional atomic co-ordinates ($x10^4$) and isotropic temperature factors ($Å^2 x10^3$) for $[Mo(\eta^2\text{-}MeC_2Ph)(dpps)(\eta\text{-}C_5H_5)][BF_4]$ **1**.

Atom	x	y	z	U
F(12)	3484(28)	4867(21)	945(14)	171(13)
F(13)	2345(18)	5929(24)	1095(13)	115(9)
F(23)	3861(24)	6381(18)	1170(13)	108(8)
H(11)	2032(7)	1267(8)	3056(4)	86(5)
H(21)	1797(8)	2949(8)	2514(4)	86(5)
H(31)	3593(11)	3817(7)	2569(4)	86(5)
H(41)	4918(7)	2565(9)	3135(4)	86(5)
H(51)	3921(8)	1018(6)	3447(3)	86(5)
H(91)	4179(6)	-1267(6)	763(4)	86(5)
H(101)	3610(7)	-1667(7)	-488(5)	86(5)
H(111)	2248(7)	-790(7)	-1118(5)	86(5)
H(121)	1447(6)	532(6)	-516(4)	86(5)
H(151)	1273(5)	-653(5)	1439(4)	86(5)
H(161)	-10(6)	-1379(6)	2169(5)	86(5)
H(171)	-1167(6)	-383(7)	2833(5)	86(5)
H(181)	-1089(6)	1344(7)	2720(4)	86(5)
H(191)	141(6)	2069(5)	1958(4)	86(5)
H(211)	-73(6)	1272(6)	179(4)	86(5)
H(221)	-1071(7)	2380(8)	-589(5)	86(5)
H(231)	-491(8)	4023(8)	-711(5)	86(5)
H(241)	1068(6)	4560(6)	-67(5)	86(5)
H(251)	2057(5)	3442(6)	721(3)	86(5)
H(291)	6265(6)	2317(5)	2316(4)	86(5)
H(301)	7947(6)	3020(7)	2333(5)	86(5)
H(311)	8368(7)	4154(7)	1404(6)	86(5)
H(321)	7097(8)	4666(7)	493(5)	86(5)
H(331)	5390(6)	4000(5)	473(4)	86(5)
H(341)	3099(6)	2136(6)	-210(3)	86(5)
H(342)	4329(6)	2018(6)	-252(3)	86(5)
H(343)	3827(6)	3078(6)	-194(3)	86(5)
H(61)	4844(47)	332(46)	2401(19)	86(5)
H(62)	5035(38)	552(51)	1547(28)	86(5)
H(71)	3073(43)	-106(45)	2043(28)	86(5)

TABLE 7.3 : Bond lengths (Å) for [Mo(η^2-MeC_2Ph)(dpps)(η-C_5H_5)][BF_4] **1**.

Atom	Bond Length	Atom	Bond Length
P(1)-Mo(1)	2.455(4)	C(1)-Mo(1)	2.362(9)
C(2)-Mo(1)	2.290(9)	C(3)-Mo(1)	2.310(9)
C(4)-Mo(1)	2.359(8)	C(5)-Mo(1)	2.409(8)
C(6)-Mo(1)	2.269(9)	C(7)-Mo(1)	2.278(9)
C(26)-Mo(1)	2.026(8)	C(27)-Mo(1)	2.005(8)
Mo(1)-P(1)	2.455(4)	C(13)-P(1)	1.803(8)
C(14)-P(1)	1.830(8)	C(20)-P(1)	1.811(8)
Mo(1)-C(1)	2.362(9)	C(2)-C(1)	1.355(11)
C(3)-C(1)	2.248(14)	C(4)-C(1)	2.218(13)
C(5)-C(1)	1.353(11)	Mo(1)-C(2)	2.290(9)
C(1)-C(2)	1.355(11)	C(3)-C(2)	1.409(12)
C(4)-C(2)	2.232(14)	C(5)-C(2)	2.207(13)
Mo(1)-C(3)	2.310(9)	C(1)-C(3)	2.248(14)
C(2)-C(3)	1.409(12)	C(4)-C(3)	1.397(12)
C(5)-C(3)	2.256(14)	Mo(1)-C(4)	2.359(8)
C(1)-C(4)	2.218(13)	C(2)-C(4)	2.232(14)
C(3)-C(4)	1.397(12)	C(5)-C(4)	1.385(11)
Mo(1)-C(5)	2.409(8)	C(1)-C(5)	1.353(11)
C(2)-C(5)	2.207(13)	C(3)-C(5)	2.256(14)
C(4)-C(5)	1.385(11)	Mo(1)-C(6)	2.269(9)
C(7)-C(6)	1.401(10)	Mo(1)-C(7)	2.277(9)
C(6)-C(7)	1.401(10)	C(8)-C(7)	1.506(10)
C(7)-C(8)	1.506(10)	C(9)-C(8)	1.373(9)
C(13)-C(8)	1.392(9)	C(8)-C(9)	1.373(9)
C(10)-C(9)	1.384(10)	C(9)-C(10)	1.384(10)
C(11)-C(10)	1.370(11)	C(10)-C(11)	1.370(11)
C(12)-C(11)	1.365(10)	C(11)-C(12)	1.365(10)
C(13)-C(12)	1.399(9)	P(1)-C(13)	1.803(8)
C(8)-C(13)	1.392(9)	C(12)-C(13)	1.399(9)
P(1)-C(14)	1.830(8)	C(15)-C(14)	1.380(9)
C(19)-C(14)	1.399(9)	C(14)-C(15)	1.380(9)
C(16)-C(15)	1.379(10)	C(15)-C(16)	1.379(10)
C(17)-C(16)	1.381(11)	C(16)-C(17)	1.381(11)
C(18)-C(17)	1.374(11)	C(17)-C(18)	1.374(11)
C(19)-C(18)	1.368(10)	C(14)-C(19)	1.399(9)
C(18)-C(19)	1.368(10)	P(1)-C(20)	1.811(8)
C(21)-C(20)	1.405(10)	C(25)-C(20)	1.366(9)
C(20)-C(21)	1.405(10)	C(22)-C(21)	1.376(11)
C(21)-C(22)	1.376(11)	C(23)-C(22)	1.385(12)
C(22)-C(23)	1.385(12)	C(24)-C(23)	1.375(11)
C(23)-C(24)	1.375(11)	C(25)-C(24)	1.399(10)
C(20)-C(25)	1.366(9)	C(24)-C(25)	1.399(10)
Mo(1)-C(26)	2.026(8)	C(27)-C(26)	1.311(9)
C(34)-C(26)	1.503(10)	Mo(1)-C(27)	2.005(8)
C(26)-C(27)	1.311(9)	C(28)-C(27)	1.447(9)
C(27)-C(28)	1.447(9)	C(29)-C(28)	1.388(9)
C(33)-C(28)	1.395(10)	C(28)-C(29)	1.388(9)
C(30)-C(29)	1.373(11)	C(29)-C(30)	1.373(11)
C(31)-C(30)	1.361(11)	C(30)-C(31)	1.361(11)
C(32)-C(31)	1.357(12)	C(31)-C(32)	1.357(12)
C(33)-C(32)	1.379(11)	C(28)-C(33)	1.395(10)
C(32)-C(33)	1.379(11)	C(26)-C(34)	1.503(10)

TABLE 7.3 cont.

Atom	Bond Length	Atom	Bond Length
F(1)-B(1)	1.337(14)	F(2)-B(1)	1.284(14)
F(3)-B(1)	1.409(16)	F(4)-B(1)	1.349(12)
F(12)-B(1)	1.424(29)	F(13)-B(1)	1.208(24)
F(23)-B(1)	1.263(27)	B(1)-F(1)	1.337(14)
F(12)-F(1)	1.388(30)	F(13)-F(1)	1.002(26)
B(1)-F(2)	1.284(14)	F(12)-F(2)	1.419(30)
F(23)-F(2)	1.004(23)	B(1)-F(3)	1.409(16)
F(13)-F(3)	1.262(29)	F(23)-F(3)	1.467(29)
B(1)-F(4)	1.349(12)	B(1)-F(12)	1.424(29)
F(1)-F(12)	1.388(30)	F(2)-F(12)	1.419(30)
F(13)-F(12)	2.056(39)	B(1)-F(13)	1.208(24)
F(1)-F(13)	1.002(26)	F(3)-F(13)	1.262(29)
F(12)-F(13)	2.056(39)	F(23)-F(13)	2.008(38)
B(1)-F(23)	1.263(27)	F(2)-F(23)	1.004(23)
F(3)-F(23)	1.467(29)	F(13)-F(23)	2.008(38)

TABLE 7.4 : Bond angles (°)for [Mo(η^2-MeC_2Ph)(dpps)(η-C_5H_5)][BF_4] **1**.

Atom	Angle	Atom	Angle
C(1)-Mo(1)-P(1)	91.6(3)	C(2)-Mo(1)-P(1)	90.2(3)
C(2)-Mo(1)-C(1)	33.8(3)	C(3)-Mo(1)-P(1)	121.3(5)
C(3)-Mo(1)-C(1)	57.5(4)	C(3)-Mo(1)-C(2)	35.7(3)
C(4)-Mo(1)-P(1)	145.9(2)	C(4)-Mo(1)-C(1)	56.0(4)
C(4)-Mo(1)-C(2)	57.4(4)	C(4)-Mo(1)-C(3)	34.8(3)
C(5)-Mo(1)-P(1)	121.0(4)	C(5)-Mo(1)-C(1)	32.9(2)
C(5)-Mo(1)-C(2)	56.0(4)	C(5)-Mo(1)-C(3)	57.1(4)
C(5)-Mo(1)-C(4)	33.8(2)	C(6)-Mo(1)-P(1)	105.1(3)
C(6)-Mo(1)-C(1)	101.8(4)	C(6)-Mo(1)-C(2)	134.3(3)
C(6)-Mo(1)-C(3)	127.7(5)	C(6)-Mo(1)-C(4)	92.9(4)
C(6)-Mo(1)-C(5)	79.8(3)	C(7)-Mo(1)-P(1)	70.5(3)
C(7)-Mo(1)-C(1)	93.4(4)	C(7)-Mo(1)-C(2)	124.5(5)
C(7)-Mo(1)-C(3)	146.7(3)	C(7)-Mo(1)-C(4)	117.2(4)
C(7)-Mo(1)-C(5)	89.8(3)	C(7)-Mo(1)-C(6)	35.9(2)
C(26)-Mo(1)-P(1)	80.5(3)	C(26)-Mo(1)-C(1)	161.1(3)
C(26)-Mo(1)-C(2)	128.4(4)	C(26)-Mo(1)-C(3)	112.5(4)
C(26)-Mo(1)-C(4)	126.5(4)	C(26)-Mo(1)-C(5)	158.5(3)
C(26)-Mo(1)-C(6)	96.8(4)	C(26)-Mo(1)-C(7)	99.9(3)
C(27)-Mo(1)-P(1)	118.3(3)	C(27)-Mo(1)-C(1)	144.6(3)
C(27)-Mo(1)-C(2)	121.4(5)	C(27)-Mo(1)-C(3)	89.2(4)
C(27)-Mo(1)-C(4)	90.1(4)	C(27)-Mo(1)-C(5)	120.6(4)
C(27)-Mo(1)-C(6)	88.9(4)	C(27)-Mo(1)-C(7)	113.4(3)
C(27)-Mo(1)-C(26)	38.0(2)	C(13)-P(1)-Mo(1)	103.3(3)
C(14)-P(1)-Mo(1)	115.9(3)	C(14)-P(1)-C(13)	104.0(4)
C(20)-P(1)-Mo(1)	122.5(3)	C(20)-P(1)-C(13)	108.6(4)

TABLE 7.4 cont.

Atom	Angle	Atom	Angle
C(20)-P(1)-C(14)	101.1(4)	C(2)-C(1)-Mo(1)	70.2(5)
C(3)-C(1)-Mo(1)	60.1(4)	C(3)-C(1)-C(2)	36.4(5)
C(4)-C(1)-Mo(1)	61.9(4)	C(4)-C(1)-C(2)	72.8(7)
C(4)-C(1)-C(3)	36.5(3)	C(5)-C(1)-Mo(1)	75.4(5)
C(5)-C(1)-C(2)	109.2(9)	C(5)-C(1)-C(3)	72.8(6)
C(5)-C(1)-C(4)	36.4(5)	C(1)-C(2)-Mo(1)	76.0(5)
C(3)-C(2)-Mo(1)	72.9(6)	C(3)-C(2)-C(1)	108.8(9)
C(4)-C(2)-Mo(1)	62.9(4)	C(4)-C(2)-C(1)	71.7(6)
C(4)-C(2)-C(3)	37.1(5)	C(5)-C(2)-Mo(1)	64.7(4)
C(5)-C(2)-C(1)	35.4(4)	C(5)-C(2)-C(3)	73.5(7)
C(5)-C(2)-C(4)	36.3(3)	C(1)-C(3)-Mo(1)	62.4(4)
C(2)-C(3)-Mo(1)	71.4(5)	C(2)-C(3)-C(1)	34.8(4)
C(4)-C(3)-Mo(1)	74.5(6)	C(4)-C(3)-C(1)	70.6(6)
C(4)-C(3)-C(2)	105.4(9)	C(5)-C(3)-Mo(1)	63.7(4)
C(5)-C(3)-C(1)	35.0(3)	C(5)-C(3)-C(2)	69.7(6)
C(5)-C(3)-C(4)	35.6(5)	C(1)-C(4)-Mo(1)	62.1(3)
C(2)-C(4)-Mo(1)	59.8(4)	C(2)-C(4)-C(1)	35.4(3)
C(3)-C(4)-Mo(1)	70.7(5)	C(3)-C(4)-C(1)	72.9(7)
C(3)-C(4)-C(2)	37.5(5)	C(5)-C(4)-Mo(1)	75.1(5)
C(5)-C(4)-C(1)	35.4(4)	C(5)-C(4)-C(2)	70.8(6)
C(5)-C(4)-C(3)	108.3(9)	C(1)-C(5)-Mo(1)	71.6(5)
C(2)-C(5)-Mo(1)	59.3(3)	C(2)-C(5)-C(1)	35.4(5)
C(3)-C(5)-Mo(1)	59.3(3)	C(3)-C(5)-C(1)	72.2(6)
C(3)-C(5)-C(2)	36.8(3)	C(4)-C(5)-Mo(1)	71.1(5)
C(4)-C(5)-C(1)	108.2(9)	C(4)-C(5)-C(2)	72.8(6)
C(4)-C(5)-C(3)	36.0(5)	C(7)-C(6)-Mo(1)	72.4(5)
C(6)-C(7)-Mo(1)	71.7(5)	C(8)-C(7)-Mo(1)	113.5(5)
C(8)-C(7)-C(6)	124.0(7)	C(9)-C(8)-C(7)	122.9(7)
C(13)-C(8)-C(7)	117.6(7)	C(13)-C(8)-C(9)	119.3(7)
C(10)-C(9)-C(8)	119.5(8)	C(11)-C(10)-C(9)	121.3(9)
C(12)-C(11)-C(10)	120.1(8)	C(13)-C(12)-C(11)	119.4(8)
C(8)-C(13)-P(1)	110.1(5)	C(12)-C(13)-P(1)	129.5(6)
C(12)-C(13)-C(8)	120.4(7)	C(15)-C(14)-P(1)	122.0(6)
C(19)-C(14)-P(1)	119.7(6)	C(19)-C(14)-C(15)	118.2(7)
C(16)-C(15)-C(14)	120.6(8)	C(17)-C(16)-C(15)	120.3(8)
C(18)-C(17)-C(16)	119.8(9)	C(19)-C(18)-C(17)	119.9(9)
C(18)-C(19)-C(14)	121.2(8)	C(21)-C(20)-P(1)	120.0(7)
C(25)-C(20)-P(1)	120.9(6)	C(25)-C(20)-C(21)	119.1(8)
C(22)-C(21)-C(20)	120.7(9)	C(23)-C(22)-C(21)	119.3(9)
C(24)-C(23)-C(22)	120.9(9)	C(25)-C(24)-C(23)	119.3(9)
C(24)-C(25)-C(20)	120.7(7)	C(27)-C(26)-Mo(1)	70.2(5)
C(34)-C(26)-Mo(1)	154.6(5)	C(34)-C(26)-C(27)	134.7(6)
C(26)-C(27)-Mo(1)	71.9(5)	C(28)-C(27)-Mo(1)	148.4(5)
C(28)-C(27)-C(26)	139.7(6)	C(29)-C(28)-C(27)	121.4(7)
C(33)-C(28)-C(27)	120.8(7)	C(33)-C(28)-C(29)	117.6(7)
C(30)-C(29)-C(28)	121.0(8)	C(31)-C(30)-C(29)	120.0(9)
C(32)-C(31)-C(30)	120.6(10)	C(33)-C(32)-C(31)	120.1(9)
C(32)-C(33)-C(28)	120.6(8)	F(2)-B(1)-F(1)	118.0(14)
F(3)-B(1)-F(1)	103.1(11)	F(3)-B(1)-F(2)	112.6(15)
F(4)-B(1)-F(1)	110.0(11)	F(4)-B(1)-F(2)	110.2(11)
F(4)-B(1)-F(3)	101.6(11)	F(12)-B(1)-F(1)	60.2(15)
F(12)-B(1)-F(2)	63.0(15)	F(12)-B(1)-F(3)	148.4(14)

TABLE 7.4 cont.

Atom	Angle	Atom	Angle
F(12)-B(1)-F(4)	109.2(15)	F(13)-B(1)-F(1)	46.0(13)
F(13)-B(1)-F(2)	135.3(15)	F(13)-B(1)-F(3)	57.1(16)
F(13)-B(1)-F(4)	114.5(15)	F(13)-B(1)-F(12)	102.4(21)
F(23)-B(1)-F(1)	133.7(14)	F(23)-B(1)-F(2)	46.4(11)
F(23)-B(1)-F(3)	66.3(15)	F(23)-B(1)-F(4)	116.3(14)
F(23)-B(1)-F(12)	104.4(20)	F(23)-B(1)-F(13)	108.7(21)
F(12)-F(1)-B(1)	63.0(14)	F(13)-F(1)-B(1)	60.2(16)
F(13)-F(1)-F(12)	117.8(23)	F(12)-F(2)-B(1)	63.4(14)
F(23)-F(2)-B(1)	65.7(18)	F(23)-F(2)-F(12)	121.7(25)
F(13)-F(3)-B(1)	53.4(12)	F(23)-F(3)-B(1)	52.1(11)
F(23)-F(3)-F(13)	94.4(18)	F(1)-F(12)-B(1)	56.7(14)
F(2)-F(12)-B(1)	53.7(13)	F(2)-F(12)-F(1)	106.3(22)
F(13)-F(12)-B(1)	35.0(11)	F(13)-F(12)-F(1)	25.5(10)
F(13)-F(12)-F(2)	80.8(17)	F(1)-F(13)-B(1)	73.8(20)
F(3)-F(13)-B(1)	69.5(17)	F(3)-F(13)-F(1)	143.2(26)
F(12)-F(13)-B(1)	42.6(13)	F(12)-F(13)-F(1)	36.7(14)
F(12)-F(13)-F(3)	108.1(18)	F(23)-F(13)-B(1)	36.6(12)
F(23)-F(13)-F(1)	99.7(20)	F(23)-F(13)-F(3)	46.8(12)
F(23)-F(13)-F(12)	63.1(12)	F(2)-F(23)-B(1)	67.9(18)
F(3)-F(23)-B(1)	61.6(16)	F(3)-F(23)-F(2)	129.2(28)
F(13)-F(23)-B(1)	34.8(12)	F(13)-F(23)-F(2)	93.9(22)
F(13)-F(23)-F(3)	38.8(11)		

7.2 Crystal Structure Determination of [Mo{η^2,η^3(5e)-*S*-$CH_2CHC(Ph)CH{=}CH$-o-$C_6H_4PPh_2$}(η-C_5H_5)] 2.

A crystal of approximate dimensions 0.3 x 0.3 x 0.07 mm was used for data collection.

Crystal Data : $C_{34}H_{29}PMo$, M = 564.5, orthorhombic, a = 10.748(1), b = 24.315(4), c = 20.348(3) Å, U = 5317.7 Å^3, space group *P*bca, Z = 8, D_c = 1.41 gcm^{-3}, μ(Mo-K_α) = 5.60 cm^{-1}, F(000) = 2320. Data were measured at room temperature on a CAD4 automatic four-circle diffractometer in the range $2 \leq \theta \leq 24°$. 4651 reflections were collected of which 1764 were unique with $I \geq 2\sigma(I)$. Data were corrected for Lorentz and polarisation effects but not for X-ray absorption effects. The structure was solved by Patterson methods and refined using the SHELX[i,ii] suite of programs. In the final least squares cycles all atoms were allowed to vibrate anisotropically. The cyclopentadienyl moiety and phenyl groups (except the one containing carbons 18-23) were refined as rigid groups. Hydrogen atoms were included at calculated positions except for H241, H251, H271, H281 and H282. These hydrogens were located after early refinements and refined at a fixed distance of 0.98Å from the relevant parent atoms. Final residues after 6 cycles of least squares were R = 0.0456, R_w =0.0378, for a weighting scheme of w = 2.7485/[σ^2(F) +0.000466(F)^2]. Max. final shift/esd was 0.010. The max. and min. residual densities were 0.19 and -0.30 eÅ^{-3}, respectively. Final fractional atomic coordinates and isotropic thermal parameters, bond distances and angles are listed in Tables 7.5/7.6, 7.7 and 7.8, respectively. The asymmetric unit is shown in Figure 2.8 (Section 2.2), along with the labelling scheme employed.

TABLE 7.5 : Fractional atomic coordinates and thermal parameters (Å) for [Mo{η^2,η^3(5e)-*S*-$CH_2CHC(Ph)CH{=}CH$-o-$C_6H_4PPh_2$}(η-C_5H_5)] **2**.

Atom	x	y	z	Uiso or Ueq (***)	
Mo1	0.24031(7)	0.20312(3)	0.13398(3)	0.0323(3)	***
P1	0.1827(2)	0.1095(1)	0.1048(1)	0.035(1)	***
C1	0.1882(9)	0.2661(4)	0.0501(5)	0.049(6)	***
C2	0.2110(9)	0.2953(4)	0.1069(5)	0.058(7)	***
C3	0.1208(12)	0.2796(5)	0.1553(5)	0.069(8)	***
C4	0.0445(9)	0.2407(5)	0.1244(7)	0.075(9)	***
C5	0.0873(11)	0.2319(4)	0.0608(6)	0.058(8)	***
C7	0.0106(5)	0.0946(2)	0.0018(3)	0.053(7)	***
C8	-0.1086(5)	0.0932(2)	-0.0253(3)	0.068(8)	***
C9	-0.2126(5)	0.0990(2)	0.0151(3)	0.068(8)	***
C10	-0.1973(5)	0.1060(2)	0.0827(3)	0.068(8)	***
C11	-0.0781(5)	0.1074(2)	0.1098(3)	0.060(7)	***
C6	0.0258(5)	0.1016(2)	0.0693(3)	0.039(5)	***
C13	0.1088(6)	0.0542(3)	0.2190(3)	0.066(7)	***
C14	0.1083(6)	0.0110(3)	0.2642(3)	0.083(9)	***
C15	0.1868(6)	-0.0340(3)	0.2550(3)	0.091(10)	***
C16	0.2659(6)	-0.0359(3)	0.2007(3)	0.081(8)	***
C17	0.2664(6)	0.0073(3)	0.1555(3)	0.055(6)	***
C12	0.1878(6)	0.0523(3)	0.1647(3)	0.042(5)	***
C18	0.2890(7)	0.0896(3)	0.0391(4)	0.035(5)	***
C19	0.2805(7)	0.0415(3)	0.0014(4)	0.040(6)	***
C20	0.3580(9)	0.0340(4)	-0.0516(5)	0.053(7)	***
C21	0.4463(8)	0.0742(4)	-0.0680(4)	0.046(6)	***
C22	0.4569(8)	0.1214(3)	-0.0300(4)	0.037(5)	***
C23	0.3810(7)	0.1288(3)	0.0249(4)	0.030(5)	***
C24	0.3982(7)	0.1775(4)	0.0694(4)	0.031(5)	***
C25	0.4202(7)	0.1656(3)	0.1378(5)	0.037(5)	***
C26	0.4219(8)	0.2156(3)	0.1795(4)	0.037(5)	***
C27	0.3342(9)	0.2156(4)	0.2306(4)	0.044(6)	***
C28	0.2544(11)	0.1698(4)	0.2391(4)	0.052(6)	***
C30	0.6176(5)	0.2541(2)	0.1302(3)	0.048(6)	***
C31	0.6996(5)	0.2975(2)	0.1187(3)	0.059(6)	***
C32	0.6731(5)	0.3498(2)	0.1431(3)	0.070(8)	***
C33	0.5645(5)	0.3587(2)	0.1791(3)	0.064(7)	***
C34	0.4824(5)	0.3153(2)	0.1906(3)	0.052(6)	***
C29	0.5090(5)	0.2630(2)	0.1662(3)	0.040(6)	***
H241	0.4408(58)	0.2079(20)	0.0476(32)	0.031(10)	
H251	0.4384(62)	0.1286(14)	0.1535(32)	0.031(10)	
H271	0.3142(64)	0.2486(17)	0.2555(28)	0.031(10)	
H281	0.2884(60)	0.1324(14)	0.2433(34)	0.031(10)	
H282	0.1836(44)	0.1739(28)	0.2687(28)	0.031(10)	

TABLE 7.6 : Fractional atomic coordinates for the hydrogen atoms of for [Mo{η^2,η^3(5e)-*S*-$CH_2CHC(Ph)CH{=}CH$-o-$C_6H_4PPh_2$}(η-C_5H_5)] **2**.

Atom	x	y	z
H11	0.2401	0.2693	0.0048
H21	0.2846	0.3250	0.1137
H31	0.1135	0.2946	0.2052
H41	-0.0351	0.2208	0.1465
H51	0.0485	0.2032	0.0258
H71	0.0911	0.0901	-0.0296
H81	-0.1204	0.0878	-0.0776
H91	-0.3048	0.0979	-0.0058
H101	-0.2778	0.1105	0.1140
H111	-0.0663	0.1128	0.1621
H131	0.0479	0.0890	0.2262
H141	0.0470	0.0124	0.3062
H151	0.1864	-0.0675	0.2900
H161	0.3267	-0.0707	0.1936
H171	0.3276	0.0059	0.1135
H191	0.2129	0.0104	0.0139
H201	0.3511	-0.0031	-0.0807
H211	0.5058	0.0685	-0.1102
H221	0.5242	0.1526	-0.0430
H301	0.6381	0.2136	0.1113
H311	0.7837	0.2905	0.0908
H321	0.7366	0.3833	0.1341
H331	0.5439	0.3992	0.1979
H341	0.3983	0.3222	0.2185

TABLE 7.7 : Bond lengths (Å) for [Mo{η^2,η^3(5e)-*S*-$CH_2CHC(Ph)CH{=}CH$-o-$C_6H_4PPh_2$} (η-C_5H_5)] **2**.

Atom	Bond Length	Atom	Bond Length
Mo1-P1	2.433(3)	Mo1-C1	2.361(9)
Mo1-C2	2.329(9)	Mo1-C3	2.302(9)
Mo1-C4	2.303(9)	Mo1-C5	2.326(10)
Mo1-C24	2.235(8)	Mo1-C25	2.139(8)
Mo1-C26	2.182(8)	Mo1-C27	2.231(9)
Mo1-C28	2.292(8)	P1-C6	1.844(7)
P1-C12	1.850(7)	P1-C18	1.824(8)
C1-C2	1.380(12)	C1-C5	1.383(13)
C2-C3	1.435(14)	C3-C4	1.401(14)
C4-C5	1.390(14)	C7-C8	1.395(1)
C7-C6	1.395(1)	C8-C9	1.395(1)
C9-C10	1.395(1)	C10-C11	1.395(1)
C11-C6	1.395(1)	C13-C14	1.395(1)
C13-C12	1.395(1)	C14-C15	1.395(1)
C15-C16	1.395(1)	C16-C17	1.395(1)
C17-C12	1.395(1)	C18-C19	1.403(11)
C18-C23	1.402(10)	C19-C20	1.374(11)
C20-C21	1.403(12)	C21-C22	1.389(11)
C22-C23	1.396(10)	C23-C24	1.502(11)
C24-C25	1.439(11)	C24-H241	0.977(19)
C25-C26	1.484(11)	C25-H251	0.974(19)
C26-C27	1.403(12)	C26-C29	1.509(10)
C27-C28	1.416(13)	C27-H271	0.973(19)
C28-H281	0.985(19)	C28-H282	0.976(19)
C30-C31	1.395(1)	C30-C29	1.395(1)
C31-C32	1.395(1)	C32-C33	1.395(1)
C33-C34	1.395(1)	C34-C29	1.395(1)

TABLE 7.8 : Bond angles (°)for [Mo{η^2,η^3(5e)-*S*-$CH_2CHC(Ph)CH$=CH-o-$C_6H_4PPh_2$} (η-C_5H_5)] **2**.

Atom	Angle	Atom	Angle
C1-Mo1-P1	111.7(3)	C2-Mo1-P1	143.9(3)
C2-Mo1-C1	34.2(3)	C3-Mo1-P1	131.3(4)
C3-Mo1-C1	58.7(3)	C3-Mo1-C2	36.1(3)
C4-Mo1-P1	96.8(3)	C4-Mo1-C1	57.6(4)
C4-Mo1-C2	58.3(3)	C4-Mo1-C3	35.4(4)
C5-Mo1-P1	86.9(3)	C5-Mo1-C1	34.3(3)
C5-Mo1-C2	57.6(3)	C5-Mo1-C3	58.9(4)
C5-Mo1-C4	34.9(4)	C24-Mo1-P1	77.8(2)
C24-Mo1-C1	86.3(3)	C24-Mo1-C2	103.4(4)
C24-Mo1-C3	139.5(4)	C24-Mo1-C4	139.0(4)
C24-Mo1-C5	104.2(4)	C25-Mo1-P1	80.8(2)
C25-Mo1-C1	121.1(4)	C25-Mo1-C2	122.8(3)
C25-Mo1-C3	147.4(4)	C25-Mo1-C4	176.7(5)
C25-Mo1-C5	142.2(4)	C25-Mo1-C24	38.3(3)
C26-Mo1-P1	117.5(2)	C26-Mo1-C1	115.4(3)
C26-Mo1-C2	95.0(3)	C26-Mo1-C3	107.9(4)
C26-Mo1-C4	143.0(4)	C26-Mo1-C5	149.6(4)
C26-Mo1-C24	67.0(3)	C26-Mo1-C25	40.1(3)
C12-P1-C6	102.0(3)	C18-P1-C6	105.0(3)
C18-P1-C12	105.4(3)	C5-C1-C2	108(1)
C3-C2-C1	108.6(9)	C4-C3-C2	105.5(9)
C5-C4-C3	109(1)	C4-C5-C1	108(1)
C6-C7-C8	120.0(1)	C9-C8-C7	120.0(1)
C10-C9-C8	120.0(1)	C11-C10-C9	120.0(1)
C6-C11-C10	120.0(1)	C7-C6-P1	120.4(2)
C11-C6-P1	119.4(2)	C11-C6-C7	120.0(1)
C12-C13-C14	120.0(1)	C15-C14-C13	120.0(1)
C16-C15-C14	120.0(1)	C17-C16-C15	120.0(1)
C12-C17-C16	120.0(1)	C13-C12-P1	118.7(2)
C17-C12-P1	121.3(2)	C17-C12-C13	120.0(1)
C19-C18-P1	125.6(6)	C23-C18-P1	114.4(6)
C23-C18-C19	120.0(8)	C20-C19-C18	120.1(8)
C21-C20-C19	120.2(9)	C22-C21-C20	120.0(8)
C23-C22-C21	120.2(8)	C22-C23-C18	119.4(8)
C24-C23-C18	119.9(7)	C24-C23-C22	120.8(8)
C25-C24-C23	116.4(8)	H241-C24-C23	112(4)
H241-C24-C25	121(4)	C26-C25-C24	113.0(7)
H251-C25-C24	122(4)	H251-C25-C26	124(4)
C27-C26-C25	114.6(8)	C29-C26-C25	122.1(7)
C29-C26-C27	123.3(7)	C28-C27-C26	119.8(8)
H271-C27-C26	122(4)	H271-C27-C28	117(4)
H281-C28-C27	121(4)	H282-C28-C27	118(4)
H282-C28-H281	109(6)	C29-C30-C31	120.0(1)
C32-C31-C30	120.0(1)	C33-C32-C31	120.0(1)
C34-C33-C32	120.0(1)	C29-C34-C33	120.0(1)
C30-C29-C26	119.6(4)	C34-C29-C26	120.4(4)
C34-C29-C30	120.0(1)		

7.3 Crystal Structure Determination of $Mo\{\eta^2,\eta^2(\mu_{Mo,C}\text{-}H)\text{-}CH_3CHC(Ph)CH{=}CH\text{-}o\text{-}C_6H_4PPh_2\}(\eta\text{-}C_5H_5)][BF_4]$ 3.

A crystal of approximate dimensions 0.3 x 0.3 x 0.2 mm was used for data collection.

Crystal Data : $C_{34}H_{30}PBF_4Mo.0.46\ CH_2Cl_2$, M = 691.0, monoclinic, a = 13.705(2), b = 12.995(2), c = 18.040(3) Å, β = 109.49(1), U = 3028.7 Å^3, space group $P2_1/c$, Z = 4, D_c = 1.52 gcm^{-3}, μ(Mo-K_α) = 5.46 cm^{-1}, F(000) = 1496. Data were measured at room temperature on a CAD4 automatic four-circle diffractometer in the range $2\leq\theta\leq24°$. 5115 reflections were collected of which 3441 were unique with $I\geq2\sigma(I)$. Data were corrected for Lorentz and polarisation effects but not for X-ray absorption effects. The structure was solved by Patterson methods and refined using the SHELX[i,ii] suite of programs. In the final least squares cycles all atoms were allowed to vibrate anisotropically. Hydrogen atoms were included at calculated positions except on carbons 24-28, where the hydrogens were located in an advanced difference Fourier map and refined at a fixed distance of 1.04Å from the relevant parent atoms. H281, located on the terminal tertiary carbon of the organic fragment (C28) exhibited agostic bonding to the metal at a distance of 1.89Å.

The sample of crystals for X-ray analysis was grown from a pentane/ dichloromethane solution and as convergence proceeded it became clear that the lattice contained solvent. A chlorine atom with a refined occupancy factor of 0.91 presented itself proximate to a centre of inversion and 2.67(2)Å away from its symmetry generated nearest partner. This distance is not untypical of the Cl-Cl distance in dichloromethane, thus indicating the presence of 0.455 molecules of this solvent per molecule of complex. Not surprisingly, the associated solvent methylene group could not be located, although the remaining maxima in the electron density map subsequent to refinement, were in this region. Therefore, it is reasonable to expect that the contentious methylene exists, on average through the

lattice, as a smeared circle about the inversion centre with all points thereon equidistant from the symmetry related chlorines. Refinement was in 2 blocks (one each for the cation and anion) and residuals after 12 cycles of least squares were R = 0.0454, R_w =0.0489, for a weighting scheme of w = 2.1567/[σ^2(F) +0.000830(F)^2]. Max. final shift/esd was 0.050. The max. and min. residual densities were 0.51 and -0.39 eÅ^{-3}, respectively. Final fractional atomic coordinates and isotropic thermal parameters, bond distances and angles are listed in Tables 7.9/7.10, 7.11 and 7.12, respectively. The asymmetric unit is shown in Figure 2.22 (Section 2.3), along with the labelling scheme employed.

TABLE 7.9 : Fractional Coordinates ($x10^4$) and equivalent isotropic factors ($Å^2 \times 10^3$) for $Mo\{\eta^2,\eta^2(\mu_{Mo,C}\text{-}H)\text{-}CH_3CHC(Ph)CH{=}CH\text{-}o\text{-}C_6H_4PPh_2\}(\eta\text{-}C_5H_5)][BF_4]$ **3**.

Atom	x	y	z	U
Mo(1)	2489	1626	1275	35
P(1)	2647(1)	1830(1)	2691(1)	36
C(1)	3663(5)	1463(5)	649(4)	62(3)
C(2)	4217(5)	1691(7)	1425(5)	79(3)
C(3)	3926(6)	2709(7)	1573(4)	75(3)
C(4)	3233(6)	3079(5)	895(5)	69(3)
C(5)	3069(5)	2320(5)	320(3)	61(3)
C(6)	3708(4)	2613(4)	3334(3)	38(2)
C(7)	4687(4)	2174(5)	3604(4)	60(3)
C(8)	5514(5)	2722(5)	4077(4)	64(3)
C(9)	5396(5)	3716(5)	4276(4)	58(2)
C(10)	4441(5)	4175(5)	3986(4)	58(3)
C(11)	3589(5)	3616(4)	3508(3)	50(2)
C(12)	1457(4)	2291(4)	2830(3)	42(2)
C(13)	1052(4)	3238(5)	2544(3)	52(2)
C(14)	102(5)	3559(5)	2594(4)	62(3)
C(15)	-451(5)	2936(6)	2912(4)	68(3)
C(16)	-61(5)	1995(7)	3200(4)	73(3)
C(17)	886(5)	1655(5)	3156(4)	54(2)
C(18)	2955(4)	565(4)	3142(3)	39(2)
C(19)	3209(5)	392(5)	3943(3)	53(2)
C(20)	3608(5)	-548(5)	4253(3)	59(3)
C(21)	3758(5)	-1297(5)	3767(4)	59(2)
C(22)	3488(4)	-1133(4)	2961(3)	48(2)
C(23)	3073(4)	-200(4)	2642(3)	38(2)
C(24)	2729(4)	-4(4)	1787(3)	38(2)
C(25)	1656(4)	266(4)	1389(3)	39(2)
C(26)	1403(4)	440(4)	557(3)	41(2)
C(27)	979(4)	1410(5)	295(3)	52(2)
C(28)	668(5)	2116(5)	832(4)	56(2)
C(29)	1621(4)	-320(4)	11(3)	43(2)
C(30)	1730(4)	-1361(5)	218(3)	51(2)
C(31)	1906(4)	-2090(5)	-292(4)	55(3)
C(32)	1953(5)	-1783(6)	-1009(4)	65(3)
C(33)	1821(5)	-781(6)	-1222(4)	64(3)
C(34)	1669(5)	-42(5)	-723(3)	55(2)
Cl(1)	9270(5)	85(5)	5334(4)	262(5)
B(1)	7146(7)	833(8)	3205(6)	79(4)
F(1)	7630(6)	1707(5)	3465(6)	181(5)
F(2)	7777(4)	83(4)	3122(3)	123(3)
F(3)	6425(9)	965(12)	2608(7)	380(9)
F(4)	6786(8)	581(6)	3773(7)	239(7)

TABLE 7.10 : Hydrogen fractional atomic co-ordinates ($x10^4$) and isotropic temperature factors ($Å^2 x10^3$) for $Mo\{\eta^2,\eta^2(\mu_{Mo,C}\text{-}H)\text{-}CH_3CHC(Ph)CH{=}CH\text{-}o\text{-}C_6H_4PPh_2\}(\eta\text{-}C_5H_5)][BF_4]$ **3**.

	x	y	z	U
H(11)	3679(5)	826(5)	385(4)	66(3)
H(21)	4704(5)	1251(7)	1795(5)	66(3)
H(31)	4173(6)	3069(7)	2065(4)	66(3)
H(41)	2915(6)	3746(5)	825(5)	93(25)
H(51)	2624(5)	2385(5)	-217(3)	66(3)
H(71)	4787(4)	1482(5)	3457(4)	66(3)
H(81)	6185(5)	2408(5)	4272(4)	66(3)
H(91)	5977(5)	4091(5)	4616(4)	66(3)
H(101)	4360(5)	4879(5)	4115(4)	66(3)
H(111)	2924(5)	3941(4)	3301(3)	66(3)
H(131)	1419(4)	3682(5)	2303(3)	66(3)
H(141)	-160(5)	4229(5)	2404(4)	66(3)
H(151)	-1111(5)	3155(6)	2932(4)	66(3)
H(161)	-438(5)	1564(7)	3442(4)	66(3)
H(171)	1136(5)	982(5)	3344(4)	66(3)
H(191)	3119(5)	928(5)	4282(3)	66(3)
H(201)	3776(5)	-684(5)	4805(3)	66(3)
H(121)	4046(5)	-1948(5)	3985(4)	66(3)
H(221)	3595(4)	-1666(4)	2628(3)	66(3)
H(301)	1686(4)	-1577(5)	714(3)	66(3)
H(311)	1991(4)	-2803(5)	-145(4)	66(3)
H(321)	2082(5)	-2278(6)	-1360(4)	66(3)
H(331)	1834(5)	-578(6)	-1731(4)	66(3)
H(341)	1597(5)	667(5)	-882(3)	66(3)
H(241)	3127(39)	-465(38)	1516(30)	66(3)
H(251)	1097(33)	325(45)	1652(30)	66(3)
H(271)	899(46)	1687(40)	-263(17)	66(3)
H(281)	1311(30)	2420(42)	1274(25)	66(3)
H(282)	494(44)	2848(24)	593(32)	66(3)
H(283)	268(40)	1786(41)	1176(29)	66(3)

TABLE 7.11 : Bond lengths (Å) for Mo{η^2,η^2($\mu_{Mo,C}$-H)-$CH_3CHC(Ph)CH{=}CH$-o-$C_6H_4PPh_2$} (η-C_5H_5)][BF_4] **3**.

Atom	Bond Length	Atom	Bond Length
P(1)-Mo(1)	2.505(4)	C(1)-Mo(1)	2.263(10)
C(2)-Mo(1)	2.294(9)	C(3)-Mo(1)	2.333(10)
C(4)-Mo(1)	2.354(10)	C(5)-Mo(1)	2.308(9)
C(24)-Mo(1)	2.290(7)	C(25)-Mo(1)	2.151(7)
C(26)-Mo(1)	2.232(7)	C(27)-Mo(1)	2.246(5)
C(28)-Mo(1)	2.437(6)	H(281)-Mo(1)	1.915(48)
C(6)-P(1)	1.835(7)	C(12)-P(1)	1.831(8)
C(18)-P(1)	1.821(7)	C(2)-C(1)	1.383(11)
C(3)-C(1)	2.264(13)	C(4)-C(1)	2.264(12)
C(5)-C(1)	1.390(10)	C(3)-C(2)	1.433(13)
C(4)-C(2)	2.264(12)	C(5)-C(2)	2.242(11)
C(4)-C(3)	1.361(11)	C(5)-C(3)	2.230(11)
C(5)-C(4)	1.395(11)	C(7)-C(6)	1.388(9)
C(11)-C(6)	1.364(9)	C(8)-C(7)	1.369(9)
C(9)-C(8)	1.365(10)	C(10)-C(9)	1.373(10)
C(11)-C(10)	1.401(9)	C(13)-C(12)	1.378(9)
C(17)-C(12)	1.395(10)	C(14)-C(13)	1.398(11)
C(15)-C(14)	1.360(12)	C(16)-C(15)	1.365(12)
C(17)-C(16)	1.399(11)	C(19)-C(18)	1.387(8)
C(23)-C(18)	1.388(9)	C(20)-C(19)	1.379(9)
C(21)-C(20)	1.371(11)	C(22)-C(21)	1.392(10)
C(23)-C(22)	1.380(8)	C(24)-C(23)	1.478(8)
C(25)-C(24)	1.448(7)	C(26)-C(25)	1.442(8)
C(27)-C(26)	1.403(9)	C(29)-C(26)	1.493(9)
C(28)-C(27)	1.496(11)	C(30)-C(29)	1.398(9)
C(34)-C(29)	1.395(9)	C(31)-C(30)	1.397(10)
C(32)-C(31)	1.374(11)	C(33)-C(32)	1.353(11)
C(34)-C(33)	1.379(11)	Cl(1)-Cl(1a)	2.668(18)
F(1)-B(1)	1.321(12)	F(2)-B(1)	1.345(12)
F(3)-B(1)	1.205(14)	F(4)-B(1)	1.319(18)
F(3)-F(1)	2.084(16)	F(4)-F(1)	2.055(15)
F(4)-F(3)	2.052(20)	H(11)-C(1)	0.960(11)
H(21)-C(2)	0.960(11)	H(31)-C(3)	0.960(12)
H(41)-C(4)	0.960(11)	H(51)-C(5)	0.960(9)
H(71)-C(7)	0.960(10)	H(81)-C(8)	0.960(10)
H(91)-C(9)	0.960(9)	H(101)-C(10)	0.960(10)
H(111)-C(11)	0.960(9)	H(131)-C(13)	0.960(10)
H(141)-C(14)	0.960(10)	H(151)-C(15)	0.960(11)
H(161)-C(16)	0.960(13)	H(171)-C(17)	0.960(9)
H(191)-C(19)	0.960(10)	H(201)-C(20)	0.960(10)
H(121)-C(21)	0.960(10)	H(221)-C(22)	0.960(10)
H(241)-C(24)	1.036(59)	H(251)-C(25)	1.028(57)
H(271)-C(27)	1.039(39)	H(281)-C(28)	1.048(40)
H(282)-C(28)	1.039(36)	H(283)-C(28)	1.047(61)
H(301)-C(30)	0.960(10)	H(311)-C(31)	0.960(10)
H(321)-C(32)	0.960(12)	H(331)-C(33)	0.960(11)
H(341)-C(34)	0.960(10)		

TABLE 7.12 : Bond angles (°) for Mo{η^2,η^2($\mu_{Mo,C}$-H)-$CH_3CHC(Ph)CH{=}CH$-o-$C_6H_4PPh_2$} (η-C_5H_5)][BF_4] **3**.

Atom	Angle	Bond	Angle
C(1)-Mo(1)-P(1)	133.2(2)	C(2)-Mo(1)-P(1)	98.1(3)
C(2)-Mo(1)-C(1)	35.3(3)	C(3)-Mo(1)-P(1)	85.5(3)
C(3)-Mo(1)-C(1)	59.0(4)	C(3)-Mo(1)-C(2)	36.1(3)
C(4)-Mo(1)-P(1)	108.3(3)	C(4)-Mo(1)-C(1)	58.7(4)
C(4)-Mo(1)-C(2)	58.3(4)	C(4)-Mo(1)-C(3)	33.8(2)
C(5)-Mo(1)-P(1)	141.8(2)	C(5)-Mo(1)-C(1)	35.4(2)
C(5)-Mo(1)-C(2)	58.3(4)	C(5)-Mo(1)-C(3)	57.4(3)
C(5)-Mo(1)-C(4)	34.8(3)	C(24)-Mo(1)-P(1)	74.6(2)
C(24)-Mo(1)-C(1)	94.8(3)	C(24)-Mo(1)-C(2)	89.0(4)
C(24)-Mo(1)-C(3)	117.9(3)	C(24)-Mo(1)-C(4)	47.3(2)
C(24)-Mo(1)-C(5)	128.5(3)	C(25)-Mo(1)-P(1)	81.8(2)
C(25)-Mo(1)-C(1)	117.4(3)	C(25)-Mo(1)-C(2)	125.4(4)
C(25)-Mo(1)-C(3)	155.2(2)	C(25)-Mo(1)-C(4)	169.2(2)
C(25)-Mo(1)-C(5)	135.9(2)	C(25)-Mo(1)-C(24)	37.9(2)
C(26)-Mo(1)-P(1)	118.6(3)	C(26)-Mo(1)-C(1)	95.4(3)
C(26)-Mo(1)-C(2)	123.8(4)	C(26)-Mo(1)-C(3)	153.9(3)
C(26)-Mo(1)-C(4)	130.9(2)	C(26)-Mo(1)-C(5)	99.5(3)
C(26)-Mo(1)-C(24)	64.8(3)	C(26)-Mo(1)-C(25)	38.4(2)
C(27)-Mo(1)-C(24)	99.9(2)	C(27)-Mo(1)-C(25)	66.1(2)
C(27)-Mo(1)-C(26)	36.5(2)	C(28)-Mo(1)-P(1)	92.26(2)
C(28)-Mo(1)-C(24)	111.6(2)	C(28)-Mo(1)-C(25)	74.2(2)
C(28)-Mo(1)-C(26)	65.1(2)	C(28)-Mo(1)-C(27)	37.0(2)
C(27)-Mo(1)-H(281)	60.8(13)	C(28)-Mo(1)-H(281)	24.3(13)
C(12)-P(1)-C(6)	106.6(3)	C(18)-P(1)-C(6)	101.6(3)
C(18)-P(1)-C(12)	108.5(4)	C(3)-C(1)-C(2)	37.3(4)
C(4)-C(1)-C(2)	72.2(6)	C(4)-C(1)-C(3)	35.0(3)
C(5)-C(1)-C(2)	107.9(7)	C(5)-C(1)-C(3)	70.6(5)
C(5)-C(1)-C(4)	35.7(3)	C(3)-C(2)-C(1)	107.0(7)
C(4)-C(2)-C(1)	72.2(5)	C(4)-C(2)-C(3)	34.8(4)
C(5)-C(2)-C(1)	36.2(4)	C(5)-C(2)-C(3)	70.9(5)
C(5)-C(2)-C(4)	36.1(3)	C(2)-C(3)-C(1)	35.7(4)
C(4)-C(3)-C(1)	72.5(6)	C(4)-C(3)-C(2)	108.2(8)
C(5)-C(3)-C(1)	36.0(3)	C(5)-C(3)-C(2)	71.8(6)
C(5)-C(3)-C(4)	36.5(4)	C(2)-C(4)-C(1)	35.6(3)
C(3)-C(4)-C(1)	72.5(6)	C(3)-C(4)-C(2)	37.0(5)
C(5)-C(4)-C(1)	35.5(3)	C(5)-C(4)-C(2)	71.1(5)
C(5)-C(4)-C(3)	108.1(7)	C(2)-C(5)-C(1)	35.9(4)
C(3)-C(5)-C(1)	73.3(5)	C(3)-C(5)-C(2)	37.4(3)
C(4)-C(5)-C(1)	108.8(6)	C(4)-C(5)-C(2)	72.8(5)
C(4)-C(5)-C(3)	35.5(4)	C(7)-C(6)-P(1)	117.6(5)
C(11)-C(6)-P(1)	123.0(5)	C(11)-C(6)-C(7)	119.2(6)
C(8)-C(7)-C(6)	120.5(7)	C(9)-C(8)-C(7)	120.7(7)
C(10)-C(9)-C(8)	119.5(6)	C(11)-C(10)-C(9)	120.1(7)
C(10)-C(11)-C(6)	119.9(6)	C(13)-C(12)-P(1)	120.4(6)
C(17)-C(12)-P(1)	121.0(5)	C(17)-C(12)-C(13)	118.3(7)
C(14)-C(13)-C(12)	120.7(7)	C(15)-C(14)-C(13)	120.7(7)
C(16)-C(15)-C(14)	119.5(8)	C(17)-C(16)-C(15)	120.9(8)
C(16)-C(17)-C(12)	120.0(7)	C(19)-C(18)-P(1)	123.5(5)
C(23)-C(18)-P(1)	114.6(5)	C(23)-C(18)-C(19)	121.2(6)
C(20)-C(19)-C(18)	119.6(7)	C(21)-C(20)-C(19)	119.6(7)
C(22)-C(21)-C(20)	121.0(7)	C(23)-C(22)-C(21)	120.0(7)

TABLE 7.12 cont.

Atom	Angle	Bond	Angle
C(22)-C(23)-C(18)	118.7(6)	C(24)-C(23)-C(18)	119.3(5)
C(24)-C(23)-C(22)	122.0(6)	C(25)-C(24)-C(23)	118.4(6)
C(26)-C(25)-C(24)	113.9(6)	C(27)-C(26)-C(25)	114.9(6)
C(29)-C(26)-C(25)	123.5(5)	C(29)-C(26)-C(27)	121.5(6)
C(28)-C(27)-C(26)	120.5(6)	C(30)-C(29)-C(26)	119.4(6)
C(34)-C(29)-C(26)	122.6(6)	C(34)-C(29)-C(30)	117.9(6)
C(31)-C(30)-C(29)	120.5(7)	C(32)-C(31)-C(30)	119.6(7)
C(33)-C(32)-C(31)	120.3(8)	C(34)-C(33)-C(32)	121.3(8)
C(33)-C(34)-C(29)	120.4(7)	F(2)-B(1)-F(1)	113.4(9)
F(3)-B(1)-F(1)	111.1(12)	F(3)-B(1)-F(2)	111.7(12)
F(4)-B(1)-F(1)	102.2(10)	F(4)-B(1)-F(2)	109.1(9)
F(4)-B(1)-F(3)	108.7(12)	F(3)-F(1)-B(1)	32.6(6)
F(4)-F(1)-B(1)	38.9(6)	F(4)-F(1)-F(3)	59.5(6)
F(1)-F(3)-B(1)	36.2(6)	F(4)-F(3)-B(1)	37.5(7)
F(4)-F(3)-F(1)	59.6(6)	F(1)-F(4)-B(1)	38.9(6)
F(3)-F(4)-B(1)	33.8(6)	F(3)-F(4)-F(1)	61.0(7)
C(2)-C(1)-H(11)	126.3(9)	C(3)-C(1)-H(11)	163.5(7)
C(4)-C(1)-H(11)	161.4(6)	C(5)-C(1)-H(11)	125.8(8)
H(21)-C(2)-C(1)	126.6(11)	C(3)-C(2)-H(21)	126.4(10)
C(4)-C(2)-H(21)	161.1(9)	C(5)-C(2)-H(21)	162.8(9)
H(31)-C(3)-C(1)	161.6(8)	H(31)-C(3)-C(2)	125.9(10)
C(4)-C(3)-H(31)	125.8(11)	C(5)-C(3)-H(31)	162.3(9)
H(41)-C(4)-C(1)	161.5(8)	H(41)-C(4)-C(2)	162.9(8)
H(41)-C(4)-C(3)	125.9(10)	C(5)-C(4)-H(41)	126.0(9)
H(51)-C(5)-C(1)	125.9(9)	H(51)-C(5)-C(2)	161.8(8)
H(51)-C(5)-C(3)	160.7(7)	H(51)-C(5)-C(4)	125.3(9)
H(71)-C(7)-C(6)	119.9(7)	C(8)-C(7)-H(71)	119.7(7)
H(81)-C(8)-C(7)	120.0(9)	C(9)-C(8)-H(81)	119.3(8)
H(91)-C(9)-C(8)	120.1(8)	C(10)-C(9)-H(91)	120.3(8)
H(101)-C(10)-C(9)	119.7(8)	C(11)-C(10)-H(101)	120.2(8)
H(111)-C(11)-C(6)	120.2(7)	H(111)-C(11)-C(10)	119.9(7)
H(131)-C(13)-C(12)	120.0(8)	C(14)-C(13)-H(131)	119.3(8)
H(141)-C(14)-C(13)	119.5(9)	C(15)-C(14)-H(141)	119.8(9)
H(151)-C(15)-C(14)	120.2(10)	C(16)-C(15)-H(151)	120.3(10)
H(161)-C(16)-C(15)	119.6(10)	C(17)-C(16)-H(161)	119.5(10)
H(171)-C(17)-C(12)	120.3(9)	H(171)-C(17)-C(16)	119.8(9)
H(191)-C(19)-C(18)	120.3(7)	C(20)-C(19)-H(191)	120.1(7)
H(201)-C(20)-C(19)	120.5(9)	C(21)-C(20)-H(201)	119.9(8)
H(121)-C(21)-C(20)	119.5(8)	C(22)-C(21)-H(121)	119.5(9)
H(221)-C(22)-C(21)	120.0(7)	C(23)-C(22)-H(221)	120.1(7)
H(241)-C(24)-C(23)	111.0(27)	H(241)-C(24)-C(25)	121.0(25)
H(251)-C(25)-C(24)	125.4(26)	H(251)-C(25)-C(26)	120.7(26)
H(271)-C(27)-C(26)	122.4(32)	H(271)-C(27)-C(28)	117.0(32)
H(281)-C(28)-C(27)	112.0(29)	H(282)-C(28)-C(27)	111.6(36)
H(282)-C(28)-H(281)	89.3(40)	H(283)-C(28)-C(27)	116.8(31)
H(283)-C(28)-H(281)	100.2(38)	H(283)-C(28)-H(282)	121.9(49)
H(301)-C(30)-C(29)	119.8(8)	C(31)-C(30)-H(301)	119.6(8)
H(311)-C(31)-C(30)	120.3(9)	C(32)-C(31)-H(311)	120.1(9)
H(321)-C(32)-C(31)	120.2(9)	C(33)-C(32)-H(321)	119.6(10)
H(331)-C(33)-C(32)	119.6(10)	C(34)-C(33)-H(331)	119.2(9)
H(341)-C(34)-C(29)	119.9(8)	H(341)-C(34)-C(33)	119.7(8)
H(281)-C(28)-Mo(1)	48.7(28)	C(28)-H(281)-Mo(1)	106.9(37)

7.4 Crystal Structure Determination of [MoI{η^2,η^2-CH_3CH=C(Ph) CH=CH-o-$C_6H_4PPh_2$}(η-C_5H_5)] 6

A crystal of approximate dimensions 0.2 x 0.2 x 0.2 mm was used for data collection.

Crystal Data : $C_{34}H_{30}PIMo$, M = 692.4, monoclinic, a = 10.455(2), b = 18.507(2), c = 15.356(2) Å, β = 109.31(1)°, U = 2804.1 Å^3, space group $P2_1/n$, Z = 4, D_c = 1.64 gcm^{-3}, μ(Mo-K_α) = 16.2 cm^{-1}, F(000) = 1376. Data were measured at room temperature on a CAD4 automatic four-circle diffractometer in the range $2\leq\theta\leq24°$. 4822 reflections were collected of which 3182 were unique with $I\geq2\sigma(I)$. Data were corrected for Lorentz and polarisation effects but not for X-ray absorption effects. The structure was solved by Patterson methods and refined using the SHELX[i,ii] suite of programs. In the final least squares cycles all atoms were allowed to vibrate anisotropically. Hydrogen atoms were included at calculated positions except in the instance of H241, H251 and H271 (attached to C24, C25 and C27, respectively). These hydrogens were located in an advanced Difference Fourier and refined at a distance of 0.96Å from the relevant parent atoms. Final residues after 10 cycles of least squares were R = 0.0316, R_w =0.0314, for a weighting scheme of w = 2.0545/[σ^2(F) +0.000541(F)^2]. Max. final shift/esd was 0.115. The max. and min. residual densities were 0.28 and -0.37 eÅ^{-3}, respectively. Final fractional atomic coordinates and isotropic thermal parameters, bond distances and angles are listed in Tables 7.13/7.14, 7.15 and 7.16, respectively. The asymmetric unit is shown in Figure 2.30 (Section 2.4), along with the labelling scheme employed.

TABLE 7.13 : Fractional atomic co-ordinates ($x10^4$) and equivalent isotropic temperature factors ($Å^2 x10^3$) for [MoI{η^2,η^2-CH_3CH=C(Ph) CH=CH-o-$C_6H_4PPh_2$}(η-C_5H_5)] **6**

Atom	x	y	z	U
Mo(1)	661.4(4)	8153.2(2)	9003.0(3)	31.8(2)
I(1)	1558.8(4)	7038.9(2)	10344.3(2)	59.0(3)
P(1)	2675(1)	7898(1)	8529(1)	32.2(6)
C(1)	-302(6)	9040(3)	9694(5)	67(3)
C(2)	3(5)	9336(3)	8942(4)	53(2)
C(3)	1441(5)	9277(3)	9139(4)	47(2)
C(4)	1977(6)	8943(3)	10021(4)	54(2)
C(5)	901(6)	8808(3)	10354(4)	61(3)
C(6)	2244(5)	8329(2)	7394(3)	36(2)
C(7)	878(5)	8504(2)	6999(3)	35(2)
C(8)	461(5)	8848(3)	6135(3)	46(2)
C(9)	1385(6)	9004(3)	5690(3)	58(3)
C(10)	2735(6)	8825(3)	6091(4)	57(2)
C(11)	3149(5)	8483(3)	6928(3)	48(2)
C(12)	4256(4)	8313(2)	9244(3)	36(2)
C(13)	5041(6)	7934(3)	10023(4)	51(2)
C(14)	6202(6)	8246(3)	10617(4)	62(2)
C(15)	6595(5)	8918(3)	10470(4)	55(2)
C(16)	5843(5)	9307(3)	9706(4)	49(2)
C(17)	4666(5)	9005(2)	9097(3)	41(2)
C(18)	3278(5)	7002(2)	8331(3)	38(2)
C(19)	2557(5)	6384(3)	8374(4)	48(2)
C(20)	3006(6)	5712(3)	8177(4)	65(3)
C(21)	4145(7)	5658(3)	7946(4)	68(3)
C(22)	4874(7)	6262(3)	7895(4)	69(3)
C(23)	4437(6)	6925(3)	8099(4)	61(3)
C(24)	-104(5)	8304(2)	7463(3)	35(2)
C(25)	-232(4)	7537(2)	7600(3)	33(2)
C(26)	-934(4)	7256(2)	8153(3)	33(2)
C(27)	-1531(5)	7757(2)	8624(3)	40(2)
C(28)	-2673(5)	8260(3)	8094(4)	50(2)
C(29)	-1045(4)	6454(2)	8242(3)	37(2)
C(30)	-1391(6)	6135(3)	8953(4)	58(3)
C(31)	-1512(6)	5396(3)	9014(4)	63(2)
C(32)	-1308(6)	4953(3)	8364(4)	63(3)
C(33)	-999(8)	5244(3)	7648(4)	78(3)
C(34)	-885(6)	5995(3)	7578(4)	59(2)

TABLE 7.14 : Hydrogen fractional atomic co-ordinates ($x10^4$) and isotropic temperature factors ($Å^2 x10^3$) for [MoI{η^2,η^2-CH_3CH=C(Ph) CH=CH-o-$C_6H_4PPh_2$}(η-C_5H_5)] **6**

Atom	x	y	z	U
H(11)	-1190(6)	9003(3)	9745(5)	65(3)
H(21)	-635(5)	9540(3)	8396(4)	65(3)
H(31)	1944(5)	9432(3)	8751(4)	65(3)
H(41)	2913(6)	8830(3)	10335(4)	65(3)
H(51)	978(6)	8593(3)	10938(4)	65(3)
H(81)	-475(5)	8977(3)	5849(3)	65(3)
H(91)	1085(6)	9238(3)	5099(3)	65(3)
H(101)	3376(6)	8940(3)	5786(4)	65(3)
H(111)	4083(5)	8346(3)	7199(3)	65(3)
H(131)	4775(6)	7459(3)	10145(4)	65(3)
H(141)	6743(6)	7980(3)	11147(4)	65(3)
H(151)	7400(5)	9125(3)	10898(4)	65(3)
H(161)	6128(5)	9731(3)	9596(4)	65(3)
H(171)	4133(5)	9277(2)	8570(3)	65(3)
H(191)	1750(5)	6416(3)	8539(4)	65(3)
H(201)	2502(6)	5285(3)	8206(4)	65(3)
H(211)	4444(7)	5192(3)	7817(4)	65(3)
H(221)	5673(7)	6225(3)	7720(4)	65(3)
H(131)	4959(6)	7347(3)	8079(4)	65(3)
H(241)	-879(34)	8618(24)	7271(33)	65(3)
H(251)	289(47)	7229(24)	7342(35)	65(3)
H(271)	-1745(51)	7553(26)	9134(23)	65(3)
H(281)	-2466(5)	8467(3)	7583(4)	65(3)
H(282)	-2769(5)	8639(3)	8495(4)	65(3)
H(283)	-3504(5)	7993(3)	7869(4)	65(3)
H(301)	-1549(6)	6437(3)	9415(4)	65(3)
H(311)	-1741(6)	5192(3)	9519(4)	65(3)
H(321)	-1382(6)	4439(3)	8412(4)	65(3)
H(331)	-857(8)	4934(3)	7187(4)	65(3)
H(341)	-691(6)	6194(3)	7057(4)	65(3)

TABLE 7.15 : Bond lengths (Å) for [MoI{η^2,η^2-CH_3CH=C(Ph) CH=CH-o-$C_6H_4PPh_2$}(η-C_5H_5)] **6**

Atom	Bond Length	Atom	Bond Length
I(1)-Mo(1)	2.845(4)	P(1)-Mo(1)	2.490(3)
C(1)-Mo(1)	2.353(7)	C(2)-Mo(1)	2.287(7)
C(3)-Mo(1)	2.218(7)	C(4)-Mo(1)	2.248(7)
C(5)-Mo(1)	2.344(7)	C(24)-Mo(1)	2.249(6)
C(25)-Mo(1)	2.341(6)	C(26)-Mo(1)	2.408(6)
C(27)-Mo(1)	2.291(7)	C(6)-P(1)	1.833(6)
C(12)-P(1)	1.825(6)	C(18)-P(1)	1.836(6)
C(2)-C(1)	1.407(9)	C(3)-C(1)	2.294(10)
C(4)-C(1)	2.274(10)	C(5)-C(1)	1.396(9)
C(3)-C(2)	1.436(8)	C(4)-C(2)	2.297(10)
C(5)-C(2)	2.278(11)	C(4)-C(3)	1.424(8)
C(5)-C(3)	2.291(10)	C(5)-C(4)	1.404(9)
C(7)-C(6)	1.392(7)	C(11)-C(6)	1.391(7)
C(8)-C(7)	1.404(7)	C(24)-C(7)	1.479(7)
C(9)-C(8)	1.386(8)	C(10)-C(9)	1.380(9)
C(11)-C(10)	1.368(8)	C(13)-C(12)	1.395(8)
C(17)-C(12)	1.392(7)	C(14)-C(13)	1.381(8)
C(15)-C(14)	1.352(9)	C(16)-C(15)	1.378(8)
C(17)-C(16)	1.393(8)	C(19)-C(18)	1.382(7)
C(23)-C(18)	1.379(8)	C(20)-C(19)	1.396(8)
C(21)-C(20)	1.354(10)	C(22)-C(21)	1.370(9)
C(23)-C(22)	1.380(8)	C(25)-C(24)	1.448(7)
C(26)-C(25)	1.393(7)	C(27)-C(26)	1.439(7)
C(29)-C(26)	1.499(7)	C(28)-C(27)	1.521(9)
C(30)-C(29)	1.390(7)	C(34)-C(29)	1.380(8)
C(31)-C(30)	1.380(8)	C(32)-C(31)	1.362(8)
C(33)-C(32)	1.355(9)	C(34)-C(33)	1.402(9)
H(11)-C(1)	0.960	H(21)-C(2)	0.960
H(31)-C(3)	0.960	H(41)-C(4)	0.960
H(51)-C(5)	0.960	H(81)-C(8)	0.960
H(91)-C(9)	0.960	H(101)-C(10)	0.960
H(111)-C(11)	0.960	H(131)-C(13)	0.960
H(141)-C(14)	0.960	H(151)-C(15)	0.960
H(161)-C(16)	0.960	H(171)-C(17)	0.960
H(191)-C(19)	0.960	H(201)-C(20)	0.960
H(211)-C(21)	0.960	H(221)-C(22)	0.960
H(131)-C(23)	0.960	H(241)-C(24)	0.960(2)
H(251)-C(25)	0.960(2)	H(271)-C(27)	0.960(2)
H(281)-C(28)	0.960	H(282)-C(28)	0.960
H(283)-C(28)	0.960	H(301)-C(30)	0.960
H(311)-C(31)	0.960	H(321)-C(32)	0.960
H(331)-C(33)	0.960	H(341)-C(34)	0.960

TABLE 7.16 : Bond angles (°) for [MoI{η^2,η^2-CH_3CH=C(Ph) CH=CH-o-$C_6H_4PPh_2$}(η-C_5H_5)] **6**

Atom	Angle	Atom	Angle
P(1)-Mo(1)-I(1)	88.1	C(1)-Mo(1)-I(1)	105.5(3)
C(1)-Mo(1)-P(1)	142.5(1)	C(2)-Mo(1)-I(1)	138.3(1)
C(2)-Mo(1)-P(1)	116.2(2)	C(2)-Mo(1)-C(1)	35.3(2)
C(3)-Mo(1)-I(1)	126.0(2)	C(3)-Mo(1)-P(1)	83.4(2)
C(3)-Mo(1)-C(1)	60.2(3)	C(3)-Mo(1)-C(2)	37.1(2)
C(4)-Mo(1)-I(1)	89.3(3)	C(4)-Mo(1)-P(1)	86.8(2)
C(4)-Mo(1)-C(1)	59.2(3)	C(4)-Mo(1)-C(2)	60.9(3)
C(4)-Mo(1)-C(3)	37.2(2)	C(5)-Mo(1)-I(1)	79.7(3)
C(5)-Mo(1)-P(1)	120.3(3)	C(5)-Mo(1)-C(1)	34.6(2)
C(5)-Mo(1)-C(2)	58.9(3)	C(5)-Mo(1)-C(3)	60.2(3)
C(5)-Mo(1)-C(4)	35.5(2)	C(24)-Mo(1)-I(1)	140.2(1)
C(24)-Mo(1)-P(1)	76.0(2)	C(24)-Mo(1)-C(1)	109.3(3)
C(24)-Mo(1)-C(2)	80.8(3)	C(24)-Mo(1)-C(3)	88.6(3)
C(24)-Mo(1)-C(4)	125.0(3)	C(24)-Mo(1)-C(5)	139.7(2)
C(25)-Mo(1)-I(1)	104.4(2)	C(25)-Mo(1)-P(1)	75.9(2)
C(25)-Mo(1)-C(1)	130.9(2)	C(25)-Mo(1)-C(2)	113.9(3)
C(25)-Mo(1)-C(3)	124.5(3)	C(25)-Mo(1)-C(4)	157.4(2)
C(25)-Mo(1)-C(5)	163.7(2)	C(25)-Mo(1)-C(24)	36.7(2)
C(26)-Mo(1)-I(1)	84.0(2)	C(26)-Mo(1)-P(1)	102.2(2)
C(26)-Mo(1)-C(1)	113.7(3)	C(26)-Mo(1)-C(2)	119.5(3)
C(26)-Mo(1)-C(3)	149.8(2)	C(26)-Mo(1)-C(4)	168.5(2)
C(26)-Mo(1)-C(5)	133.5(2)	C(26)-Mo(1)-C(24)	64.8(2)
C(26)-Mo(1)-C(25)	34.1(1)	C(27)-Mo(1)-I(1)	90.8(2)
C(27)-Mo(1)-P(1)	137.5(1)	C(27)-Mo(1)-C(1)	78.2(3)
C(27)-Mo(1)-C(2)	91.9(3)	C(27)-Mo(1)-C(3)	129.0(3)
C(27)-Mo(1)-C(4)	135.7(2)	C(27)-Mo(1)-C(5)	101.2(3)
C(27)-Mo(1)-C(24)	78.1(3)	C(27)-Mo(1)-C(25)	63.2(3)
C(27)-Mo(1)-C(26)	35.6(2)	C(12)-P(1)-C(6)	106.2(3)
C(18)-P(1)-C(6)	103.1(3)	C(18)-P(1)-C(12)	100.8(3)
C(3)-C(1)-C(2)	36.6(3)	C(4)-C(1)-C(2)	73.0(5)
C(4)-C(1)-C(3)	36.3(2)	C(5)-C(1)-C(2)	108.8(6)
C(5)-C(1)-C(3)	72.1(5)	C(5)-C(1)-C(4)	35.8(3)
C(3)-C(2)-C(1)	107.6(6)	C(4)-C(2)-C(1)	71.2(5)
C(4)-C(2)-C(3)	36.4(3)	C(5)-C(2)-C(1)	35.5(3)
C(5)-C(2)-C(3)	72.1(5)	C(5)-C(2)-C(4)	35.7(2)
C(2)-C(3)-C(1)	35.8(3)	C(4)-C(3)-C(1)	71.1(4)
C(4)-C(3)-C(2)	106.8(6)	C(5)-C(3)-C(1)	35.5(2)
C(5)-C(3)-C(2)	71.2(4)	C(5)-C(3)-C(4)	35.6(3)
C(2)-C(4)-C(1)	35.8(2)	C(3)-C(4)-C(1)	72.6(4)
C(3)-C(4)-C(2)	36.8(3)	C(5)-C(4)-C(1)	35.6(3)
C(5)-C(4)-C(2)	71.4(5)	C(5)-C(4)-C(3)	108.2(6)
C(2)-C(5)-C(1)	35.8(3)	C(3)-C(5)-C(1)	72.4(5)
C(3)-C(5)-C(2)	36.6(2)	C(4)-C(5)-C(1)	108.6(6)
C(4)-C(5)-C(2)	72.8(5)	C(4)-C(5)-C(3)	36.2(3)
C(7)-C(6)-P(1)	114.2(4)	C(11)-C(6)-P(1)	125.6(5)
C(11)-C(6)-C(7)	120.2(5)	C(8)-C(7)-C(6)	118.1(5)
C(24)-C(7)-C(6)	120.5(5)	C(24)-C(7)-C(8)	121.4(5)
C(9)-C(8)-C(7)	120.7(6)	C(10)-C(9)-C(8)	120.5(6)
C(11)-C(10)-C(9)	119.3(6)	C(10)-C(11)-C(6)	121.3(6)
C(13)-C(12)-P(1)	117.6(4)	C(17)-C(12)-P(1)	123.8(5)
C(17)-C(12)-C(13)	118.4(5)	C(14)-C(13)-C(12)	119.7(6)
C(15)-C(14)-C(13)	121.6(6)	C(16)-C(15)-C(14)	120.2(6)

TABLE 7.16 cont.

Atom	Angle	Atom	Angle
C(17)-C(16)-C(15)	119.4(6)	C(16)-C(17)-C(12)	120.7(6)
C(19)-C(18)-P(1)	121.2(5)	C(23)-C(18)-P(1)	121.0(5)
C(23)-C(18)-C(19)	117.8(5)	C(20)-C(19)-C(18)	119.9(6)
C(21)-C(20)-C(19)	120.7(6)	C(22)-C(21)-C(20)	120.6(6)
C(23)-C(22)-C(21)	118.6(7)	C(22)-C(23)-C(18)	122.4(6)
C(25)-C(24)-C(7)	115.3(5)	C(26)-C(25)-C(24)	123.2(5)
C(27)-C(26)-C(25)	118.0(5)	C(29)-C(26)-C(25)	119.8(5)
C(29)-C(26)-C(27)	122.2(5)	C(28)-C(27)-C(26)	121.3(5)
C(30)-C(29)-C(26)	122.7(5)	C(34)-C(29)-C(26)	120.7(5)
C(34)-C(29)-C(30)	116.4(5)	C(31)-C(30)-C(29)	121.9(6)
C(32)-C(31)-C(30)	120.4(6)	C(33)-C(32)-C(31)	119.5(6)
C(34)-C(33)-C(32)	120.4(6)	C(33)-C(34)-C(29)	121.3(6)
C(2)-C(1)-H(11)	125.6(4)	C(3)-C(1)-H(11)	162.3(2)
C(4)-C(1)-H(11)	161.4(2)	C(5)-C(1)-H(11)	125.6(5)
H(21)-C(2)-C(1)	126.2(4)	C(3)-C(2)-H(21)	126.2(4)
C(4)-C(2)-H(21)	162.6(2)	C(5)-C(2)-H(21)	161.7(2)
H(31)-C(3)-C(1)`	162.4(2)	H(31)-C(3)-C(2)	126.6(4)
C(4)-C(3)-H(31)	126.6(4)	C(5)-C(3)-H(31)	162.2(2)
H(41)-C(4)-C(1)	161.5(2)	H(41)-C(4)-C(2)	162.7(2)
H(41)-C(4)-C(3)	125.9(4)	C(5)-C(4)-H(41)	125.9(5)
H(51)-C(5)-C(1)	125.7(5)	H(51)-C(5)-C(2)	161.5(2)
H(51)-C(5)-C(3)	161.9(2)	H(51)-C(5)-C(4)	125.7(5)
H(81)-C(8)-C(7)	119.7(4)	C(9)-C(8)-H(81)	119.7(4)
H(91)-C(9)-C(8)	119.8(4)	C(10)-C(9)-H(91)	119.8(4)
H(101)-C(10)-C(9)	120.3(4)	C(11)-C(10)-H(101)	120.3(4)
H(111)-C(11)-C(6)	119.4(4)	H(111)-C(11)-C(10)	119.4(4)
H(131)-C(13)-C(12)	120.2(4)	C(14)-C(13)-H(131)	120.1(4)
H(141)-C(14)-C(13)	119.2(4)	C(15)-C(14)-H(141)	119.2(4)
H(151)-C(15)-C(14)	119.9(4)	C(16)-C(15)-H(151)	119.9(4)
H(161)-C(16)-C(15)	120.3(4)	C(17)-C(16)-H(161)	120.3(4)
H(171)-C(17)-C(12)	119.6(4)	H(171)-C(17)-C(16)	119.6(4)
H(191)-C(19)-C(18)	120.1(4)	C(20)-C(19)-H(191)	120.1(4)
H(201)-C(20)-C(19)	119.6(4)	C(21)-C(20)-H(201)	119.7(4)
H(211)-C(21)-C(20)	119.7(4)	C(22)-C(21)-H(211)	119.7(5)
H(221)-C(22)-C(21)	120.7(5)	C(23)-C(22)-H(221)	120.7(5)
H(131)-C(23)-C(18)	118.8(4)	H(131)-C(23)-C(22)	118.8(5)
H(241)-C(24)-C(7)	110.5(33)	C(25)-C(24)-H(241)	121.9(34)
H(251)-C(25)-C(24)	115.5(34)	C(26)-C(25)-H(251)	121.0(34)
H(271)-C(27)-C(26)	114.4(34)	C(28)-C(27)-H(271)	109.0(33)
H(281)-C(28)-C(27)	109.5(4)	H(282)-C(28)-C(27)	109.5(4)
H(282)-C(28)-H(281)	109.5	H(283)-C(28)-C(27)	109.5(4)
H(283)-C(28)-H(281)	109.5	H(283)-C(28)-H(282)	109.5
H(301)-C(30)-C(29)	119.0(4)	C(31)-C(30)-H(301)	119.0(4)
H(311)-C(31)-C(30)	119.8(4)	C(32)-C(31)-H(311)	119.8(4)
H(321)-C(32)-C(31)	120.2(4)	C(33)-C(32)-H(321)	120.2(4)
H(331)-C(33)-C(32)	119.8(4)	C(34)-C(33)-H(331)	119.8(4)
H(341)-C(34)-C(29)	119.4(4)	H(341)-C(34)-C(33)	119.4(4)

7.5 Crystal Structure Determination of [Re=C(Ph)-η^3-{C(Me)CHCH $C_6H_4PPh_2$-*o*}(η-C_5H_5)][BF_4] 13

A crystal of approximate dimensions 0.2 x 0.2 x 0.15 mm was used for data collection.

Crystal Data : $C_{34}H_{29}PBF_4Re$, M = 741.6, monoclinic, a = 11.324(1), b = 15.033(2), c = 17.598(2) Å, β = 98.08(1)°, U = 2966.0 Å^3, space group $P2_1/c$, Z = 4, D_c = 1.66 gcm^{-3}, μ(Mo-K_α) = 40.3 cm^{-1}, F(000) = 1456. Data were measured at room temperature on a CAD4 automatic four-circle diffractometer in the range $2\leq\theta\leq24°$. 5099 reflections were collected of which 2741 were unique with $I\geq2\sigma(I)$. Data were corrected for Lorentz and polarisation also for absorption.[iii] The structure was solved by Patterson methods and refined using the SHELX[i,ii] suite of programs. In the final least squares cycles all atoms were allowed to vibrate anisotropically except for the boron as disorder in the anion, which could not be successfully modelled, precluded a clean refinement in this region. Thus, in the latter stages of convergence the terafluoroborate moiety was refined as a rigid group, in a block separate from the cation. Hydrogen atoms were included at calculated positions except those hydrogens attached to C6 and C7. These hydrogens (H61 and H71) were located in an advanced Difference Fourier and refined at a distance of 0.96Å from the relevant parent atoms. Final residues after 36 cycles of a blocked-matrix least squares were R = 0.0406, R_w =0.0406, for a weighting scheme of w = 2.2345/[σ^2(F) +0.000242(F)^2]. Max. final shift/esd values in the two blocks were -0.010 (in the fractional z coordinate of H61 and -1.321 (in the isotropic thermal parameter of B1). The max. and min. residual densities were 0.64 and -0.56 eÅ^{-3}, respectively. Final fractional atomic coordinates and isotropic thermal parameters, bond distances and angles are listed in Tables 7.17/7.18, 7.19 and 7.20, respectively. The asymmetric unit is shown in Figure 2.44 (Section 2.7), along with the labelling scheme employed.

---

iii N. Walker and D. Stewart, *Acta Crystallogr., Sect. A,* 158, 39, **1983**.

TABLE 7.17 : Fractional atomic co-ordinates ($x10^4$) and equivalent isotropic temperature factors ($Å^2 x10^3$) for [Re=C(Ph)-η^3-{C(Me)CHCHC$_6$H$_4$PPh$_2$-o}(η-C$_5$H$_5$)][BF$_4$] **13**.

Atom	x	y	z	U
Re(1)	1213	2392	1348	39
P(1)	2915(2)	2345(2)	2304(2)	35(1)
C(1)	-271(14)	2187(14)	2052(10)	91(8)
C(2)	-751(14)	2228(15)	1318(13)	103(9)
C(3)	-540(18)	3098(22)	1044(13)	135(13)
C(4)	86(20)	3574(13)	1661(17)	128(12)
C(5)	256(15)	2973(15)	2274(11)	94(8)
C(6)	2578(11)	3039(7)	792(7)	44(4)
C(7)	1779(10)	2591(8)	205(6)	48(5)
C(8)	1463(10)	1687(7)	272(6)	42(5)
C(9)	1782(9)	1269(7)	1001(6)	40(4)
C(10)	568(12)	1281(9)	-358(8)	79(6)
C(11)	2066(10)	350(7)	1146(7)	43(4)
C(12)	2602(11)	-135(9)	609(8)	64(6)
C(13)	2864(12)	-1045(10)	720(10)	79(7)
C(14)	2576(15)	-1445(10)	1372(12)	96(8)
C(15)	2080(12)	-978(10)	1913(8)	71(6)
C(16)	1784(11)	-73(8)	1792(7)	61(5)
C(17)	3844(9)	2738(7)	1033(6)	39(4)
C(18)	4750(10)	2879(7)	577(6)	46(4)
C(19)	5891(11)	2670(9)	859(9)	65(5)
C(20)	6218(10)	2378(8)	1608(9)	60(5)
C(21)	5354(10)	2249(7)	2050(7)	48(5)
C(22)	4173(9)	2415(6)	1765(6)	35(4)
C(23)	3206(11)	3293(7)	2939(6)	44(4)
C(24)	3022(12)	4154(7)	2623(7)	61(6)
C(25)	3312(14)	4897(8)	3059(8)	65(6)
C(26)	3844(13)	4833(8)	3793(8)	66(6)
C(27)	4020(11)	3975(8)	4111(7)	59(5)
C(28)	3699(12)	3224(7)	3686(7)	56(5)
C(29)	3090(10)	1398(7)	2955(6)	38(4)
C(30)	3988(11)	773(7)	2962(7)	56(5)
C(31)	4050(14)	66(9)	3496(10)	94(9)
C(32)	3210(15)	-1(9)	3984(8)	77(7)
C(33)	2307(13)	601(8)	3952(7)	61(6)
C(34)	2227(12)	1317(7)	3448(7)	53(5)
F(1)	9247(7)	1478(8)	3966(6)	215(9)
F(2)	7723(9)	1249(6)	3323(5)	206(8)
F(3)	8432(11)	341(5)	4043(7)	281(11)
F(4)	7774(10)	1429(8)	4428(6)	241(10)

TABLE 7.18 : Hydrogen fractional atomic co-ordinates ($x10^4$) and isotropic temperature factors ($Å^2 x10^3$) for [Re=C(Ph)-η^3-{C(Me)CHCHC$_6$H$_4$PPh$_2$-o}(η-C$_5$H$_5$)][BF$_4$] **13**

Atom	x	y	z	U
B(1)	8294(5)	1124(4)	3940(3)	90(2)
H(11)	-308(14)	1684(14)	2384(10)	90(8)
H(21)	-1145(14)	1747(15)	1027(13)	90(8)
H(31)	-776(18)	3312(22)	531(13)	90(8)
H(41)	317(20)	4187(13)	1646(17)	90(8)
H(51)	686(15)	3108(15)	2770(11)	90(8)
H(61)	2405(107)	3660(20)	710(71)	90(8)
H(71)	1277(86)	2937(68)	-170(51)	90(8)
H(101)	440(12)	667(9)	-244(8)	90(8)
H(102)	874(12)	1325(9)	-839(8)	90(8)
H(103)	-174(12)	1598(9)	-392(8)	90(8)
H(121)	2799(11)	157(9)	158(8)	90(8)
H(131)	3227(12)	-1378(10)	349(10)	90(8)
H(141)	2741(15)	-2067(10)	1449(12)	90(8)
H(151)	1926(12)	-1270(10)	2375(8)	90(8)
H(161)	1390(11)	249(8)	2155(7)	90(8)
H(181)	4559(10)	3116(7)	68(6)	90(8)
H(191)	6497(11)	2739(9)	534(9)	90(8)
H(201)	7038(10)	2265(8)	1804(9)	90(8)
H(211)	5569(10)	2037(7)	2566(7)	90(8)
H(241)	2685(12)	4222(7)	2095(7)	90(8)
H(251)	3168(14)	5478(8)	2839(8)	90(8)
H(261)	4066(13)	5352(8)	4098(8)	90(8)
H(271)	4375(11)	3914(8)	4637(7)	90(8)
H(281)	3833(12)	2650(7)	3921(7)	90(8)
H(301)	4565(11)	812(7)	2612(7)	90(8)
H(311)	4678(14)	-366(9)	3517(10)	90(8)
H(321)	3272(15)	-473(9)	4355(8)	90(8)
H(331)	1710(13)	530(8)	4285(7)	90(8)
H(341)	1593(12)	1743(7)	3434(7)	90(8)

TABLE 7.19 : Bond lengths (Å) for [Re=C(Ph)-η^3-{C(Me)CHCHC$_6$H$_4$PPh$_2$-o}(η-C$_5$H$_5$)] [BF$_4$] **13**

Atom	Bond Length	Atom	Bond Length
P(1)-Re(1)	2.375(5)	C(1)-Re(1)	2.244(20)
C(2)-Re(1)	2.230(19)	C(3)-Re(1)	2.248(26)
C(4)-Re(1)	2.299(24)	C(5)-Re(1)	2.256(22)
C(6)-Re(1)	2.172(14)	C(7)-Re(1)	2.216(13)
C(8)-Re(1)	2.222(13)	C(9)-Re(1)	1.936(12)
Re(1)-P(1)	2.375(5)	C(22)-P(1)	1.822(13)
C(23)-P(1)	1.812(13)	C(29)-P(1)	1.821(13)
Re(1)-C(1)	2.244(20)	C(2)-C(1)	1.330(28)
C(5)-C(1)	1.356(30)	Re(1)-C(2)	2.230(19)
C(1)-C(2)	1.330(28)	C(3)-C(2)	1.425(40)
Re(1)-C(3)	2.248(26)	C(2)-C(3)	1.425(40)
C(4)-C(3)	1.406(36)	Re(1)-C(4)	2.299(24)
C(3)-C(4)	1.406(36)	C(5)-C(4)	1.399(34)
Re(1)-C(5)	2.256(22)	C(1)-C(5)	1.356(30)
C(4)-C(5)	1.399(34)	Re(1)-C(6)	2.172(14)
C(7)-C(6)	1.441(16)	C(17)-C(6)	1.506(17)
Re(1)-C(7)	2.216(13)	C(6)-C(7)	1.441(16)
C(8)-C(7)	1.415(18)	Re(1)-C(8)	2.222(13)
C(7)-C(8)	1.415(18)	C(9)-C(8)	1.427(16)
C(10)-C(8)	1.521(18)	Re(1)-C(9)	1.936(12)
C(8)-C(9)	1.427(16)	C(11)-C(9)	1.433(15)
C(8)-C(10)	1.521(18)	C(9)-C(11)	1.433(15)
C(12)-C(11)	1.399(19)	C(16)-C(11)	1.379(19)
C(11)-C(12)	1.399(19)	C(13)-C(12)	1.408(21)
C(12)-C(13)	1.408(21)	C(14)-C(13)	1.374(28)
C(13)-C(14)	1.374(28)	C(15)-C(14)	1.366(26)
C(14)-C(15)	1.366(26)	C(16)-C(15)	1.409(20)
C(11)-C(16)	1.379(19)	C(15)-C(16)	1.409(20)
C(6)-C(17)	1.506(17)	C(18)-C(17)	1.405(17)
C(22)-C(17)	1.378(15)	C(17)-C(18)	1.405(17)
C(19)-C(18)	1.354(17)	C(18)-C(19)	1.354(17)
C(20)-C(19)	1.388(22)	C(19)-C(20)	1.388(22)
C(21)-C(20)	1.347(20)	C(20)-C(21)	1.347(20)
C(22)-C(21)	1.383(15)	P(1)-C(22)	1.822(13)
C(17)-C(22)	1.378(15)	C(21)-C(22)	1.383(15)
P(1)-C(23)	1.812(13)	C(24)-C(23)	1.412(16)
C(28)-C(23)	1.358(17)	C(23)-C(24)	1.412(16)
C(25)-C(24)	1.370(18)	C(24)-C(25)	1.370(18)
C(26)-C(25)	1.350(20)	C(25)-C(26)	1.350(20)
C(27)-C(26)	1.410(18)	C(26)-C(27)	1.410(18)
C(28)-C(27)	1.374(18)	C(23)-C(28)	1.358(17)
C(27)-C(28)	1.374(18)	P(1)-C(29)	1.821(13)
C(30)-C(29)	1.383(17)	C(34)-C(29)	1.399(19)
C(29)-C(30)	1.383(17)	C(31)-C(30)	1.414(21)
C(30)-C(31)	1.414(21)	C(32)-C(31)	1.372(26)
C(31)-C(32)	1.372(26)	C(33)-C(32)	1.361(22)
C(32)-C(33)	1.361(22)	C(34)-C(33)	1.390(17)
C(29)-C(34)	1.399(19)	C(33)-C(34)	1.390(17)
F(1)-B(1)	1.199(12)	F(2)-B(1)	1.198(11)
F(3)-B(1)	1.198(10)	F(4)-B(1)	1.199(14)
B(1)-F(1)	1.199(12)	B(1)-F(2)	1.198(11)

TABLE 7.19cont.

Atom	Bond Length	Atom	Bond Length
B(1)-F(3)	1.198(10)	B(1)-F(4)	1.199(14)
H(11)-C(1)	0.960(29)	C(1)-H(11)	0.960(29)
H(21)-C(2)	0.960(31)	C(2)-H(21)	0.960(31)
H(31)-C(3)	0.960(33)	C(3)-H(31)	0.960(33)
H(41)-C(4)	0.960(28)	C(4)-H(41)	0.960(28)
H(51)-C(5)	0.960(26)	C(5)-H(51)	0.960(26)
H(61)-C(6)	0.960(43)	C(6)-H(61)	0.960(43)
H(71)-C(7)	0.960(93)	C(7)-H(71)	0.960(93)
H(101)-C(10)	0.960(20)	H(102)-C(10)	0.960(21)
H(103)-C(10)	0.960(20)	C(10)-H(101)	0.960(20)
C(10)-H(102)	0.960(21)	C(10)-H(103)	0.960(20)
H(121)-C(12)	0.960(21)	C(12)-H(121)	0.960(21)
H(131)-C(13)	0.960(25)	C(13)-H(131)	0.960(25)
H(141)-C(14)	0.960(23)	C(14)-H(141)	0.960(23)
H(151)-C(15)	0.960(22)	C(15)-H(151)	0.960(22)
H(161)-C(16)	0.960(20)	C(16)-H(161)	0.960(20)
H(181)-C(18)	0.960(16)	C(18)-H(181)	0.960(16)
H(191)-C(19)	0.960(22)	C(19)-H(191)	0.960(22)
H(201)-C(20)	0.960(17)	C(20)-H(201)	0.960(17)
H(211)-C(21)	0.960(18)	C(21)-H(211)	0.960(18)
H(241)-C(24)	0.960(18)	C(24)-H(241)	0.960(18)
H(251)-C(25)	0.960(18)	C(25)-H(251)	0.960(18)
H(261)-C(26)	0.960(18)	C(26)-H(261)	0.960(18)
H(271)-C(27)	0.960(18)	C(27)-H(271)	0.960(18)
H(281)-C(28)	0.960(16)	C(28)-H(281)	0.960(16)
H(301)-C(30)	0.960(20)	C(30)-H(301)	0.960(20)
H(311)-C(31)	0.960(22)	C(31)-H(311)	0.960(22)
H(321)-C(32)	0.960(21)	C(32)-H(321)	0.960(21)
H(331)-C(33)	0.960(21)	C(33)-H(331)	0.960(21)
H(341)-C(34)	0.960(18)	C(34)-H(341)	0.960(18)

TABLE 7.20 : Bond angles (°) for [Re=C(Ph)-η^3-{C(Me)CHCHC$_6$H$_4$PPh$_2$-o}(η-C$_5$H$_5$)][BF$_4$] **13**

Atom	Angle	Atom	Angle
C(1)-Re(1)-P(1)	101.6(5)	C(2)-Re(1)-P(1)	136.1(6)
C(2)-Re(1)-C(1)	34.6(7)	C(3)-Re(1)-P(1)	141.6(7)
C(3)-Re(1)-C(1)	59.4(9)	C(3)-Re(1)-C(2)	37.1(10)
C(4)-Re(1)-P(1)	106.0(7)	C(4)-Re(1)-C(1)	59.3(9)
C(4)-Re(1)-C(2)	60.4(9)	C(4)-Re(1)-C(3)	36.0(9)
C(5)-Re(1)-P(1)	85.6(5)	C(5)-Re(1)-C(1)	35.1(7)
C(5)-Re(1)-C(2)	58.8(8)	C(5)-Re(1)-C(3)	59.4(8)
C(5)-Re(1)-C(4)	35.8(9)	C(6)-Re(1)-P(1)	76.9(4)
C(6)-Re(1)-C(1)	161.0(6)	C(6)-Re(1)-C(2)	144.0(6)
C(6)-Re(1)-C(3)	110.0(9)	C(6)-Re(1)-C(4)	102.4(8)
C(6)-Re(1)-C(5)	126.6(7)	C(7)-Re(1)-P(1)	109.7(4)
C(7)-Re(1)-C(1)	148.7(5)	C(7)-Re(1)-C(2)	114.1(7)
C(7)-Re(1)-C(3)	94.5(8)	C(7)-Re(1)-C(4)	110.7(9)
C(7)-Re(1)-C(5)	146.4(6)	C(7)-Re(1)-C(6)	38.3(4)
C(8)-Re(1)-P(1)	113.7(4)	C(8)-Re(1)-C(1)	126.9(7)
C(8)-Re(1)-C(2)	100.0(7)	C(8)-Re(1)-C(3)	103.7(8)
C(8)-Re(1)-C(4)	135.6(8)	C(8)-Re(1)-C(5)	158.7(5)
C(8)-Re(1)-C(6)	69.3(5)	C(8)-Re(1)-C(7)	37.2(4)
C(9)-Re(1)-P(1)	85.7(4)	C(9)-Re(1)-C(1)	111.3(7)
C(9)-Re(1)-C(2)	105.7(8)	C(9)-Re(1)-C(3)	131.2(8)
C(9)-Re(1)-C(4)	165.9(6)	C(9)-Re(1)-C(5)	141.3(6)
C(9)-Re(1)-C(6)	87.6(5)	C(9)-Re(1)-C(7)	71.3(6)
C(9)-Re(1)-C(8)	39.4(4)	C(22)-P(1)-Re(1)	104.2(4)
C(23)-P(1)-Re(1)	118.2(5)	C(23)-P(1)-C(22)	100.9(6)
C(29)-P(1)-Re(1)	118.3(5)	C(29)-P(1)-C(22)	110.4(6)
C(29)-P(1)-C(23)	103.5(6)	C(2)-C(1)-Re(1)	72.1(12)
C(5)-C(1)-Re(1)	72.9(12)	C(5)-C(1)-C(2)	110.0(20)
C(1)-C(2)-Re(1)	73.3(11)	C(3)-C(2)-Re(1)	72.1(12)
C(3)-C(2)-C(1)	107.8(20)	C(2)-C(3)-Re(1)	70.8(14)
C(4)-C(3)-Re(1)	74.0(13)	C(4)-C(3)-C(2)	107.2(21)
C(3)-C(4)-Re(1)	70.0(15)	C(5)-C(4)-Re(1)	70.4(12)
C(5)-C(4)-C(3)	105.5(20)	C(1)-C(5)-Re(1)	72.0(13)
C(4)-C(5)-Re(1)	73.8(14)	C(4)-C(5)-C(1)	109.5(18)
C(7)-C(6)-Re(1)	72.5(8)	C(17)-C(6)-Re(1)	116.6(8)
C(17)-C(6)-C(7)	122.6(11)	C(6)-C(7)-Re(1)	69.2(7)
C(8)-C(7)-Re(1)	71.6(7)	C(8)-C(7)-C(6)	122.0(11)
C(7)-C(8)-Re(1)	71.2(7)	C(9)-C(8)-Re(1)	59.4(7)
C(9)-C(8)-C(7)	117.6(10)	C(10)-C(8)-Re(1)	131.3(9)
C(10)-C(8)-C(7)	118.3(10)	C(10)-C(8)-C(9)	122.5(11)
C(8)-C(9)-Re(1)	81.2(7)	C(11)-C(9)-Re(1)	149.3(9)
C(11)-C(9)-C(8)	127.4(11)	C(12)-C(11)-C(9)	119.3(12)
C(16)-C(11)-C(9)	121.4(12)	C(16)-C(11)-C(12)	119.3(11)
C(13)-C(12)-C(11)	121.0(14)	C(14)-C(13)-C(12)	118.1(16)
C(15)-C(14)-C(13)	121.8(16)	C(16)-C(15)-C(14)	120.1(15)
C(15)-C(16)-C(11)	119.5(13)	C(18)-C(17)-C(6)	122.5(10)
C(22)-C(17)-C(6)	119.4(11)	C(22)-C(17)-C(18)	117.6(10)
C(19)-C(18)-C(17)	119.5(12)	C(20)-C(19)-C(18)	122.3(14)
C(21)-C(20)-C(19)	118.4(12)	C(22)-C(21)-C(20)	120.5(12)
C(17)-C(22)-P(1)	112.2(8)	C(21)-C(22)-P(1)	126.0(9)
C(21)-C(22)-C(17)	121.6(11)	C(24)-C(23)-P(1)	118.3(9)
C(28)-C(23)-P(1)	123.4(9)	C(28)-C(23)-C(24)	117.9(11)

TABLE 7.20 cont.

Atom	Angle	Atom	Angle
C(25)-C(24)-C(23)	121.2(12)	C(26)-C(25)-C(24)	121.2(12)
C(27)-C(26)-C(25)	117.7(12)	C(28)-C(27)-C(26)	121.5(12)
C(27)-C(28)-C(23)	120.4(11)	C(30)-C(29)-P(1)	123.5(10)
C(34)-C(29)-P(1)	115.7(9)	C(34)-C(29)-C(30)	120.8(11)
C(31)-C(30)-C(29)	119.0(14)	C(32)-C(31)-C(30)	119.8(14)
C(33)-C(32)-C(31)	120.6(14)	C(34)-C(33)-C(32)	121.5(15)
C(33)-C(34)-C(29)	118.3(12)	F(2)-B(1)-F(1)	109.4(10)
F(3)-B(1)-F(1)	109.5(10)	F(3)-B(1)-F(2)	
F(4)-B(1)-F(1)	109.4(10)	F(4)-B(1)-F(2)	109.4(9)
F(4)-B(1)-F(3)	109.5(11)	H(11)-C(1)-Re(1)	122.9(18)
C(2)-C(1)-H(11)	125.5(23)	C(5)-C(1)-H(11)	124.5(21)
H(21)-C(2)-Re(1)	118.8(20)	H(21)-C(2)-C(1)	125.4(27)
C(3)-C(2)-H(21)	126.7(26)	H(31)-C(3)-Re(1)	120.1(24)
H(31)-C(3)-C(2)	126.0(33)	C(4)-C(3)-H(31)	126.8(37)
H(41)-C(4)-Re(1)	125.0(25)	H(41)-C(4)-C(3)	125.3(34)
C(5)-C(4)-H(41)	129.2(32)	H(51)-C(5)-Re(1)	120.3(18)
H(51)-C(5)-C(1)	126.4(25)	H(51)-C(5)-C(4)	124.2(26)
H(61)-C(6)-Re(1)	111.1(78)	C(7)-C(6)-H(61)	104.6(68)
C(17)-C(6)-H(61)	120.0(71)	H(71)-C(7)-Re(1)	118.5(61)
H(71)-C(7)-C(6)	119.4(61)	C(8)-C(7)-H(71)	116.4(61)
H(101)-C(10)-C(8)	109.7(14)	H(102)-C(10)-C(8)	109.2(15)
H(102)-C(10)-H(101)	109.5(18)	H(103)-C(10)-C(8)	109.5(15)
H(103)-C(10)-H(101)	109.5(19)	H(103)-C(10)-H(102)	109.5(18)
H(121)-C(12)-C(11)	119.6(15)	C(13)-C(12)-H(121)	119.4(17)
H(131)-C(13)-C(12)	120.9(20)	C(14)-C(13)-H(131)	120.9(19)
H(141)-C(14)-C(13)	118.7(24)	C(15)-C(14)-H(141)	119.5(25)
H(151)-C(15)-C(14)	119.8(18)	C(16)-C(15)-H(151)	120.1(18)
H(161)-C(16)-C(11)	119.9(15)	H(161)-C(16)-C(15)	120.6(16)
H(181)-C(18)-C(17)	120.2(14)	C(19)-C(18)-H(181)	120.4(16)
H(191)-C(19)-C(18)	118.8(17)	C(20)-C(19)-H(191)	118.9(15)
H(201)-C(20)-C(19)	120.8(17)	C(21)-C(20)-H(201)	120.8(18)
H(211)-C(21)-C(20)	119.0(14)	C(22)-C(21)-H(211)	120.5(15)
H(241)-C(24)-C(23)	119.7(14)	C(25)-C(24)-H(241)	119.1(14)
H(251)-C(25)-C(24)	120.2(16)	C(26)-C(25)-H(251)	118.6(15)
H(261)-C(26)-C(25)	121.5(15)	C(27)-C(26)-H(261)	120.7(16)
H(271)-C(27)-C(26)	119.1(15)	C(28)-C(27)-H(271)	119.4(15)
H(281)-C(28)-C(23)	120.3(14)	H(281)-C(28)-C(27)	119.3(15)
H(301)-C(30)-C(29)	121.3(14)	C(31)-C(30)-H(301)	119.8(15)
H(311)-C(31)-C(30)	120.1(20)	C(32)-C(31)-H(311)	120.1(19)
H(321)-C(32)-C(31)	119.3(20)	C(33)-C(32)-H(321)	120.1(20)
H(331)-C(33)-C(32)	119.4(15)	C(34)-C(33)-H(331)	119.1(16)
H(341)-C(34)-C(29)	120.8(14)	H(341)-C(34)-C(33)	120.9(16)

7.6 Crystal Structure Determination of [Re{η^4-CH(Ph)=C(Ph) CH=CH($C_6H_4PPh_2$-o)}(η-C_5H_5)] 15.

A crystal of approximate dimensions 0.2 x 0.2 x 0.25 mm was used for data collection.

Crystal Data : $C_{39}H_{32}PRe$, M = 717.82, monoclinic, a = 11.100(3), b = 17.539(4), c = 16.023(4) Å, β = 105.78(2)°, U = 3001.8(13) Å^3, space group $P2_1/c$, Z = 4, D_c = 1.588 gcm^{-3}, μ(Mo-K_α) = 4.128 mm^{-1}, F(000) = 1424. Data were measured at room temperature on a CAD4 automatic four-circle diffractometer in the range $2 \leq \theta \leq 24°$. Data were corrected for Lorentz and polarisation effects also for X-ray absorption effects.[iii] (Max. and min absorption corrections; 1.00 and 0.467, respectively). The structure was solved by Patterson methods and refined using the SHELX[i,ii] suite of programs. In the final least squares cycles all atoms were allowed to vibrate anisotropically. Hydrogen atoms were included at calculated positions except those hydrogens attached to C6, C7 and C9. These hydrogens (H61, H71 and H91) were located in the penultimate difference Fourier map and refined at a distance of 0.98Å from the relevant parent atoms. The solution of the structure[iv] and refinement[v] converged to conventional [i.e. based on 3613 with $F_0 > 4\sigma(F_0)$] R = 0.0402 and R_w = 0.1397. Goodness of fit = 1.083. The max. and min. residual densities were 1.631 and -0.830 eÅ^{-3}, respectively. Final fractional atomic coordinates and isotropic thermal parameters, bond distances and angles are listed in Tables 7.21/7.24, 7.22 and 7.23, respectively. The asymmetric unit is shown in Figure 2.68 (Section 2.8), along with the labelling scheme employed.

---

iv G.M. Sheldrick, *Acta Cryst.*, 467, A46, **1990**.

v G.M. Sheldrick, *J. Appl. Cryst.*, in preparation, **1995**

Table 7.21 : Atomic coordinates (x 10^4) and equivalent isotropic displacement parameters ($Å^2$ x 10^3) for [Re{η^4-CH(Ph)=C(Ph)CH=CH($C_6H_4PPh_2$-o)}(η-C_5H_5)] **15**. U(eq) is defined as one third of the trace of the orthogonalized Uij tensor.

Atom	x	y	z	U(eq)
Re(1)	1244(1)	1315(1)	1123(1)	34(1)
P(1)	3054(2)	822(2)	2078(2)	35(1)
C(1)	215(11)	761(7)	1998(9)	57(3)
C(2)	-143(10)	382(7)	1196(8)	49(3)
C(3)	-717(10)	942(7)	560(9)	50(3)
C(4)	-725(10)	1654(7)	1028(8)	49(3)
C(5)	-170(11)	1519(8)	1885(8)	52(3)
C(6)	2438(11)	943(6)	283(7)	41(2)
C(7)	1657(9)	1568(6)	-105(7)	37(2)
C(8)	1581(9)	2273(6)	331(6)	38(2)
C(9)	2433(10)	2370(6)	1166(7)	37(2)
C(10)	3787(9)	994(6)	645(7)	36(2)
C(11)	4328(9)	939(6)	1565(6)	35(2)
C(12)	5602(11)	997(7)	1953(8)	50(3)
C(13)	6364(10)	1124(7)	1427(8)	50(3)
C(14)	5920(10)	1139(7)	534(8)	52(3)
C(15)	4644(11)	1072(8)	134(8)	51(3)
C(16)	721(11)	2883(6)	-152(7)	44(3)
C(17)	1134(16)	3625(7)	-137(9)	62(4)
C(18)	393(15)	4222(7)	-591(8)	63(4)
C(19)	-829(17)	4058(9)	-1022(9)	74(4)
C(20)	-1273(15)	3330(10)	-1057(9)	72(4)
C(21)	-528(12)	2736(7)	-627(7)	51(3)
C(22)	2327(10)	3041(6)	1721(7)	40(2)
C(23)	1202(12)	3296(7)	1839(8)	51(3)
C(24)	1130(12)	3931(8)	2354(9)	58(3)
C(25)	2207(13)	4307(7)	2757(8)	56(3)
C(26)	3303(12)	4088(8)	2635(8)	58(3)
C(27)	3371(11)	3450(7)	2119(8)	49(3)
C(28)	2983(9)	-203(6)	2268(7)	41(3)
C(29)	2643(12)	-487(8)	2985(9)	59(3)
C(30)	2547(16)	-1266(8)	3101(10)	78(5)
C(31)	2855(17)	-1770(9)	2570(12)	89(6)
C(32)	3167(16)	-1498(8)	1838(11)	79(5)
C(33)	3253(11)	-734(6)	1674(7)	49(3)
C(34)	3712(11)	1173(7)	3182(6)	43(3)
C(35)	3268(12)	1837(7)	3463(8)	51(3)
C(36)	3835(12)	2128(8)	4296(9)	60(3)
C(37)	4777(17)	1741(11)	4834(10)	86(5)
C(38)	5212(14)	1064(9)	4582(9)	70(4)
C(39)	4710(13)	785(9)	3770(8)	66(4)

Table 7. 22 : Bond lengths [Å] for [Re{η^4-CH(Ph)=C(Ph)CH=CH($C_6H_4PPh_2$-o)}(η-C_5H_5)] **15**

Atom	Bond Length	Atom	Bond Length
Re(1)-C(7)	2.184(11)	C(12)-C(13)	1.36(2)
Re(1)-C(8)	2.199(10)	C(13)-C(14)	1.38(2)
Re(1)-C(3)	2.216(11)	C(14)-C(15)	1.39(2)
Re(1)-C(6)	2.229(11)	C(16)-C(17)	1.38(2)
Re(1)-C(4)	2.230(10)	C(16)-C(21)	1.41(2)
Re(1)-C(1)	2.254(12)	C(17)-C(18)	1.41(2)
Re(1)-C(5)	2.263(11)	C(18)-C(19)	1.38(2)
Re(1)-C(9)	2.264(9)	C(19)-C(20)	1.36(3)
Re(1)-C(2)	2.270(10)	C(20)-C(21)	1.39(2)
Re(1)-P(1)	2.335(3)	C(22)-C(27)	1.37(2)
P(1)-C(34)	1.828(10)	C(22)-C(23)	1.39(2)
P(1)-C(28)	1.829(11)	C(23)-C(24)	1.40(2)
P(1)-C(11)	1.831(10)	C(24)-C(25)	1.36(2)
C(1)-C(5)	1.39(2)	C(25)-C(26)	1.34(2)
C(1)-C(2)	1.41(2)	C(26)-C(27)	1.40(2)
C(2)-C(3)	1.43(2)	C(28)-C(29)	1.40(2)
C(3)-C(4)	1.46(2)	C(28)-C(33)	1.42(2)
C(4)-C(5)	1.36(2)	C(29)-C(30)	1.39(2)
C(6)-C(7)	1.43(2)	C(30)-C(31)	1.33(3)
C(6)-C(10)	1.45(2)	C(31)-C(32)	1.39(3)
C(7)-C(8)	1.43(2)	C(32)-C(33)	1.38(2)
C(8)-C(9)	1.424(14)	C(34)-C(35)	1.39(2)
C(8)-C(16)	1.500(14)	C(34)-C(39)	1.42(2)
C(9)-C(22)	1.50(2)	C(35)-C(36)	1.41(2)
C(10)-C(15)	1.42(2)	C(36)-C(37)	1.35(2)
C(10)-C(11)	1.435(14)	C(37)-C(38)	1.38(2)
C(11)-C(12)	1.38(2)	C(38)-C(39)	1.36(2)

TABLE 7.23: Bond Angles (°) for [Re{η^1-CH(Ph)=C(Ph)CH=CH($C_6H_4PPh_2$-o)}(η-C_5H_5)] **15**

Atom	Angle	Atom	Angle
C(7)-Re(1)-C(8)	38.2(4)	C(3)-C(4)-Re(1)	70.3(6)
C(7)-Re(1)-C(3)	96.7(4)	C(4)-C(5)-C(1)	109.6(11)
C(8)-Re(1)-C(3)	107.0(4)	C(4)-C(5)-Re(1)	71.0(6)
C(7)-Re(1)-C(6)	37.8(4)	C(1)-C(5)-Re(1)	71.7(7)
C(8)-Re(1)-C(6)	69.6(4)	C(7)-C(6)-C(10)	124.4(10)
C(3)-Re(1)-C(6)	110.4(4)	C(7)-C(6)-Re(1)	69.4(6)
C(7)-Re(1)-C(4)	109.0(4)	C(10)-C(6)-Re(1)	117.2(8)
C(8)-Re(1)-C(4)	94.2(4)	C(6)-C(7)-C(8)	123.9(9)
C(3)-Re(1)-C(4)	38.3(5)	C(6)-C(7)-Re(1)	72.8(6)
C(6)-Re(1)-C(4)	140.3(4)	C(8)-C(7)-Re(1)	71.5(6)
C(7)-Re(1)-C(1)	156.0(4)	C(9)-C(8)-C(7)	116.7(9)
C(8)-Re(1)-C(1)	152.0(4)	C(9)-C(8)-C(16)	124.4(10)
C(3)-Re(1)-C(1)	61.2(5)	C(7)-C(8)-C(16)	118.5(9)
C(6)-Re(1)-C(1)	137.3(5)	C(9)-C(8)-Re(1)	73.9(6)
C(4)-Re(1)-C(1)	60.3(5)	C(7)-C(8)-Re(1)	70.4(6)
C(7)-Re(1)-C(5)	143.1(5)	C(16)-C(8)-Re(1)	131.2(8)
C(8)-Re(1)-C(5)	116.3(5)	C(8)-C(9)-C(22)	120.9(10)
C(3)-Re(1)-C(5)	61.2(5)	C(8)-C(9)-Re(1)	68.9(6)
C(6)-Re(1)-C(5)	170.3(4)	C(22)-C(9)-Re(1)	121.4(7)
C(4)-Re(1)-C(5)	35.3(5)	C(15)-C(10)-C(11)	116.1(9)
C(1)-Re(1)-C(5)	35.9(5)	C(15)-C(10)-C(6)	123.6(10)
C(7)-Re(1)-C(9)	66.3(4)	C(11)-C(10)-C(6)	120.3(9)
C(8)-Re(1)-C(9)	37.2(4)	C(12)-C(11)-C(10)	123.2(10)
C(3)-Re(1)-C(9)	138.9(4)	C(12)-C(11)-P(1)	128.7(9)
C(6)-Re(1)-C(9)	79.6(4)	C(10)-C(11)-P(1)	108.1(7)
C(4)-Re(1)-C(9)	109.6(4)	C(13)-C(12)-C(11)	117.6(11)
C(1)-Re(1)-C(9)	136.3(4)	C(12)-C(13)-C(14)	122.5(11)
C(5)-Re(1)-C(9)	109.8(4)	C(13)-C(14)-C(15)	120.4(11)
C(7)-Re(1)-C(2)	120.3(4)	C(14)-C(15)-C(10)	120.0(11)
C(8)-Re(1)-C(2)	143.5(4)	C(17)-C(16)-C(21)	117.1(11)
C(3)-Re(1)-C(2)	37.2(4)	C(17)-C(16)-C(8)	120.2(11)
C(6)-Re(1)-C(2)	110.1(4)	C(21)-C(16)-C(8)	122.7(10)
C(4)-Re(1)-C(2)	62.0(4)	C(16)-C(17)-C(18)	123(2)
C(1)-Re(1)-C(2)	36.2(5)	C(19)-C(18)-C(17)	117.5(14)
C(5)-Re(1)-C(2)	60.5(5)	C(20)-C(19)-C(18)	120.9(13)
C(9)-Re(1)-C(2)	170.2(4)	C(19)-C(20)-C(21)	121.4(14)
C(7)-Re(1)-P(1)	108.2(3)	C(20)-C(21)-C(16)	119.6(13)
C(8)-Re(1)-P(1)	114.2(3)	C(27)-C(22)-C(23)	116.6(10)
C(3)-Re(1)-P(1)	137.1(3)	C(27)-C(22)-C(9)	119.8(10)
C(6)-Re(1)-P(1)	75.0(3)	C(23)-C(22)-C(9)	123.6(10)
C(4)-Re(1)-P(1)	142.8(3)	C(22)-C(23)-C(24)	122.3(11)
C(1)-Re(1)-P(1)	85.7(4)	C(25)-C(24)-C(23)	118.7(12)
C(5)-Re(1)-P(1)	107.7(4)	C(26)-C(25)-C(24)	120.4(12)
C(9)-Re(1)-P(1)	83.8(3)	C(25)-C(26)-C(27)	120.7(11)
C(2)-Re(1)-P(1)	100.0(3)	C(22)-C(27)-C(26)	121.3(11)
C(34)-P(1)-C(28)	101.2(5)	C(29)-C(28)-C(33)	118.2(11)
C(34)-P(1)-C(11)	104.0(5)	C(29)-C(28)-P(1)	121.4(10)
C(28)-P(1)-C(11)	105.0(5)	C(33)-C(28)-P(1)	120.4(8)
C(34)-P(1)-Re(1)	123.7(4)	C(30)-C(29)-C(28)	120.6(14)
C(28)-P(1)-Re(1)	113.9(3)	C(31)-C(30)-C(29)	122(2)
C(11)-P(1)-Re(1)	107.2(3)	C(30)-C(31)-C(32)	118.4(14)
C(5)-C(1)-C(2)	109.4(12)	C(33)-C(32)-C(31)	123(2)

TABLE 7.23 cont.

Atom	Angle	Atom	Angle
C(5)-C(1)-Re(1)	72.4(7)	C(32)-C(33)-C(28)	118.1(13)
C(2)-C(1)-Re(1)	72.5(7)	C(35)-C(34)-C(39)	118.0(10)
C(1)-C(2)-C(3)	106.6(11)	C(35)-C(34)-P(1)	120.9(9)
C(1)-C(2)-Re(1)	71.3(6)	C(39)-C(34)-P(1)	121.0(9)
C(3)-C(2)-Re(1)	69.3(6)	C(34)-C(35)-C(36)	120.4(12)
C(2)-C(3)-C(4)	106.6(11)	C(37)-C(36)-C(35)	119.6(13)
C(2)-C(3)-Re(1)	73.5(6)	C(36)-C(37)-C(38)	121.2(13)
C(4)-C(3)-Re(1)	71.4(6)	C(39)-C(38)-C(37)	120.2(14)
C(5)-C(4)-C(3)	107.7(11)	C(38)-C(39)-C(34)	120.4(14)
C(5)-C(4)-Re(1)	73.7(6)		

Table 7.24: Hydrogen coordinates (x 10^4) and isotropic displacement parameters ($Å^2$ x 10^3) for [Re{η^4-CH(Ph)=C(Ph)CH=CH($C_6H_4PPh_2$-o)}(η-C_5H_5)] **15**

Atom	x	y	z	U(eq)
H(1)	643(11)	541(7)	2522(9)	69
H(2)	-30(10)	-132(7)	1096(8)	59
H(3)	-1024(10)	866(7)	-34(9)	60
H(4)	-1051(10)	2117(7)	786(8)	59
H(5)	-65(11)	1877(8)	2326(8)	62
H(61)	2323(104)	488(39)	-84(60)	50
H(71)	971(71)	1516(63)	-633(42)	44
H(91)	3334(28)	2312(60)	1251(70)	44
H(12)	5926(11)	952(7)	2551(8)	59
H(13)	7213(10)	1203(7)	1680(8)	60
H(14)	6478(10)	1194(7)	198(8)	62
H(15)	4352(11)	1078(8)	-467(8)	61
H(17)	1943(16)	3737(7)	191(9)	74
H(18)	718(15)	4710(7)	-600(8)	76
H(19)	-1359(17)	4448(9)	-1294(9)	89
H(20)	-2092(15)	3230(10)	-1375(9)	86
H(21)	-851(12)	2244(7)	-652(7)	61
H(23)	470(12)	3036(7)	1567(8)	62
H(24)	363(12)	4093(8)	2419(9)	70
H(25)	2180(13)	4718(7)	3118(8)	67
H(26)	4027(12)	4361(8)	2894(8)	69
H(27)	4142(11)	3304(7)	2047(8)	59
H(29)	2479(12)	-151(8)	3390(9)	71
H(30)	2260(16)	-1442(8)	3560(10)	94
H(31)	2861(17)	-2290(9)	2686(12)	106
H(32)	3325(16)	-1849(8)	1445(11)	94
H(33)	3481(11)	-568(6)	1186(7)	59
H(35)	2592(12)	2091(7)	3099(8)	61
H(36)	3559(12)	2585(8)	4473(9)	72
H(37)	5143(17)	1932(11)	5386(10)	103
H(38)	5850(14)	798(9)	4969(9)	84
H(39)	5023(13)	337(9)	3598(8)	79

7.7 Crystal Structure Determination of $[ReH_2(\eta^4\text{-}C_4Ph_4)(\eta\text{-}C_5H_5)]$ 20

A crystal of approximate dimensions 0.2 x 0.2 x 0.1 mm was used for data collection.

Crystal Data : $C_{33}H_{27}Re$, $M = 609.6$, monoclinic, $a = 10.037(1)$, $b = 26.110(4)$, $c = 18.967(3)$ Å, $\beta = 98.34(2)°$, $U = 4918.0$ Å^3, space group $P2_1/n$, $Z = 8$, $D_c = 1.65$ gcm^{-3}, μ(Mo-K_α) = 47.5 cm^{-1}, $F(000) = 2400$. Data were measured at room temperature on a CAD4 automatic four-circle diffractometer in the range $2 \leq \theta \leq 24°$. 8043 reflections were collected of which 5358 were unique with $I \geq 2\sigma(I)$. Data were corrected for Lorentz and polarisation effects also for absorption effects.[iii] (Max. and min. absorption corrections; 1.153 and 0.829, respectively). The structure was solved by Patterson methods and refined using the SHELX[i,ii] suite of programs. The asymmetric unit consisted of two molecules which were treated as separate blocks in the latter stages of convergence. In the final least squares cycles all atoms were allowed to vibrate anisotropically. Hydrogen atoms were included at calculated positions on relevant carbon atoms. Unfortunately, the metal hydride ligands could not be located, even by considering a difference Fourier map based on low angle data. Final residues after 12 cycles of a blocked-matrix least squares were $R = 0.0315$, $R_w = 0.0301$, for a weighting scheme of $w = 1.9052/[\sigma^2(F) + 0.000440(F)^2]$. Max. final shift/esd was 0.001. The max. and min. residual densities were 0.38 and -0.32 eÅ^{-3}, respectively. Final fractional atomic coordinates and isotropic thermal parameters, bond distances and angles are listed in Tables 7.25/7.26, 7.26 and 7.28, respectively. The asymmetric unit is shown in Figure 3.22 (Section 3.3), along with the labelling scheme employed.

TABLE 7.25 : Fractional atomic co-ordinates ($x10^4$) and equivalent isotropic temperature factors ($Å^2 x10^3$) for $[ReH_2(\eta^4\text{-}C_4Ph_4)(\eta\text{-}C_5H_5)]$ **20**

Atom	x	y	z	U
Re(1)	699.4(3)	1292.0(1)	1870.3(1)	40.0(2)
C(1)	222(9)	1863(4)	2706(5)	75(4)
C(2)	1171(8)	1497(3)	3032(4)	58(3)
C(3)	2356(8)	1560(3)	2711(4)	55(3)
C(4)	2111(9)	1952(3)	2200(4)	63(3)
C(5)	796(11)	2137(3)	2210(5)	77(4)
C(6)	189(7)	711(2)	1062(3)	39(2)
C(7)	1495(6)	937(3)	988(3)	40(2)
C(8)	2072(6)	666(3)	1646(3)	39(2)
C(9)	762(6)	463(2)	1739(3)	36(2)
C(11)	-925(4)	634(2)	-182(2)	48(2)
C(12)	-2064(4)	568(2)	-690(2)	56(3)
C(13)	-3326(4)	507(2)	-474(2)	62(3)
C(14)	-3448(4)	513(2)	249(2)	59(3)
C(15)	-2309(4)	579(2)	757(2)	47(3)
C(10)	-1047(4)	640(2)	542(2)	39(2)
C(17)	2753(5)	854(2)	-28(3)	60(3)
C(18)	3184(5)	1047(2)	-642(3)	76(4)
C(19)	2900(5)	1553(2)	-847(3)	68(3)
C(20)	2186(5)	1866(2)	-438(3)	78(4)
C(21)	1755(5)	1673(2)	177(3)	60(3)
C(16)	2038(5)	1167(2)	382(3)	40(2)
C(23)	3811(4)	104(2)	2319(2)	45(2)
C(24)	5144(4)	-9(2)	2592(2)	57(3)
C(25)	6162(4)	341(2)	2512(2)	64(3)
C(26)	5846(4)	803(2)	2158(2)	58(3)
C(27)	4512(4)	916(2)	1884(2)	51(3)
C(22)	3494(4)	566(2)	1965(2)	38(2)
C(29)	673(5)	75(2)	2944(2)	58(3)
C(30)	164(5)	-287(2)	3377(2)	68(3)
C(31)	-749(5)	-656(2)	3074(2)	64(3)
C(32)	-1152(5)	-664(2)	2338(2)	62(3)
C(33)	-643(5)	-302(2)	1906(2)	49(3)
C(28)	270(5)	67(2)	2209(2)	41(2)
Re(2)	7582.9(3)	2733.0(1)	328.9(1)	37.0(2)
C(34)	7450(10)	1872(3)	35(5)	70(4)
C(35)	6125(10)	2079(3)	-18(5)	68(4)
C(36)	5991(8)	2451(3)	-554(4)	59(3)
C(37)	7232(9)	2485(3)	-821(4)	64(3)
C(38)	8122(9)	2130(3)	-451(4)	60(3)
C(39)	7426(6)	3549(3)	467(3)	37(2)
C(40)	8044(6)	3313(3)	1145(3)	38(2)
C(41)	6752(7)	3071(3)	1213(3)	40(2)
C(42)	6135(7)	3337(2)	565(3)	39(2)
C(44)	8534(5)	3941(2)	-526(2)	45(3)
C(45)	8920(5)	4367(2)	-891(2)	58(3)
C(46)	8628(5)	4859(2)	-670(2)	64(3)
C(47)	7950(5)	4924(2)	-85(2)	79(4)
C(48)	7564(5)	4498(2)	280(2)	64(3)
C(43)	7856(5)	4006(2)	60(2)	42(3)
C(50)	10395(5)	3628(2)	1338(2)	54(3)

TABLE 7.25 cont.

Atom	x	y	z	U
C(51)	11571(5)	3754(2)	1791(2)	65(4)
C(52)	11642(5)	3685(2)	2525(2)	67(3)
C(53)	10536(5)	3490(2)	2806(2)	67(3)
C(54)	9360(5)	3364(2)	2353(2)	56(3)
C(49)	9290(5)	3433(2)	1619(2)	39(2)
C(56)	6820(4)	2362(2)	2122(3)	58(3)
C(57)	6405(4)	2150(2)	2730(3)	62(3)
C(58)	5392(4)	2387(2)	3044(3)	60(3)
C(59)	4793(4)	2836(2)	2750(3)	66(3)
C(60)	5208(4)	3047(2)	2142(3)	54(3)
C(55)	6221(4)	2810(2)	1828(3)	43(2)
C(62)	4531(5)	3768(2)	-355(3)	58(3)
C(63)	3233(5)	3847(2)	-714(3)	81(4)
C(64)	2158(5)	3563(2)	-528(3)	86(4)
C(65)	2382(5)	3200(2)	15(3)	82(4)
C(66)	3680(5)	3121(2)	374(3)	63(3)
C(61)	4754(5)	3405(2)	189(3)	44(2)

TABLE 7.26 : Hydrogen fractional atomic co-ordinates ($x10^4$) and isotropic temperature factors ($Å^2 x10^3$) for $[ReH_2(\eta^4\text{-}C_4Ph_4)(\eta\text{-}C_5H_5)]$ **20**

Atom	x	y	z	U
H(11)	-675(9)	1910(4)	2815(5)	81(5)
H(21)	1037(8)	1255(3)	3397(4)	81(5)
H(31)	3176(8)	1368(3)	2822(4)	81(5)
H(41)	2732(9)	2073(3)	1898(4)	81(5)
H(51)	373(11)	2410(3)	1920(5)	81(5)
H(111)	-56(4)	676(2)	-330(2)	81(5)
H(121)	-1979(4)	564(2)	-1187(2)	81(5)
H(131)	-4109(4)	461(2)	-824(2)	81(5)
H(141)	-4317(4)	471(2)	397(2)	81(5)
H(151)	-2394(4)	583(2)	1255(2)	81(5)
H(171)	2948(5)	506(2)	114(3)	81(5)
H(181)	3675(5)	832(2)	-924(3)	81(5)
H(191)	3197(5)	1686(2)	-1270(3)	81(5)
H(201)	1991(5)	2214(2)	-579(3)	81(5)
H(211)	1264(5)	1888(2)	459(3)	81(5)
H(231)	3110(4)	-137(2)	2374(2)	81(5)
H(241)	5362(4)	-327(2)	2836(2)	81(5)
H(251)	7080(4)	264(2)	2700(2)	81(5)
H(261)	6546(4)	1044(2)	2103(2)	81(5)
H(271)	4294(4)	1234(2)	1641(2)	81(5)
H(291)	1301(5)	329(2)	3153(2)	81(5)
H(301)	442(5)	-282(2)	3883(2)	81(5)
H(311)	-1099(5)	-905(2)	3371(2)	81(5)
H(321)	-1780(5)	-918(2)	2130(2)	81(5)
H(331)	-921(5)	-307(2)	1400(2)	81(5)
H(341)	7813(10)	1603(3)	349(5)	81(5)
H(351)	5445(10)	1982(3)	264(5)	81(5)
H(361)	5199(8)	2650(3)	-712(4)	81(5)
H(371)	7429(9)	2709(3)	-1194(4)	81(5)
H(381)	9040(9)	2076(3)	-520(4)	81(5)
H(441)	8736(5)	3602(2)	-678(2)	81(5)
H(451)	9387(5)	4322(2)	-1294(2)	81(5)
H(461)	8893(5)	5152(2)	-921(2)	81(5)
H(471)	7748(5)	5263(2)	68(2)	81(5)
H(481)	7097(5)	4543(2)	684(2)	81(5)
H(501)	10347(5)	3675(2)	833(2)	81(5)
H(511)	12332(5)	3888(2)	1598(2)	81(5)
H(521)	12451(5)	3772(2)	2837(2)	81(5)
H(531)	10585(5)	3442(2)	3311(2)	81(5)
H(541)	8599(5)	3229(2)	2546(2)	81(5)
H(561)	7517(4)	2199(2)	1907(3)	81(5)
H(571)	6817(4)	1841(2)	2932(3)	81(5)
H(581)	5106(4)	2241(2)	3462(3)	81(5)
H(591)	4096(4)	2999(2)	2965(3)	81(5)
H(601)	4796(4)	3356(2)	1940(3)	81(5)
H(621)	5270(5)	3963(2)	-483(3)	81(5)
H(631)	3079(5)	4097(2)	-1088(3)	81(5)
H(641)	1265(5)	3618(2)	-775(3)	81(5)
H(651)	1642(5)	3005(2)	143(3)	81(5)
H(661)	3834(5)	2871(2)	748(3)	81(5)

TABLE 7.27 : Bond lengths (Å) for $[ReH_2(\eta^4\text{-}C_4Ph_4)(\eta\text{-}C_5H_5)]$ **20**

Atom	Bond Length	Atom	Bond Length
C(1)-Re(1)	2.277(12)	C(2)-Re(1)	2.250(9)
C(3)-Re(1)	2.241(9)	C(4)-Re(1)	2.261(11)
C(5)-Re(1)	2.297(11)	C(6)-Re(1)	2.164(8)
C(7)-Re(1)	2.164(9)	C(8)-Re(1)	2.219(9)
C(9)-Re(1)	2.181(8)	C(2)-C(1)	1.426(13)
C(5)-C(1)	1.373(16)	C(3)-C(2)	1.423(13)
C(4)-C(3)	1.407(12)	C(5)-C(4)	1.408(15)
C(7)-C(6)	1.462(10)	C(8)-C(6)	2.051(11)
C(9)-C(6)	1.480(9)	C(10)-C(6)	1.481(8)
C(8)-C(7)	1.478(10)	C(9)-C(7)	2.099(11)
C(16)-C(7)	1.471(10)	C(9)-C(8)	1.452(10)
C(22)-C(8)	1.490(8)	C(28)-C(9)	1.495(9)
C(12)-C(11)	1.395(6)	C(10)-C(11)	1.395(7)
C(13)-C(12)	1.395(7)	C(14)-C(13)	1.395(7)
C(15)-C(14)	1.395(6)	C(10)-C(15)	1.395(7)
C(18)-C(17)	1.395(8)	C(16)-C(17)	1.395(8)
C(19)-C(18)	1.395(7)	C(20)-C(19)	1.395(8)
C(21)-C(20)	1.395(8)	C(16)-C(21)	1.395(7)
C(24)-C(23)	1.395(7)	C(22)-C(23)	1.395(7)
C(25)-C(24)	1.395(7)	C(26)-C(25)	1.395(7)
C(27)-C(26)	1.395(7)	C(22)-C(27)	1.395(7)
C(30)-C(29)	1.395(8)	C(28)-C(29)	1.395(7)
C(31)-C(30)	1.395(7)	C(32)-C(31)	1.395(7)
C(33)-C(32)	1.395(8)	C(28)-C(33)	1.395(7)
C(34)-Re(2)	2.315(10)	C(35)-Re(2)	2.282(11)
C(36)-Re(2)	2.264(10)	C(37)-Re(2)	2.254(10)
C(38)-Re(2)	2.278(10)	C(39)-Re(2)	2.156(9)
C(40)-Re(2)	2.167(8)	C(41)-Re(2)	2.166(9)
C(42)-Re(2)	2.233(9)	C(35)-C(34)	1.426(15)
C(38)-C(34)	1.391(14)	C(36)-C(35)	1.398(13)
C(37)-C(36)	1.414(14)	C(38)-C(37)	1.404(13)
C(40)-C(39)	1.479(10)	C(41)-C(39)	2.072(11)
C(42)-C(39)	1.446(10)	C(43)-C(39)	1.518(10)
C(41)-C(40)	1.464(10)	C(42)-C(40)	2.067(11)
C(49)-C(40)	1.464(8)	C(42)-C(41)	1.468(10)
C(55)-C(41)	1.514(10)	C(61)-C(42)	1.474(9)
C(45)-C(44)	1.395(7)	C(43)-C(44)	1.395(8)
C(46)-C(45)	1.395(7)	C(47)-C(46)	1.395(8)
C(48)-C(47)	1.395(7)	C(43)-C(48)	1.395(7)
C(51)-C(50)	1.395(7)	C(49)-C(50)	1.395(8)
C(52)-C(51)	1.395(6)	C(53)-C(52)	1.395(8)
C(54)-C(53)	1.395(7)	C(49)-C(54)	1.395(6)
C(57)-C(56)	1.395(8)	C(55)-C(56)	1.395(7)
C(58)-C(57)	1.395(8)	C(59)-C(58)	1.395(7)
C(60)-C(59)	1.395(8)	C(55)-C(60)	1.395(8)
C(63)-C(62)	1.395(8)	C(61)-C(62)	1.395(8)
C(64)-C(63)	1.395(8)	C(65)-C(64)	1.395(8)
C(66)-C(65)	1.395(8)	C(61)-C(66)	1.395(8)
H(11)-C(1)	0.960(15)	H(21)-C(2)	0.960(12)
H(31)-C(3)	0.960(12)	H(41)-C(4)	0.960(14)
H(51)-C(5)	0.960(14)	H(111)-C(11)	0.960(7)
H(121)-C(12)	0.960(7)	H(131)-C(13)	0.960(6)

TABLE 7.27 cont.

Atom	Bond Length	Atom	Bond Length
H(141)-C(14)	0.960(7)	H(151)-C(15)	0.960(7)
H(171)-C(17)	0.960(7)	H(181)-C(18)	0.960(8)
H(191)-C(19)	0.960(8)	H(201)-C(20)	0.960(7)
H(211)-C(21)	0.960(8)	H(231)-C(23)	0.960(7)
H(241)-C(24)	0.960(7)	H(251)-C(25)	0.960(7)
H(261)-C(26)	0.960(7)	H(271)-C(27)	0.960(7)
H(291)-C(29)	0.960(7)	H(301)-C(30)	0.960(7)
H(311)-C(31)	0.960(8)	H(321)-C(32)	0.960(7)
H(331)-C(33)	0.960(7)	H(341)-C(34)	0.960(13)
H(351)-C(35)	0.960(15)	H(361)-C(36)	0.960(12)
H(371)-C(37)	0.960(13)	H(381)-C(38)	0.960(14)
H(441)-C(44)	0.960(7)	H(451)-C(45)	0.960(8)
H(461)-C(46)	0.960(7)	H(471)-C(47)	0.960(7)
H(481)-C(48)	0.960(8)	H(501)-C(50)	0.960(6)
H(511)-C(51)	0.960(8)	H(521)-C(52)	0.960(7)
H(531)-C(53)	0.960(6)	H(541)-C(54)	0.960(8)
H(561)-C(56)	0.960(8)	H(571)-C(57)	0.960(7)
H(581)-C(58)	0.960(8)	H(591)-C(59)	0.960(8)
H(601)-C(60)	0.960(7)	H(621)-C(62)	0.960(8)
H(631)-C(63)	0.960(8)	H(641)-C(64)	0.960(8)
H(651)-C(65)	0.960(8)	H(661)-C(66)	0.960(8)

TABLE 7.28 : Bond angles (°) for $[ReH_2(\eta^4\text{-}C_4Ph_4)(\eta\text{-}C_5H_5)]$ **20**

Atom	Angle	Atom	Angle
C(2)-Re(1)-C(1)	36.7(3)	C(3)-Re(1)-C(1)	60.7(4)
C(3)-Re(1)-C(2)	36.9(3)	C(4)-Re(1)-C(1)	59.7(4)
C(4)-Re(1)-C(2)	60.9(4)	C(4)-Re(1)-C(3)	36.4(3)
C(5)-Re(1)-C(1)	34.9(4)	C(5)-Re(1)-C(2)	60.2(4)
C(5)-Re(1)-C(3)	60.3(4)	C(5)-Re(1)-C(4)	36.0(4)
C(6)-Re(1)-C(1)	154.1(3)	C(6)-Re(1)-C(2)	148.8(3)
C(6)-Re(1)-C(3)	142.9(3)	C(6)-Re(1)-C(4)	143.5(3)
C(6)-Re(1)-C(5)	150.2(3)	C(7)-Re(1)-C(1)	163.1(3)
C(7)-Re(1)-C(2)	144.1(3)	C(7)-Re(1)-C(3)	111.4(4)
C(7)-Re(1)-C(4)	104.7(4)	C(7)-Re(1)-C(5)	128.5(4)
C(7)-Re(1)-C(6)	39.5(2)	C(8)-Re(1)-C(1)	144.6(3)
C(8)-Re(1)-C(2)	108.3(4)	C(8)-Re(1)-C(3)	87.1(4)
C(8)-Re(1)-C(4)	103.5(4)	C(8)-Re(1)-C(5)	139.4(3)
C(8)-Re(1)-C(6)	55.8(3)	C(8)-Re(1)-C(7)	39.4(2)
C(9)-Re(1)-C(1)	137.9(3)	C(9)-Re(1)-C(2)	110.0(4)
C(9)-Re(1)-C(3)	111.1(4)	C(9)-Re(1)-C(4)	139.5(3)
C(9)-Re(1)-C(5)	170.0(3)	C(9)-Re(1)-C(6)	39.8(2)
C(9)-Re(1)-C(7)	57.8(3)	C(9)-Re(1)-C(8)	38.5(2)
C(2)-C(1)-Re(1)	70.6(6)	C(5)-C(1)-Re(1)	73.3(7)
C(5)-C(1)-C(2)	109.1(9)	C(1)-C(2)-Re(1)	72.7(6)
C(3)-C(2)-Re(1)	71.2(5)	C(3)-C(2)-C(1)	106.5(8)
C(2)-C(3)-Re(1)	71.8(5)	C(4)-C(3)-Re(1)	72.6(5)
C(4)-C(3)-C(2)	107.8(8)	C(3)-C(4)-Re(1)	71.0(6)
C(5)-C(4)-Re(1)	73.4(6)	C(5)-C(4)-C(3)	108.2(9)
C(1)-C(5)-Re(1)	71.7(6)	C(4)-C(5)-Re(1)	70.6(6)
C(4)-C(5)-C(1)	108.5(9)	C(7)-C(6)-Re(1)	70.3(5)
C(8)-C(6)-Re(1)	63.4(4)	C(8)-C(6)-C(7)	46.1(4)
C(9)-C(6)-Re(1)	70.7(4)	C(9)-C(6)-C(7)	91.0(6)
C(9)-C(6)-C(8)	45.0(3)	C(10)-C(6)-Re(1)	130.5(4)
C(10)-C(6)-C(7)	131.6(5)	C(10)-C(6)-C(8)	166.0(5)
C(10)-C(6)-C(9)	134.9(6)	C(6)-C(7)-Re(1)	70.3(5)
C(8)-C(7)-Re(1)	72.3(5)	C(8)-C(7)-C(6)	88.5(6)
C(9)-C(7)-Re(1)	61.5(4)	C(9)-C(7)-C(6)	44.8(3)
C(9)-C(7)-C(8)	43.8(4)	C(16)-C(7)-Re(1)	130.5(4)
C(16)-C(7)-C(6)	132.7(5)	C(16)-C(7)-C(8)	135.4(6)
C(16)-C(7)-C(9)	167.9(5)	C(6)-C(8)-Re(1)	60.8(4)
C(7)-C(8)-Re(1)	68.3(5)	C(7)-C(8)-C(6)	45.4(4)
C(9)-C(8)-Re(1)	69.3(5)	C(9)-C(8)-C(6)	46.1(3)
C(9)-C(8)-C(7)	91.5(6)	C(22)-C(8)-Re(1)	129.5(5)
C(22)-C(8)-C(6)	169.3(5)	C(22)-C(8)-C(7)	131.4(6)
C(22)-C(8)-C(9)	135.9(5)	C(6)-C(9)-Re(1)	69.5(4)
C(7)-C(9)-Re(1)	60.7(4)	C(7)-C(9)-C(6)	44.1(4)
C(8)-C(9)-Re(1)	72.1(5)	C(8)-C(9)-C(6)	88.8(6)
C(8)-C(9)-C(7)	44.7(3)	C(28)-C(9)-Re(1)	126.9(5)
C(28)-C(9)-C(6)	134.5(5)	C(28)-C(9)-C(7)	172.3(5)
C(28)-C(9)-C(8)	135.1(5)	C(10)-C(11)-C(12)	120.0(5)
C(13)-C(12)-C(11)	120.0(5)	C(14)-C(13)-C(12)	120.0(4)
C(15)-C(14)-C(13)	120.0(5)	C(10)-C(15)-C(14)	120.0(5)
C(11)-C(10)-C(6)	118.1(5)	C(15)-C(10)-C(6)	121.9(5)
C(15)-C(10)-C(11)	120.0(4)	C(16)-C(17)-C(18)	120.0(5)
C(19)-C(18)-C(17)	120.0(6)	C(20)-C(19)-C(18)	120.0(6)
C(21)-C(20)-C(19)	120.0(5)	C(16)-C(21)-C(20)	120.0(6)

TABLE 7.28 cont.

Atom	Angle	Atom	Angle
C(17)-C(16)-C(7)	118.4(5)	C(21)-C(16)-C(7)	121.4(6)
C(21)-C(16)-C(17)	120.0(6)	C(22)-C(23)-C(24)	120.0(5)
C(25)-C(24)-C(23)	120.0(5)	C(26)-C(25)-C(24)	120.0(5)
C(27)-C(26)-C(25)	120.0(5)	C(22)-C(27)-C(26)	120.0(5)
C(23)-C(22)-C(8)	119.0(5)	C(27)-C(22)-C(8)	121.0(5)
C(27)-C(22)-C(23)	120.0(5)	C(28)-C(29)-C(30)	120.0(5)
C(31)-C(30)-C(29)	120.0(5)	C(32)-C(31)-C(30)	120.0(5)
C(33)-C(32)-C(31)	120.0(5)	C(28)-C(33)-C(32)	120.0(5)
C(29)-C(28)-C(9)	120.9(5)	C(33)-C(28)-C(9)	119.1(5)
C(33)-C(28)-C(29)	120.0(5)	C(35)-Re(2)-C(34)	36.1(3)
C(36)-Re(2)-C(34)	59.7(4)	C(36)-Re(2)-C(35)	35.8(3)
C(37)-Re(2)-C(34)	59.5(4)	C(37)-Re(2)-C(35)	60.2(4)
C(37)-Re(2)-C(36)	36.5(3)	C(38)-Re(2)-C(34)	35.2(3)
C(38)-Re(2)-C(35)	59.9(4)	C(38)-Re(2)-C(36)	60.2(4)
C(38)-Re(2)-C(37)	36.1(3)	C(39)-Re(2)-C(34)	170.5(3)
C(39)-Re(2)-C(35)	136.0(3)	C(39)-Re(2)-C(36)	110.8(4)
C(39)-Re(2)-C(37)	113.4(4)	C(39)-Re(2)-C(38)	142.3(3)
C(40)-Re(2)-C(34)	148.2(3)	C(40)-Re(2)-C(35)	142.2(3)
C(40)-Re(2)-C(36)	144.1(3)	C(40)-Re(2)-C(37)	151.6(3)
C(40)-Re(2)-C(38)	154.2(3)	C(40)-Re(2)-C(39)	40.0(2)
C(41)-Re(2)-C(34)	124.6(4)	C(41)-Re(2)-C(35)	103.0(4)
C(41)-Re(2)-C(36)	113.3(4)	C(41)-Re(2)-C(37)	147.4(3)
C(41)-Re(2)-C(38)	159.8(3)	C(41)-Re(2)-C(39)	57.3(3)
C(41)-Re(2)-C(40)	39.5(2)	C(42)-Re(2)-C(34)	135.8(3)
C(42)-Re(2)-C(35)	100.2(4)	C(42)-Re(2)-C(36)	88.2(4)
C(42)-Re(2)-C(37)	112.4(4)	C(42)-Re(2)-C(38)	147.2(3)
C(42)-Re(2)-C(39)	38.4(2)	C(42)-Re(2)-C(40)	56.0(3)
C(42)-Re(2)-C(41)	38.9(2)	C(35)-C(34)-Re(2)	70.7(6)
C(38)-C(34)-Re(2)	71.0(6)	C(38)-C(34)-C(35)	107.9(8)
C(34)-C(35)-Re(2)	73.2(6)	C(36)-C(35)-Re(2)	71.4(6)
C(36)-C(35)-C(34)	107.7(9)	C(35)-C(36)-Re(2)	72.8(6)
C(37)-C(36)-Re(2)	71.4(5)	C(37)-C(36)-C(35)	107.9(8)
C(36)-C(37)-Re(2)	72.1(6)	C(38)-C(37)-Re(2)	72.9(6)
C(38)-C(37)-C(36)	107.9(8)	C(34)-C(38)-Re(2)	73.8(6)
C(37)-C(38)-Re(2)	71.0(6)	C(37)-C(38)-C(34)	108.5(9)
C(40)-C(39)-Re(2)	70.4(5)	C(41)-C(39)-Re(2)	61.6(4)
C(41)-C(39)-C(40)	45.0(4)	C(42)-C(39)-Re(2)	73.7(5)
C(42)-C(39)-C(40)	89.9(6)	C(42)-C(39)-C(41)	45.1(4)
C(43)-C(39)-Re(2)	133.1(4)	C(43)-C(39)-C(40)	131.0(5)
C(43)-C(39)-C(41)	165.1(5)	C(43)-C(39)-C(42)	133.9(5)
C(39)-C(40)-Re(2)	69.6(4)	C(41)-C(40)-Re(2)	70.2(5)
C(41)-C(40)-C(39)	89.5(6)	C(42)-C(40)-Re(2)	63.6(3)
C(42)-C(40)-C(39)	44.4(4)	C(42)-C(40)-C(41)	45.2(3)
C(49)-C(40)-Re(2)	131.5(4)	C(49)-C(40)-C(39)	131.1(6)
C(49)-C(40)-C(41)	136.6(6)	C(49)-C(40)-C(42)	164.5(5)
C(39)-C(41)-Re(2)	61.1(4)	C(40)-C(41)-Re(2)	70.3(5)
C(40)-C(41)-C(39)	45.5(3)	C(42)-C(41)-Re(2)	73.0(5)
C(42)-C(41)-C(39)	44.3(4)	C(42)-C(41)-C(40)	89.7(6)
C(55)-C(41)-Re(2)	129.2(5)	C(55)-C(41)-C(39)	169.7(5)
C(55)-C(41)-C(40)	132.6(5)	C(55)-C(41)-C(42)	134.9(6)
C(39)-C(42)-Re(2)	67.9(5)	C(40)-C(42)-Re(2)	60.4(4)
C(40)-C(42)-C(39)	45.7(4)	C(41)-C(42)-Re(2)	68.1(5)
C(41)-C(42)-C(39)	90.6(6)	C(41)-C(42)-C(40)	45.1(4)

TABLE 7.28 cont.

Atom	Angle	Atom	Angle
C(61)-C(42)-Re(2)	125.5(5)	C(61)-C(42)-C(39)	133.5(6)
C(61)-C(42)-C(40)	174.0(5)	C(61)-C(42)-C(41)	135.7(6)
C(43)-C(44)-C(45)	120.0(5)	C(46)-C(45)-C(44)	120.0(5)
C(47)-C(46)-C(45)	120.0(5)	C(48)-C(47)-C(46)	120.0(5)
C(43)-C(48)-C(47)	120.0(5)	C(44)-C(43)-C(39)	121.1(5)
C(48)-C(43)-C(39)	118.9(6)	C(48)-C(43)-C(44)	120.0(5)
C(49)-C(50)-C(51)	120.0(5)	C(52)-C(51)-C(50)	120.0(5)
C(53)-C(52)-C(51)	120.0(5)	C(54)-C(53)-C(52)	120.0(5)
C(49)-C(54)-C(53)	120.0(5)	C(50)-C(49)-C(40)	120.0(5)
C(54)-C(49)-C(40)	120.0(6)	C(54)-C(49)-C(50)	120.0(5)
C(55)-C(56)-C(57)	120.0(5)	C(58)-C(57)-C(56)	120.0(5)
C(59)-C(58)-C(57)	120.0(5)	C(60)-C(59)-C(58)	120.0(5)
C(55)-C(60)-C(59)	120.0(5)	C(56)-C(55)-C(41)	120.5(6)
C(60)-C(55)-C(41)	119.3(5)	C(60)-C(55)-C(56)	120.0(5)
C(61)-C(62)-C(63)	120.0(6)	C(64)-C(63)-C(62)	120.0(5)
C(65)-C(64)-C(63)	120.0(5)	C(66)-C(65)-C(64)	120.0(6)
C(61)-C(66)-C(65)	120.0(5)	C(62)-C(61)-C(42)	118.6(6)
C(66)-C(61)-C(42)	121.4(6)	C(66)-C(61)-C(62)	120.0(5)
H(11)-C(1)-Re(1)	122.1(10)	C(2)-C(1)-H(11)	125.4(12)
C(5)-C(1)-H(11)	125.5(12)	H(21)-C(2)-Re(1)	121.2(9)
H(21)-C(2)-C(1)	126.8(11)	C(3)-C(2)-H(21)	126.7(10)
H(31)-C(3)-Re(1)	121.2(8)	H(31)-C(3)-C(2)	126.1(10)
C(4)-C(3)-H(31)	126.1(11)	H(41)-C(4)-Re(1)	121.3(9)
H(41)-C(4)-C(3)	125.9(11)	C(5)-C(4)-H(41)	125.9(11)
H(51)-C(5)-Re(1)	123.7(10)	H(51)-C(5)-C(1)	125.8(14)
H(51)-C(5)-C(4)	125.7(14)	H(111)-C(11)-C(12)	120.0(6)
H(111)-C(11)-C(10)	120.0(5)	H(121)-C(12)-C(11)	120.0(5)
H(121)-C(12)-C(13)	120.0(5)	H(131)-C(13)-C(12)	120.0(6)
H(131)-C(13)-C(14)	120.0(6)	H(141)-C(14)-C(13)	120.0(5)
H(141)-C(14)-C(15)	120.0(6)	H(151)-C(15)-C(14)	120.0(5)
H(151)-C(15)-C(10)	120.0(5)	H(171)-C(17)-C(18)	120.0(7)
H(171)-C(17)-C(16)	120.0(7)	H(181)-C(18)-C(17)	120.0(6)
H(181)-C(18)-C(19)	120.0(7)	H(191)-C(19)-C(18)	120.0(7)
H(191)-C(19)-C(20)	120.0(6)	H(201)-C(20)-C(19)	120.0(7)
H(201)-C(20)-C(21)	120.0(7)	H(211)-C(21)-C(20)	120.0(6)
H(211)-C(21)-C(16)	120.0(7)	H(231)-C(23)-C(24)	120.0(6)
H(231)-C(23)-C(22)	120.0(6)	H(241)-C(24)-C(23)	120.0(6)
H(241)-C(24)-C(25)	120.0(6)	H(251)-C(25)-C(24)	120.0(6)
H(251)-C(25)-C(26)	120.0(6)	H(261)-C(26)-C(25)	120.0(6)
H(261)-C(26)-C(27)	120.0(6)	H(271)-C(27)-C(26)	120.0(6)
H(271)-C(27)-C(22)	120.0(6)	H(291)-C(29)-C(30)	120.0(6)
H(291)-C(29)-C(28)	120.0(6)	H(301)-C(30)-C(29)	120.0(6)
H(301)-C(30)-C(31)	120.0(6)	H(311)-C(31)-C(30)	120.0(6)
H(311)-C(31)-C(32)	120.0(6)	H(321)-C(32)-C(31)	120.0(6)
H(321)-C(32)-C(33)	120.0(6)	H(331)-C(33)-C(32)	120.0(6)
H(331)-C(33)-C(28)	120.0(6)	H(341)-C(34)-Re(2)	124.0(9)
C(35)-C(34)-H(341)	126.0(13)	C(38)-C(34)-H(341)	126.1(13)
H(351)-C(35)-Re(2)	121.0(9)	H(351)-C(35)-C(34)	126.3(11)
C(36)-C(35)-H(351)	126.0(11)	H(361)-C(36)-Re(2)	121.3(9)
H(361)-C(36)-C(35)	126.2(11)	C(37)-C(36)-H(361)	125.9(11)
H(371)-C(37)-Re(2)	121.2(9)	H(371)-C(37)-C(36)	126.1(11)
C(38)-C(37)-H(371)	126.0(12)	H(381)-C(38)-Re(2)	120.9(9)
H(381)-C(38)-C(34)	125.9(10)	H(381)-C(38)-C(37)	125.7(11)

TABLE 7.28 cont.

Atom	Angle	Atom	Angle
H(441)-C(44)-C(45)	120.0(6)	H(441)-C(44)-C(43)	120.0(6)
H(451)-C(45)-C(44)	120.0(6)	H(451)-C(45)-C(46)	120.0(6)
H(461)-C(46)-C(45)	120.0(6)	H(461)-C(46)-C(47)	120.0(6)
H(471)-C(47)-C(46)	120.0(6)	H(471)-C(47)-C(48)	120.0(6)
H(481)-C(48)-C(47)	120.0(6)	H(481)-C(48)-C(43)	120.0(6)
H(501)-C(50)-C(51)	120.0(6)	H(501)-C(50)-C(49)	120.0(6)
H(511)-C(51)-C(50)	120.0(5)	H(511)-C(51)-C(52)	120.0(6)
H(521)-C(52)-C(51)	120.0(6)	H(521)-C(52)-C(53)	120.0(5)
H(531)-C(53)-C(52)	120.0(6)	H(531)-C(53)-C(54)	120.0(6)
H(541)-C(54)-C(53)	120.0(5)	H(541)-C(54)-C(49)	120.0(6)
H(561)-C(56)-C(57)	120.0(6)	H(561)-C(56)-C(55)	120.0(6)
H(571)-C(57)-C(56)	120.0(7)	H(571)-C(57)-C(58)	120.0(7)
H(581)-C(58)-C(57)	120.0(6)	H(581)-C(58)-C(59)	120.0(6)
H(591)-C(59)-C(58)	120.0(6)	H(591)-C(59)-C(60)	120.0(6)
H(601)-C(60)-C(59)	120.0(7)	H(601)-C(60)-C(55)	120.0(7)
H(621)-C(62)-C(63)	120.0(6)	H(621)-C(62)-C(61)	120.0(6)
H(631)-C(63)-C(62)	120.0(7)	H(631)-C(63)-C(64)	120.0(6)
H(641)-C(64)-C(63)	120.0(7)	H(641)-C(64)-C(65)	120.0(7)
H(651)-C(65)-C(64)	120.0(6)	H(651)-C(65)-C(66)	120.0(6)
H(661)-C(66)-C(65)	120.0(7)	H(661)-C(66)-C(61)	120.0(6)

7.8 Crystal Structure Determination of [ReH{O(C)OCF$_3$}{η^2,η^2-PhC(H)=C(Ph)C(Ph)=C(Ph)H} (η-C$_5$H$_5$)] 22

A crystal of approximate dimensions 0.3 x 0.3 x 0.35 mm was used for data collection.

Crystal Data : $C_{35}H_{28}F_3O_2Re$, M = 723.77, triclinic, a = 13.466(4), b = 18.894(5), c = 22.210(7) Å, α = 109.75(2)°, β = 98.95(3)°, γ = 107.18(3)° U = 4872(3) Å^3, space group P-1 (No. 2), Z = 6, D_c = 0.987 gcm^{-3}, μ(Mo-K_α) = 2.524 mm^{-1}, F(000) = 1424. Crystallographic measurements were made at 293(2)°K on a CAD4 automatic four-circle diffractometer in the range 2.03≤θ≤23.99°. Data (6823 reflections) were corrected for Lorentz and polarisation but not for absorption. The asymmetric unit consisted of three independent organometallic molecules. In the final least squares cycles the rhenium atoms were allowed to vibrate anisotropically. All other atoms were treated isotropically. Hydrogen atoms were included at calculated positions where relevant, except on the terminal butadienyl carbon atoms. The hydrogens on these atoms could not be located, nor could the hydride ligand attached to the metal centre.

Unfortunately, refinement of this structure was severely hampered by many factors. In the first instance, the crystals developed cracks as they grew in solution in what were initially very small gem-like blocks. The crystal batch also had inherent handling difficulties in that the crystals quickly powdered due to solvent loss, and the only remotely "suitable" sample for single-crystal analysis was sub-standard. Poor quality was quickly manifested in broad scan widths during early search routines on the diffractometer. In addition the diffracting ability of the sample fell off rapidly with increasing Bragg angle, and much of the higher angle data collected were flagged as weak, and bore negative intensity. As a consequence of a poor data set, convergence was inhibited, but improved by omitting reflections with negative intensity from the final refinement cycles, treating phenyl groups as rigid hexagons, cyclopentadienyl rings as pentagons, and by restricting the C-C distances

pentagons, and by restricting the C-C distances in the butadiene moieties to 1.42Å. Blocked-matrix refinement attempts proved unstable, and attempts to treat more atoms anisotropically served to yield non-positive definites, due to shrinking thermal parameters. Bond distances and angles are not reliable for comparison purposes, but the structural analysis did attain some of its objectives by providing proof of a novel cyclobutadienyl ring opening reaction, while also confirming the relative configuration of the organic fragments attached to the rhenium centres. The solution of the structure (SHELX86)[iv] and refinement (SHELX93)[v] converged to a conventional [i.e. based on 3097 with $Fo>4\sigma(Fo)$] R = 0.1042 and R_w = 0.2544. Goodness of fit = 1.067. The max. and min. residual densities were 1.500 and -1.379 eÅ^{-3}, respectively. Final fractional atomic co-ordinates and isotropic thermal parameters, bond distances and angles are listed in Tables 7.29/7.32, 7.30 and 7.31, respectively. The asymmetric unit is shown in Figure 3.30a, 3.30b and 3.30c (Section 3.4), along with the labelling scheme employed.

Table 7.29 : Atomic coordinates (x 10^4) and equivalent isotropic displacement parameters ($Å^2$ x 10^3) for [ReH{η^2,η^2-PhC(H)=C(Ph) C(Ph)=C(Ph)H}($CF_3C(O)O$)(η-C_5H_5)] **22**
U(eq) is defined as one third of the trace of the orthogonalized Uij tensor.

Atom	x	y	z	U(eq)
Re(1)	2505(2)	8901(1)	1747(1)	24(1)
O(1)	3149(28)	8241(20)	2151(14)	20(7)
O(2)	2001(28)	7695(21)	2654(14)	20(7)
F(1)	3425(40)	7046(29)	2919(20)	83(12)
F(2)	4115(30)	7234(22)	2191(15)	46(8)
F(3)	2528(40)	6378(28)	1918(19)	79(11)
C(1)	4320(41)	9780(29)	2045(18)	21(10)
C(2)	3955(32)	9900(24)	2624(18)	18(9)
C(3)	2966(31)	10009(26)	2687(21)	24(10)
C(4)	2399(41)	10105(35)	2145(25)	38(13)
C(5)	5181(23)	9527(18)	1907(15)	34(12)
C(6)	5520(24)	9030(18)	2159(12)	25(10)
C(7)	6353(24)	8794(16)	1978(13)	23(10)
C(8)	6846(22)	9055(18)	1546(14)	33(12)
C(9)	6507(25)	9552(18)	1294(12)	33(12)
C(10)	5674(25)	9788(17)	1475(15)	36(12)
C(11)	4711(26)	9900(24)	3228(14)	23(10)
C(12)	4358(24)	9487(24)	3615(15)	42(13)
C(13)	5060(29)	9637(25)	4212(15)	31(11)
C(14)	6115(26)	10201(26)	4423(15)	48(15)
C(15)	6467(24)	10614(26)	4037(16)	31(11)
C(16)	5765(28)	10463(24)	3439(15)	42(13)
C(17)	2679(33)	10182(21)	3327(13)	23(10)
C(18)	3335(31)	10932(21)	3835(14)	20(10)
C(19)	3158(39)	11155(22)	4460(14)	45(14)
C(20)	2323(41)	10627(27)	4578(15)	68(19)
C(21)	1667(38)	9877(26)	4071(17)	45(14)
C(22)	1844(38)	9654(21)	3445(15)	56(16)
C(23)	1373(26)	10250(22)	2027(17)	24(10)
C(24)	563(30)	9937(20)	2290(15)	46(14)
C(25)	-384(28)	10093(22)	2206(17)	48(15)
C(26)	-521(29)	10562(24)	1858(19)	63(18)
C(27)	288(33)	10875(21)	1594(17)	58(17)
C(28)	1235(29)	10719(21)	1679(15)	48(15)
C(29)	2641(55)	7790(40)	2448(27)	36(13)
C(30)	3121(48)	7200(36)	2357(24)	23(10)
C(31)	2272(29)	7855(22)	794(19)	26(11)
C(32)	1259(28)	7807(21)	923(17)	49(15)
C(33)	1073(28)	8506(24)	915(19)	31(12)
C(34)	1971(33)	8985(22)	781(21)	76(21)
C(35)	2712(27)	8582(24)	706(18)	47(15)
Re(2)	4877(2)	7223(1)	-2159(1)	33(1)
O(201)	6062(30)	7739(22)	-1240(15)	26(7)
O(202)	6428(45)	9143(30)	-900(20)	53(10)
F(201)	8199(39)	8376(31)	-596(19)	75(11)
F(202)	8141(42)	9309(31)	82(21)	88(12)
F(203)	7323(32)	8161(23)	28(15)	52(8)
C(201)	3122(58)	6801(44)	-2525(22)	50(15)
C(202)	3471(39)	7059(32)	-1798(21)	37(12)
C(203)	3909(39)	6569(29)	-1555(25)	36(12)

TABLE 7.29 cont.

Atom	x	y	z	U
C(204)	4231(43)	6002(29)	-2021(24)	33(12)
C(205)	2443(34)	7210(26)	-2787(20)	65(19)
C(206)	2765(31)	8036(24)	-2631(17)	47(15)
C(207)	2109(37)	8325(20)	-2951(20)	56(16)
C(208)	1131(34)	7787(28)	-3426(21)	69(19)
C(209)	809(31)	6961(25)	-3582(17)	74(20)
C(210)	1465(37)	6673(20)	-3262(20)	45(14)
C(211)	2984(33)	7633(24)	-1346(19)	31(12)
C(212)	1870(32)	7331(21)	-1441(18)	86(24)
C(213)	1364(27)	7846(25)	-1152(19)	46(14)
C(214)	1972(35)	8665(23)	-767(19)	54(16)
C(215)	3085(34)	8967(21)	-671(20)	88(25)
C(216)	3591(27)	8452(25)	-961(20)	69(19)
C(217)	4054(35)	6693(21)	-826(12)	27(11)
C(218)	4540(33)	7420(17)	-263(16)	49(15)
C(219)	4667(39)	7417(20)	369(13)	33(12)
C(220)	4308(44)	6686(25)	438(13)	82(22)
C(221)	3822(38)	5960(20)	-125(17)	77(21)
C(222)	3695(36)	5963(18)	-757(14)	20(9)
C(223)	4982(30)	5669(23)	-1794(18)	46(14)
C(224)	5859(34)	6092(18)	-1223(16)	41(13)
C(225)	6512(28)	5706(25)	-1043(14)	47(14)
C(226)	6288(31)	4896(26)	-1433(20)	61(17)
C(227)	5411(35)	4473(18)	-2004(17)	56(16)
C(228)	4758(28)	4859(22)	-2184(13)	25(10)
C(229)	6680(69)	8469(46)	-857(30)	48(15)
C(230)	7490(54)	8569(40)	-322(26)	36(12)
C(231)	4995(39)	7435(25)	-3054(22)	63(18)
C(232)	6038(37)	7730(23)	-2600(20)	58(17)
C(233)	6241(33)	7055(33)	-2545(22)	101(28)
C(234)	5324(40)	6343(24)	-2965(23)	60(17)
C(235)	4554(32)	6578(25)	-3279(17)	35(12)
Re(3)	-648(2)	6343(1)	3131(1)	30(1)
O(301)	-954(31)	6047(23)	3937(15)	30(8)
O(302)	-2679(34)	5211(25)	3569(17)	39(9)
F(301)	-1795(37)	5924(28)	5045(19)	73(11)
F(302)	-2357(31)	4759(23)	4527(15)	52(8)
F(303)	-691(38)	5409(30)	4819(19)	77(11)
C(301)	-610(46)	7304(32)	2849(22)	31(11)
C(302)	-988(35)	7516(31)	3433(19)	34(12)
C(303)	-149(30)	7633(24)	3979(19)	18(9)
C(304)	787(31)	7492(23)	3853(19)	13(9)
C(305)	-1484(26)	7153(26)	2151(15)	35(12)
C(306)	-2582(27)	6677(26)	1951(14)	28(11)
C(307)	-3243(23)	6565(25)	1353(16)	41(13)
C(308)	-2807(28)	6930(28)	955(16)	37(12)
C(309)	-1709(29)	7406(28)	1156(16)	55(16)
C(310)	-1047(23)	7518(27)	1753(16)	34(12)
C(311)	-1939(27)	7682(23)	3505(21)	56(17)
C(312)	-2879(30)	7166(18)	3547(18)	29(11)
C(313)	-3771(26)	7390(20)	3577(15)	27(11)
C(314)	-3723(31)	8130(23)	3566(23)	67(19)
C(315)	-2783(36)	8646(19)	3524(20)	65(18)

TABLE 7.29 cont.

Atom	x	y	z	U
C(316)	-1891(29)	8422(21)	3493(16)	37(13)
C(317)	-246(30)	7944(20)	4703(13)	45(14)
C(318)	-1154(28)	7598(19)	4881(13)	14(9)
C(319)	-1267(27)	7991(23)	5505(15)	44(14)
C(320)	-473(34)	8732(22)	5951(14)	43(14)
C(321)	435(31)	9078(21)	5773(13)	41(13)
C(322)	549(26)	8685(22)	5149(14)	19(9)
C(323)	1681(26)	7450(23)	4341(16)	29(11)
C(324)	1498(23)	7166(21)	4831(15)	31(11)
C(325)	2346(26)	7115(22)	5237(14)	27(11)
C(326)	3378(24)	7348(23)	5154(17)	31(11)
C(327)	3561(24)	7632(26)	4664(18)	85(23)
C(328)	2713(29)	7684(26)	4258(16)	49(15)
C(329)	-1853(49)	5530(36)	3928(24)	31(11)
C(330)	-1609(41)	5374(30)	4603(20)	12(9)
C(331)	773(26)	5940(24)	2790(18)	22(10)
C(332)	112(33)	5287(26)	2905(21)	48(14)
C(333)	-961(31)	5014(29)	2494(23)	70(19)
C(334)	-963(28)	5499(29)	2126(21)	45(14)
C(335)	109(31)	6071(24)	2308(20)	51(15)

Table 7.30 : Bond lengths [Å] for [ReH{η^2,η^2-PhC(H)=C(Ph) C(Ph)=C(Ph)H}($CF_3C(O)O$) (η-C_5H_5)] **22**.

Atom	Bond Length	Atom	Bond Length
Re(1)-O(1)	2.07(5)	C(211)-C(212)	1.39
Re(1)-C(33)	2.19(4)	C(211)-C(216)	1.39
Re(1)-C(4)	2.20(7)	C(212)-C(213)	1.39
Re(1)-C(32)	2.21(3)	C(213)-C(214)	1.39
Re(1)-C(34)	2.23(4)	C(214)-C(215)	1.39
Re(1)-C(31)	2.26(4)	C(215)-C(216)	1.39
Re(1)-C(3)	2.24(4)	C(217)-C(218)	1.39
Re(1)-C(35)	2.27(3)	C(217)-C(222)	1.39
Re(1)-C(2)	2.31(4)	C(218)-C(219)	1.39
Re(1)-C(1)	2.35(4)	C(219)-C(220)	1.39
O(1)-C(29)	1.34(5)	C(220)-C(221)	1.39
O(2)-C(29)	1.03(7)	C(221)-C(222)	1.39
F(1)-C(30)	1.40(7)	C(223)-C(224)	1.39
F(2)-C(30)	1.43(8)	C(223)-C(228)	1.39
F(3)-C(30)	1.41(6)	C(224)-C(225)	1.39
C(1)-C(2)	1.42(3)	C(225)-C(226)	1.39
C(1)-C(5)	1.41(7)	C(226)-C(227)	1.39
C(2)-C(3)	1.43(3)	C(227)-C(228)	1.39
C(2)-C(11)	1.55(6)	C(229)-C(230)	1.40(11)
C(3)-C(4)	1.42(3)	C(231)-C(232)	1.42
C(3)-C(17)	1.49(5)	C(231)-C(235)	1.42
C(4)-C(23)	1.49(8)	C(232)-C(233)	1.42
C(5)-C(6)	1.39	C(233)-C(234)	1.42
C(5)-C(10)	1.39	C(234)-C(235)	1.42
C(6)-C(7)	1.39	Re(3)-O(301)	2.11(3)
C(7)-C(8)	1.39	Re(3)-C(334)	2.15(5)
C(8)-C(9)	1.39	Re(3)-C(301)	2.10(7)

TABLE 7.30 cont.

Atom	Bond Length	Atom	Bond Length
C(9)-C(10)	1.39	Re(3)-C(333)	2.30(6)
C(11)-C(12)	1.39	Re(3)-C(335)	2.21(5)
C(11)-C(16)	1.39	Re(3)-C(304)	2.29(3)
C(12)-C(13)	1.39	Re(3)-C(302)	2.29(6)
C(13)-C(14)	1.39	Re(3)-C(303)	2.34(4)
C(14)-C(15)	1.39	Re(3)-C(332)	2.44(6)
C(15)-C(16)	1.39	Re(3)-C(331)	2.40(5)
C(17)-C(18)	1.39	O(301)-C(329)	1.30(5)
C(17)-C(22)	1.39	O(302)-C(329)	1.11(7)
C(18)-C(19)	1.39	F(301)-C(330)	1.28(8)
C(19)-C(20)	1.39	F(302)-C(330)	1.23(4)
C(20)-C(21)	1.39	F(303)-C(330)	1.23(9)
C(21)-C(22)	1.39	C(301)-C(302)	1.44(3)
C(23)-C(24)	1.39	C(301)-C(305)	1.67(7)
C(23)-C(28)	1.39	C(302)-C(303)	1.43(3)
C(24)-C(25)	1.39	C(302)-C(311)	1.43(7)
C(25)-C(26)	1.39	C(303)-C(304)	1.41(3)
C(26)-C(27)	1.39	C(303)-C(317)	1.56(4)
C(27)-C(28)	1.39	C(304)-C(323)	1.53(6)
C(29)-C(30)	1.42(12)	C(305)-C(306)	1.39
C(31)-C(32)	1.42	C(305)-C(310)	1.39
C(31)-C(35)	1.42	C(306)-C(307)	1.39
C(32)-C(33)	1.42	C(307)-C(308)	1.39
C(33)-C(34)	1.42	C(308)-C(309)	1.39
C(34)-C(35)	1.42	C(309)-C(310)	1.39
Re(2)-O(201)	2.09(3)	C(311)-C(312)	1.39
Re(2)-C(232)	2.13(4)	C(311)-C(316)	1.39
Re(2)-C(202)	2.15(5)	C(312)-C(313)	1.39
Re(2)-C(231)	2.18(4)	C(313)-C(314)	1.39
Re(2)-C(201)	2.18(8)	C(314)-C(315)	1.39
Re(2)-C(233)	2.21(5)	C(315)-C(316)	1.39
Re(2)-C(235)	2.27(3)	C(317)-C(318)	1.39
Re(2)-C(234)	2.29(5)	C(317)-C(322)	1.39
Re(2)-C(204)	2.35(5)	C(318)-C(319)	1.39
Re(2)-C(203)	2.39(4)	C(319)-C(320)	1.39
O(201)-C(229)	1.28(6)	C(320)-C(321)	1.39
O(202)-C(229)	1.44(14)	C(321)-C(322)	1.39
F(201)-C(230)	1.29(10)	C(323)-C(324)	1.39
F(202)-C(230)	1.31(6)	C(323)-C(328)	1.39
F(203)-C(230)	1.26(7)	C(324)-C(325)	1.39
C(201)-C(202)	1.47(3)	C(325)-C(326)	1.39
C(201)-C(205)	1.53(11)	C(326)-C(327)	1.39
C(202)-C(203)	1.43(3)	C(327)-C(328)	1.39
C(202)-C(211)	1.58(8)	C(329)-C(330)	1.63(7)
C(203)-C(204)	1.44(3)	C(331)-C(332)	1.42
C(203)-C(217)	1.53(5)	C(331)-C(335)	1.42
C(204)-C(223)	1.45(8)	C(332)-C(333)	1.42
C(205)-C(206)	1.39	C(333)-C(334)	1.42
C(205)-C(210)	1.39	C(334)-C(335)	1.42
C(206)-C(207)	1.39	C(208)-C(209)	1.39
C(207)-C(208)	1.39	C(209)-C(210)	1.39

TABLE 7.31 : Bond Angles for [ReH{η^2,η^2-PhC(H)=C(Ph) C(Ph)=C(Ph)H}($CF_3C(O)O$) (η-C_5H_5)] **22**.

Atom	Angle	Atom	Angle
O(1)-Re(1)-C(33)	130.8(13)	C(2)-C(1)-C(5)	128(5)
O(1)-Re(1)-C(4)	135.1(14)	C(2)-C(1)-Re(1)	71(2)
C(33)-Re(1)-C(4)	89(2)	C(5)-C(1)-Re(1)	125(3)
O(1)-Re(1)-C(32)	93.4(14)	C(1)-C(2)-C(3)	126(5)
C(33)-Re(1)-C(32)	37.7(5)	C(1)-C(2)-C(11)	116(4)
C(4)-Re(1)-C(32)	126(2)	C(3)-C(2)-C(11)	119(3)
O(1)-Re(1)-C(34)	142(2)	C(1)-C(2)-Re(1)	74(2)
C(33)-Re(1)-C(34)	37.5(7)	C(3)-C(2)-Re(1)	69(3)
C(4)-Re(1)-C(34)	82(2)	C(11)-C(2)-Re(1)	133(3)
C(32)-Re(1)-C(34)	62.4(7)	C(4)-C(3)-C(2)	115(5)
O(1)-Re(1)-C(31)	81(2)	C(4)-C(3)-C(17)	122(5)
C(33)-Re(1)-C(31)	62.2(6)	C(2)-C(3)-C(17)	122(4)
C(4)-Re(1)-C(31)	143(2)	C(4)-C(3)-Re(1)	70(3)
C(32)-Re(1)-C(31)	37.1(5)	C(2)-C(3)-Re(1)	75(3)
C(34)-Re(1)-C(31)	61.6(6)	C(17)-C(3)-Re(1)	135(2)
O(1)-Re(1)-C(3)	97.8(14)	C(3)-C(4)-C(23)	131(5)
C(33)-Re(1)-C(3)	123(2)	C(3)-C(4)-Re(1)	73(3)
C(4)-Re(1)-C(3)	37.3(9)	C(23)-C(4)-Re(1)	124(3)
C(32)-Re(1)-C(3)	151(2)	C(6)-C(5)-C(10)	120.0
C(34)-Re(1)-C(3)	118(2)	C(6)-C(5)-C(1)	124(3)
C(31)-Re(1)-C(3)	172.2(13)	C(10)-C(5)-C(1)	116(3)
O(1)-Re(1)-C(35)	107(2)	C(5)-C(6)-C(7)	120.0
C(33)-Re(1)-C(35)	62.0(7)	C(8)-C(7)-C(6)	120.0
C(4)-Re(1)-C(35)	111(2)	C(7)-C(8)-C(9)	120.0
C(32)-Re(1)-C(35)	61.8(6)	C(10)-C(9)-C(8)	120.0
C(34)-Re(1)-C(35)	36.8(5)	C(9)-C(10)-C(5)	120.0
C(31)-Re(1)-C(35)	36.6(5)	C(12)-C(11)-C(16)	120.0
C(3)-Re(1)-C(35)	138.2(13)	C(12)-C(11)-C(2)	125(2)
O(1)-Re(1)-C(2)	77.5(14)	C(16)-C(11)-C(2)	115(2)
C(33)-Re(1)-C(2)	152(2)	C(13)-C(12)-C(11)	120.0
C(4)-Re(1)-C(2)	64(2)	C(14)-C(13)-C(12)	120.0
C(32)-Re(1)-C(2)	170(2)	C(13)-C(14)-C(15)	120.0
C(34)-Re(1)-C(2)	123.5(12)	C(16)-C(15)-C(14)	120.0
C(31)-Re(1)-C(2)	136(2)	C(15)-C(16)-C(11)	120.0
C(3)-Re(1)-C(2)	36.5(8)	C(18)-C(17)-C(22)	120.0
C(35)-Re(1)-C(2)	117.4(10)	C(18)-C(17)-C(3)	115(2)
O(1)-Re(1)-C(1)	85(2)	C(22)-C(17)-C(3)	125(2)
C(33)-Re(1)-C(1)	134(2)	C(19)-C(18)-C(17)	120.0
C(4)-Re(1)-C(1)	78(2)	C(18)-C(19)-C(20)	120.0
C(32)-Re(1)-C(1)	141.7(13)	C(19)-C(20)-C(21)	120.0
C(34)-Re(1)-C(1)	96.8(14)	C(20)-C(21)-C(22)	120.0
C(31)-Re(1)-C(1)	105.3(14)	C(21)-C(22)-C(17)	120.0
C(3)-Re(1)-C(1)	66.9(14)	C(24)-C(23)-C(28)	120.0
C(35)-Re(1)-C(1)	82.1(11)	C(24)-C(23)-C(4)	119(3)
C(2)-Re(1)-C(1)	35.4(7)	C(28)-C(23)-C(4)	121(3)
C(29)-O(1)-Re(1)	124(5)	C(25)-C(24)-C(23)	120.0
C(32)-C(31)-C(35)	108.0	C(24)-C(25)-C(26)	120.0
C(32)-C(31)-Re(1)	69.6(13)	C(27)-C(26)-C(25)	120.0
C(35)-C(31)-Re(1)	72.2(14)	C(28)-C(27)-C(26)	120.0
C(33)-C(32)-C(31)	108.0	C(27)-C(28)-C(23)	120.0
C(33)-C(32)-Re(1)	71(2)	O(2)-C(29)-O(1)	142(9)

TABLE 7.31 cont.

Atom	Angle	Atom	Angle
C(31)-C(32)-Re(1)	73(2)	O(2)-C(29)-C(30)	115(6)
C(32)-C(33)-C(34)	108.0	O(1)-C(29)-C(30)	103(6)
C(32)-C(33)-Re(1)	72(2)	F(1)-C(30)-F(2)	94(6)
C(34)-C(33)-Re(1)	72.7(13)	F(1)-C(30)-F(3)	96(5)
C(35)-C(34)-C(33)	108.0	F(2)-C(30)-F(3)	96(6)
C(35)-C(34)-Re(1)	73(2)	F(1)-C(30)-C(29)	116(6)
C(33)-C(34)-Re(1)	69.8(12)	F(2)-C(30)-C(29)	128(4)
C(34)-C(35)-C(31)	108.0	F(3)-C(30)-C(29)	121(6)
C(34)-C(35)-Re(1)	70(2)	C(202)-C(201)-C(205)	117(7)
C(31)-C(35)-Re(1)	71(2)	C(202)-C(201)-Re(2)	69(3)
O(201)-Re(2)-C(232)	90.7(14)	C(205)-C(201)-Re(2)	129(3)
O(201)-Re(2)-C(202)	98(2)	C(203)-C(202)-C(201)	117(6)
C(232)-Re(2)-C(202)	157(2)	C(203)-C(202)-C(211)	120(4)
O(201)-Re(2)-C(231)	128.2(13)	C(201)-C(202)-C(211)	119(6)
C(232)-Re(2)-C(231)	38.5(6)	C(203)-C(202)-Re(2)	81(3)
C(202)-Re(2)-C(231)	125(2)	C(201)-C(202)-Re(2)	71(4)
O(201)-Re(2)-C(201)	138(2)	C(211)-C(202)-Re(2)	136(3)
C(232)-Re(2)-C(201)	127(2)	C(202)-C(203)-C(204)	117(5)
C(202)-Re(2)-C(201)	39.8(11)	C(202)-C(203)-C(217)	120(4)
C(231)-Re(2)-C(201)	89(2)	C(204)-C(203)-C(217)	124(5)
O(201)-Re(2)-C(233)	82(2)	C(202)-C(203)-Re(2)	63(3)
C(232)-Re(2)-C(233)	38.2(7)	C(204)-C(203)-Re(2)	71(3)
C(202)-Re(2)-C(233)	164(2)	C(217)-C(203)-Re(2)	136(3)
C(231)-Re(2)-C(233)	63.2(8)	C(203)-C(204)-C(223)	121(5)
C(201)-Re(2)-C(233)	138(2)	C(203)-C(204)-Re(2)	74(3)
O(201)-Re(2)-C(235)	144(2)	C(223)-C(204)-Re(2)	121(3)
C(232)-Re(2)-C(235)	62.8(7)	C(206)-C(205)-C(210)	120.0
C(202)-Re(2)-C(235)	116(2)	C(206)-C(205)-C(201)	126(3)
C(231)-Re(2)-C(235)	37.1(5)	C(210)-C(205)-C(201)	114(3)
C(201)-Re(2)-C(235)	77(2)	C(205)-C(206)-C(207)	120.0
C(233)-Re(2)-C(235)	61.7(8)	C(206)-C(207)-C(208)	120.0
O(201)-Re(2)-C(234)	111(2)	C(209)-C(208)-C(207)	120.0
C(232)-Re(2)-C(234)	62.5(9)	C(208)-C(209)-C(210)	120.0
C(202)-Re(2)-C(234)	132(2)	C(209)-C(210)-C(205)	120.0
C(231)-Re(2)-C(234)	61.8(7)	C(212)-C(211)-C(216)	120.0
C(201)-Re(2)-C(234)	104(2)	C(212)-C(211)-C(202)	117(3)
C(233)-Re(2)-C(234)	36.8(8)	C(216)-C(211)-C(202)	122(3)
C(235)-Re(2)-C(234)	36.3(6)	C(211)-C(212)-C(213)	120.0
O(201)-Re(2)-C(204)	90(2)	C(214)-C(213)-C(212)	120.0
C(232)-Re(2)-C(204)	136(2)	C(215)-C(214)-C(213)	120.0
C(202)-Re(2)-C(204)	66(2)	C(214)-C(215)-C(216)	120.0
C(231)-Re(2)-C(204)	131(2)	C(215)-C(216)-C(211)	120.0
C(201)-Re(2)-C(204)	76(3)	C(218)-C(217)-C(222)	120.0
C(233)-Re(2)-C(204)	99(2)	C(218)-C(217)-C(203)	128(3)
C(235)-Re(2)-C(204)	93(2)	C(222)-C(217)-C(203)	112(3)
C(234)-Re(2)-C(204)	77(2)	C(219)-C(218)-C(217)	120.0
O(201)-Re(2)-C(203)	79.7(13)	C(218)-C(219)-C(220)	120.0
C(232)-Re(2)-C(203)	166(2)	C(221)-C(220)-C(219)	120.0
C(202)-Re(2)-C(203)	36.3(9)	C(222)-C(221)-C(220)	120.0
C(231)-Re(2)-C(203)	152(2)	C(221)-C(222)-C(217)	120.0
C(201)-Re(2)-C(203)	66(2)	C(224)-C(223)-C(228)	120.0
C(233)-Re(2)-C(203)	130(2)	C(224)-C(223)-C(204)	125(3)
C(235)-Re(2)-C(203)	120.9(13)	C(228)-C(223)-C(204)	115(3)

TABLE 7.31 cont.

Atom	Angle	Atom	Angle
C(234)-Re(2)-C(203)	112(2)	C(225)-C(224)-C(223)	120.0
C(204)-Re(2)-C(203)	35.3(8)	C(224)-C(225)-C(226)	120.0
C(229)-O(201)-Re(2)	133(5)	C(227)-C(226)-C(225)	120.0
O(301)-Re(3)-C(334)	126.2(14)	C(226)-C(227)-C(228)	120.0
O(301)-Re(3)-C(301)	136(2)	C(227)-C(228)-C(223)	120.0
C(334)-Re(3)-C(301)	93(2)	C(230)-C(229)-O(201)	116(8)
O(301)-Re(3)-C(333)	91(2)	C(230)-C(229)-O(202)	122(6)
C(334)-Re(3)-C(333)	37.1(9)	O(201)-C(229)-O(202)	121(8)
C(301)-Re(3)-C(333)	130(2)	F(202)-C(230)-C(229)	118(8)
O(301)-Re(3)-C(335)	143(2)	F(202)-C(230)-F(203)	107(5)
C(334)-Re(3)-C(335)	38.0(8)	C(229)-C(230)-F(203)	123(4)
C(301)-Re(3)-C(335)	79(2)	F(202)-C(230)-F(201)	96(5)
C(333)-Re(3)-C(335)	61.2(11)	C(229)-C(230)-F(201)	104(6)
O(301)-Re(3)-C(304)	90.1(12)	F(203)-C(230)-F(201)	105(8)
C(334)-Re(3)-C(304)	133.8(13)	C(232)-C(231)-C(235)	108.0
C(301)-Re(3)-C(304)	70(2)	C(232)-C(231)-Re(2)	69(2)
C(333)-Re(3)-C(304)	138(2)	C(235)-C(231)-Re(2)	75(2)
C(335)-Re(3)-C(304)	95.9(12)	C(231)-C(232)-C(233)	108.0
O(301)-Re(3)-C(302)	98(2)	C(231)-C(232)-Re(2)	73(2)
C(334)-Re(3)-C(302)	126(2)	C(233)-C(232)-Re(2)	74(2)
C(301)-Re(3)-C(302)	38.0(11)	C(234)-C(233)-C(232)	108.0
C(333)-Re(3)-C(302)	156(2)	C(234)-C(233)-Re(2)	74.9(13)
C(335)-Re(3)-C(302)	117.2(14)	C(232)-C(233)-Re(2)	68(2)
C(304)-Re(3)-C(302)	64.6(14)	C(233)-C(234)-C(235)	108.0
O(301)-Re(3)-C(303)	78.9(14)	C(233)-C(234)-Re(2)	68.4(14)
C(334)-Re(3)-C(303)	154.8(14)	C(235)-C(234)-Re(2)	71(2)
C(301)-Re(3)-C(303)	62(2)	C(234)-C(235)-C(231)	108.0
C(333)-Re(3)-C(303)	167(2)	C(234)-C(235)-Re(2)	73(2)
C(335)-Re(3)-C(303)	124.3(12)	C(231)-C(235)-Re(2)	68(2)
C(304)-Re(3)-C(303)	35.5(8)	C(312)-C(311)-C(316)	120.0
C(302)-Re(3)-C(303)	35.9(8)	C(312)-C(311)-C(302)	126(3)
O(301)-Re(3)-C(332)	84(2)	C(316)-C(311)-C(302)	114(3)
C(334)-Re(3)-C(332)	59.6(12)	C(313)-C(312)-C(311)	120.0
C(301)-Re(3)-C(332)	137(2)	C(312)-C(313)-C(314)	120.0
C(333)-Re(3)-C(332)	34.7(8)	C(315)-C(314)-C(313)	120.0
C(335)-Re(3)-C(332)	58.9(11)	C(316)-C(315)-C(314)	120.0
C(304)-Re(3)-C(332)	104(2)	C(315)-C(316)-C(311)	120.0
C(302)-Re(3)-C(332)	168.0(13)	C(318)-C(317)-C(322)	120.0
C(303)-Re(3)-C(332)	134.8(14)	C(318)-C(317)-C(303)	123(2)
O(301)-Re(3)-C(331)	110(2)	C(322)-C(317)-C(303)	116(2)
C(334)-Re(3)-C(331)	60.4(10)	C(317)-C(318)-C(319)	120.0
C(301)-Re(3)-C(331)	105(2)	C(320)-C(319)-C(318)	120.0
C(333)-Re(3)-C(331)	58.6(11)	C(319)-C(320)-C(321)	120.0
C(335)-Re(3)-C(331)	35.6(7)	C(320)-C(321)-C(322)	120.0
C(304)-Re(3)-C(331)	82.0(14)	C(321)-C(322)-C(317)	120.0
C(302)-Re(3)-C(331)	135.8(12)	C(324)-C(323)-C(328)	120.0
C(303)-Re(3)-C(331)	117.6(12)	C(324)-C(323)-C(304)	124(2)
C(332)-Re(3)-C(331)	34.1(7)	C(328)-C(323)-C(304)	116(2)
C(329)-O(301)-Re(3)	126(3)	C(323)-C(324)-C(325)	120.0
C(302)-C(301)-C(305)	114(5)	C(326)-C(325)-C(324)	120.0
C(302)-C(301)-Re(3)	78(3)	C(325)-C(326)-C(327)	120.0
C(305)-C(301)-Re(3)	121(3)	C(328)-C(327)-C(326)	120.0
C(303)-C(302)-C(301)	107(4)	C(327)-C(328)-C(323)	120.0

TABLE 7.31 cont.

Atom	Angle	Atom	Angle
C(303)-C(302)-C(311)	124(4)	O(302)-C(329)-O(301)	133(5)
C(301)-C(302)-C(311)	129(5)	O(302)-C(329)-C(330)	120(4)
C(303)-C(302)-Re(3)	74(3)	O(301)-C(329)-C(330)	107(4)
C(301)-C(302)-Re(3)	64(3)	F(301)-C(330)-F(302)	101(4)
C(311)-C(302)-Re(3)	133(3)	F(301)-C(330)-F(303)	109(4)
C(304)-C(303)-C(302)	119(4)	F(302)-C(330)-F(303)	116(7)
C(304)-C(303)-C(317)	121(4)	F(301)-C(330)-C(329)	105(6)
C(302)-C(303)-C(317)	120(4)	F(302)-C(330)-C(329)	107(4)
C(304)-C(303)-Re(3)	70(2)	F(303)-C(330)-C(329)	117(4)
C(302)-C(303)-Re(3)	70(3)	C(332)-C(331)-C(335)	108.0
C(317)-C(303)-Re(3)	134(2)	C(332)-C(331)-Re(3)	75(2)
C(303)-C(304)-C(323)	127(3)	C(335)-C(331)-Re(3)	65(2)
C(303)-C(304)-Re(3)	74(2)	C(331)-C(332)-C(333)	108.0
C(323)-C(304)-Re(3)	121(3)	C(331)-C(332)-Re(3)	71(2)
C(306)-C(305)-C(310)	120.0	C(333)-C(332)-Re(3)	67(2)
C(306)-C(305)-C(301)	124(2)	C(332)-C(333)-C(334)	108.0
C(310)-C(305)-C(301)	116(2)	C(332)-C(333)-Re(3)	78(2)
C(307)-C(306)-C(305)	120.0	C(334)-C(333)-Re(3)	66(2)
C(306)-C(307)-C(308)	120.0	C(335)-C(334)-C(333)	108.0
C(309)-C(308)-C(307)	120.0	C(335)-C(334)-Re(3)	74(2)
C(308)-C(309)-C(310)	120.0	C(333)-C(334)-Re(3)	77(2)
C(309)-C(310)-C(305)	120.0	C(334)-C(335)-C(331)	108.0
C(331)-C(335)-Re(3)	79(2)	C(334)-C(335)-Re(3)	69(2)

TABLE 7.32 : Hydrogen coordinates (x 10^4) and isotropic displacement parameters ($Å^2$ x 10^3) for [ReH{η^2,η^2-PhC(H)=C(Ph) C(Ph)=C(Ph)H}($CF_3C(O)O$)(η-C_5H_5)] **22**

Atom	x	y	z	U(eq)
H(6)	5190(31)	8855(24)	2448(16)	30
H(7)	6580(31)	8461(21)	2146(19)	28
H(8)	7403(28)	8897(24)	1425(21)	40
H(9)	6837(33)	9727(25)	1005(16)	40
H(10)	5447(33)	10121(23)	1307(21)	44
H(12)	3653(28)	9110(35)	3473(21)	50
H(13)	4824(39)	9361(36)	4471(21)	37
H(14)	6584(34)	10301(38)	4823(21)	58
H(15)	7173(28)	10991(37)	4178(22)	37
H(16)	6001(38)	10740(35)	3181(21)	50
H(18)	3894(45)	11285(29)	3756(19)	24
H(19)	3597(57)	11657(29)	4800(19)	54
H(20)	2205(59)	10777(37)	4997(19)	82
H(21)	1108(53)	9524(35)	4150(23)	54
H(22)	1405(55)	9152(28)	3106(20)	68
H(24)	655(39)	9623(27)	2523(22)	55
H(25)	-925(34)	9883(30)	2382(24)	58
H(26)	-1155(34)	10666(33)	1801(28)	75
H(27)	197(43)	11189(28)	1361(23)	69
H(28)	1777(35)	10929(29)	1503(22)	58
H(31)	2592(29)	7476(22)	771(19)	31
H(32)	799(36)	7392(27)	1000(28)	59
H(33)	469(34)	8628(32)	985(29)	38
H(34)	2058(45)	9476(27)	748(33)	91

TABLE 7.32 cont.

Atom	x	y	z	U
H(35)	3369(32)	8764(32)	616(28)	56
H(206)	3419(35)	8395(31)	-2313(22)	56
H(207)	2324(49)	8877(21)	-2846(29)	67
H(208)	692(43)	7980(37)	-3640(30)	83
H(209)	155(35)	6602(33)	-3900(23)	89
H(210)	1250(49)	6120(20)	-3367(28)	55
H(212)	1464(40)	6783(22)	-1699(27)	103
H(213)	619(28)	7644(32)	-1216(28)	55
H(214)	1633(44)	9010(29)	-573(28)	65
H(215)	3491(43)	9515(22)	-414(28)	106
H(216)	4336(28)	8654(32)	-897(29)	83
H(218)	4780(46)	7908(19)	-309(22)	59
H(219)	4992(55)	7903(24)	746(16)	40
H(220)	4393(62)	6684(33)	861(15)	98
H(221)	3582(52)	5471(23)	-79(24)	92
H(222)	3370(51)	5477(20)	-1134(17)	24
H(224)	6009(46)	6634(19)	-962(23)	49
H(225)	7099(33)	5989(34)	-661(17)	56
H(226)	6725(39)	4638(35)	-1313(30)	73
H(227)	5261(47)	3931(19)	-2265(24)	67
H(228)	4172(33)	4576(30)	-2566(15)	30
H(231)	4660(39)	7749(25)	-3181(22)	76
H(232)	6506(50)	8270(26)	-2377(28)	69
H(233)	6865(39)	7075(47)	-2280(32)	121
H(234)	5242(57)	5816(27)	-3024(36)	72
H(235)	3879(36)	6232(34)	-3580(23)	41
H(306)	-2874(36)	6433(37)	2216(20)	33
H(307)	-3978(24)	6247(36)	1219(22)	49
H(308)	-3249(35)	6855(40)	555(22)	44
H(309)	-1417(38)	7650(41)	890(22)	66
H(310)	-313(25)	7836(38)	1887(22)	41
H(312)	-2912(40)	6670(22)	3555(28)	34
H(313)	-4400(29)	7044(25)	3606(22)	33
H(314)	-4320(38)	8280(32)	3586(35)	81
H(315)	-2750(47)	9141(23)	3516(31)	78
H(316)	-1262(34)	8768(26)	3465(24)	45
H(318)	-1685(39)	7102(26)	4583(17)	16
H(319)	-1875(35)	7759(31)	5624(20)	53
H(320)	-549(47)	8995(30)	6368(19)	52
H(321)	967(43)	9574(27)	6071(18)	50
H(322)	1156(33)	8917(30)	5030(20)	22
H(324)	808(24)	7010(30)	4887(22)	37
H(325)	2224(33)	6924(31)	5565(19)	33
H(326)	3946(27)	7313(31)	5425(23)	37
H(327)	4252(27)	7788(36)	4608(25)	102
H(328)	2836(37)	7874(36)	3931(21)	59
H(331)	1512(26)	6231(24)	2994(18)	27
H(332)	341(44)	5075(38)	3198(31)	57
H(333)	-1558(38)	4593(41)	2471(34)	84
H(334)	-1560(33)	5450(42)	1819(30)	54
H(335)	337(42)	6463(34)	2142(31)	61

7.9 Crystal Structure Determination of Complex 26.

A crystal of approximate dimensions 0.2 x 0.2 x 0.2 mm was used for data collection.

Crystal Data : $C_{21}H_{16}F_{12}Mo$, $M = 592.3$, monoclinic, $a = 8.847(2)$, $b = 13.574(3)$, $c = 17.336(4)$ Å, $\beta = 93.94(2)°$, $U = 2076.9$ Å^3, space group $P2_1/n$, $Z = 4$, $D_c = 1.89$ gcm^{-3}, μ(Mo-K_α) = 6.49 cm^{-1}, $F(000)$ = 1168. Data were measured at room temperature on a CAD4 automatic four-circle diffractometer in the range $2 \leq \theta \leq 24°$. 3661 reflections were collected of which 2431 were unique with $I \geq 2\sigma(I)$. Data were corrected for Lorentz and polarisation effects but not for X-ray absorption effects. The structure was solved by direct methods and refined using the SHELX[i,ii] suite of programs. In the final least squares cycles all atoms were allowed to vibrate anisotropically. Hydrogen atoms were included at calculated positions except in the case of those hydrogens attached to C6 and C9. These hydrogens (H61 and H91) were located in the penultimate Difference Fourier and refined at a distance of 1.08Å from the relevant parent atoms. Final residues after 8 cycles of least squares were $R = 0.0309$, $R_w = 0.0354$, for a weighting scheme of $w = 1.5695/[\sigma^2(F) + 0.001500(F)^2]$. Max. final shift/esd was 0.150 (z coordinate of H61). The max. and min. residual densities were 0.25 and -0.31 eÅ^{-3}, respectively. Final fractional atomic coordinates and isotropic thermal parameters, bond distances and angles are listed in Tables 7.33/7.34, 7.35 and 7.36, respectively. The asymmetric unit is shown in Figure 4.17 (Section 4.4), along with the labelling scheme employed.

TABLE 7.33 : Fractional atomic coordinates and thermal parameters (Å) for complex **26**.

Atom	x	y	z	Uiso or Ueq	(***)
Mo1	0.22047(3)	0.17901(2)	0.40376(2)	0.0341(2)	***
C1	0.1775(4)	0.3090(3)	0.3381(2)	0.034(2)	***
C2	0.2461(4)	0.2393(3)	0.2879(2)	0.042(2)	***
C3	0.1363(5)	0.1626(3)	0.2796(2)	0.044(2)	***
C4	0.0065(5)	0.1873(3)	0.3240(2)	0.041(2)	***
C5	0.0032(4)	0.3001(3)	0.3338(2)	0.039(2)	***
C6	-0.0346(5)	0.3394(4)	0.4126(3)	0.055(3)	***
C7	0.0732(6)	0.2854(4)	0.4741(2)	0.055(3)	***
C8	0.2231(6)	0.3239(3)	0.4766(3)	0.056(3)	***
C9	0.2769(5)	0.3399(3)	0.4037(3)	0.048(2)	***
C10	0.3892(6)	0.2582(4)	0.2458(3)	0.072(3)	***
C11	0.1522(7)	0.0809(5)	0.2223(3)	0.077(4)	***
C12	-0.1294(6)	0.1234(4)	0.3184(3)	0.066(3)	***
C13	-0.0712(5)	0.3559(4)	0.2637(3)	0.054(3)	***
C14	-0.1972(7)	0.3549(6)	0.4363(4)	0.089(4)	***
C15	0.3233(8)	0.3418(5)	0.5490(3)	0.095(5)	***
C16	0.0107(9)	0.2484(5)	0.5493(3)	0.101(5)	***
C17	0.2874(6)	0.0148(4)	0.4007(3)	0.068(3)	***
C18	0.2206(6)	0.0322(4)	0.4705(3)	0.069(3)	***
C19	0.3148(7)	0.0957(4)	0.5146(3)	0.070(3)	***
C20	0.4402(6)	0.1168(4)	0.4706(4)	0.071(4)	***
C21	0.4215(6)	0.0673(4)	0.4019(4)	0.074(4)	***
F1	0.2903(4)	0.0486(3)	0.2189(2)	0.107(3)	***
F2	0.1065(6)	0.1113(4)	0.1530(2)	0.138(4)	***
F3	0.0703(6)	0.0008(3)	0.2361(3)	0.132(4)	***
F4	-0.1912(4)	0.1103(3)	0.2472(2)	0.104(3)	***
F5	-0.1067(4)	0.0332(2)	0.3474(2)	0.104(3)	***
F6	-0.2409(4)	0.1625(3)	0.3556(3)	0.128(4)	***
F7	-0.2129(3)	0.3280(2)	0.2446(2)	0.076(2)	***
F8	0.0053(4)	0.3414(3)	0.2000(2)	0.077(2)	***
F9	-0.0724(3)	0.4539(2)	0.2742(2)	0.075(2)	***
F10	-0.1929(5)	0.4194(3)	0.4946(3)	0.123(3)	***
F11	-0.2850(4)	0.3958(4)	0.3792(3)	0.115(3)	***
F12	-0.2680(5)	0.2772(4)	0.4618(3)	0.140(4)	***
H61	-0.0001(58)	0.4141(18)	0.4079(31)	0.076(6)	
H91	0.3860(32)	0.3644(38)	0.3924(30)	0.076(6)	

TABLE 7.34 : Fractional atomic coordinates for the hydrogen atoms of complex **26**.

Atom	x	y	z
H101	0.4150	0.1940	0.2123
H102	0.4826	0.2732	0.2876
H103	0.3716	0.3208	0.2078
H151	0.2610	0.3252	0.5989
H152	0.3585	0.4179	0.5512
H153	0.4219	0.2948	0.5490
H161	-0.1035	0.2217	0.5375
H162	0.0105	0.3082	0.5904
H163	0.0814	0.1894	0.5730
H171	0.2421	-0.0317	0.3541
H181	0.1148	0.0016	0.4869
H191	0.2959	0.1237	0.5715
H201	0.5345	0.1640	0.4882
H211	0.4985	0.0690	0.3562

TABLE 7.35 : Bond lengths (Å) for complex **26**.

Atom	Bond Length	Atom	Bond Length
Mo1-C1	2.119(4)	Mo1-C2	2.196(4)
Mo1-C3	2.239(4)	Mo1-C4	2.269(4)
Mo1-C5	2.747(4)	Mo1-C7	2.343(4)
Mo1-C8	2.337(4)	Mo1-C9	2.241(4)
Mo1-C17	2.308(5)	Mo1-C18	2.304(5)
Mo1-C19	2.334(5)	Mo1-C20	2.350(4)
C1-C2	1.447(6)	C1-C3	2.249(6)
C1-C4	2.241(5)	C1-C5	1.543(5)
C1-C9	1.451(6)	C2-C3	1.424(6)
C2-C10	1.525(6)	C3-C4	1.465(6)
C3-C11	1.502(7)	C4-C5	1.541(6)
C4-C12	1.480(6)	C5-C6	1.525(6)
C5-C13	1.542(6)	C6-H61	1.064(19)
C6-C7	1.563(7)	C6-C14	1.537(7)
C7-C8	1.423(7)	C7-C16	1.535(7)
C8-C9	1.399(7)	C8-C15	1.505(7)
C9-H91	1.052(19)	C11-F1	1.303(7)
C11-F2	1.308(7)	C11-F3	1.337(8)
C12-F4	1.328(7)	C12-F5	1.333(6)
C12-F6	1.327(7)	C13-F7	1.329(5)
C13-F8	1.349(6)	C13-F9	1.343(6)
C14-F10	1.335(8)	C14-F11	1.336(8)
C14-F12	1.319(8)	C17-C18	1.402(8)
C17-C19	2.259(8)	C17-C20	2.233(8)
C17-C21	1.383(8)	C18-C19	1.392(8)
C18-C20	2.257(7)	C18-C21	2.256(8)
C19-C20	1.419(8)	C19-C21	2.261(9)
C20-C21	1.367(8)	F1-F3	2.092(7)
F4-F6	2.084(7)		

TABLE 7.36 : Bond angles (°) for complex **26**.

Atom	Angle	Atom	Angle
C2-Mo1-C1	39.1(2)	C3-Mo1-C1	62.0(2)
C3-Mo1-C2	37.4(2)	C4-Mo1-C1	61.3(1)
C4-Mo1-C2	63.8(1)	C4-Mo1-C3	37.9(2)
C5-Mo1-C1	34.0(1)	C5-Mo1-C2	59.1(1)
C5-Mo1-C3	57.3(1)	C5-Mo1-C4	34.1(1)
C7-Mo1-C1	71.4(2)	C7-Mo1-C2	110.0(2)
C7-Mo1-C3	113.7(2)	C7-Mo1-C4	79.4(2)
C7-Mo1-C5	57.6(1)	C8-Mo1-C1	65.5(2)
C8-Mo1-C2	100.6(2)	C8-Mo1-C3	126.4(2)
C8-Mo1-C4	105.3(2)	C8-Mo1-C5	73.5(2)
C8-Mo1-C7	35.4(2)	C9-Mo1-C1	38.8(2)
C9-Mo1-C2	66.4(2)	C9-Mo1-C3	99.0(2)
C9-Mo1-C4	97.3(1)	C9-Mo1-C5	64.3(1)
C9-Mo1-C7	62.0(2)	C9-Mo1-C8	35.5(2)
C17-Mo1-C1	145.9(2)	C17-Mo1-C2	107.2(2)
C17-Mo1-C3	87.2(2)	C17-Mo1-C4	103.8(2)
C17-Mo1-C5	137.8(2)	C17-Mo1-C7	139.5(2)
C17-Mo1-C8	146.3(2)	C17-Mo1-C9	152.1(2)
C3-C1-C2	38.1(2)	C4-C1-C2	76.2(3)
C4-C1-C3	38.1(2)	C5-C1-C2	112.3(3)
C5-C1-C3	77.3(2)	C5-C1-C4	43.4(2)
C9-C1-C2	113.8(4)	C9-C1-C3	132.8(3)
C9-C1-C4	131.9(3)	C9-C1-C5	127.6(4)
C3-C2-C1	103.1(3)	C10-C2-C1	125.1(4)
C10-C2-C3	131.1(4)	C2-C3-C1	38.8(2)
C4-C3-C1	70.7(2)	C4-C3-C2	109.5(4)
C11-C3-C1	158.6(4)	C11-C3-C2	120.8(5)
C11-C3-C4	128.9(4)	C3-C4-C1	71.2(3)
C5-C4-C1	43.4(2)	C5-C4-C3	107.9(4)
C12-C4-C1	167.9(4)	C12-C4-C3	119.6(4)
C12-C4-C5	124.6(4)	C4-C5-C1	93.2(3)
C6-C5-C1	102.1(3)	C6-C5-C4	117.0(4)
C13-C5-C1	111.8(3)	C13-C5-C4	114.2(4)
C13-C5-C6	115.3(4)	H61-C6-C5	100(3)
C7-C6-C5	106.6(3)	C7-C6-H61	109(3)
C14-C6-C5	123.7(5)	C14-C6-H61	100(3)
C14-C6-C7	114.9(5)	C8-C7-C6	111.9(4)
C16-C7-C6	119.6(5)	C16-C7-C8	118.9(5)
C9-C8-C7	113.8(4)	C15-C8-C7	125.4(5)
C15-C8-C9	120.7(5)	C8-C9-C1	115.9(4)
H91-C9-C1	117(3)	H91-C9-C8	126(3)
F1-C11-C3	114.1(5)	F2-C11-C3	109.7(5)
F2-C11-F1	107.2(6)	F3-C11-C3	114.0(5)
F3-C11-F1	104.9(5)	F3-C11-F2	106.4(5)
F4-C12-C4	114.8(5)	F5-C12-C4	114.4(4)
F5-C12-F4	105.6(5)	F6-C12-C4	111.2(4)
F6-C12-F4	103.5(5)	F6-C12-F5	106.4(5)
F7-C13-C5	113.6(4)	F8-C13-C5	111.3(4)
F8-C13-F7	105.8(4)	F9-C13-C5	112.7(4)
F9-C13-F7	107.5(4)	F9-C13-F8	105.3(4)
F10-C14-C6	108.2(6)	F11-C14-C6	111.5(5)
F11-C14-F10	105.9(5)	F12-C14-C6	117.0(5)

TABLE 7.36 cont.

Atom	Angle	Atom	Angle
F12-C14-F10	105.1(6)	F12-C14-F11	108.4(6)
C19-C17-C18	35.9(3)	C20-C17-C18	72.7(4)
C20-C17-C19	36.8(2)	C21-C17-C18	108.2(5)
C21-C17-C19	72.3(4)	C21-C17-C20	35.5(3)
C19-C18-C17	107.9(5)	C20-C18-C17	70.9(4)
C20-C18-C19	37.0(3)	C21-C18-C17	35.6(3)
C21-C18-C19	72.3(4)	C21-C18-C20	35.3(2)
C18-C19-C17	36.2(3)	C20-C19-C17	70.6(4)
C20-C19-C18	106.8(5)	C21-C19-C17	35.6(2)
C21-C19-C18	71.8(4)	C21-C19-C20	35.0(3)
C18-C20-C17	36.4(2)	C19-C20-C17	72.6(4)
C19-C20-C18	36.2(3)	C21-C20-C17	35.9(3)
C21-C20-C18	72.3(4)	C21-C20-C19	108.5(5)
C18-C21-C17	36.2(3)	C19-C21-C17	72.1(4)
C19-C21-C18	35.9(2)	C20-C21-C17	108.6(5)
C20-C21-C18	72.4(4)	C20-C21-C19	36.5(3)
F3-F1-C11	38.1(3)	F1-F3-C11	37.0(3)
F6-F4-C12	38.2(3)	F4-F6-C12	38.3(3)